

Design and Synthesis of Novel
PPAR Agonists for the Treatment of
the Metabolic Syndrome and
Diabetes Type II

Anju Hina Yushma Bhurruth

Imperial College London

A thesis submitted for the degree of
Doctor of Philosophy of the University of London
and for the
Diploma of Membership of Imperial College London

October 2007

Declaration

I hereby declare that the work described here is entirely my own, except where specifically acknowledged in the text.

Anju Hina Yushma Bhurruth

October 2007

Acknowledgements

First of all, I am grateful to Professor Andrew Miller for allowing me to start this new medicinal chemistry project in his group. Thank you for trusting me and for allowing me to be independent in my research project. I wish to acknowledge both the GTC and IC-VEC Ltd. for funding my project and for my bursary.

Next, I want to thank Dr Michael Jorgensen for his constant support and guidance. Thank you so much for being present and for all your help, you've always been there when I needed you. I have learnt a lot from you, thank you also for being a good friend, for taking us out for drinks and for some delicious barbecues!

I wish to express my gratitude towards Professors Christopher Schofield and William Motherwell for accepting to be my examiners.

I am really grateful to Therese Røst, Dr Jon Skorve and Professor Rolf Berge from the Institute of Medicine, Bergen and Thia Medica AS, Norway, for the biology testing. Big thanks to Therese for looking after me in Bergen and for replying to all my questions and emails about the assay!

I would like to extend some special acknowledgements towards the following people for technical support: John Barton for HRMS, Stephen Boyer for elemental analysis, Andrew White for x-ray crystallography, Pete Haycock for NOE experiments, the chemistry research technicians without whom the lab would not function and chemistry stores.

This manuscript would not be what it is today if it had not been for Mike J, Steve, Mike W and last but not least, Damien, whom I wish to acknowledge for proof reading. Your efforts and comments were strongly appreciated. Thank you for your time!

Some especial acknowledgements to Professor Charles Rees and Dr Alan Spivey for a few stimulating discussions about heterocyclic chemistry. Thank you for your kindness and for being attentive to my questions. Thank you to Alan for having accepted to be my examiner for my transfer and for keeping in touch since then.

The past three years would not have been the same without the support of the group, in particular Nic, Arnaud, Mike W, Wayne, Jim, Ben, Top, Mike K, Nazila and Steve. I

will always remember Nic who showed me around the lab and who made me discover the Thai Square! Arnaud, thanks for looking after me during my first week and for being so friendly and caring. Mike W, thank you so much for your help with POs and computer problems... But most important of all, thanks for being a good friend and for your constant support. Wayne, you've taught me so much, can I really write everything here? We've had so many good times in the lab and I really enjoyed sharing my cooking recipes with you while doing columns! Thanks for being such a good friend and for your jokes, I miss them so much! Nazila, we started our PhDs on the same day and we've been through so much together, hang on, you are nearly there too! Top, you're joking! Steve, you were only here for a couple of months, but it was really good fun and "chilaxing". Thanks for being so supportive and so helpful, I really appreciate it. Peerada, Soumia and Taka, you've only been here over the past year, but it's been great to have you around. Thank you for being so caring and supportive.

Of course, I have some very especial thoughts for my family, in particular my grandmother and my parents. I've been away from you for so long, it is always hard for me not to have you around. My heart is always with you and I would not be here if it was not for your love and support. Yash, it's been great to have you in London for the past year, sorry for not being present all the time, but you know how much I love you. Nana, I miss you too, I am sure you would have been happy to share this moment with me. Warm thanks to Damien's family for being caring and thoughtful.

Finally, Damien, what would I be today had it not been for you? No words could ever be enough to say how much I am grateful for having you by my side everyday and how happy I am with you. I can't wait for us to start a new chapter of our life in Paris...

To Mum and Dad

This thesis is for you.

May your love and support guide me throughout my life, as always.

“All religions, arts and sciences are branches of the same tree. All these aspirations are directed toward ennobling man's life, lifting it from the sphere of mere physical existence and leading the individual towards freedom.”

- Albert Einstein

Abstract

The metabolic syndrome and diabetes type II are a major public health problem throughout the world. One current class of pharmaceutical drugs is the thiazolidinediones, which are peroxisome proliferator-activated receptor (PPAR) γ agonists. However, their side-effects include weight gain, oedema and liver toxicity. New effective drugs with an improved side-effect profile are needed.

PPARs are transcription factors which control gene expression by binding to specific response elements within promoters; there are three subtypes α , γ , and δ . Both PPAR α and PPAR δ have been shown to be regulators of fatty acid β -oxidation while PPAR γ has been implicated with adipocyte differentiation, triglyceride synthesis and fatty acid β -oxidation. Given the critical physiological role of all the PPAR subtypes as lipid sensors and regulators of lipid metabolism, the aim of this project is to synthesise novel dual or pan PPAR agonists as potential drugs for the treatment of metabolic disorders.

The first part of the project consisted of the synthesis of lipid analogues in collaboration with Thia Medica AS, Norway. Tetradecylthioacetic acid (TTA), a fatty acid analogue, developed by Thia Medica AS, was found to be a potent pan PPAR agonist. Although it is presently in clinical studies, TTA suffers from poor absorption, distribution, metabolism and elimination (ADME) characteristics. I have synthesised new lipid analogues of TTA as natural prodrugs in order to improve its bioavailability. Preliminary biological analyses with the new TTA analogues have shown better results *in vitro* and *in vivo* than with TTA.

Furthermore, two novel heterocyclic scaffolds were designed as dual PPAR α/γ agonists using proprietary software by an *in silico* screening company, *Prosarix Ltd*, UK. The synthesis of the indole scaffold was carried out using a variety of solution phase chemistry. The *in vitro* PPAR activation assay showed potency on both PPAR α and PPAR δ . The synthesis of the second heterocyclic scaffold consisting of a pyrrolidine core, is also described.

Table of Contents

CHAPTER 1 <i>Introduction to PPARs and the therapeutic area</i>	21
1.1 Peroxisome proliferator-activated receptors.....	22
1.1.1 Introduction to PPARs.....	22
1.1.2 Receptor structure.....	23
1.1.3 Mechanism of action of PPARs.....	24
1.1.4 The three PPAR isoforms PPAR α , PPAR γ and PPAR δ	26
1.1.5 Natural and synthetic ligands.....	30
1.2 The Metabolic syndrome and diabetes type II.....	32
1.2.1 The metabolic syndrome.....	32
1.2.2 Insulin and its role in glucose level.....	34
1.2.3 Diabetes type II and its treatment.....	36
1.2.4 New therapeutic approaches.....	42
1.2.4.1 <i>Reducing excessive hepatic glucose production</i>	42
1.2.4.2 <i>Enhancing glucose-stimulated insulin secretion</i>	42
1.2.4.3 <i>Targeting the insulin signalling pathway</i>	44
1.2.4.4 <i>Targeting obesity, lipid metabolism and 'lipotoxicity'</i>	44
1.2.4.5 <i>Peroxisome proliferator-activated receptors (PPAR) α/γ dual agonists</i>	44
1.3 Neurological diseases.....	46
1.3.1 Alzheimer's disease (AD).....	46
1.3.1.1 <i>Etiology</i>	46
1.3.1.2 <i>Treatment of Alzheimer's disease</i>	48
1.3.2 Multiple Sclerosis (MS).....	48
1.3.2.1 <i>Etiology</i>	48
1.3.2.2 <i>Types of multiple sclerosis</i>	49
1.3.2.3 <i>Treatment of multiple sclerosis</i>	50
1.3.3 Targeting the brain: brain glucose levels and the blood brain barrier.....	51
1.3.4 Targeting AD and MS via the effects of PPAR agonists.....	54
1.3.4.1 <i>Alzheimer's disease</i>	54
1.3.4.2 <i>Multiple Sclerosis</i>	55
CHAPTER 2 <i>Project outline</i>	56
2.1 Objectives of the project.....	57
2.2 Synthesis of new lipid analogues.....	60
2.3 Design and synthesis of novel heterocycles.....	61

CHAPTER 3	<i>Synthesis of new lipid analogues of tetradecylthioacetic acid</i>	64
3.1	Tetradecylthioacetic acid	65
3.2	Synthesis of the first two analogues of TTA	67
3.2.1	Synthesis of TTA-PC 32	67
3.2.2	Synthesis of TTA-TAG 33	69
3.3	Synthesis of four new lipid analogues of TTA	73
3.3.1	Synthesis of lyso TTA-PC 34	74
3.3.2	Synthesis of TTA-PS 35	75
3.3.3	Synthesis of TTA-PG 36	77
3.3.4	Synthesis of TTA-Chol 37	80
3.3.5	Preliminary biology results with the four new analogues	81
3.3.5.1	<i>Luciferase reporter gene assay</i>	81
3.3.5.2	<i>PPAR activation assay results and discussion</i>	83
CHAPTER 4	<i>Synthesis of novel heterocyclic leads</i>	88
4.1	Identification of leads by <i>de novo</i> design	89
4.2	Synthesis of the indole scaffold	93
4.2.1	Indole scaffold: retrosynthesis and envisaged strategy	93
4.2.2	Synthesis of the indole leads: 1 st synthetic approach	95
4.2.2.2	<i>Hydrazine formation and Fischer Indole synthesis</i>	103
4.2.3	Synthesis of the indole leads: 2 nd synthetic approach	107
4.2.3.1	<i>Preliminary research on the 2nd synthetic approach</i>	110
4.2.3.2	<i>Synthesis of indole targets 38 and 39</i>	112
4.2.3.3	<i>Feasibility of convergent synthesis</i>	114
4.2.3.4	<i>Synthesis of indole leads 40 and 41</i>	123
4.2.3.5	<i>Synthesis of indole leads 42 and 43</i>	129
4.2.4	Indoles <i>in vitro</i> PPAR activation assay: results and discussions	133
4.2.4.1	<i>PPARα activation assay with the indole leads</i>	135
4.2.4.2	<i>PPARγ activation assay with the indole leads</i>	136
4.2.4.3	<i>PPARδ activation assay with the indole leads</i>	137
4.3	Work towards the pyrrolidine scaffold	139
4.3.1	Pyrrolidine scaffold: retrosynthetic analysis	139
4.3.2	Synthesis of the pyrrolidine scaffold	141
4.4	Summary	147
CHAPTER 5	<i>Conclusions and future directions</i>	149
CHAPTER 6	<i>Experimental</i>	157
6.1	General information	158

6.2 Chemistry	159
6.3 Biological methods.....	217
6.3.1 Preparation of the samples for the PPAR activation assay	217
6.3.2 Transfection procedure	218
CHAPTER 7 <i>References</i>	219
Appendices	234

List of Figures

Figure 1 Structure of PPAR receptors.....	24
Figure 2 The x-ray crystal structures of PPAR α , PPAR γ and PPAR δ ¹⁹	24
Figure 3 Binding of PPAR-RXR heterodimer to PPRE.....	26
Figure 4 Structure of GW-501516, a selective PPAR δ agonist.....	30
Figure 5 PPAR α fatty acid ligands.....	30
Figure 6 PPAR α fibrate ligands.....	31
Figure 7 PPAR γ natural ligands.....	31
Figure 8 PPAR α/γ dual agonists.....	31
Figure 9 Structure of L165.041, a PPAR δ agonist.....	32
Figure 10 The metabolic syndrome.....	32
Figure 11 Insulin's structure ⁸⁷	34
Figure 12 The pancreas and its β cells ⁸⁸	35
Figure 13 Regulation of blood glucose levels by the pancreas and the liver ⁸⁹	36
Figure 14 Structures of glimepiride and repaglinide.....	40
Figure 15 Metformin and phenformin.....	40
Figure 16 Acarbose.....	40
Figure 17 Structures of thiazolidinediones.....	41
Figure 18 Structure of LAF-237.....	43
Figure 19 Structure of GW 409544, a dual PPAR α/γ agonist.....	45
Figure 20 Amyloid plaques and neurofibrillary tangles in Alzheimer's disease (left) ¹²³	46
Figure 21 Difference between a normal brain (left) and a brain affected by AD (right) ¹²⁴	47
Figure 22 Difference between normal nerve cells (left) and those affected by MS (right) ¹²⁸	49
Figure 23 The blood brain barrier ¹³⁶	52
Figure 24 Difference between a brain capillary and a capillary found.....	53
Figure 25 Structures of different PPAR α/γ dual agonists.....	58
Figure 26 Tetradecylthioacetic acid.....	60
Figure 27 Structures of novel lipid analogues of TTA.....	61
Figure 28 Indole scaffold.....	62
Figure 29 Pyrrolidine scaffold.....	63
Figure 30 Tetradecylthioacetic acid.....	65
Figure 31 3-glycerophosphoric acid and glycerol.....	66
Figure 32 Absorption of lipids into the blood stream ^{190,191}	66

Figure 33 Structure of TTA-PC	67
Figure 34 Structure of TTA-TAG	67
Figure 35 Effects of TTA, TTA-PC and TTA-TAG on plasma lipid levels	71
Figure 36 Effects of TTA, TTA-PC and TTA-TAG on the activity of key enzymes involved in fatty acid oxidation	72
Figure 37 Structures of four novel lipid analogues	73
Figure 38 New lipid analogues: <i>lyso</i> TTA-PC, TTA-PS and TTA-PG.....	74
Figure 39 DSPC.....	74
Figure 40 ³¹ P NMR of DSPC.....	80
Figure 41 Luciferase reporter gene assay.....	83
Figure 42 Specific PPAR agonists used as positive controls.....	84
Figure 43 PPAR α , γ and δ activation results with <i>lyso</i> TTA-PC and TTA-PG	85
Figure 44 Structure of GI262570.....	90
Figure 45 Indole scaffold.....	90
Figure 46 Indole leads 38 to 43	91
Figure 47 Proposed interaction of indole 42 with PPAR γ	92
Figure 48 Retrosynthesis envisaged for the indole leads	94
Figure 49 Stabilisation of the enol form by mesomeric effects.....	97
Figure 50 Resins used for solid phase reductions	98
Figure 51 Other alternative routes for the synthesis of the ether 91	102
Figure 52 Different R groups for the 2-position of the indole	107
Figure 53 2 nd retrosynthetic analysis of the indole leads	108
Figure 54 Retrosynthesis of the different phosphonoacetates 129 and 130	109
Figure 55 C2 lithiation.....	115
Figure 56 Side-product 169 isolated in entry 2 of Table 11	121
Figure 57 1-(phenylsulfonyl)-1 <i>H</i> -indole-5-carbaldehyde.....	122
Figure 58 Indole lead 40	123
Figure 59 Structure of 2-benzyl indole 194	125
Figure 60 Crystal structure of 2-benzyl indole 194	126
Figure 61 Indole side-product 198 isolated after arylation reaction.....	130
Figure 62 BOC protected cyano indole 171	130
Figure 63 Structure of 2-naphthylmethyl indole 195	132
Figure 64 Crystal structure of 2-naphthylmethyl indole 195	132
Figure 65 Indole leads tested <i>in vitro</i>	134
Figure 66 PPAR α activation results with the six indole leads 38 to 43	135
Figure 67 PPAR γ activation with the six indole leads 38 to 43	136
Figure 68 PPAR δ activation with the six indole targets 38 to 43	137

Figure 69 PPAR activation with indole targets 40 to 43	138
Figure 70 Pyrrolidine scaffold.....	139
Figure 71 Proposed interaction of the pyrrolidine scaffold.....	139
Figure 72 Retrosynthetic analysis of the pyrrolidine scaffold.....	140
Figure 73 Proposed forward synthesis of the pyrrolidine scaffold.....	141
Figure 74 Possible side-products of the Heck reaction.....	143
Figure 75 Indole leads 38-43	148
Figure 76 First two TTA analogues synthesised.....	150
Figure 77 Structures of novel lipid analogues of TTA.....	152
Figure 78 Novel class of indoles synthesised as PPAR agonists	155
Figure 79 PPAR activation results with indoles 40 to 43	155

List of Schemes

Scheme 1 Interconversion of cortisone and cortisol as catalysed by 11 β -HSD types 1 and 2	43
Scheme 2 Coupling reaction between TTA 31 and GPC 47	67
Scheme 3 Synthesis of TTA 31	68
Scheme 4 Synthesis of TTA-PC, 70%	69
Scheme 5 Synthesis of TTA-TAG	69
Scheme 6 Mechanism of coupling reaction between TTA and glycerol	70
Scheme 7 Synthesis of lyso DSPC 58	75
Scheme 8 Synthesis of lyso TTA-PC 34	75
Scheme 9 Synthesis of DSPS 60	76
Scheme 10 Synthesis of TTA PBOC Ser 61	76
Scheme 11 Synthesis of TTA-PSerinol 64	77
Scheme 12 Synthesis of DSPG 65	77
Scheme 13 Synthesis of TTA-PE 67	78
Scheme 14 Synthesis of TTA-PG 36	78
Scheme 15 Synthesis of TTA-PG 36 in 2 steps	79
Scheme 16 Synthesis of TTA-Chol	81
Scheme 17 The reaction catalysed by the luciferase enzyme found in <i>Photinus pyralis</i>	82
Scheme 18 Proposed forward enantioselective synthesis of indoles 38-43	94
Scheme 19 Proposed route to the racemic synthesis of precursors 81 and 82	95
Scheme 20 Reduction into α -hydroxy acid 80 using NaBH ₄	96
Scheme 21 Synthesis of <i>para</i> -nitrophenyl pyruvic acid 77	96
Scheme 22 Mechanism of ozonolysis	97
Scheme 23 Synthesis of the methyl ester 90	97
Scheme 24 Reduction into the α -hydroxy ester 91	98
Scheme 25 One pot ozonolysis-reduction	99
Scheme 26 Reaction mechanism for the reduction using NaBH ₄	99
Scheme 27 Ether synthesis using silver oxide	100
Scheme 28 Conversion into methyl ester 96 , followed by the synthesis of ether 97	100
Scheme 29 Ether synthesis by opening the acetal 99 with a Grignard reagent	101
Scheme 30 Ether synthesis using sodium hydride and ethyl iodide	101
Scheme 31 Transesterification observed	102
Scheme 32 Mechanism for the Fischer Indole synthesis	103

Scheme 33 Synthesis of hydrazine 109 <i>via</i> formation of the diazonium salt.....	104
Scheme 34 Esterification of amine 96	104
Scheme 35 Fischer Indole synthesis with octanal	104
Scheme 36 Indole synthesis from phenyl hydrazine hydrochloride.....	105
Scheme 37 Fischer Indole synthesis on substituted hydrazone 119	106
Scheme 38 Regioselectivity of the cyclisation in the Fischer Indole synthesis.....	106
Scheme 39 Forward racemic synthesis for indoles 38 and 39 ($R_1 = H$)	108
Scheme 40 Proposed forward synthesis for indoles 40-43 ($R_1 \neq H$)	109
Scheme 41 Preparation of the phosphonoacetate 129	110
Scheme 42 Synthesis of 2,2,2-trifluorophosphonoacetate 130	111
Scheme 43 HWE coupling	111
Scheme 44 Mechanism of the HWE coupling	112
Scheme 45 Reduction of the double bond using magnesium	112
Scheme 46 Synthesis of indole lead 38	113
Scheme 47 Synthesis of indole lead 39	114
Scheme 48 Electrophilic substitution on an indole ring.....	114
Scheme 49 Protection of indole 113 with a benzenesulfonyl group.....	115
Scheme 50 Benzoylation on the 2-position of the indole 160 using LDA.....	116
Scheme 51 Deprotonation with LDA and quenching with MeOD	116
Scheme 52 Synthesis of benzyl iodide 164 by Finkelstein halogen exchange.....	116
Scheme 53 Benzoylation of indole 160 using <i>t</i> -BuLi.....	117
Scheme 54 Hydrolysis of benzenesulfonyl group of indole 161	117
Scheme 55 Feasibility of convergent synthesis with indole 135	118
Scheme 56 Competition between reactive sites of indole 166 under arylation conditions	119
Scheme 57 Bromination of indole 160	119
Scheme 58 Benzoylation on the bromo derivative 168	120
Scheme 59 Route chosen for the synthesis of the indole leads.....	122
Scheme 60 Benzoylation of acetal 172	124
Scheme 61 Hydrolysis of benzenesulfonyl group of indole 191	124
Scheme 62 3 rd alternate route towards indole aldehyde precursors 177 and 178 ...	124
Scheme 63 Comparison between routes A and B	127
Scheme 64 Synthesis of indole lead 40	128
Scheme 65 Synthesis of indole lead 41	129
Scheme 66 Synthesis of indole lead 42	131
Scheme 67 Synthesis of indole lead 43	133
Scheme 68 Protection of 3-pyrroline with benzyl chloroformate, followed by Heck reaction	142

Scheme 69 Protection of 3-pyrroline with methyl chloroformate, followed by Heck reaction	143
Scheme 70 Mechanism of Heck coupling.....	144
Scheme 71 Reduction of pyrroline 211 into pyrrolidine 218	144
Scheme 72 Cleavage of carbamate group of protected pyrrolidine 218	145
Scheme 73 Buchwald-Hartwig synthesis of tertiary amine 220	145
Scheme 74 Buchwald-Hartwig synthesis of tertiary amine using acetal 220	146
Scheme 75 Buchwald-Hartwig amination on the desired pyrrolidine 201	146
Scheme 76 Synthesis of the pyrrolidine target 44	147
Scheme 77 Synthesis of the pyrrolidine lead 44	148
Scheme 78 Synthesis of indole leads 38 and 39	153
Scheme 79 Route chosen for the synthesis of the last four indole leads	154
Scheme 80 Synthesis of the pyrrolidine lead 44	156

List of Tables

Table 1 The three PPAR isoforms ³⁴	27
Table 2 Current therapeutic targets for diabetes type II	38
Table 3 Advantages and disadvantages of the current therapeutic classes for diabetes type II	39
Table 4 PPAR agonist candidates in pipelines of pharmaceutical companies	45
Table 5 Indole leads 38 to 43	62
Table 6 ³¹ P NMR shifts in ppm	80
Table 7 Different experimental conditions for the synthesis of the hydrazone 117 ..	105
Table 8 Arylation attempts on indole derivative 166	119
Table 9 Bromination attempts.....	120
Table 10 Benzylation attempts on the bromo derivative 168	120
Table 11 Arylation conditions through transmetallation using Zn	121
Table 12 Different conditions for the introduction of the naphthylmethyl group	130
Table 13 Heck coupling conditions on 3-pyrroline	142

Abbreviations

AcOH	acetic acid
AD	alzheimer's disease
ADME	absorption, distribution, metabolism and elimination
AF	activation function
aq	aqueous
AgNO ₃	silver(I) nitrate
Ag ₂ O	silver(I) oxide
aP	adipocyte fatty acid binding protein
BBB	blood brain barrier
Bn	benzyl
BOC	<i>tert</i> -butoxycarbonyl
Br ₂	bromine
<i>n</i> -BuLi	<i>n</i> -butyllithium
<i>t</i> -BuLi	<i>tert</i> -butyllithium
<i>t</i> -BuMgCl	<i>tert</i> -butylmagnesium chloride
(<i>n</i> Bu) ₄ NBr	<i>tetrabutylammonium</i> bromide
<i>t</i> BuOK	potassium <i>tert</i> -butoxylate
Bz	benzene
cat.	catalytic
CDCl ₃	deuterated chloroform
CDI	<i>N,N'</i> -carbonyl-diimidazole
Chol	cholesterol (cholesr-5-en- β -ol)
CNS	central nervous system
CoA	coenzyme A
<i>conc.</i>	concentrated
d	doublet
DBD	DNA binding domain
DBU	1,8-diazabicyclo(5.4.0.)undec-1-ene
DCM	dichloromethane
DMAP	4-dimethylaminopyridine
DMF	<i>N,N</i> -dimethylformamide
DMSO	dimethylsulfoxide
DNA	deoxyribonucleic acid
DOPC	1,2-dioleoyl- <i>sn</i> -glycero-3-phosphocholine
DPP4	dipeptidylpeptidase IV
DSPC	1,2-distearoyl- <i>sn</i> -glycero-3-phosphocholine

DTT	dithiothreitol
EDCI	1-(3-dimethylaminopropyl)-3-ethylcarbodiimide
EDTA	ethylenediamine tetraacetic acid
EI	electron ionisation
eq	equivalent
EtOAc	ethyl acetate
EtOH	ethanol
FA	fatty acid
FDA	food and drug administration
FFA	free fatty acid
GIP	gastric inhibitory peptide
GLP	glucagon-like-peptide
GPC	L- α -glycerophosphocholine
H ₂	hydrogen
HBTU	O-benzotriazole- <i>N, N, N', N'</i> -tetramethyl-uronium-hexafluoro-phosphate
HDL	high-density lipoprotein
HMG-CoA	3-hydroxy-3-methylglutaryl coenzyme A
hr	hour
HRMS	high resolution mass spectrometry
H ₂ SO ₄	sulfuric acid
HWE	Horner Wadsworth Emmons
I ₂	iodine
IL	interleukin
iNOS	inducible nitric oxide synthase
IR	infra red
<i>J</i>	coupling constant
LBD	ligand binding domain
LDA	lithium diisopropylamide
LDL	low-density lipoprotein
LPL	lipoprotein lipase
m	multiplet
MeOD	deuterated methanol
MeOH	methanol
min	minutes
mmol	millimole
MS	multiple sclerosis
<i>m/z</i>	mass-to-charge ratio

NaBH ₄	sodium borohydride
NaH	sodium hydride
NaNO ₂	sodium nitrite
NaOH	sodium hydroxide
NaphBr	2-(bromomethyl)naphthalene
NaphI	2-(iodomethyl)naphthalene
NaO ^t Bu	sodium <i>tert</i> -butoxide
NMDA	<i>N</i> -methyl-D-aspartate
NMR	nuclear magnetic resonance
NO	nitric oxide
NOE	nuclear overhauser effect
O ₃	ozone
PC	phosphatidylcholine
PDH	pyruvate dehydrogenase
PDK1	phosphoinositide-dependent protein kinase-1
Pd(OAc) ₂	palladium(II) acetate
PE	phosphatidylethanolamine
PEPCK	phosphoenolpyruvate carboxykinase
PG	phosphatidylglycerol
PhSO ₂ Cl	benzenesulfonyl chloride
PI	phosphatidylinositol
PLD	phospholipase D
PPAR	peroxisome proliferator-activated receptor
PPh ₃ CHCN	(cyanomethylene)triphenylphosphorane
PPRE	peroxisome proliferator response element
PS	phosphatidylserine
PTP	protein tyrosine phosphatase
RA	retinoic acid
R _f	retention time
RT	room temperature
RXR	retinoid X receptor
s	singlet
sat.	saturated
SnCl ₂	tin(II) chloride
SOCl ₂	thionyl chloride
SU	sulfonylurea
t	triplet
TAE	tris-acetate EDTA

TFA	trifluoroacetic acid
THF	tetrahydrofuran
TLC	thin layer chromatography
TNF- α	tumour necrosis factor
<i>p</i> -TsOH	<i>para</i> -toluenesulfonic acid
TTA	tetradecylthioacetic acid
TTA-Chol	cholesterol tetradecylthioacetate
TTA-PC	<i>di</i> -tetradecylthioacetyl- <i>sn</i> -glycero-3-phosphocholine
TTA PE	<i>di</i> -tetradecylthioacetyl- <i>sn</i> -glycero-3-phosphoethanolamine
TTA-PG	<i>di</i> -tetradecylthioacetyl- <i>sn</i> -glycero-3-phosphoglycerol
TTA-PS	<i>di</i> -tetradecylthioacetyl- <i>sn</i> -glycero-3-phosphoserine
TTA-TAG	<i>tri</i> -tetradecylthioacetyl glyceride
TZD	thiazolidinedione
UV	ultraviolet
VLDL	very low-density lipoprotein
v/v	by volume
ZnCl ₂	zinc(II) chloride

CHAPTER 1

Introduction to PPARs and the therapeutic area

1.1 Peroxisome proliferator-activated receptors

1.1.1 Introduction to PPARs

Peroxisome Proliferator-Activated Receptors (PPARs) are nuclear receptors belonging to the superfamily of ligand-activated transcription factors;^{1,2,3} these include receptors for steroids, thyroid hormone, vitamin A- and D- derived hormones and some fatty acids.⁴ Structurally, they share common features. Nuclear receptors generally bind to DNA in the form of dimers, either homodimers or more often heterodimers with the receptor for 9-*cis* retinoic acid known as retinoid receptor X (RXR).⁵

The first cloning of PPARs occurred while searching for the molecular target of hepatic peroxisome proliferating agents in rodents in 1990.⁶ Peroxisome proliferators, located in the nuclei of cells, influence both the size and number of peroxisomes. Peroxisomes, so-called because of the production of hydrogen peroxide during fatty acid oxidation, contain various fatty acid oxidising enzymes such as acyl-CoA oxidase.⁷ These organelles, bounded by a single membrane, perform various metabolic functions within the cell, including peroxide-derived respiration, beta oxidation of fatty acids and cholesterol metabolism. Peroxisomes are also an intracellular site of expression for the hydrogen peroxide-destroying enzyme, catalase.

PPARs are transcription factors which play an important role during cell signalling when activated by specific ligands. There are three subtypes of PPARs: PPAR α , PPAR γ and PPAR δ . Over the past years, it has been shown that PPARs play a critical physiological role as lipid sensors and regulators of lipid metabolism and they have become an important target for the treatment of diabetes type II amongst other diseases in the pharmaceutical industry.^{8,9} Therefore, a significant understanding of the molecular and physiological characteristics of these receptors has become extremely important. Lately, many research teams have published research connecting PPARs to various medical indications such as inflammation, cancer and diseases of the central nervous system.^{10,11,12,7,13,14,15}

1.1.2 Receptor structure

The protein domain structure of PPARs is similar to that of the other members of the nuclear receptor gene family. This consists of (**Figure 1**):¹⁶

- a variable N-terminal domain which contains the ligand-independent transcriptional activation function 1 domain (AF-1);
- a highly conserved central DNA binding domain (DBD), which consists of two zinc fingers. One is responsible for specific recognition of the response element and the other is involved in dimerisation;
- a hinge region, D;
- a ligand binding domain (LBD) in the COOH- terminal region which has been shown by crystallographic studies to be composed of 13 α -helices and a small 4-stranded β -sheet (**Figure 2**). Within the LBD lies a C-terminal region which contains the ligand-dependent transcriptional activation function 2 domain (AF-2). The ligand binding pocket of PPARs, which is much larger than that of other nuclear receptors with a volume of $\sim 1300\text{\AA}^3$, is occupied to 30-40% by its ligand.^{17,18,19} The LBD contains some conserved amino acids, critical for the role of the receptor in signal transduction. However, there is also a significant sequence variation in the residues that line the ligand-binding pocket, which is reflected in the pharmacological distinction of each receptor subtype.²⁰ The main differences between the three PPAR LBDs are that the PPAR δ pocket is narrower in the region adjacent to the AF-2 helix, and that a histidine is present at the carboxylate-binding residue in PPAR γ rather than a tyrosine as in PPAR α . Most PPAR agonists share a common binding mode, in which the acidic head group of the ligand forms a network of hydrogen bonds within the ligand binding pocket. These interactions stabilise a charge clamp between AF-2 and a highly conserved lysine residue on the surface of the receptor, through which coactivator proteins are recruited to the receptor.²¹ In addition to ligand binding, the LBD is essential for receptor dimerisation; and
- a domain of unknown function F.

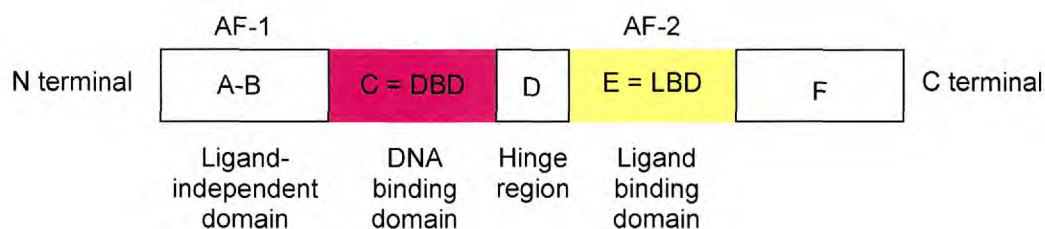
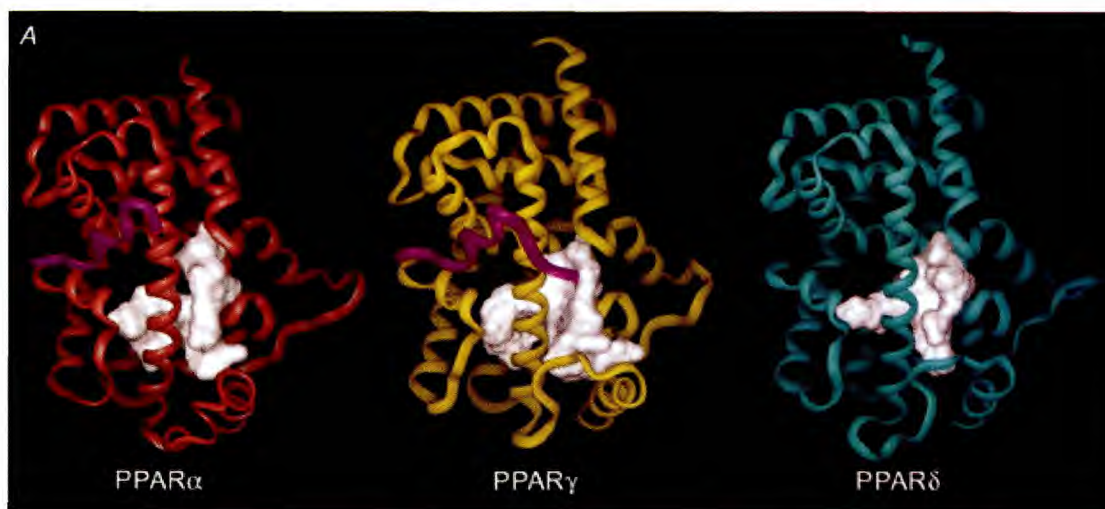


Figure 1 Structure of PPAR receptors



Representation of the PPARs' x-ray crystal structures: PPAR α (red worm), PPAR γ (yellow worm) and PPAR δ (green worm). Each PPAR is complexed to a high-affinity ligand (not shown). PPAR α and PPAR γ are complexed to the co-activator which consists of LXXLL (X = any amino acid) peptides represented by purple worms. The white surface represents the solvent-accessible ligand binding domain.

Figure 2 The x-ray crystal structures of PPAR α , PPAR γ and PPAR δ ¹⁹

1.1.3 Mechanism of action of PPARs

PPARs control gene expression by binding to specific peroxisome proliferator response elements (PPREs) within promoters.²² This results in activation or suppression of a target gene. PPREs have been identified in the regulatory regions of a large number of genes, including many that encode proteins involved in lipid metabolism and energy balance, such as aP2,²³ phosphoenolpyruvate carboxykinase (PEPCK),²⁴ acyl-CoA synthetase, and lipoprotein lipase (LPL).^{25,26} All natural PPREs consist of a direct repeat of two more-or-less conserved AGGTCA hexamers separated by a single base pair.

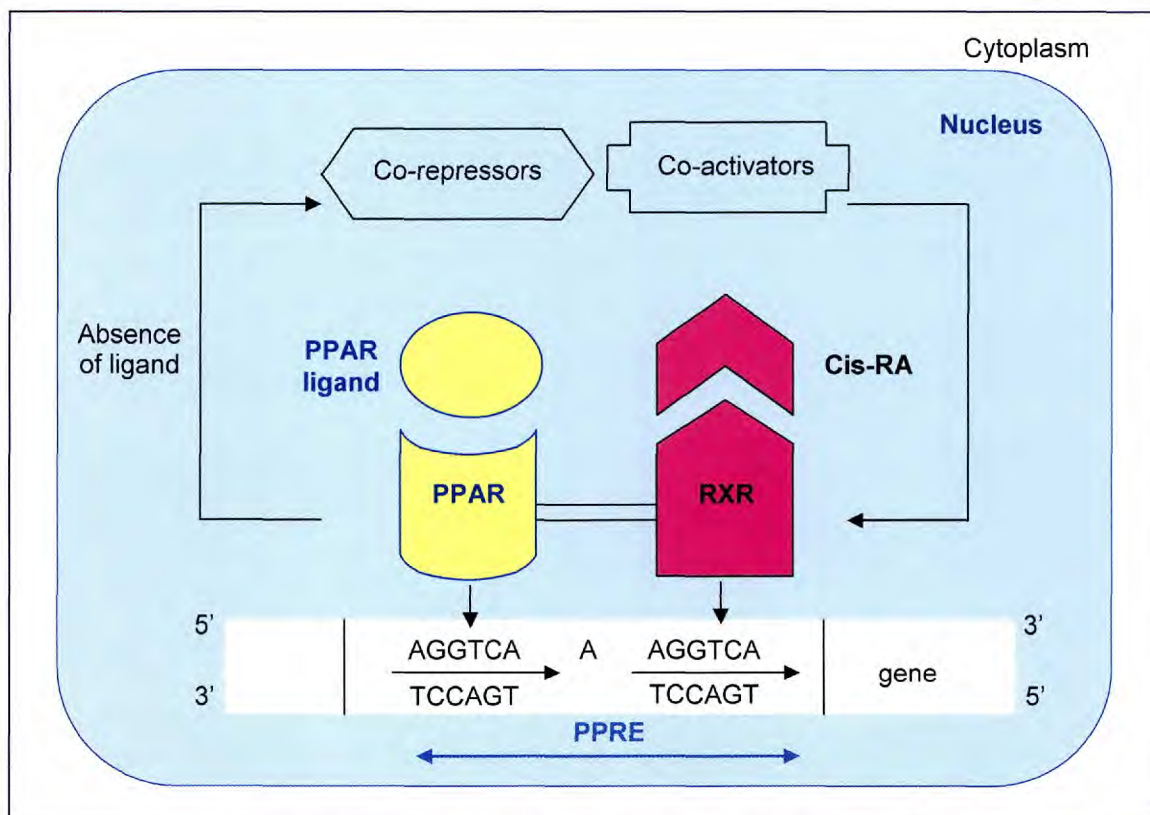
Dimerisation is essential for the function of PPARs. Before binding to the PPREs occurs, PPARs form heterodimers with the 9-*cis* retinoic acid receptor (RXR) which

stimulate gene activity.²⁷ Upon binding an agonist, the conformation of a PPAR is altered and stabilised such that a binding cleft is created and recruitment of transcriptional coactivators occurs. This results in gene transcription. A 'mouse trap' model of receptor activation has been proposed, in which the AF-2 helix closes on the ligand-binding site in response to the ligand and establishes a transcriptionally active form of the receptor.^{28,29}

The coactivators or cofactor proteins mediate the ability of nuclear receptors to initiate or suppress the transcription process.³⁰ These coactivators interact with nuclear receptors in an agonist-independent manner through a conserved LXXLL motif where X is any amino acid. One example of a coactivator of PPAR γ is 3-phosphoinositide-dependent protein kinase-1 (PDK1).³¹ The coactivators allow further contacts to be made with the PPRE, which lead to an enhancement of transcription of the target gene. Ligand binding leads to preferential recruitment of chromatin-decondensing coactivator complexes and favours dismissal of the corepressor complex.

In the absence of a PPAR ligand, the heterodimer forms high-affinity complexes with nuclear co-repressor proteins. This prevents transcription activation by sequestration of the receptor complex from the promoter. Dissociation of corepressors occurs as a consequence of a ligand-induced conformational change, and the activated heterodimer can subsequently bind to the PPRE.

Figure 3 shows the binding of the heterodimer PPAR-RXR to the corresponding PPRE.³²



Upon activation by a ligand, the PPAR receptor forms a heterodimer with the RXR receptor, itself complexed to its ligand *cis*-retinoic acid (*cis*-RA). Coactivator proteins are recruited and the PPAR-RXR heterodimer binds to the PPRE in the promoter region of specific genes. In the absence of a PPAR ligand, the heterodimer binds to corepressor proteins which block transcription.

Figure 3 Binding of PPAR-RXR heterodimer to PPRE

1.1.4 The three PPAR isoforms $PPAR\alpha$, $PPAR\gamma$ and $PPAR\delta$

Three PPAR isoforms, encoded by different genes, have been identified so far: $PPAR\alpha$, $PPAR\gamma$ and $PPAR\delta$.³³ Their main characteristics are summarised in **Table 1**.

	<i>PPARα</i>	<i>PPARγ</i>	<i>PPARδ</i>
<i>Primary sites of expression</i>	Liver, heart, kidney	Adipose tissue	Adipose tissue, skin, brain
<i>Cellular processes involved</i>	Fatty acid β -oxidation, lipoprotein synthesis, amino acid catabolism	Adipocyte differentiation, triglyceride synthesis	Fatty acid β -oxidation
<i>Physiological function</i>	Coordination of metabolic response to fasting	Differentiation of adipocytes, fatty acid trapping	Currently being investigated
<i>Key target genes</i>	Carnitine palmitoyl transferase I, HMG CoA synthase 2, apoA-I	Fatty acid-binding protein 4, lipoprotein lipase, adiponectin	Acyl-CoA oxidase
<i>Metabolic phenotype of knockout mice</i>	Fasting hypoglycaemia, hypothermia, hypoketonaemia and hepatic steatosis	-/- Lethal, -/+ more insulin sensitive at baseline	Reduced base-line adiposity; increased obesity on high-fat feeding

Table 1 The three PPAR isoforms³⁴

PPAR α

PPAR α is abundantly expressed in catabolically active tissues such as the liver, heart, kidneys, skeletal muscle and brown fat. It is also present in monocytic, vascular endothelial and vascular smooth muscle cells.

It is important in the oxidation of fatty acids in various organelles such as mitochondria, peroxisomes and microsomes. It stimulates the uptake of fatty acids and has an important role in lipoprotein metabolism. *PPAR α* has mainly been studied in the liver where it is highly expressed. In the liver, *PPAR α* 's target genes participate in many aspects of lipid catabolism, such as intracellular binding by fatty acid binding proteins, activation by the acyl-CoA synthase, as well as catabolism by β -oxidation in the peroxisomes and mitochondria, and ω -oxidation in the microsomes.³⁵ Research conducted by Wahli *et al.* has shown that *PPAR α* regulates amino acid metabolism by regulating genes that lead to a decrease in amino acid degradation.^{36,13} Oxidation of amino acids contributes largely to energy production in several organs, including the liver and gut. Finally, recent evidence also implicates *PPAR α* in the regulation of carbohydrate metabolism and in gluconeogenesis. Indeed, *PPAR α* activation has

been shown to cause triglyceride lowering.³⁷ As a result, PPAR α acts as a global regulator of energy metabolism in the liver thereby coordinating the rates of utilisation of the different energy substrates with respect to food availability.

A new interesting development is that PPAR α has been demonstrated to play an important role in the control of inflammation.^{38,39} The influence of PPAR α inhibitors on plasma cytokine levels as well as on acute-phase proteins was subsequently determined by Staels *et al.*^{40,11} Furthermore, it has been reported that PPAR α agonists reduce microglial activation.^{41,42}

PPAR γ

PPAR γ was first cloned in 1992.⁴³ It exists in two different isoforms: $\gamma 1$ is expressed in a broad range of metabolically active tissues such as skeletal muscle, kidneys and intestine and predominantly in adipose tissue while $\gamma 2$ is exclusively expressed in adipose tissue. PPAR $\gamma 2$ has 30 additional amino acids, encoded by a single exon, at its N-terminus.^{44,45} This confers a 5- to 6-fold increase in transcription-stimulating activity of the ligand-independent activating function AF-1.²³

PPAR γ has a significant role in fat cell differentiation as it controls the expression of genes encoding proteins involved in lipid metabolism and fat-derived hormones. It promotes fatty acid storage in fat depots through fatty acid transport protein¹ and regulates the expression of adipocyte-secreted hormones that impact on glucose homeostasis.^{46,47,48} PPAR γ enhances lipoprotein triglyceride hydrolysis by endothelial lipoprotein lipase (LPL) and modifies triglycerides synthesis starting with free fatty acids' esterification by acyl CoA synthase. PPAR γ stimulates the binding and activation of fatty acids in the cytosol, events that are required for the synthesis of triglycerides. Direct target genes of PPAR γ in lipid metabolism include those that code for the adipocyte fatty acid binding protein aP2,²³ lipoprotein lipase,²⁵ acyl-CoA synthase³⁵ and fatty acid transport protein.⁴⁹ Moreover, PPAR γ regulates genes that control cellular energy homeostasis.¹

One particular gene to which PPAR γ has been associated is tumour necrosis factor TNF- α , a pro-inflammatory cytokine that is expressed by adipocytes. This gene has been linked to insulin resistance and diminished insulin signal transduction. The inhibitory effects of PPAR γ on TNF- α action have led research groups to investigate the anti-inflammatory properties of PPAR γ agonists. PPAR γ agonists were shown to

inhibit TNF- α and interleukins expression in monocytes,⁵⁰ as well as inducible nitric oxide synthase (iNOS) in macrophages.^{51,52} Some recent studies have shown anti-proliferative and pre-apoptotic effects of PPAR γ ligands on T cells, whose activation has been shown to be crucial for the initiation and clinical progression of demyelinating diseases, such as multiple sclerosis.^{53,54} Moreover, activation of PPAR γ exerts anti-inflammatory effects in brain glial cells and neurons, with decreased expression of pro-inflammatory cytokines.^{55,56}

PPAR δ

PPAR δ , also first cloned in 1992, is expressed in a wide range of tissues and cells, with relatively higher levels of expression in the brain, adipose and skin.⁴³

It is involved in the regulation of lipid metabolism and cholesterol efflux.^{13,57} There are three major types of blood cholesterol combined with protein: high-density lipoprotein (HDL) cholesterol, low-density lipoprotein (LDL) cholesterol and very low-density lipoprotein (VLDL) cholesterol. Each type contains a specific combination of cholesterol, protein and triglyceride and a blood fat. HDL, known as “good” cholesterol, consists of very small amounts of cholesterol and triglycerides, coated with an especial protein that distinguishes it from VLDL. It plays a protective role through the process of reverse cholesterol transport whereby cholesterol is removed from peripheral cells, including macrophage-derived foam cells, and returned to the liver.⁵⁸ Small dense LDL particles are prone to accumulate in the arterial wall leading to the formation of atherosclerotic cholesterol-laden foam cells.⁵⁹ VLDL cholesterol contains the highest amount of triglyceride and is considered as “bad” cholesterol, like LDL. Elevated levels of VLDL lead to an increased risk of coronary artery disease. Agents that raise the levels of HDL through reverse cholesterol transport could be potential drugs for the prevention of atherosclerotic cardiovascular disease. Oliver *et al.* reported that the potent and selective PPAR δ agonist GW-501516 **1** (**Figure 3**) could induce a substantial increase in HDL-cholesterol levels as well as a reduction in triglyceride levels in obese Rhesus monkeys.⁶⁰

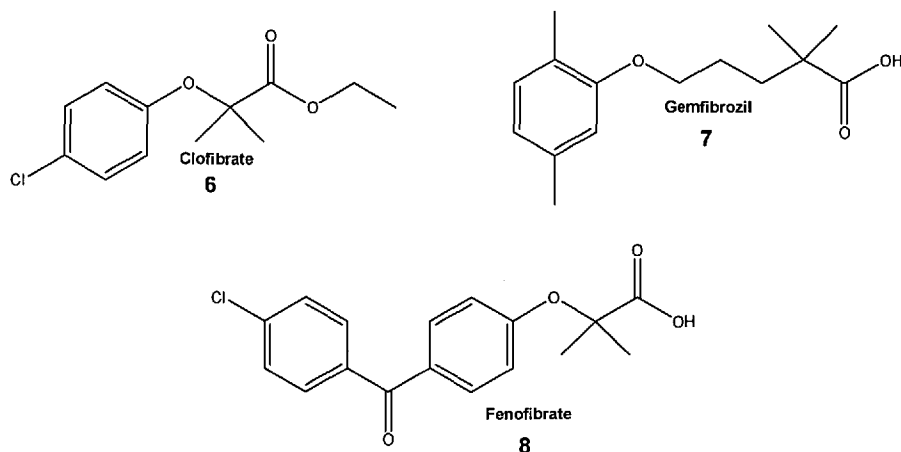


Figure 6 PPAR α fibrate ligands

Various fatty acids such as linoleic acid, linolenic acid **9**, arachidonic acid and eicosapentaenoic acid **10** and eicosanoid derivatives bind and activate PPAR γ at micromolar concentrations (Figure 7).⁶⁹ An example of synthetic ligands are the thiazolidinediones which are a class of anti-diabetic agents.⁷⁰

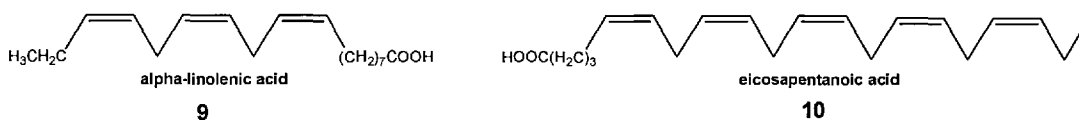


Figure 7 PPAR γ natural ligands

Some non-steroidal anti-inflammatory drugs (NSAIDs) such as indomethacin **11**, fenopfen **12** and ibuprofen **13** are dual PPAR α/γ agonists (Figure 8).^{71,9}

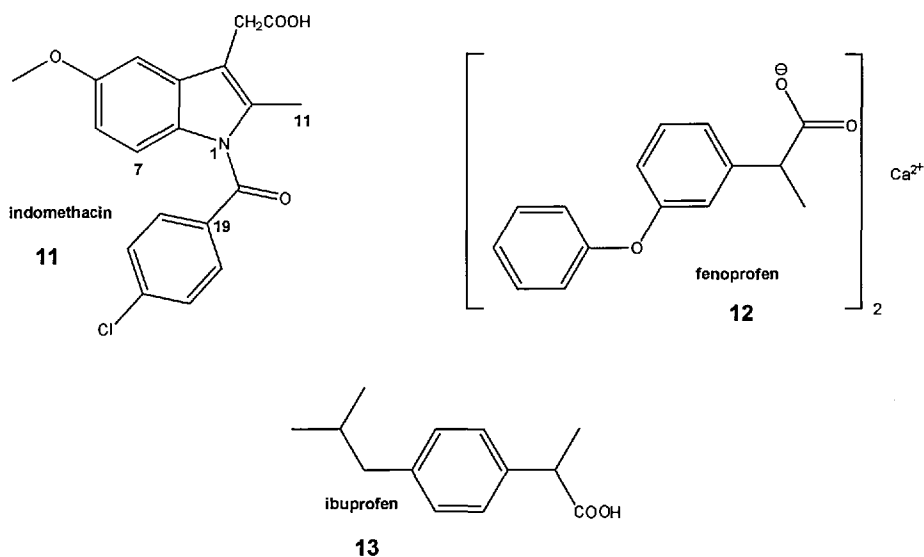


Figure 8 PPAR α/γ dual agonists

PPAR δ also binds to saturated and unsaturated fatty acids such as dihomo- δ -linolenic acid, eicosapentaenoic acid, arachidonic acid, palmitic acid and to some eicosanoids.⁷² Some synthetic ligands include L165.041 **14** (Figure 9) and GW-501516 **1** (Figure 4).^{73,60}

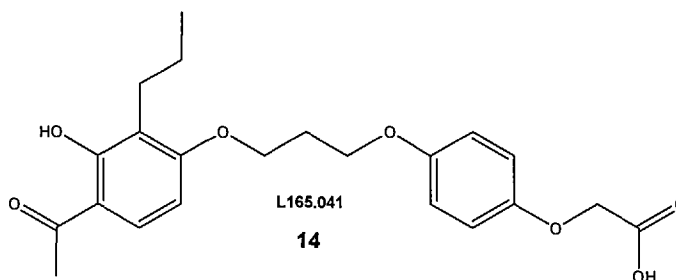


Figure 9 Structure of L165.041, a PPAR δ agonist

Given the implication of PPARs in lipid and carbohydrate metabolism, PPAR agonists could be potential drugs for the treatment of the metabolic syndrome and diabetes type II. On the other hand, PPAR agonists could also be used in the treatment of neurological inflammatory diseases such as Alzheimer's disease and multiple sclerosis since they have anti-proliferative and anti-inflammatory effects in brain glial cells, T-cells and macrophages.^{14,74,75}

1.2 The Metabolic syndrome and diabetes type II

1.2.1 The metabolic syndrome

The metabolic syndrome is a complex set of disorders that significantly increases the risk of heart disease (Figure 10).^{76,77} The clustering of the atherosclerotic risk factors that identify the metabolic syndrome was first recognised in 1983.⁷⁸ It was in 1988 that Professor Gerald Reaven named this cluster of disorders syndrome X, now termed as the *metabolic syndrome* by the World Health Organisation.^{79,80}

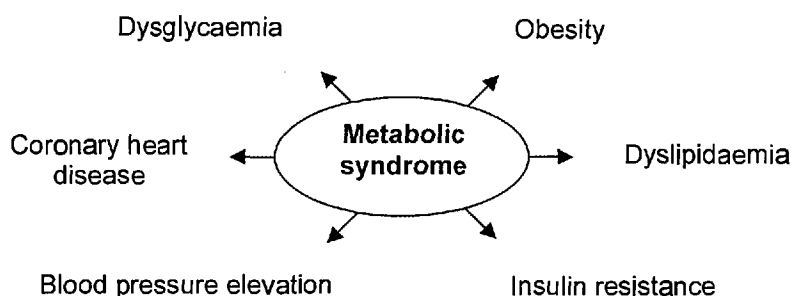


Figure 10 The metabolic syndrome

Features of the metabolic syndrome⁸¹

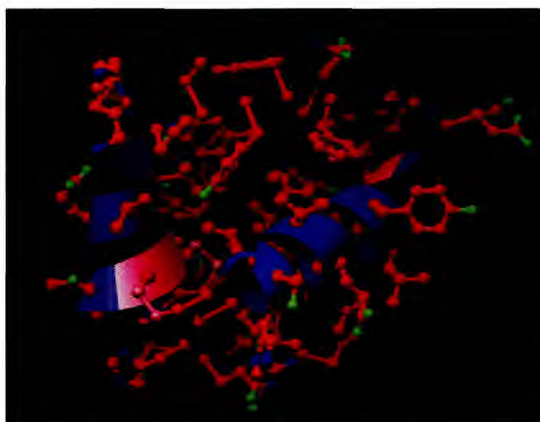
Blood pressure elevation is an arterial disease which consists of chronic high blood pressure. It is a risk factor for stroke and heart disease. Coronary heart disease occurs as a result of fat build up in the coronary arteries. Dysglycaemia is characterised by an abnormal blood glucose level, without defining a threshold whereas dyslipidaemia is characterised by high levels of triglycerides and low levels of high-density lipoproteins in the blood, leading to build-up of plaque in blood vessel walls. Excess abdominal obesity is associated with a potentially atherogenic lipoprotein profile: increased proportion of small, dense LDL particles and reduced HDL cholesterol concentrations.⁸²

Insulin sensitivity is defined as the ability of insulin to lower blood glucose concentrations. This reduction is achieved by stimulating glucose uptake of muscle and adipose tissues (the two primary tissues affected by insulin resistance) and by suppressing hepatic glucose production. A central cause of the metabolic syndrome is insulin resistance, a condition of low insulin sensitivity.⁸³ Therefore, patients suffering from the metabolic syndrome have an excess of glucose in the blood. Due to the compensatory hyperinsulinemia caused by insulin resistance, the sympathetic nervous system is stimulated, causing vasoconstriction, increased cardiac input and renal absorption of sodium, which in turn leads to elevated blood pressure. Several components of the metabolic syndrome have proatherogenic properties and have an adverse effect on the vascular endothelium, producing endothelial dysfunction. The latter is an underlying and inciting process that propagates atherosclerosis because of the following combined effects of elevated concentration of free fatty acid circulation and all the effects associated with insulin resistance.

The metabolic syndrome affects a quarter of the world's adults. People with the metabolic syndrome are twice as likely to die, and three times as likely to have a heart attack or stroke compared to people without the syndrome.⁸⁴ Moreover, people with the metabolic syndrome have a five fold greater risk of developing diabetes type II.⁸⁵ The number of deaths from the metabolic syndrome and diabetes is a lot higher than from AIDS, yet the problem is being recognised very slowly.⁸⁶

1.2.2 Insulin and its role in glucose level

Insulin is a polypeptide hormone (6000 Daltons), of empirical formula $C_{257}H_{383}N_{65}O_{77}S_6$, that consists of two peptide chains A (21 amino acids) and B (30 amino acids), linked together by two disulfide bonds. There is an additional disulfide in the A chain. **Figure 11** shows the structure of this protein.



Red: carbon, green: oxygen; blue: nitrogen; pink: sulfur. The blue/purple ribbons denote the skeleton $[-N-C-C-]_n$ in the protein's amino acid sequence $H-[NH-CHR-CO-]_n-OH$.

Figure 11 Insulin's structure⁸⁷

Insulin is produced in the islets of Langerhans in the pancreas (**Figure 12**). In healthy individuals, the β -cells secrete small amounts of insulin every 8-10 minutes in a continuous pulsatile, oscillating pattern, without regard to food. The human pancreas has two main functions: the production of pancreatic endocrine hormones (e.g. insulin and glucagon), which help regulate many aspects of our metabolism, and the production of pancreatic digestive enzymes.

Insulin facilitates the entry of glucose into muscle, adipose tissue and several other tissues. It also stimulates the liver to store glucose in the form of glycogen. In lipid metabolism, insulin promotes the synthesis of fatty acids in the liver and inhibits the breakdown of fat in adipose tissue. In each case, insulin triggers these effects by binding to the insulin receptor.

Glucagon secretion is stimulated by low, and inhibited by high, concentrations of glucose and fatty acids in blood plasma. Glucagon counterbalances the action of insulin, increasing the levels of blood glucose and stimulating protein breakdown in muscle. It is a major catabolic hormone which acts primarily on the liver to stimulate glycogenolysis (glycogen breakdown) and gluconeogenesis (synthesis of glucose

from non-carbohydrate sources), and inhibiting glycogenesis (glycogen synthesis) and glycolysis, increasing hepatic glucose output and ketone body formation.

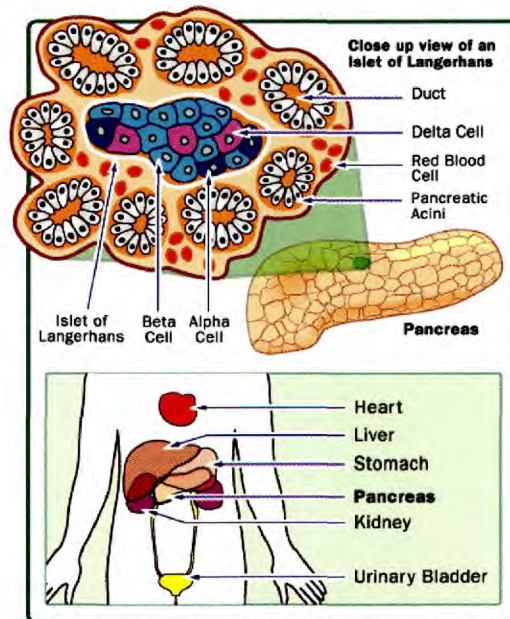


Figure 12 The pancreas and its β -cells⁸⁸

The liver is a central fat metabolising organ that controls the levels of fats, amino acids and glucose in the blood. It coordinates the synthesis of free fatty acids, esterification of triacylglycerols (TAG) and their packaging into dense VLDL after ingestion of food. Upon absorption of excess cholesterol from tissues, HDL in the circulation becomes mature and returns to the liver. The liver recognises its lipoprotein coat and directs the cholesterol to the liver pool. HDL is capable of helping us maintain a good balance of cholesterol delivery and removal. The liver and the pancreas together regulate blood glucose levels in the body (**Figure 13**).⁸⁹

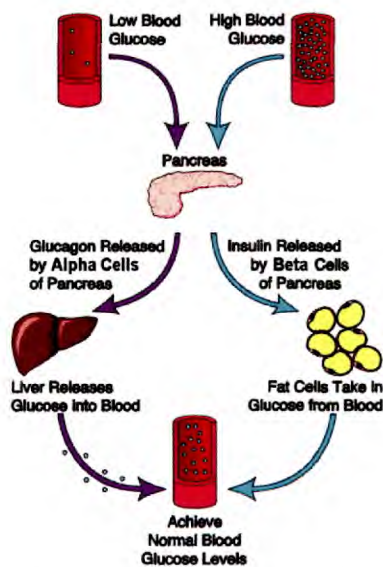


Figure 13 Regulation of blood glucose levels by the pancreas and the liver⁸⁹

1.2.3 Diabetes type II and its treatment

Diabetes is a major health problem throughout the world. It is defined as a group of metabolic diseases, characterised by hyperglycaemia (elevation of blood glucose), arising as a consequence of a relative or absolute deficiency of insulin secretion, resistance to insulin action or both.⁹⁰ Hyperglycaemia desensitises β -cells and reduces insulin secretion. Also, it directly increases insulin resistance in muscle tissue. The causes of diabetes can be genetic but obesity, a sedentary lifestyle and aging also contribute to its onset. The number of people with diabetes is expected to increase alarmingly in the coming decades. According to the World Health Organisation, the global figure of people with diabetes is expected to rise from the current figure of 194 million to 366 million in 2030. There are two types of diabetes:

Type I

It is characterised by a deficiency of insulin, usually due to an immune-mediated destruction of the insulin secreting cells, the pancreatic islet β -cells. Therefore, there is the need to replace insulin.

Type II

It is the more common type as it accounts for about 90-95% of all the cases of diabetes. Diabetes type II is usually due to resistance to insulin action by inappropriate response of the target tissues and to pancreatic β -cell impairment.⁹¹ Both factors have important roles to play in the onset of diabetes type II.^{92,93} Diabetes type II arises in people who have a defect in insulin secretory capacity; thus

pancreatic insulin secretion fails to compensate for the insulin resistance. Patients suffering from diabetes type II have an increased pancreatic α -cell mass, an exaggerated response of glucagon to amino acids and an impaired suppression of glucagons secretion by hyperglycaemia. An important morphological feature is the amyloid deposition in the islets of the pancreas.

Diabetes type II is a serious chronic disease that leads to the development of microvascular complications including retinopathy, neuropathy and nephropathy as well as macrovascular complications such as heart disease, stroke and peripheral vascular disease. As a consequence of these complications, it is a major cause of blindness, kidney failure, amputation and cardiovascular disease. It is estimated that 200 million people will suffer from diabetes type II worldwide by the year 2010.⁹⁴ About 47 million people are affected by the metabolic syndrome in the United States today and more and more people in the developing world are being diagnosed everyday. Given these important figures, there is an urgent need to cure this metabolic disease.

Current treatments for diabetes type II act by different mechanisms to attempt to regulate blood glucose levels and prevent the complications that affect the kidneys, cardiovascular, ophthalmic and nervous systems. **Table 2** below shows the different classes of drugs and their targets while **Table 3** compares the advantages and disadvantages of the different classes of drugs. These treatments include:^{95,96,97}

- diet and exercise;
- insulin;

Insulin was the first used therapeutic agent, however it is not suitable for most type II patients as it is not effective if the degree of insulin resistance is high.

- 1st generation drug therapies: sulfonylureas (SUs), meglitinides, biguanides, acarbose and thiazolidinediones (TZDs).

Drug class	Molecular target	Site of action	FDA administration status	Effect
<i>Insulin</i>	Insulin receptor	Liver, muscle, fat	Combination with SUs, metformin, TZDs	Suppresses glucose production Augments glucose utilisation
<i>Sulfonylureas (SUs)</i>	SU receptor/K ⁺ ATP channel	Pancreatic β -cell	Monotherapy or combination with insulin, metformin, acarbose, TZDs	Stimulate the pancreas to produce more insulin
<i>Meglitinides</i>	K ⁺ channel	Pancreatic β -cell	Monotherapy or combination with metformin, TZDs	Stimulate the pancreas to produce more insulin
<i>Biguanides-metformin</i>	Unknown	Liver (muscle)	Monotherapy or combination with insulin, SUs, TZDs	Suppress glucose production by the liver Increase the responsiveness of tissues to insulin (not proven)
<i>Acarbose</i>	α -Glucosidase	Intestine	Monotherapy or combination with SUs	α -Glucosidase inhibitor which interferes with gut glucose absorption
<i>Thiazolidinediones (TZDs) and glitazones</i>	PPAR γ	Fat, muscle, liver	Monotherapy or combination with insulin (pioglitazone only), SUs, metformin	New class of compounds that enhance insulin activity in peripheral tissues, such as liver, fat cells and skeletal muscle

Table 2 Current therapeutic targets for diabetes type II

Drug Class	Advantages	Disadvantages
<i>Insulin</i>	Endogenous hormone	Hypoglycaemia Weight gain
<i>Sulfonylureas</i>	Well established Improve fasting and postprandial glucose Decrease microvascular risk Convenient once-daily dosing	Hypoglycaemia Weight gain Associated with increased cardiovascular complications Adverse drug-drug interactions Diminished effectiveness over time
<i>Meglitinides</i>	Quick onset and short duration of action	Hypoglycaemia Weight gain
<i>Biguanides- metformin</i>	Well established Weight loss No hypoglycaemia Decrease micro- and macro-vascular risk Nonglycemic benefits (decreased lipid levels and hyperinsulinemia) Convenient once- or twice-daily dosing	Gastrointestinal side-effects Lactic acidosis Contraindicated in > 50% of patients with type II diabetes including the elderly and those with kidney, liver and respiratory problems
<i>Acarbose</i>	Targets postprandial glycaemia No hypoglycaemia Nonsystemic	Gastrointestinal disturbances More complex dosing schedule No long-term data
<i>Thiazolidine- diones and glitazones</i>	Decreased hepatic glucose output No hypoglycaemia Improve insulin sensitivity Nonglycemic effects (decreased triglycerides levels and hyperinsulinemia, increased fibrinolysis and improved endothelial function) Increase adiponectin levels Possible β -cell preservation Convenient once- or twice-daily dosing	Weight gain Oedema Anaemia Possible liver dysfunction Slow onset of action No long-term data May be associated with colon tumours Adverse drug-drug interactions

Table 3 Advantages and disadvantages of the current therapeutic classes for diabetes type II

The sulfonylureas (SUs) were introduced in the 1950's and are still in use today, due in part to the advent of combination therapy, a new approach which involves an enhanced treatment through the use of two or more drugs for complex diseases. The major side-effects of SUs include hypoglycaemia and lack of efficacy in 10-20% patients. A small amount of the SU market loss was to repaglinide **16** (**Figure 13**) which belongs to the meglitinide class of drugs.

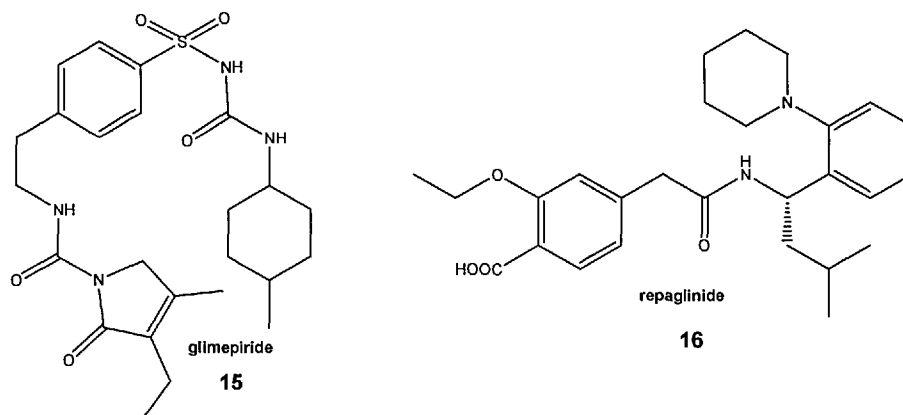


Figure 14 Structures of glimepiride and repaglinide

Introduced in the late 1950's, the biguanide, metformin **17** (**Figure 14**) has maintained its strong footing in the market and remains the only biguanide in clinical use. It is particularly appropriate for use in obese patients because it does not cause weight gain. Phenformin **18** (**Figure 15**) was removed from the market in 1977 due to fatalities caused by lactic acidosis.^{98,99,100}

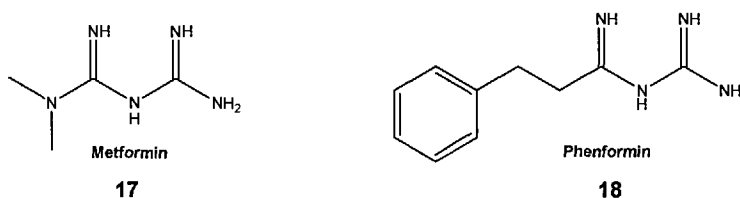


Figure 15 Metformin and phenformin

In contrast, the α -glucosidase inhibitor, acarbose **19** (**Figure 16**) which was introduced in the early 1990's, has been commercially less successful. This is largely attributed to the drug's adverse side effect profile which includes gastrointestinal side effects and hypoglycaemia when used in combination therapy.

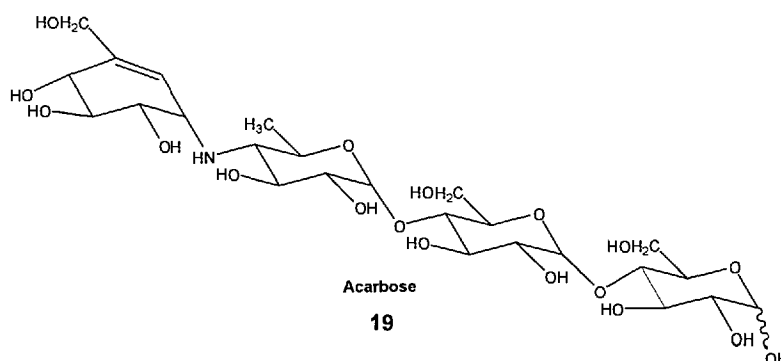


Figure 16 Acarbose

The major new medicines in the oral antihyperglycaemic market are the new thiazolidinediones, or glitazones which are selective PPAR γ agonists (**Figure 17**). Both rosiglitazone **20** (GlaxoSmith-Kline's Avandia) and pioglitazone **21** (Takeda/Lilly's Actos) were marketed in 1999.^{101,70}

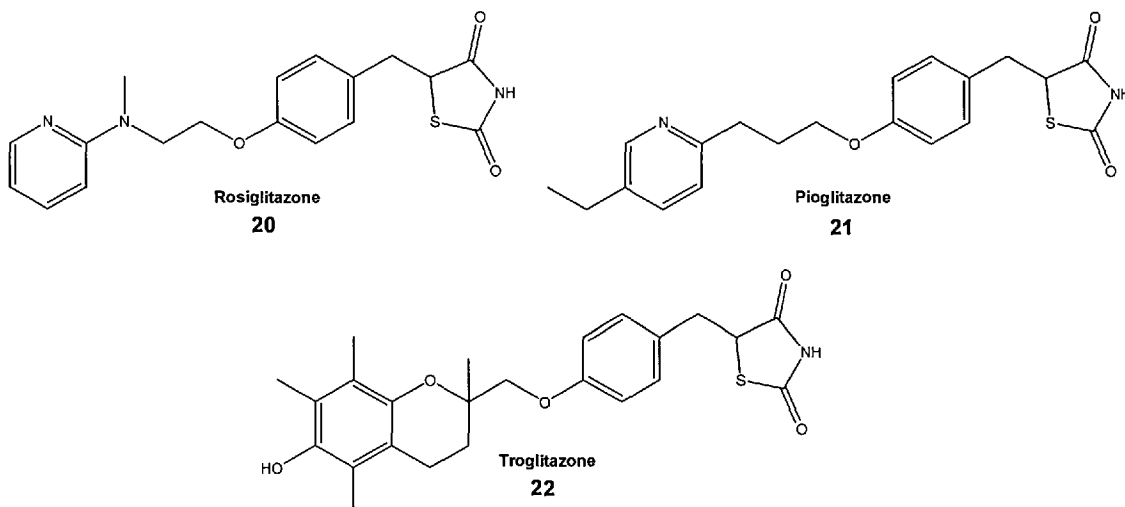


Figure 17 Structures of thiazolidinediones

Thiazolidinediones (TZDs) appear to be the only oral anti-diabetic drugs that normalise pro-insulin levels, suggesting a reduction in pancreatic workload and preservation of β -cell function.^{102,103} Rosiglitazone **20**, the most commonly used TZD, decreases the fasting and postprandial glucose concentrations, C peptide, insulin and non-esterified fatty acids in patients with diabetes type II.¹⁰⁴ However, the hepatic toxicity effects seen with the earlier compound, troglitazone **22**, have caused some doubts about the safety of this class of drugs. Indeed, this compound was removed from the market after three years by its manufacturer, Warner-Lambert, due to liver toxicity side-effects. The main side-effects encountered with the TZDs include oedema, hemodilution and weight gain.^{105,106} Recently, there has been some concern about the safety of rosiglitazone in patients suffering from heart failure.^{107,108} Current data suggests that only patients with severe cardiovascular problems have to be cautious when taking the drug.¹⁰⁹

A new drug called Avandaryl, which combines two other diabetes drugs, Avandia and Amaryl, has reached the market in February 2006. This drug, marketed by GlaxoSmithKline, is the first fixed-dose tablet combining these two different classes of diabetes medications. Specifically, Avandia (rosiglitazone **20**) is a PPAR γ agonist while Amaryl (glimepiride **15**) is a sulfonylurea that lowers blood glucose.

1.2.4 New therapeutic approaches

Considering the adverse effects of these treatments shown in **Table 3**, newer approaches that preserve normal endocrine responses to food intake are needed. The understanding of biochemical pathways related to the development of diabetes and the metabolic syndrome has expanded and the following new therapeutic approaches are now being considered.^{110,96}

1.2.4.1 Reducing excessive hepatic glucose production

The liver has a critical role in regulating endogenous glucose production from *de novo* synthesis (gluconeogenesis) or the catabolism of glycogen.¹¹¹ There are several drug targets in the liver that can offer ways of reducing hepatic glucose production.⁹⁶ Glucagon is a hormone that contributes to hyperglycaemia through the induction of both gluconeogenic and glycogenolytic pathways. The glucagon receptor is one target for the development of small-molecule antagonists. Enzymes that regulate rate-controlling steps in the gluconeogenic and glycogenolytic pathways are other potential targets. Increasing the activity of pyruvate dehydrogenase (PDH) by inhibiting the PDH kinase is expected to decrease blood glucose by increasing the glucose oxidation in peripheral tissues and by decreasing the supply of the gluconeogenic precursors, lactate and alanine to the liver. The potential liabilities to this approach include hypoglycaemia, accumulation of hepatic triglycerides and increased plasma lactate levels.

1.2.4.2 Enhancing glucose-stimulated insulin secretion

Researchers have been able to reduce insulin secretion in a glucose-dependent way by targeting two peptide hormones: glucagon-like-peptide (GLP-1) and gastric inhibitory peptide (GIP).^{112,113} Administration of these two hormones can induce insulin secretion. GLP-1 stimulates the release of insulin from pancreatic β -cells as long as blood glucose levels are high. One promising GLP-1 analogue, approved in 2005, is Exenatide. However, both GLP-1 and GIP are subject to rapid amino-terminal degradation by dipeptidylpeptidase IV (DPP4). DPP4 inhibitors can thus represent an indirect therapeutic approach to stabilising endogenous GLP-1.¹¹⁴ GLP-1 analogues and DPP4 inhibitors have the potential to overcome the hypoglycaemia, weight gain and other failures associated with the sulfonylureas. DPP4 inhibitors are expected to compete with oral drugs such as sulfonylureas and metformin. They could be recommended for early stage or prediabetes to help manage

hyperglycaemia. Sitagliptin, commercialised by Merck, was put on the market in 2006. LAF-237 **23**, vildagliptin, is in clinical trials at the moment and may be marketed by Novartis in 2007 (**Figure 18**). The main drawback to GLP-1 therapy is nausea due to delayed gastric emptying. One important risk with DPP4 is that it is not a one-substrate enzyme and it clips off the end of many proteins that have an alanine or proline at the 2-position.¹¹⁵

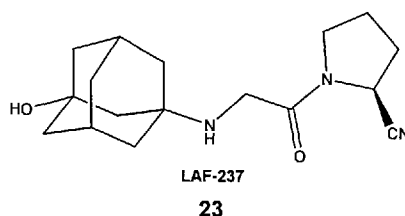
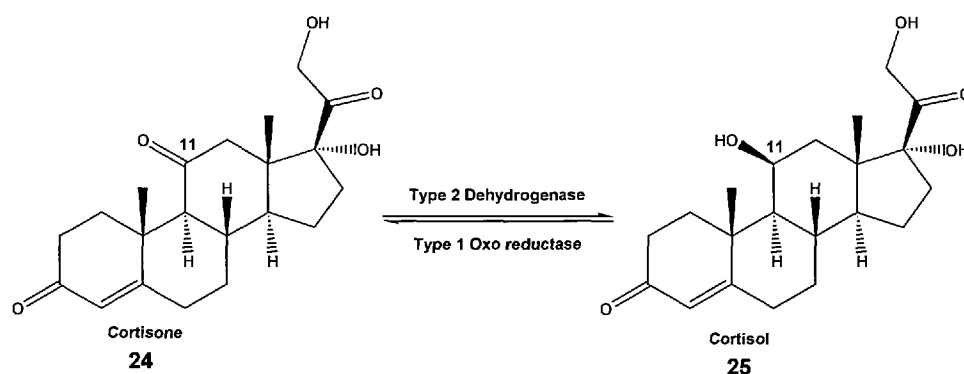


Figure 18 Structure of LAF-237

Another target is cortisol, an important glucocorticoid. This primary stress hormone is secreted by the adrenal glands when blood levels of amino acids, carbohydrates or fats fall below normal, or when there is inflammation from infection, injury, allergens or toxins. It is essential for life and regulates and supports a variety of important cardiovascular, metabolic, immunologic, and homeostatic functions. One of the ways cortisol functions is by stimulating gluconeogenesis in the liver: the conversion of fat and protein into intermediate metabolites that are ultimately converted into glucose. However, elevated levels of cortisol can disrupt blood sugar regulation. 11β -hydroxysteroid dehydrogenase type 1 activates inactive cortisone **24** to cortisol **25** as illustrated in **Scheme 1**. Research into 11β -HSD1 inhibitors is now being investigated to uncover novel therapeutic options for the metabolic syndrome.^{116,117}



Scheme 1 Interconversion of cortisone and cortisol as catalysed by 11β -HSD types 1 and 2

Analogues of amylin, a β -cell hormone, are also being investigated. Amylin plays a complementary role to insulin by regulating the rate of glucose in the circulation

during the postprandial period. Its levels are low in people suffering from both diabetes types. Pramlintide was the first amylin analogue approved in 2005.¹¹⁸

1.2.4.3 Targeting the insulin signalling pathway

Insulin resistance can be caused by multiple defects in signal transduction such as impaired activation of insulin receptor-tyrosine kinase. Molecular targets that can enhance insulin-mediated signal transduction are now being investigated. An alternative approach to targeting the insulin receptor is to inhibit enzymes responsible for deactivation of the receptor or downstream targets in the signalling pathway. Protein tyrosine phosphatase 1B (PTP-1B) is an intracellular enzyme specifically implicated in the negative regulation of insulin signalling.¹¹⁹

1.2.4.4 Targeting obesity, lipid metabolism and 'lipotoxicity'

Approaches to attenuate appetite and/or enhance energy expenditure will benefit the prevention and treatment of diabetes type II. One example is adiponectin, a protein that has recently been shown to produce beneficial metabolic effects in mice, including the ability to reduce glucose, triglycerides and free fatty acids. Another potential hormone could be leptin which can improve insulin resistance. Thus mimetic compounds could be envisaged as new therapeutic approaches.

1.2.4.5 Peroxisome proliferator-activated receptors (PPAR) α/γ dual agonists

PPARs are a very promising area of research as they present multiple targets.^{96,120} Thiazolidinediones (TZDs) previously discussed are selective PPAR γ activators. Given the importance of controlling both glucose and lipid levels in diabetes type II, it would be interesting to develop ligands that bind and activate both PPAR α and PPAR γ . The dual agonism should produce additive and hopefully synergistic results.^{121,105} One such dual agonist, GW 409544 **25 (Figure 19)**, currently in clinical trials, has indeed been shown to induce lowered serum insulin, triglycerides and non-high density lipoprotein cholesterol.¹⁹ "Pan-agonists" (molecules that activate the three PPAR subtypes) could even be better in the treatment of diabetes. As described earlier, all three PPAR subtypes have important roles in the regulation of lipid and glucose metabolism. Activation of the three isoforms could potentially lead to increased positive effects though the targeting of multiple genes in complicated diseases such as the metabolic syndrome and diabetes type II. **Table 4** shows how much PPAR agonists have attracted researchers in drug discovery. All the major

pharmaceutical companies have at least one PPAR agonist in their pipeline. The challenge lies in finding the PPAR agonists leading to the optimal activation of PPAR α , PPAR γ and PPAR δ such that they are potent compounds for treating metabolic diseases and they balance the possible toxicity seen with some of the selective PPAR γ agonists.

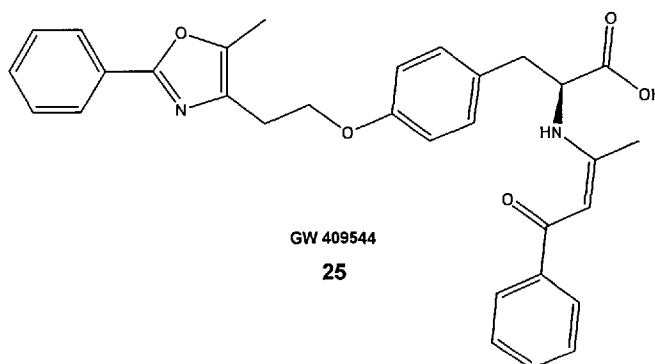


Figure 19 Structure of GW 409544, a dual PPAR α/γ agonist

Company	Drug	Development status	Activity on PPARs	Indication targeted
Sanofi-Aventis	AVE-0847	Phase 2a	α/γ agonist	Diabetes type II
AstraZeneca	AZD 6610	Phase 2	α/γ agonist	Metabolic disorder
Roche	R1439	Phase 2	α/γ agonist	Diabetes type II
Wyeth/Plexikon	PLX204	Phase 1	pan agonist	Metabolic disorder
Bristol-Myers Squibb Co	Muraglitazar	Late stage clinical trials	α/γ agonist	Metabolic disorder
Eli Lilly & Co	LY-465608	Phase 2	pan agonist	Diabetes type II
GlaxoSmithKline	GW-2433	Research tool	α/δ agonist	Hyperlipidaemia
GlaxoSmithKline	GSK-677954	Phase 2	pan agonist	Obesity, diabetes type II
Novartis	LBM-642	Phase 1	α/γ agonist	Obesity, lipid metabolism and diabetes type II

Table 4 PPAR agonist candidates in pipelines of pharmaceutical companies

1.3 Neurological diseases

1.3.1 Alzheimer's disease (AD)

1.3.1.1 Etiology

Alzheimer's disease is a progressive neurodegenerative disorder which leads to irreversible brain damage.^{14,122} During the course of the disease, "plaques" and "tangles" are developed in the brain and these lead to the death of brain cells (**Figure 20**).¹²³ The plaques are due to the accumulation of beta amyloid in the brain while the neurofibrillary tangles consist of mainly the tau protein. This results in shrinkage of the brain cortex and enlargement of the ventricles (**Figure 21**).¹²⁴

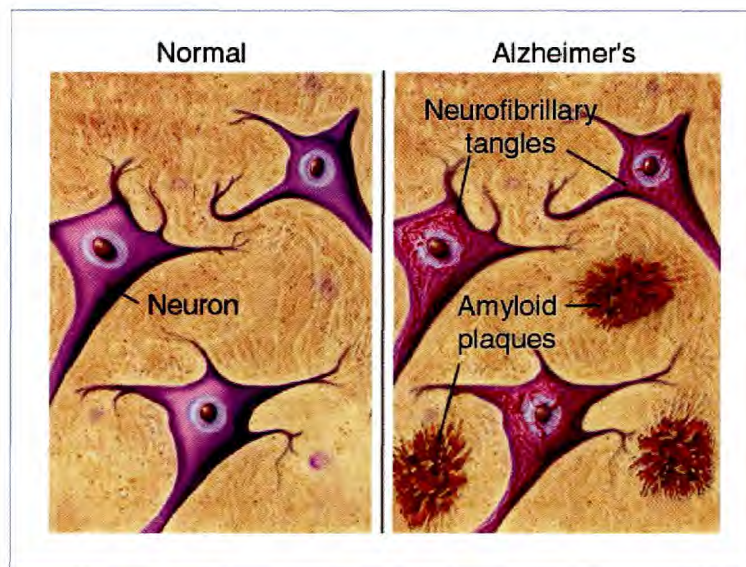


Figure 20 Amyloid plaques and neurofibrillary tangles in Alzheimer's disease (left)¹²³

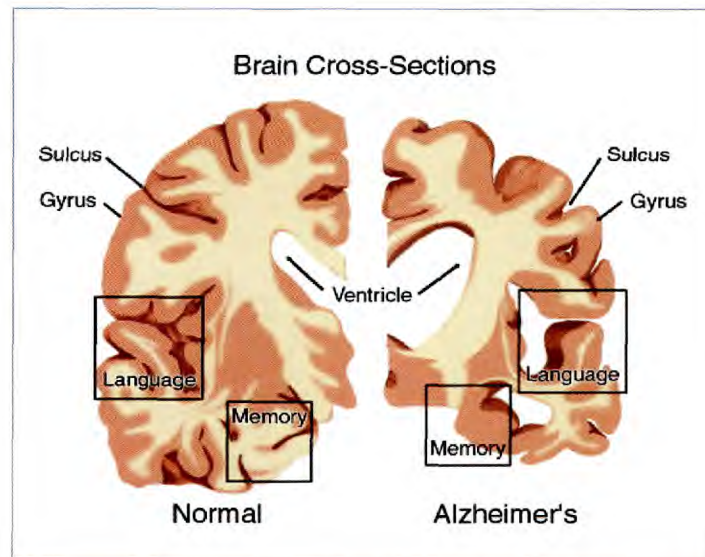


Figure 21 Difference between a normal brain (left) and a brain affected by AD (right)¹²⁴

Progressive mental deterioration in old age had been recognised and described throughout history. However, it was not until the early part of the 20th century that a collection of brain cell abnormalities were specifically identified by Dr. Alois Alzheimer, a German physician, in 1906. He studied the brain of a woman who had died after years of experiencing severe memory problems, confusion, and difficulty understanding questions. The autopsy revealed the presence of dense deposits outside and around the nerve cells (neuritic plaques). Inside the nerve cells, he noted the presence of twisted bands of fibres (neurofibrillary tangles). Today, this degenerative brain disorder bears his name. The observation of the plaques and tangles at autopsy is still required to obtain a definitive diagnosis of Alzheimer's disease. The duration of the disease varies between 3 to 20 years and eventual extensive neuronal loss leads to death. The symptoms of the disease are as follows: disturbances in memory, attention, orientation and language difficulties. While there are some common symptoms of Alzheimer's disease, it is important to remember that everyone is unique. No two cases of AD are likely to be the same. People always experience illness in their own individual way.

Some factors that are believed to cause the disease are age, genetic inheritance, environmental factors, diet and the overall general health. However, no one single factor has been identified as a cause.¹²⁵ According to the World Health Organisation, 24 million people suffer from dementia worldwide.¹²⁶ Dementia affects 1 in 20 people over the age of 65 and 1 in 5 over the age of 80. By 2040 the number will have risen to 81 million. Alzheimer's disease makes up 55% of all cases of dementia.

1.3.1.2 Treatment of Alzheimer's disease

At present, there is no cure for AD. The first few drugs are all cholinesterase inhibitors which can slow down the progression of the disease by maintaining the levels of acetylcholine. In 1993, the FDA approved the first drug to treat Alzheimer's disease: Cognex (Tacrine) increases the amount of the neurotransmitter acetylcholine in the brain and can slow cognitive decline. A number of other acetylcholinesterase inhibitors followed: Aricept (1996), Exelon (2000) and Razadyne (2001). In 1997, studies indicated that vitamin E and a drug normally used in the treatment of Parkinson's disease, Eldepryl (Selegiline), were helpful in slowing mental deterioration in patients with moderate Alzheimer's disease; however, further studies are necessary to corroborate these findings. In 2003, the FDA approved the first drug to treat moderate-to-severe Alzheimer's disease. Namenda is an *N*-methyl-D-aspartate (NMDA) receptor antagonist, and appears to protect the brain's nerve cells against excess amounts of glutamate, a messenger chemical released in large amounts by cells damaged by this devastating neurological disease.

1.3.2 Multiple Sclerosis (MS)

1.3.2.1 Etiology

Multiple sclerosis is a chronic, autoimmune, inflammatory disease of the central nervous system (CNS).^{14,127} During the course of this disease, the myelin sheath insulating nerve cells is destroyed as illustrated in **Figure 22**.¹²⁸ The symptoms of the disease include visual difficulties, emotional disturbances, speech disorders, convulsions, paralysis, bladder disturbances and muscular weakness.

The exact causes of MS are unknown. Some potential factors are thought to be autoimmunity, exposure to pathogens and genetics. The National Multiple Sclerosis Society estimates about 2.5 million people are affected worldwide, out of which 85,000 live in the UK. Diagnosis is usually between 20 and 40 years of age - rarely under 12 or over 55. Three women have MS for every two men.¹²⁹

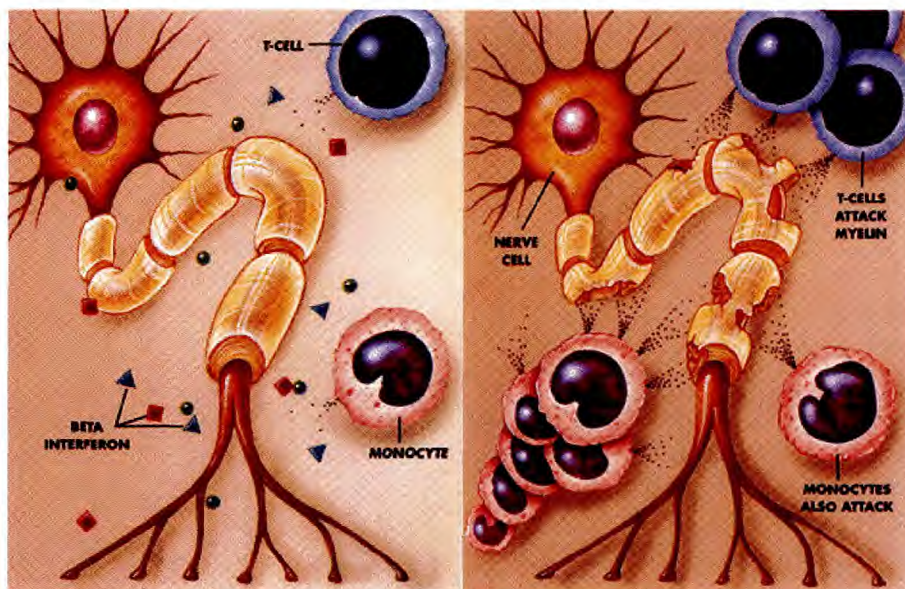


Figure 22 Difference between normal nerve cells (left) and those affected by MS (right)¹²⁸

1.3.2.2 Types of multiple sclerosis

1. Relapsing/remitting multiple sclerosis

It is the most common form of MS, affecting about 85% of people with the condition. Relapsing/remitting MS is characterised by sporadic attacks of degeneration (relapses) intermingled with remissions, periods of near-normal health that can last for months or years. Some people even go into permanent remission, but most experience a slow increase in permanent nerve damage.

2. Secondary progressive multiple sclerosis

This is a later stage of the relapsing/remitting form of MS where attack rate is reduced and the condition changes to a gradual but steady deterioration of body functions unrelated to acute attacks. Within 10 years, 50% of all patients with relapsing/remitting MS move into the secondary progressive type.

3. Primary progressive multiple sclerosis

After onset of symptoms, there is a gradual but steady deterioration of body functions without acute attacks in about 10% of sufferers. In the very worst cases, primary progressive MS can accelerate, leading to complete disability or death within just a few months.

4. Progressive/relapsing multiple sclerosis

It is the most severe form of MS, affecting about 5% of people with the condition. Progressive/relapsing MS begins with a progressive course although these people also experience acute attacks.

1.3.2.3 Treatment of multiple sclerosis

There is no cure for this disease. There are now drugs that can modify its course for some patients and many symptoms can be successfully treated or managed. The different types of drugs on the market focus mainly on decreasing the rate and severity of relapse, reducing the number of MS lesions, delaying the progression of the disease, and providing symptomatic relief for the patient. The drug classes are as follows:

- *Corticosteroids*: these natural chemicals released by the body are frequently used for visual symptoms of MS and can prolong the onset of MS if used early in the disease course;
- *Interferons*: substances produced by the body to regulate the immune system, mainly to combat viral infections. They decrease the worsening or relapse of MS. However, they do not stop the overall disease progression and they have significant side effects;
- *Glatiramer acetate*: mixture of amino acids which decreases the relapse rates of MS by 30% and appears to also have an effect on the overall disability of MS. It is better tolerated than interferons and has fewer side effects;
- *Natalizumab (Tysabri)*: monoclonal antibody that binds to white blood cells and interferes with their movement from the bloodstream into the brain and spinal cord. White blood cells are thought to play a role in causing nervous system damage in MS.

Several drugs that suppress the immune system and are used in the treatment of cancer have been used as well; however they make patients very ill. Four MS disease modifying drugs are licensed in the UK: Avonex and Rebif (both β interferon 1a), Betaferon (β interferon 1b) and Copaxone (glatiramer acetate).

However, the main drawback with these drugs is that they are only effective in about 30% of the patients. New research and treatment methods are currently being investigated and are expected to offer some hope to people with MS. Some preclinical studies have shown that Pioglitazone **21 (Figure 17)** delays the onset and reduces the severity of clinical symptoms in an animal model of multiple sclerosis. It was therefore tested in a patient with secondary MS by Feinstein *et al.* and an improvement in orientation, short-term memory and attention span was seen after 8 months of the therapy.¹³⁰ The possible neuroprotective effects of PPAR γ agonists were reviewed by Feinstein.¹³¹

1.3.3 Targeting the brain: brain glucose levels and the blood brain barrier

Glucose is the main fuel of cerebral tissue. Because neurons cannot store glucose, they depend on the bloodstream to deliver a constant supply of this important fuel. Although the brain represents only 2% of the body weight, it receives 25% of total body glucose utilisation. Hexokinase metabolises glucose transported to the cerebral tissue to glucose-6-phosphate, a very important intermediate in the glucose catabolism system. Glucose-6-phosphate then enters a metabolic pathway where it is catabolised to generate high-energy phosphate compounds, such as ATP, through its linked phosphorylation reaction.

Mental performance is strongly dependent on brain glucose utilisation whose rate is not uniform throughout the brain. Certain brain portions and cell types, such as astrocytes, have been found to be clearly insulin sensitive.¹³² Astrocytes are important communicating cells whose glucose utilisation is severely affected by diabetes as they can develop insulin resistance. So far, it is known that brain glucose utilisation is not altered in relation to diet, insulin treatment or diabetes.

Memory loss and dementia generally develop with age. Not only does glucose utilisation in the brain decrease with age, but insulin-stimulated fuel utilisation in peripheral tissues, such as skeletal muscle, also declines with age, thereby leading to insulin resistance. This is often due to a reduced amplification of the insulin signalling process. As a consequence, insulin is less efficient in activating the normal insulin response. This suggests that insulin resistance in discrete brain areas and cell types may play a role in central glucose utilisation, resulting in reduced mental performance. However, glucose utilisation in the brain is under complex control and it cannot be predicted how significant the impact of insulin resistance on age-decreased brain glucose utilisation is.¹³³

Since neural tissue is entirely dependent on glucose for normal metabolic activity, metabolism in the brain is dependent upon adequate glucose delivery from the systemic circulation.¹³⁴ Changes in endothelial glucose transport may have profound consequences on glucose delivery to these tissues and major implications in the development of two major diabetic complications, namely insulin-induced hypoglycaemia and diabetic retinopathy.

The main issue with treating dementia by increasing brain glucose metabolism is that it is crucial to treat only brain glucose metabolism for patients with normal serum glucose. Accordingly, it is important to deliver agents for treating brain glucose metabolism to the cerebral tissue. Unfortunately, the blood brain barrier (BBB) is the major obstacle for delivering most medication to the central nervous system (**Figure 23**).¹³⁵

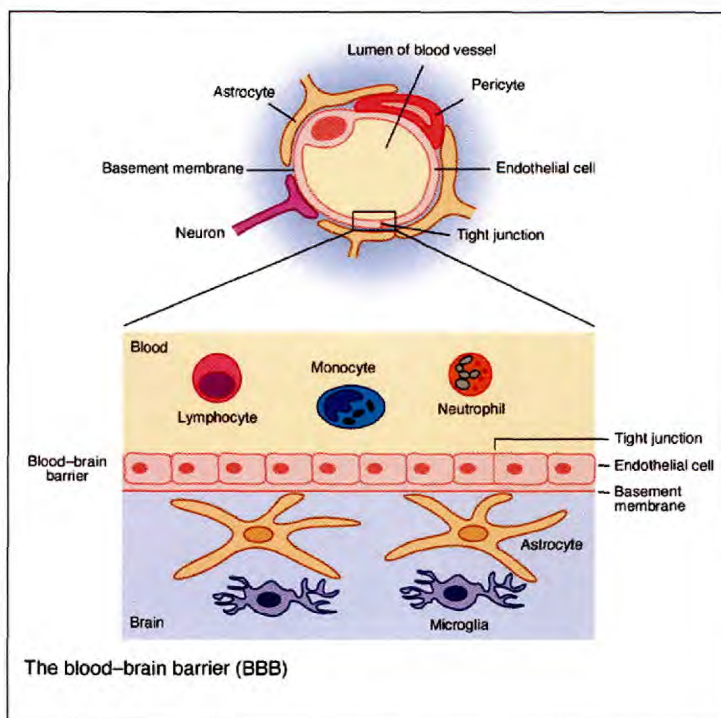


Figure 23 The blood brain barrier¹³⁶

The BBB is formed by the tight apposition of endothelial cells lining blood vessels in the brain, forming a barrier between the circulation and the brain parenchyma (e.g. astrocytes, microglia). A thin basement membrane, comprising laminin, fibronectin and other proteins, surrounds the endothelial cells and associated pericytes, and provides both mechanical support and a barrier function. Brain capillaries, unlike all other capillaries in the body, have no gaps which allow permeation of substances into and out of the blood (**Figure 24**).¹³⁷ Diffusion through the BBB depends mainly on the lipid

solubility of the solute as the cell membranes' main constituents are lipids. Water-soluble molecules such as glucose and glutamate enter the brain almost exclusively by carrier-mediated transport. Blood-borne immune cells such as lymphocytes, monocytes and neutrophils cannot penetrate this barrier.

Thus, the BBB is crucial for preventing infiltration of pathogens and restricting antibody-mediated immune responses in the central nervous system, as well as for preventing disorganisation of the fragile neural network. This, together with a generally muted immune environment within the brain itself, protects the fragile neuronal network from the risk of damage that could ensue from a full-blown immune response.

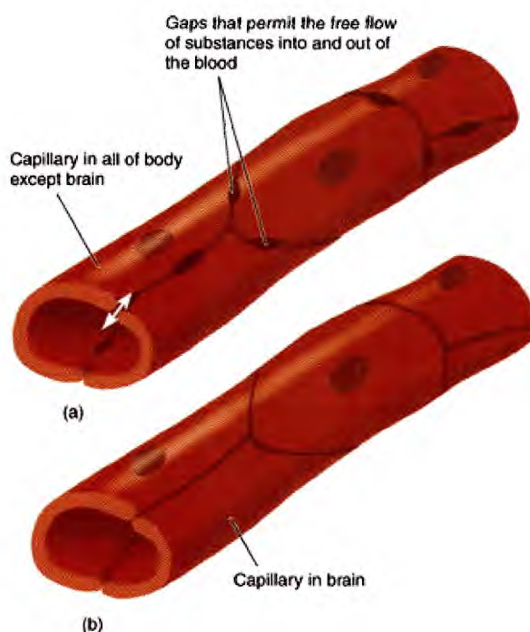


Figure 24 Difference between a brain capillary and a capillary found anywhere else in the body¹³⁷

Some non-invasive methods for drug delivery into the central nervous system include the use of chimeric cell-penetrating peptides and the use of "prodrugs" such as lipophilic esters or amides of the molecule amongst others.^{138,139,140,141} Prodrugs are biologically inactive compounds that subsequently decompose to yield the active compound. Depending on the nature of the active compound, different modifications are possible in order to make a prodrug. One possibility includes converting an anionic group such as a sulfate or sulfonate into the corresponding ester. The prodrug, when administered to a patient, is either cleaved, enzymatically or

nonenzymatically, reductively or hydrolytically, to reveal the therapeutic target or is actively transported *in vivo* and is selectively taken up by target organs. It can be selected to allow specific targeting of the therapeutic moieties to the brain.

Carrier molecules may also be used to transport active compounds to the brain. The carrier molecule, which can be natural or synthetic, may include a moiety capable of targeting the therapeutic compound to the brain by either active or passive transport such as a redox moiety.^{142,143,144} These carriers include lipids, proteins, peptides, fatty acids, inositol and 1,4-dihydropyridine. Some examples of useful protein carriers include antibodies specific for receptors within the brain, albumin, insulin, drugs, or growth factors.

1.3.4 Targeting AD and MS via the effects of PPAR agonists

1.3.4.1 Alzheimer's disease

There are a number of abnormalities in brain glucose-sensing neurons, the transmitters and peptides that affect them, and the physiological responses to changes in glucose levels that occur in both obesity and diabetes. But there is no direct link yet between these defects and the pathophysiology of obesity and diabetes. Both animal models and studies with Type II diabetic elderly patients have shown that altered glucose regulation impairs learning and memory processes. People with type II diabetes have a 9% increased risk of developing dementia and Alzheimer's disease.¹³³ Moreover, insulin degrading enzyme was found to inhibit the degradation of the *beta* amyloid produced in AD¹⁴⁵ and to play a significant role in the regulation of the phosphorylation of the tau protein, the main component of the tangles.¹⁴⁶ Insulin resistance and the resulting hyperinsulinemia appear to increase the risk of AD.¹⁴⁷ As such a link exists, the next logical step would be to determine whether AD patients could benefit from treatments aimed at normalising blood glucose regulation and improving insulin sensitivity.

In view of the fact that inflammatory responses are an important component in AD, and that glucose metabolism is perturbed in AD,¹⁴⁸ PPARs could play an important role in the treatment of this disease.^{55,149,150,51,50,74,151} Studies with pioglitazone **21** have shown that it significantly increases glucose consumption in astrocytes.¹⁵² Studies with rosiglitazone **20** are currently being undertaken.¹⁵³

1.3.4.2 Multiple Sclerosis

MS lesions have been associated with increased levels of nitric oxide (NO) and pro-inflammatory cytokines such as interleukin-1 β (IL-1 β) and tumour necrosis factor (TNF- α).^{154,155}

Nitric oxide transmits messages between nerve cells and is associated with the processes of learning, memory, sleeping, feeling pain, and, probably, depression. It is a mediator in inflammation and rheumatism. Scientists are currently investigating the participation of NO in brain cell damage that occurs in a variety of diseases.

Interleukin-1 β is a member of the interleukin-1 (IL-1) family. IL-1 is a cytokine that is secreted by macrophages, monocytes and dendritic cells and is an important part of the inflammatory response of the body against infection. It increases the expression of adhesion factors on endothelial cells to enable transmigration of leukocytes, the cells that fight pathogens, to sites of infection. It also re-sets the hypothalamus thermoregulatory center, leading to an increased body temperature, which expresses itself as fever. It is therefore called an endogenous pyrogen. The increased body temperature helps the body's immune system to fight infection.

Tumor Necrosis Factor (TNF- α , cachexin or cachectin) is an important cytokine involved in systemic inflammation and the acute phase response: it can cause cytolysis of certain tumor cell lines; it is involved in the induction of cachexia; it is a potent pyrogen, causing fever by direct action or by stimulation of interleukin-1 secretion; finally, it can stimulate cell proliferation and induce cell differentiation under certain conditions.

An interesting study by Drew *et al.* has demonstrated that PPAR α agonists inhibit microglia production of nitric oxide, IL-1 β and TNF- α .¹⁵⁶ Another study has shown that PPAR α agonists inhibited IL-1 β induction in astrocytes.¹⁵⁷ Furthermore, Watanabe *et al.* have shown that PPAR γ activation increases neurite extension in brain cells.¹⁵⁸ With the findings that PPAR agonists could prevent anti-inflammatory activation of glial cells, reduce T cell activation and also regulate myelin gene expression,^{63,159} they could also become potential drugs for the treatment of multiple sclerosis.^{160,161,162}

CHAPTER 2

Project outline

2.1 Objectives of the project

In the first chapter, we discussed how peroxisome proliferator-activated receptors (PPARs) have been established as a prime target in drug discovery for the treatment of metabolic diseases because of their critical role in the regulation of lipid metabolism and fat cell differentiation. In particular, study into PPAR γ agonists have founded a class of drugs known as the thiazolidinediones (TZDs). The TZDs have the following beneficial effects: improved insulin sensitivity, decreased hepatic glucose output, nonglycemic effects (decreased triglycerides levels and hyperinsulinemia, increased fibrinolysis and improved endothelial function) and increased adiponectin levels.¹⁰⁴ In addition, they are the only first generation drugs that have a possible potential to preserve the pancreatic β -cells.^{102,103} Moreover, unlike insulin and sulfonylureas, they do not induce hypoglycaemia and they do not provoke gastric disturbances and lactic acidosis found with biguanide therapy. Their convenient once- or twice-daily dosing makes them easier to use by patients. Nevertheless, they do have side effects such as weight gain, oedema, anaemia and possible liver dysfunction and care has to be taken in the case of patients suffering from severe cardiovascular complications.^{106,105} As a consequence of these side effects and given the complexity of the metabolic syndrome and diabetes, combination therapy is sometimes employed, for example, TZDs can be prescribed with metformin which does not induce any weight gain.

We propose to design novel PPAR dual (*i.e.* an agonist of two of the three PPAR subtypes) or pan (*i.e.* an agonist of the three subtypes) agonists, which would hopefully lead to complementary and synergistic actions in improving lipid homeostasis, insulin sensitivity and inflammation control. PPAR γ is abundantly expressed in adipose tissue and has an important role in adipocyte differentiation and triglyceride synthesis. Selective PPAR γ agonists increase the diversion of fatty acids into adipose tissue and enhance glucose-metabolic insulin sensitivity. All this provides the rationale for the use of TZDs in the treatment of diabetes type II. On the other hand, PPAR α , expressed mainly in the liver, skeletal muscle and heart, is involved in fatty acid oxidation and lipoprotein synthesis. PPAR α agonists may protect against obesity and enhance insulin-mediated muscle glucose metabolism.^{163,164} Also, they could improve small dense VLDL triglyceride hydrolysis by lipoprotein lipase.¹⁶⁵ Bergeron *et al.* showed that chronic treatment with a PPAR α agonist stopped the development of diabetes in Zucker diabetic rats mainly by improving the pancreatic insulin response without side effects on body weight gain

and cardiomegaly.¹⁶⁶ The established actions of PPAR γ and the positive results obtained with PPAR α activation have thus led to the hypothesis that combined PPAR α/γ activation could give much better results than single activation of one PPAR subtype. The properties of the ligand-binding domains of each of the two subtypes are such that dual agonists could be developed. Moreover, dual activation of PPAR α and PPAR γ could also limit the occurrence of certain effects associated with currently used glitazones.¹²¹ The propensity for adipogenesis from PPAR γ activation could be offset by the propensity of PPAR α activation to stimulate lipid catabolism. In this respect, a new class of compounds called the glitazars has emerged over the past few years.¹⁰⁵ Some examples of these synthetic dual agonists are shown in **Figure 25**.

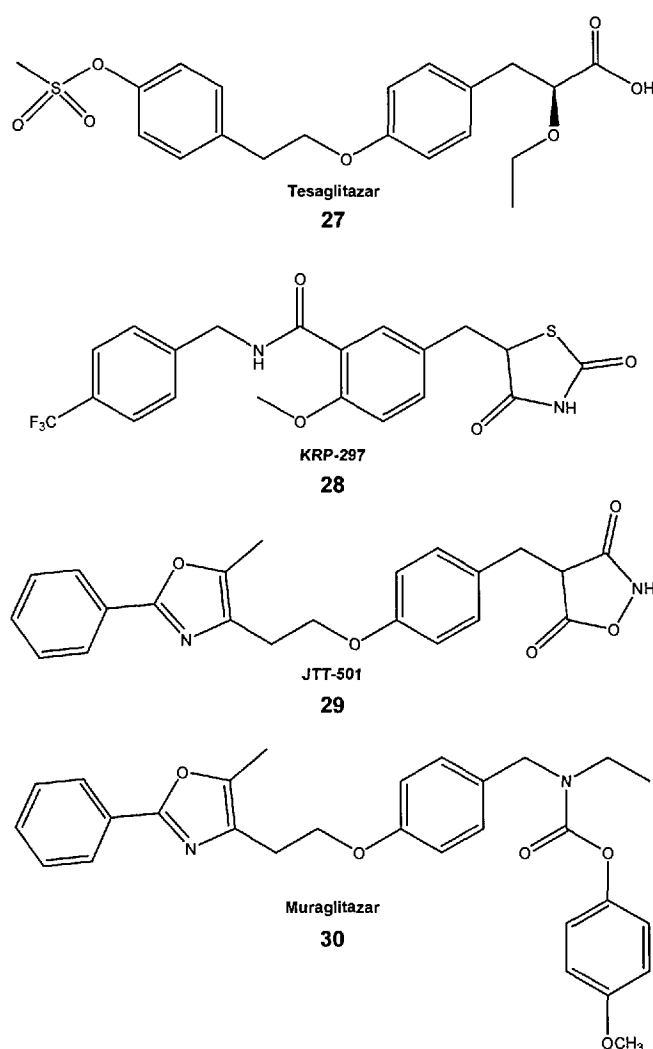


Figure 25 Structures of different PPAR α/γ dual agonists

Plasma triacylglycerol concentrations and hepatic triacylglycerol accumulation were reduced by dual PPAR α/γ agonists.^{167,168,169,170,171} Treatment of Zucker rats (obese,

diabetic rat model) with the dual agonist LY465608 (Eli Lilly) did not enhance food consumption and resulted in significantly less fat accumulation and body weight gain.^{172,173} Another dual agonist, JTT-501 **29**, was shown to reduce the diabetic complications such as cataract, nephropathy and osteopenia in Zucker rats.¹⁷⁴ Muraglitazar **30**, developed by Bristol-Myers Squibb, was shown to prevent the development of diabetes if administered before the onset of diabetes and, when initiated after the onset of diabetes, prevented the worsening of the disease.¹⁷⁵ However, the progress of glitazars to the market has been hampered by idiosyncratic side-effects.¹⁰⁶ Given the potential of the PPAR nuclear receptor family in glucose and lipid metabolism, it is important to find the right optimal activity of the receptor subtypes with the best side-effect profile.

One new development in PPAR activation is its effect on the control of inflammation. Indeed, recent studies have shown that PPAR α agonists reduce microglial activation whereas PPAR γ activation inhibits TNF- α and interleukins expression in monocytes, and inducible nitric acid synthase in macrophages. Feinstein *et al.* have reported some promising data from the treatment of a patient suffering from multiple sclerosis with the TZD, pioglitazone **21**.¹³⁰ All these effects strongly suggest that PPAR agonists could have a significant potential in the treatment of neurological inflammatory diseases.

Moreover, the studies showing the link between altered glucose regulation and the impairment of learning and memory processes in Type II diabetic patients have led to the hypothesis that treatments regulating blood glucose and improving insulin sensitivity could be useful for the treatment of Alzheimer's disease.

Our aim is to synthesise and develop new potential drugs for the treatment of the metabolic syndrome and diabetes type II and, also for neurological inflammatory brain diseases. Given all the findings about the nuclear receptors, PPARs in both the regulation of glucose and lipid metabolism, as well as in the control of inflammation, we propose to develop new dual or pan PPAR agonists. This thesis describes the design and development of two families of orthogonal PPAR agonists; firstly lipid analogues of tetradecylthioacetic acid and, secondly, small molecule heterocyclic structures.

2.2 Synthesis of new lipid analogues

The first part of the project involved the synthesis of lipids based on work previously carried out in our group and in collaboration with Professor Berge from the Institute of Medicine, Bergen and Thia Medica AS (Norway). Tetradecylthioacetic acid (TTA) **31** has been developed as a potential treatment for many of the indications related to the metabolic syndrome, including diabetes II, by Thia Medica AS (**Figure 26**).

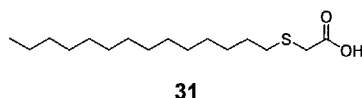


Figure 26 Tetradecylthioacetic acid

This acid, found to be a potent PPAR agonist of all three subtypes, has very good lipid lowering effects and improved insulin action. However, it is easily excreted by the body and has very poor bioavailability. We proposed to synthesise phospholipids analogues of TTA as natural “prodrugs” in order to improve the absorption, distribution, metabolism and excretion (ADME) properties of this acid. Phospholipids (and other classes of lipids) were shown to have better absorption characteristics compared to the parent fatty acid as preliminary *in vivo* data on TTA-PC **32** and TTA-TAG **33** suggested these new molecules to have better activity than the parent TTA. Thus, several new lipid analogues (**Figure 27**) have been synthesised and were screened *in vitro* and *in vivo* by Thia Medica AS for their action as potential diabetes II treatments.

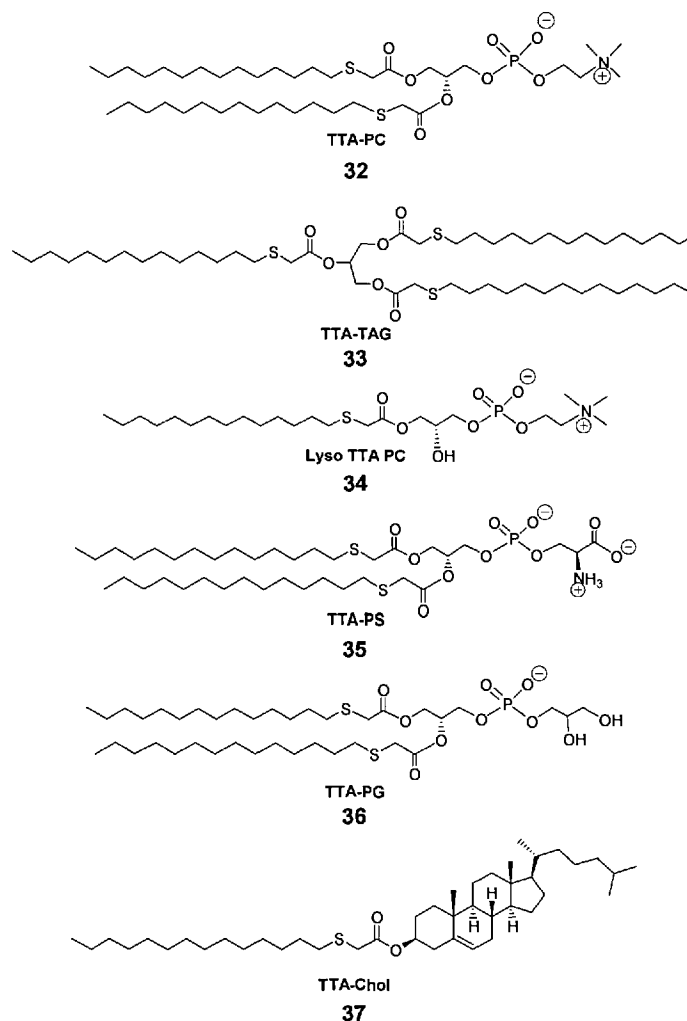


Figure 27 Structures of novel lipid analogues of TTA

2.3 Design and synthesis of novel heterocycles

The second part of the project consisted of the synthesis of novel heterocyclic structures, designed using *de novo* design technology. This strategy was adopted in order to develop small molecule heterocycles with drug-like properties in order to help to achieve the ADME characteristics required for the development of an oral drug. Prosarix Ltd is an *in silico* screening company based in Cambridge, UK. Using its proprietary drug design software, Prosarix Ltd modelled the interaction of known drugs with the PPAR receptors and subsequently used this data to predict and design novel heterocyclic scaffolds as potential PPAR α/γ dual agonists. The first scaffold displays the classical carboxylic acid moiety found in many PPAR agonists linked to an indole core (**Figure 28**).

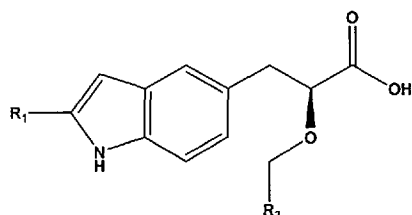


Figure 28 Indole scaffold

The screening study suggested the synthesis of molecules **38** to **43**, with $R_1 = \text{H}$, phenyl and naphthylmethyl groups, and $R_2 = \text{methyl}$ or trifluoro group (**Table 5**). The racemic synthesis of the six indoles leads **38** to **43**, as well as their *in vitro* luciferase reporter gene PPAR activation assay, is described in Chapter 4.

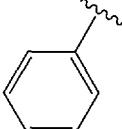
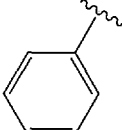
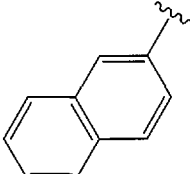
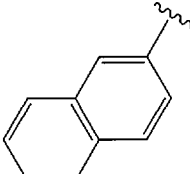
Target	R_1	R_2
38	H	CH_3
39	H	CF_3
40		CH_3
41		CF_3
42		CH_3
43		CF_3

Table 5 Indole leads 38 to 43

Some indole-based structures have recently been published as PPAR agonists in the literature by GlaxoSmithKline and Hoffman-La Roche. GlaxoSmithKline's 2,3-disubstituted compounds were found to be potent PPAR γ agonists *in vitro* and are currently being investigated in animal models.¹⁷⁶ Hoffman-La Roche's 1,5-disubstituted indole molecules were found to be potent PPAR α/γ agonists *in vitro* and are being studied *in vivo*.¹⁷⁷

Furthermore, a second heterocyclic scaffold was designed by Prosarix Ltd as potential PPAR α/γ dual agonists. It consists of a pyrrolidine core with different aryl groups on the 3-position (**Figure 29**).

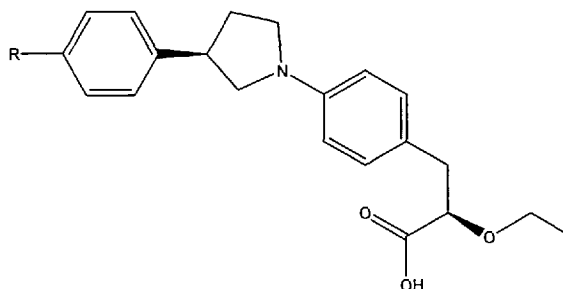


Figure 29 Pyrrolidine scaffold

The racemic synthesis of the first pyrrolidine molecule **44**, with R = H, is also described in Chapter 4.

CHAPTER 3

Synthesis of new lipid analogues of tetradecylthioacetic acid

3.1 Tetradecylthioacetic acid

Tetradecylthioacetic acid (TTA) **31** is a 3-thia fatty acid with a 14-carbon chain length (Figure 30).

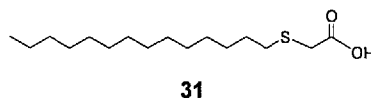


Figure 30 Tetradecylthioacetic acid

TTA **31** was first synthesised by Spydevold *et al.* and was found to induce peroxosomal β -oxidation.¹⁷⁸ TTA's effects were further studied by Professor Rolf Berge at the Institute of Medicine, Bergen, in collaboration with Thia Medica AS, and it was found to have powerful effects both *in vitro* and *in vivo*.^{179,180,181} *In vivo* studies of biological effects of TTA in rats have shown the following effects after administration: lipid lowering,¹⁸² improved insulin action,^{183,184} hepatic lipid content decrease, decrease of hyperinsulinemia, increased fatty acid oxidation,¹⁸⁵ anti-oxidising and anti-inflammatory action,¹⁸⁶ as well as modification of cell proliferation and apoptosis.¹⁸⁷

TTA is involved in lipid metabolism *via* its agonist action on the peroxisome proliferator-activated receptors (PPARs); it is a potent ligand of the three PPAR subtypes.¹⁸⁷ The ratio of PPAR α/δ activation is cell specific. Human PPARs are activated in the following order: $\delta > \alpha > \gamma$.¹⁸⁸

TTA is currently in phase III clinical trials. Phases I and II clinical trials have shown that it is effective at acceptable doses and that it has little acute toxicity. However, it suffers from poor bioavailability due to its poor ADME (absorption, distribution, metabolism and excretion) properties.¹⁸¹ Particularly, this fatty acid is poorly absorbed into the bloodstream. In order to improve the absorption and bioavailability of TTA, it was decided to couple it with phospholipids since these natural prodrugs should be better absorbed in the gut. Phospholipids are di-acyl derivatives of 3-glycerophosphoric acid **45** (Figure 31).¹⁸⁹ Glycerol **46** is a prochiral molecule with the prochiral carbon carrying two CH₂OH groups (Figure 31). To designate the stereochemistry of glycerol-containing components, the carbon atoms are stereospecifically numbered (*sn*). When the glycerol molecule is represented by a Fischer projection with the secondary hydroxyl to the left of the central carbon atom, and the carbon atoms are numbered 1, 2, and 3 from top to bottom. The major

glycerophospholipids are phosphatidylcholines (PC), phosphatidylethanolamines (PE), phosphatidylserines (PS), phosphatidylinositols (PI) and phosphatidylglycerols (PG).

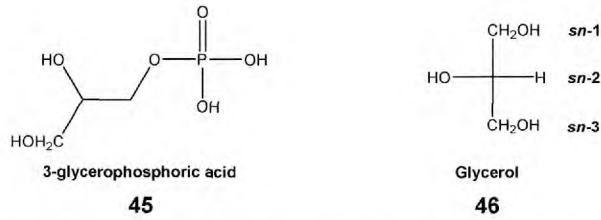


Figure 31 3-glycerophosphoric acid and glycerol

The mechanism of absorption and digestion of phospholipids explains their better absorption in the gut. Degradation by pancreatic lipases releases fatty acids from the *sn*-1 and *sn*-3 positions of triacylglycerols and of phospholipids. Micelles are formed with 2-monoacylglycerols, lysophospholipids, cholesterol, bile salts and free acids and are absorbed into the enterocytes by simple diffusion across the plasma membrane. Within the epithelial cells of the gut wall, a combination of triglycerides, and cholesterol, and fatty acids are coated with protein to form large lipoproteins known as chylomicrons. These pass into the general circulation *via* the thoracic duct and are transported in the bloodstream to the liver where they are absorbed and broken down to contribute to the triglyceride and the cholesterol pool within the liver. This is illustrated in **Figure 32**.^{190,191}

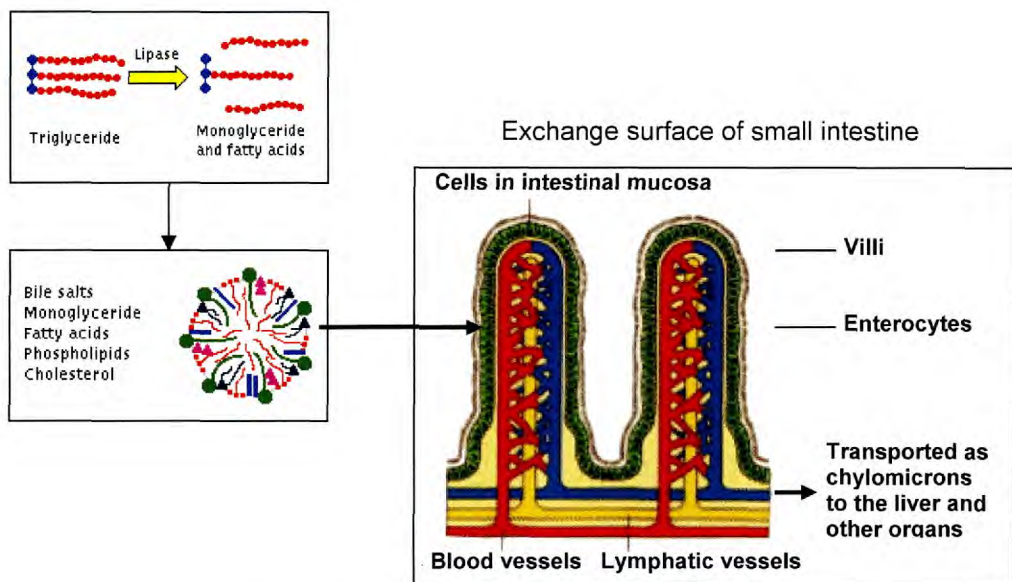


Figure 32 Absorption of lipids into the blood stream^{190,191}

Two new lipid analogues: TTA-PC **32** and TTA-TAG **33** were first synthesised. The coupling of TTA with L- α -glycerophosphocholine (GPC) gave *di*-tetradecylthioacetoyl-*sn*-glycero-3-phosphocholine, TTA-PC **32** (Figure 33).

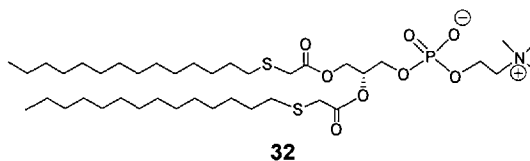


Figure 33 Structure of TTA-PC

TTA was also coupled with glycerol to give *tri*-tetradecylthioacetoyltriglyceride, TTA-TAG **33** (Figure 34).

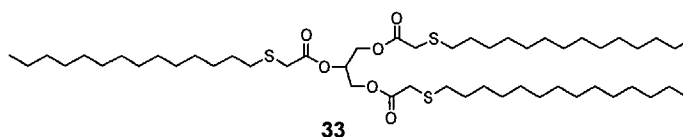
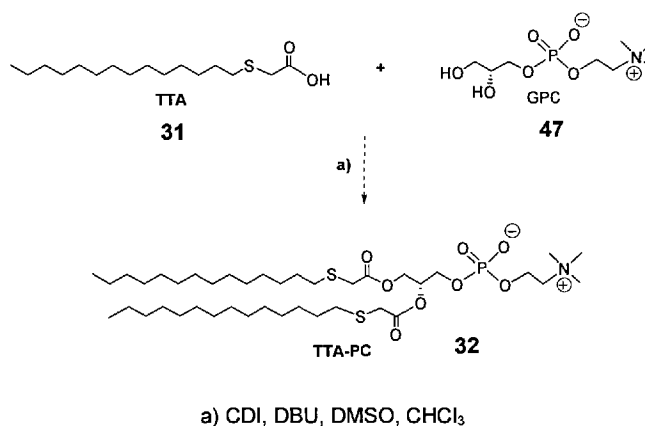


Figure 34 Structure of TTA-TAG

3.2 Synthesis of the first two analogues of TTA

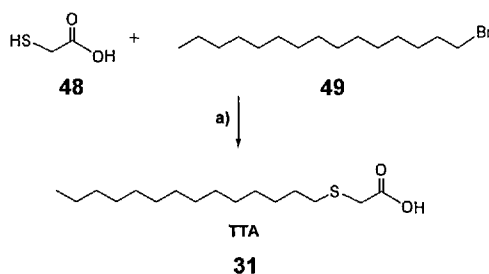
3.2.1 Synthesis of TTA-PC 32

TTA-PC **32**, is made from the coupling reaction between TTA **31** and L- α -glycerophosphocholine **47** (GPC).



Scheme 2 Coupling reaction between TTA **31** and GPC **47**

TTA **31** was first made by reacting thioglycolic acid **48**, under basic conditions, with tetradecylbromide **49** (**Scheme 3**). TTA was isolated as a white solid in an excellent yield (91%).¹⁷⁸



a) NaOH/MeOH, RT, 48 hr, 91%

Scheme 3 Synthesis of TTA **31**

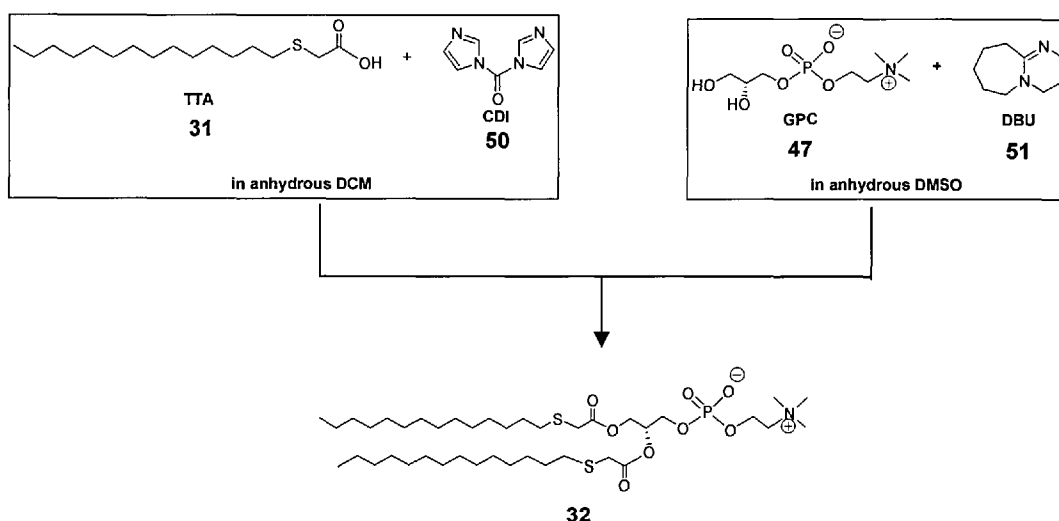
The coupling reaction between TTA and L- α -glycerophosphatidylcholine (GPC) is made difficult by the low solubility of GPC. CdCl_2 (as it is commercially provided) in most organic solvents. Furthermore, the secondary alcohol in GPC is less nucleophilic and becomes more hindered due to the first esterification occurring predominantly at the primary alcohol position.

Many different conditions were investigated to optimise the coupling reaction:

- coupling reagents: isobutyl and ethyl chloroformates, *N*-hydroxysuccinimide, dicyclohexylcarbodiimide, *N,N'*-carbonyl-diimidazole and pentafluorophenol.
- bases: 4-methylmorpholine, DBU and triethylamine.
- solvents: chloroform, dichloromethane, dimethylformamide, acetonitrile and dimethylsulfoxide.

The optimised coupling conditions required a mixed solvent system: dichloromethane-DMSO (**Scheme 4**), adapted from a method developed by Warner *et al.*^{192,193,194} Although DMSO is a high boiling solvent, thus difficult to remove, it has the advantage of efficiently dissolving GPC. CdCl_2 . TTA **31** was first activated separately with *N,N'*-carbonyldiimidazole (CDI) **50** in anhydrous DCM to form a reactive TTA-imidazolide. CO_2 is given off as the reaction proceeds, making this reaction simple to monitor. Once the acid has been fully activated, the evolution of CO_2 ceases, and the nucleophile can be introduced. The latter must only be added after the activation of the acid has finished, otherwise carbonates will result. The two alcohols of GPC were deprotonated with the non-nucleophilic base, DBU and the

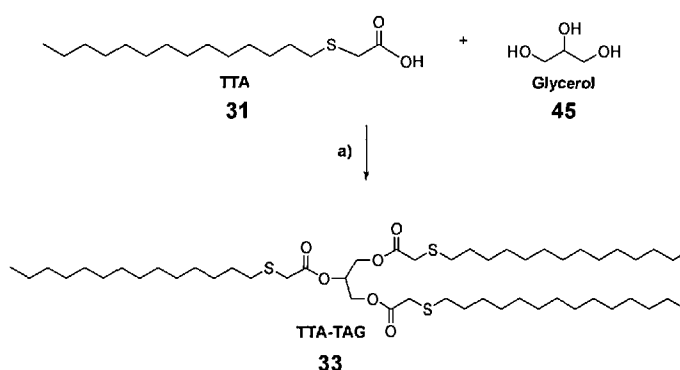
resultant solution reacted with the preformed TTA-imidazolide at slightly elevated temperature (ca. 40 °C), thereby giving the desired TTA-PC **32** in a yield 70%.¹⁹⁵



Scheme 4 Synthesis of TTA-PC, 70%

3.2.2 Synthesis of TTA-TAG **33**

The coupling reaction between TTA **31** and glycerol **45** was conducted using HBTU as coupling agent and DMAP as a nucleophilic catalyst (**Scheme 5**). TTA and glycerol were dissolved in anhydrous DCM after which HBTU and DMAP were added under inert atmosphere. The reaction was carried out at room temperature overnight. An increase in the number of equivalents of TTA significantly improved the yield. TTA-TAG **33** was isolated with a yield of 83% after chromatography on silica gel.

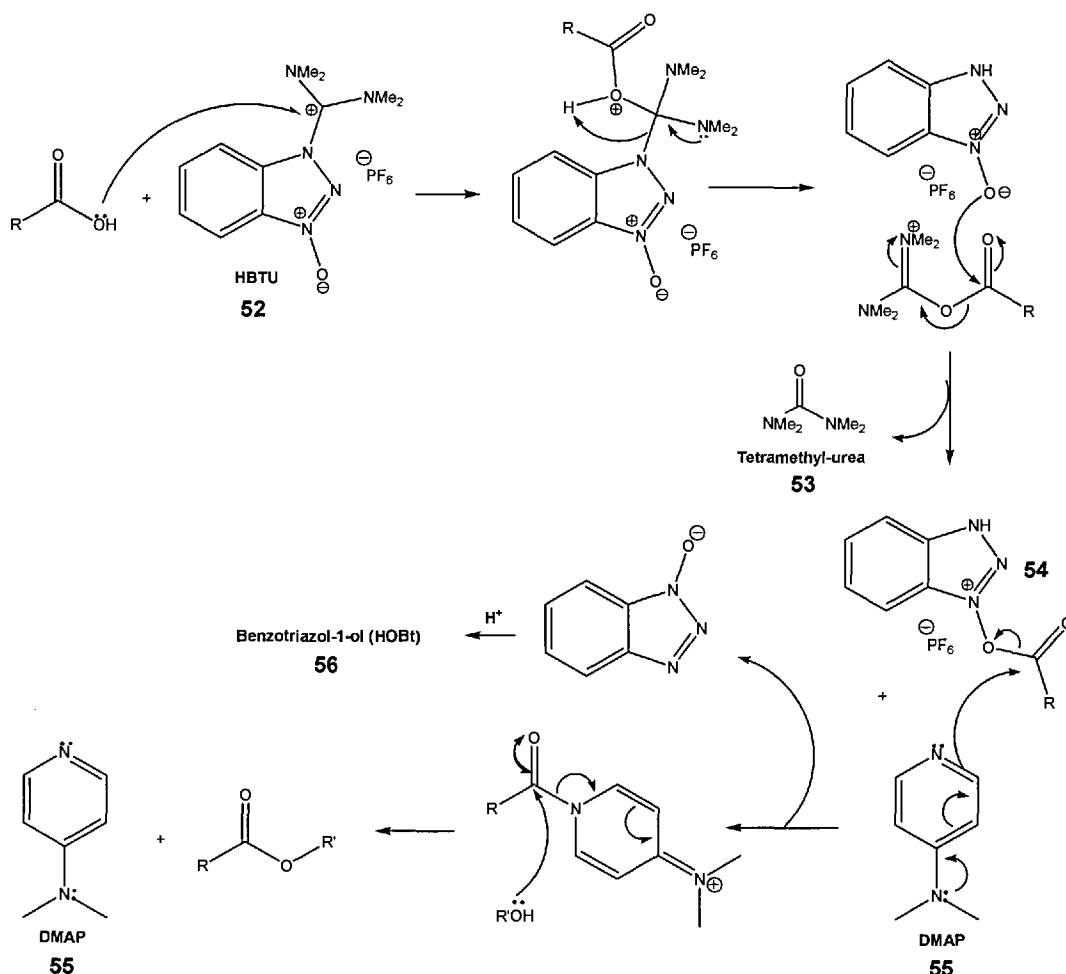


a) HBTU, DMAP, anhydrous DCM, RT, 83%

Scheme 5 Synthesis of TTA-TAG

The mechanism of the reaction is shown in **Scheme 6**. TTA is represented by RCOOH. It is first activated by HBTU **52**, giving tetramethylurea **53** as a side product. DMAP **55** subsequently further activates intermediate **54**. DMAP is a particular type

of aminopyridine in which the amino group reinforces the nucleophilic nature of the pyridinyl nitrogen atom. The nucleophilic oxygen of the alcohol attacks the carbon of the carbonyl group to yield back DMAP **55** which is a good leaving group and gives the desired ester product.



Scheme 6 Mechanism of coupling reaction between TTA and glycerol

3.2.3 Preliminary biological results with TTA-PC and TTA-TAG

In order to evaluate the biological potential of the new analogues, biological tests were carried out on TTA-PC and TTA-TAG by Thia Medica AS in Norway.¹⁹⁵ Male Wistar rats (4-5 rats in each treatment group) were fed TTA, TTA-PC or TTA-TAG at equimolar doses of TTA (1mmole/day/kg body weight) for 6 days. Negative control rats received only 0.5% of carboxymethylcellulose, CMC. The animals were sacrificed and lipid lowering effects were evaluated.

As described in Chapter 1, patients suffering from the metabolic syndrome and diabetes type II have an unusually high level of triacylglycerol and cholesterol. The

levels of plasma triacylglycerol, cholesterol and hepatic triacylglycerol levels were therefore measured after treatment with the different compounds. The results, normalised to the control, are shown in **Figure 35**. All three treatments showed a decrease in plasma triacylglycerol, cholesterol and hepatic triacylglycerol levels, with the largest decrease being affected by TTA-PC.

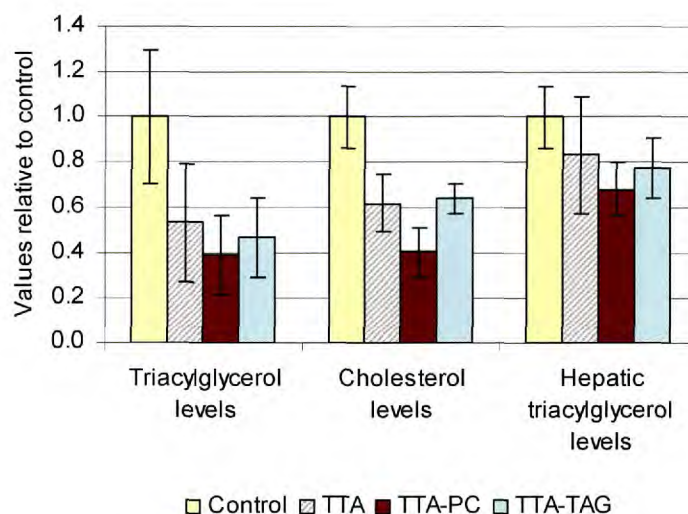


Figure 35 Effects of TTA, TTA-PC and TTA-TAG on plasma lipid levels

Fatty acid oxidation and the activity of key mitochondrial enzymes involved in fatty acid oxidation and transport were also measured (**Figure 36**) as these are very important dysfunctions in the metabolic syndrome and diabetes type II as previously explained. Palmitoyl-CoA is a fatty acid coenzyme derivative that plays a key role in fatty acid oxidation and biosynthesis. The catabolism of fatty acid palmitoyl-CoA reduces the production and secretion of VLDL by the liver, therefore a high rate of palmitoyl-CoA indicates a high rate of fatty acid metabolism. TTA-PC and TTA-TAG led to comparable levels of activity, with respect to TTA. Carnitine palmitoyl transferase-II is an important enzyme for the transport of fatty acids into the mitochondrion, a high activity of this enzyme implicates a high rate of fatty acid metabolism. CPT-II activity was found to be increased with the three compounds, with the highest increase effected by TTA-PC. 3-Hydroxy-3-methylglutaryl-CoA synthase (HMG-CoA synthase) is a rate-limiting enzyme for the production of ketone bodies in the mitochondrion whose activity increases with fatty acid oxidation. Similarly to CPT-II activity, HMG-CoA synthase activity was found to be increased with the three compounds, with the highest increase effected by TTA-PC. Fatty acyl-CoA is the rate determining enzyme in peroxisomal oxidation of fatty acids in rodents. Its gene expression is regulated by PPAR α . The activity of fatty acyl-CoA was

strongly increased with the three compounds and the highest activity was given by TTA-PC. In the case of these three enzymes, TTA, and TTA-PC showed significant activity, whereas TTA-TAG was slightly less effective in general. It must be highlighted that TTA-PC improved the activity of the key enzymes by nearly two-fold compared to TTA.

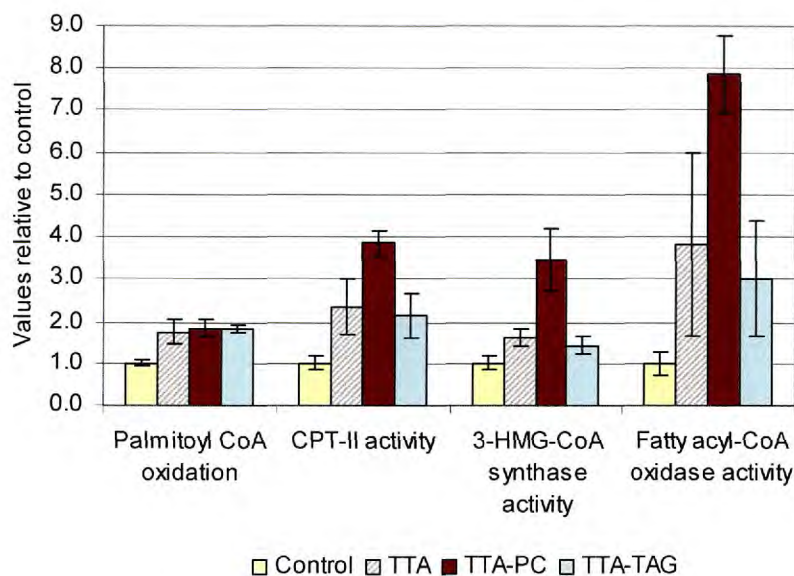


Figure 36 Effects of TTA, TTA-PC and TTA-TAG on the activity of key enzymes involved in fatty acid oxidation

Given this promising set of data, it was decided to synthesise further lipid analogues of TTA, such as phosphoglycerols and phosphoserines which are naturally occurring phospholipids in cell membranes, in order to improve the absorption and distribution properties of the active molecule TTA (**Figure 37**).

- i. *lyso-di-tetradecylthioacetoyl-sn-glycero-3-phosphocholine*, *lyso* TTA-PC **34**,
- ii. *di-tetradecylthioacetoyl-sn-glycero-3-phosphoserine*, TTA-PS **35**,
- iii. *di-tetradecylthioacetoyl-sn-glycero-3-phosphoglycerol*, TTA-PG **36**, and
- iv. *cholesterol-tetradecylthioacetate*, TTA-Chol **37**.

Lyso TTA-PC, TTA-PG and TTA-PS can be synthesised by enzymatic hydrolysis (in the case of *lyso* TTA-PC) or by enzymatic transphosphatidylation reactions (in the case of TTA-PG and TTA-PS) directly from TTA-PC whilst TTA-Chol is formed from the direct coupling of cholesterol and TTA.

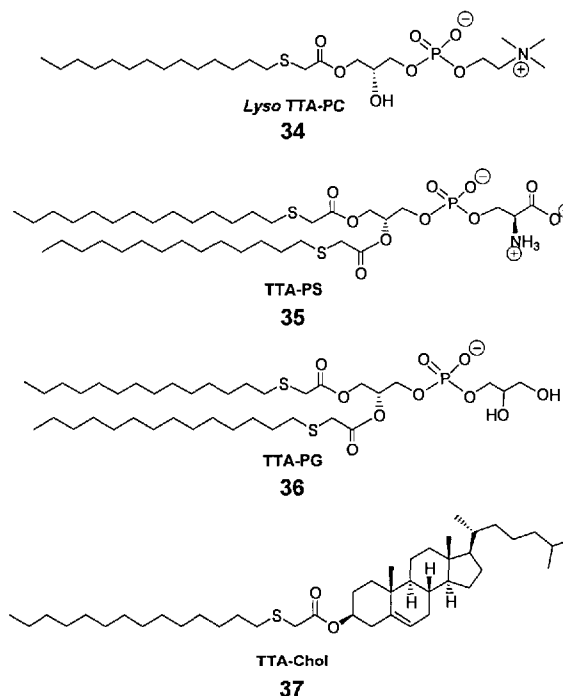


Figure 37 Structures of four novel lipid analogues

3.3 Synthesis of four new lipid analogues of TTA

TTA-PC **32** is the precursor to three of the new lipids shown in **Figure 37**: *lyso* TTA-PC **34**, TTA-PS **35** and TTA-PG **36**. Phospholipases were used to catalyse the synthesis of these lipids as shown in **Figure 38**. Phospholipase A_2 causes deacylation at the *sn*-2 position to yield *lyso* TTA-PC **34** and the fatty acid TTA **31**. Phospholipase D cleaves the phosphate ester bond to give choline and phosphatidic acids. It then re-esterifies the phosphatidic acid to give TTA-PS **35** and TTA-PG **36**. The overall reaction is an exchange between choline and serine or glycerol respectively. This type of enzyme transphosphatidylations reactions has been carried out with a wide variety of nucleophiles such as ethanolamine, azasugars, nucleosides and peptides by Wong *et al.*¹⁹⁶ The only pre-requisite for the nucleophile is that it bears a primary hydroxyl group, for which phospholipase D is chemoselective.

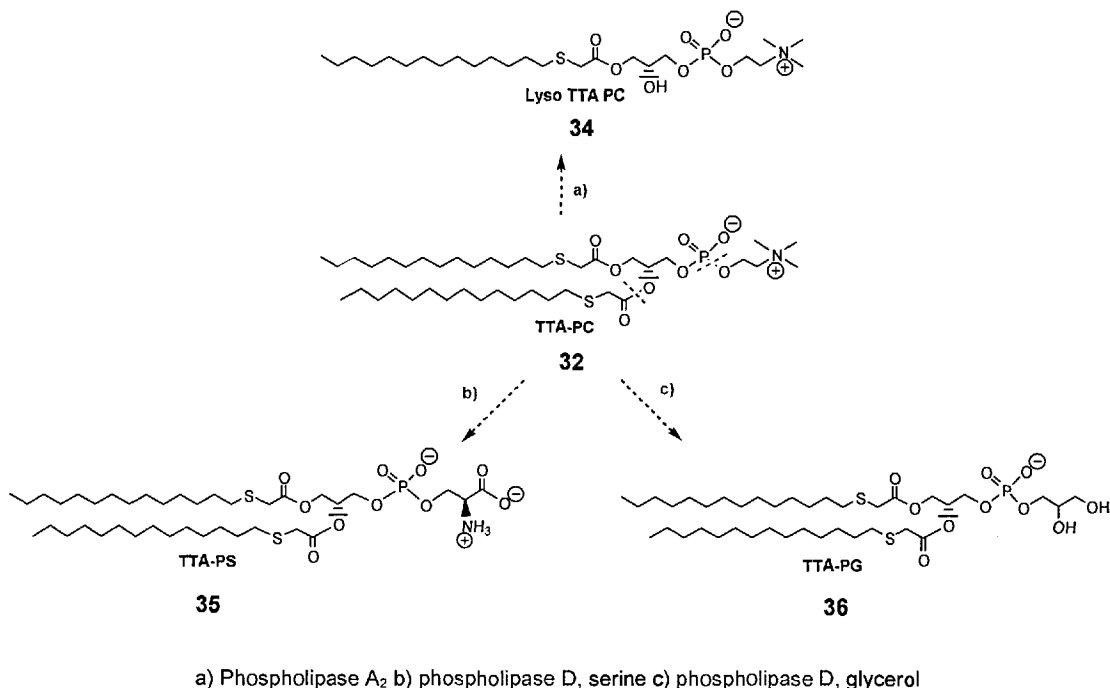


Figure 38 New lipid analogues: *lyso* TTA-PC, TTA-PS and TTA-PG

Due to limited resources of TTA-PC **32**, model studies for the enzymatic transformations were initially conducted with distearoyl phosphatidylcholine, DSPC **57** (Figure 39) which is commercially available and inexpensive.

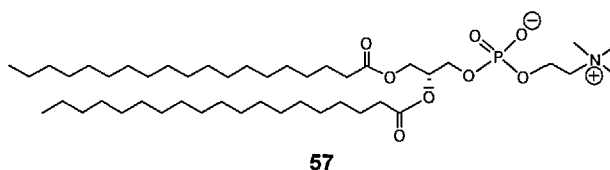
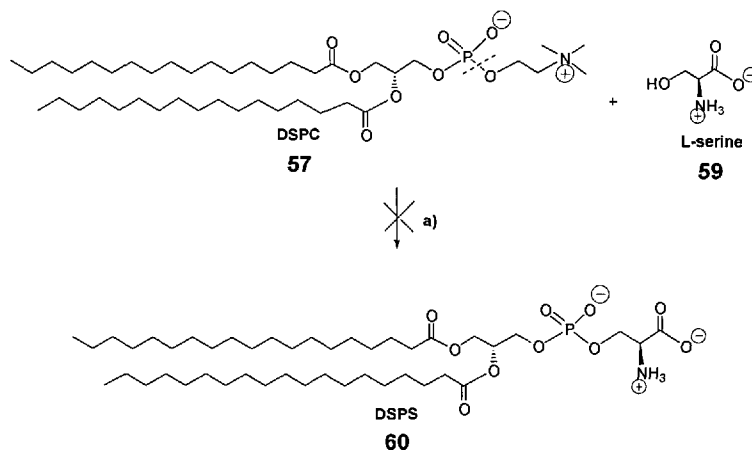


Figure 39 DSPC

The last analogue, TTA-Chol **37**, was made by reacting TTA with cholesterol using standard coupling conditions.

3.3.1 Synthesis of *lyso* TTA-PC **34**

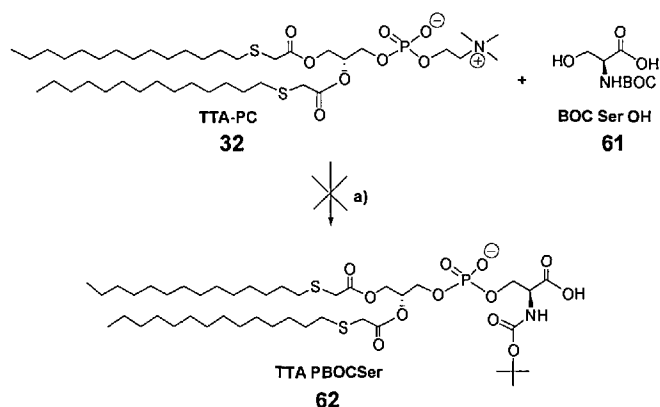
The synthesis of *lyso* DSPC **58** from DSPC **57** was conducted using the conditions shown in **Scheme 7**.¹⁹⁷ To a solution of the starting material in the organic phase were added trisHCl buffer (pH ~ 8.4) and finally the enzyme, phospholipase A₂. The reaction mixture was stirred at 37 °C for 3-5 hours. The model *lyso* product was isolated with a yield of 87% after chromatography.



a) Phospholipase D, chloroform, buffer: NaOAc (100 mM), CaCl₂ (50 mM), pH 6.4, 30 °C

Scheme 9 Synthesis of DSPS 60

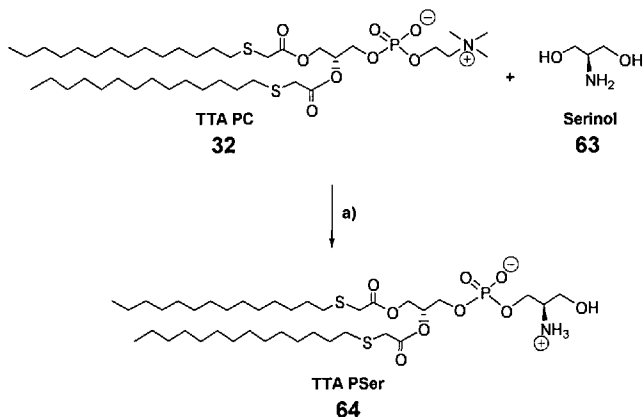
One important factor preventing the exchange of serine could be the poor solubility of serine in chloroform. This could be overcome by using protected serine. Thus the serine transphosphatidylation was carried out using BOC-serine **61** (Scheme 10). However, this reaction did not proceed to completion and purification of the product from the starting material was unsuccessful. De-protection of the amine by cleaving the BOC group did not render the purification easier as a more complex mixture of products was obtained.



a) Phospholipase D, hipersolv chloroform, buffer: NaOAc (100 mM), CaCl₂ (50 mM), pH 6.4, 30 °C

Scheme 10 Synthesis of TTA PBOC Ser 61

Due to the difficulties encountered to synthesise TTA-PS, it was decided to employ a derivative of serine as the nucleophile. Thus, the transphosphatidylation was carried out with serinol **63** as shown in Scheme 11. This reaction proceeded smoothly giving the desired product **64** in 87% yield.

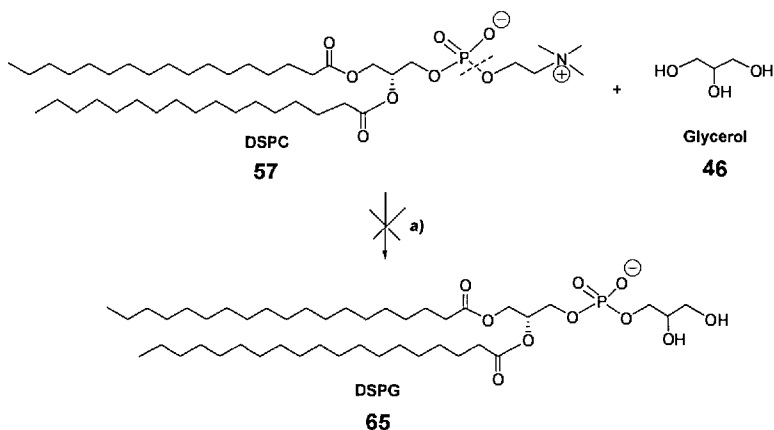


a) Phospholipase D, hipersolv chloroform, buffer: NaOAc (100 mM), CaCl₂ (50 mM), pH 6.4, 30 °C, 87%

Scheme 11 Synthesis of TTA-PSerinol **64**

3.3.3 Synthesis of TTA-PG 36

The model reaction for the synthesis of TTA-PG was first performed with DSPC **57** using the same conditions that proved successful with serinol **63** (**Scheme 12**).

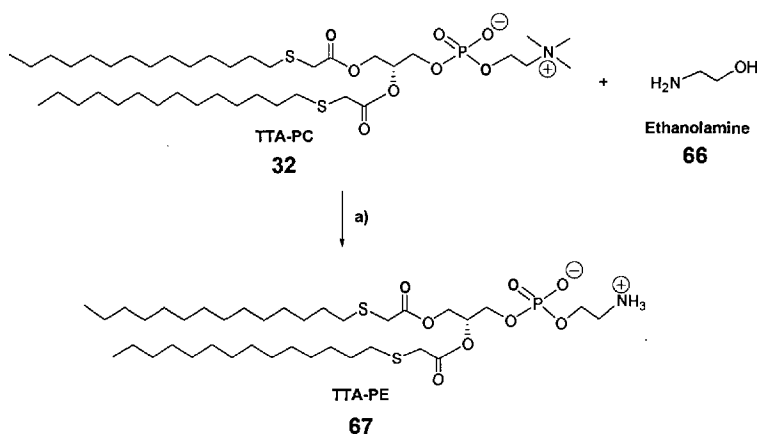


a) Phospholipase D, hipersolv chloroform, buffer: NaOAc (100 mM), CaCl₂ (50 mM), pH 6.4, 30 °C

Scheme 12 Synthesis of DSPG **65**

Again, it proved to be very difficult to follow the reaction by TLC or mass spectrometry. At this point the difficulty relating to the detection and handling of DSPC as a model study compound resulted in a slight change of strategy. 1,2-Dioleoyl-*sn*-glycero-3-phosphocholine (DOPC) would have probably been a better candidate for these model studies since unsaturation on its hydrocarbon chain is more liable to chemical changes (for *e.g.* oxidation), hence making it easier to detect this compound by TLC stains. Instead, it was decided to optimise the enzymatic reaction through the synthesis of *di*-tetradecyl-thioacetoyl-*sn*-glycero-3-phosphoethanolamine **67** (TTA-PE) as this reaction had been successfully carried out

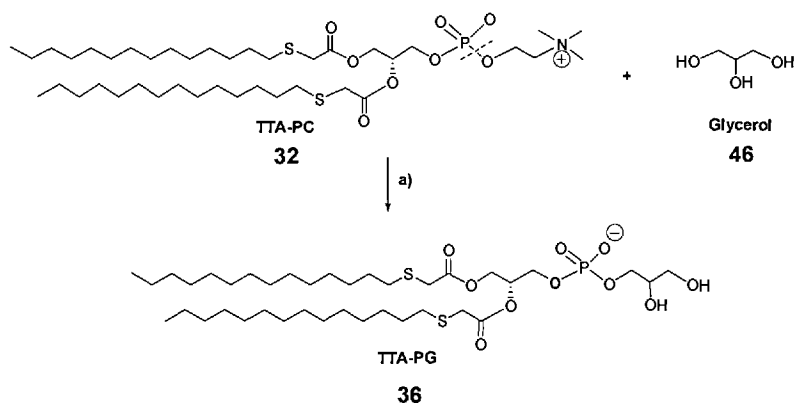
previously in our laboratory. The reaction was carried out as shown in **Scheme 13** and was easily followed by TLC. The sulfur on the fatty acid chain makes it liable to chemical changes such as oxidation and thus allows staining of the compounds by regular stains such as ammonium molybdate reagent. The product, TTA-PE **67**, was isolated after chromatography, in an excellent 95% yield.



a) Phospholipase D, hipsolv chloroform, buffer: NaOAc (100 mM), CaCl₂ (50 mM), pH 6.4, 30 °C, 95%

Scheme 13 Synthesis of TTA-PE **67**

Having validated our experimental procedure, TTA-PG was synthesised in a similar fashion (**Scheme 14**). The conditions were optimised using two units of enzyme per mmol of starting material and the desired product was isolated with a yield of 63% after silica gel chromatography.

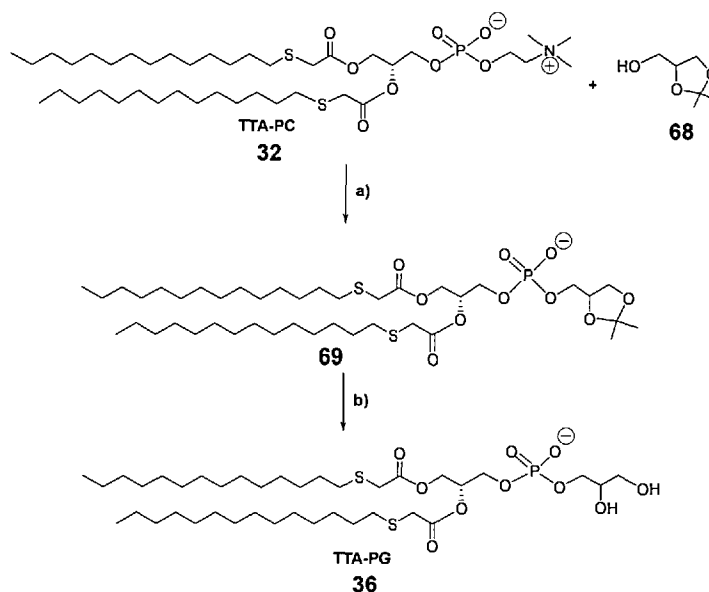


a) Phospholipase D, hipsolv chloroform, buffer: NaOAc (100 mM), CaCl₂ (50 mM), pH 6.4, 30 °C, 63%

Scheme 14 Synthesis of TTA-PG **36**

In an effort to improve the yield, the transphosphatidyltion was attempted with the protected acetal of glycerol **68** as it has a better solubility in chloroform (**Scheme 15**). The reaction proceeded smoothly and TTA-Pdioxolglycerol **69** was isolated with a

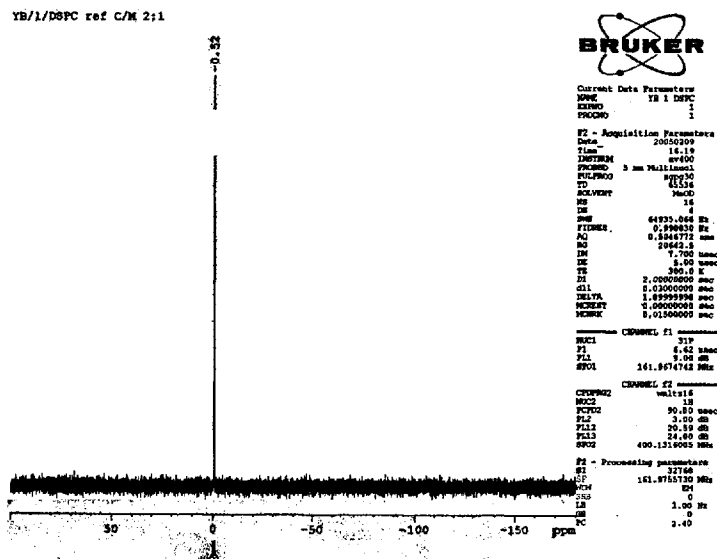
yield of 97%. The acetal was next cleaved using trifluoroacetic acid in dichloromethane. TTA-PG **36** was isolated with an overall yield of 67% over the two steps thus providing a slight improvement of the yield compared to the one-step synthesis of TTA-PG with unprotected glycerol.



a) Phospholipase D, hipersolv chloroform, buffer: NaOAc (100 mM), CaCl₂ (50 mM), pH 6.4, 30 °C, 97% b) TFA, DCM, 69%

Scheme 15 Synthesis of TTA-PG **36** in 2 steps

Proton and carbon NMR of phospholipids can be rendered difficult due to the overlap of many diagnostic signals and the splitting of peaks due to the phosphorus-carbon coupling. Hence, phosphorus NMR was used as an additional method of characterisation of the synthesised phospholipids. Decoupled ³¹P experiments were run, so each peak corresponds to one phosphorus atom. One example of a ³¹P NMR spectrum is shown in **Figure 40**.

Figure 40 ^{31}P NMR of DSPC

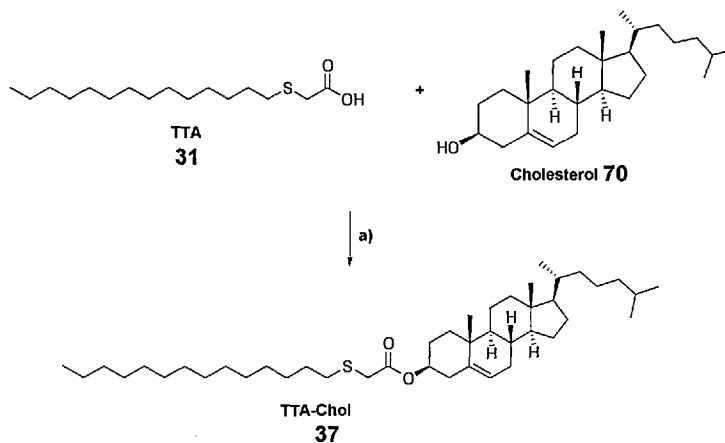
The ^{31}P chemical shifts, measured in ppm, are summarised in Table 6.

	<i>1,2-Distearoyl</i>	<i>1,2-TTA</i>
Phosphocholine	-0.52	-0.68
Lyso phosphocholine	-0.18	-0.17
Phosphoglycerol	-1.02	-1.41
Phosphodioxolaneglycerol	-3.20	X
Phosphoserinol	X	-0.93
Phosphoserine	-0.56	X

Table 6 ^{31}P NMR shifts in ppm

3.3.4 Synthesis of TTA-Chol 37

The last target, TTA-Chol **37**, consists in the direct coupling of TTA **31** with cholesterol **70**. This reaction was conducted using HBTU as coupling agent and DMAP as a nucleophilic catalyst, and TTA-Chol **37** was isolated with an excellent yield of 99% after chromatography on silica gel (Scheme 16).



a) HBTU, DMAP, anhydrous DCM, RT, 99%

Scheme 16 Synthesis of TTA-Chol

The mechanism for the synthesis of TTA-Chol is identical to the one for TTA-TAG (Scheme 6).

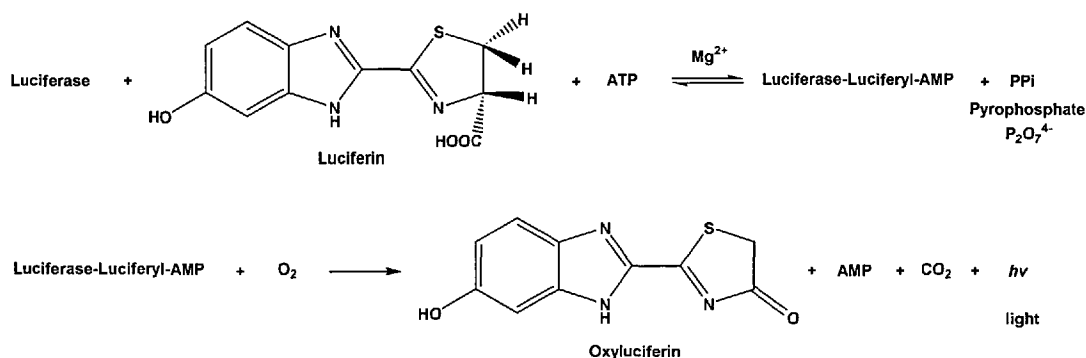
The novel lipid analogues *lyso* TTA-PC **34**, TTA-PSer **64**, TTA-PG **36** and TTA-Chol **37** were therefore successfully synthesised using the optimised conditions developed on preliminary model studies on the analogue DSPC **57**. Phospholipase A2 afforded the *lyso* TTA-PC in a good yield of 70% while transphosphatidylation with phospholipase D yielded both TTA-PSer **64** and TTA-PG **36** in good yields of 87% and 69% respectively. TTA-Chol **37** was obtained in 99% yield by the coupling between TTA **31** and cholesterol. The next step was to test the effects of the new compounds with respect to TTA.

3.3.5 Preliminary biology results with the four new analogues

3.3.5.1 Luciferase reporter gene assay

The activation of the three PPAR subtypes by the new lipids *lyso* TTA-PC **34**, TTA-PSer **64**, TTA-PG **36** and TTA-Chol **37** was studied *in vitro* using reporter gene assays. It is known that upon activation by potent ligands, PPARs regulate gene expression by binding to peroxisome proliferator response elements (PPREs) found in the promoter region of specific genes. Hence, a promoter sequence is linked to an easily detectable reporter gene such as that encoding for the firefly luciferase, and this offers a means to measure PPAR activity. Specifically, a plasmid containing genes encoding for each subtype of PPARs, as well as a luciferase reporter gene which has PPREs in the promoter region of the gene is transfected into human breast cancer MCF-7 cells. The firefly luciferase catalyses the bioluminescent oxidation of

luciferin in the presence of ATP, magnesium and oxygen (**Scheme 17**).¹⁹⁸ The luciferase protein complexes with the luciferin substrate to form a luciferyl-adenylate complex in the presence of magnesium ions and ATP. In the presence of oxygen, this complex is oxidised to oxyluciferin with the release of carbon dioxide and adenosine as well as a light emission with a wavelength of 560 nm. The measurement of the amount of luciferase protein expressed can be detected on a luminometer and is expressed in relative light units (RLU), which can be used to quantify the efficiency of the PPAR activation.



Scheme 17 The reaction catalysed by the luciferase enzyme found in *Photinus pyralis*

The advantages of the luciferase assay are the high sensitivity, the absence of luciferase activity inside most of the cell types, the wide dynamic range, rapidity and low costs.

The procedure, briefly outlined in **Figure 41**, was carried out as follows: human MCF-7 breast cancer cells were seeded at a density of 85,000 cells per well of a 12-well plate. The following day, they were transiently transfected using a peroxisome proliferator response element (PPRE)-luciferase reporter plasmid and DNA with the three subtypes of PPARs. The total amount of plasmid was kept constant at 2.65 μ g by compensating with pCMV-5 which is an empty expression plasmid. 24 hours after transfection, the cells were treated with the TTA analogues. After another 48 hours, the cells were washed once with PBS, lysed and the cell extracts were used for luciferase determination on a LUCY-1 luminometer. The luciferase assay was performed in accordance with the protocol of the Luciferase Assay Kit (BIO Thema AB, Sweden).

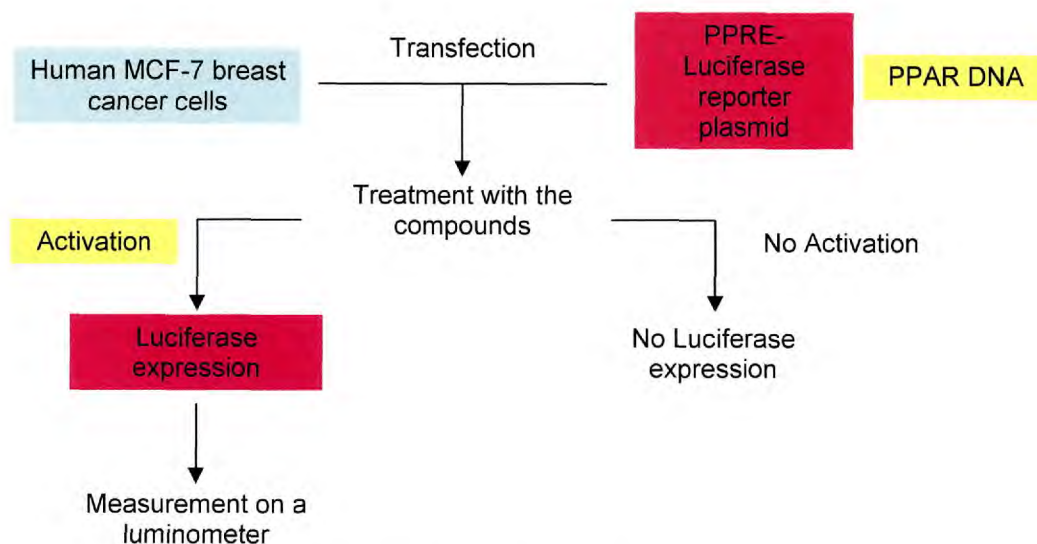


Figure 41 Luciferase reporter gene assay

3.3.5.2 PPAR activation assay results and discussion

First of all, cells used for the PPAR assays were checked for any endogenous PPAR activity through performing transfection in the absence of the PPAR DNA. In these conditions, no significant luciferase expression was detected. For each of the experiments, the control was done by carrying out the assay without treating the cells with any of the compounds. The following selective potent PPAR agonists, whose structures are given in **Figure 42**, were used as positive controls at concentrations of 1 μM or 30 μM : WY14.643 **71** for PPAR α , BRL49653 **20** (rosiglitazone) for PPAR γ , and L165.041 **14** for PPAR δ . Also, TTA, at different concentrations between 1 μM and 75 μM , was run in parallel in order to allow for comparison of the new lipid analogues. The compounds were prepared in serum solutions as they were insoluble in DMSO. Due to the very poor solubility of the lipid analogues TTA-PSer **64** and TTA-Chol **37**, only *lyso* TTA-PC and TTA-PG's activities could be tested. It was decided to run four to five different concentrations of the compounds (between 1 μM and 75 μM) to get a preliminary indication of their effects on the PPARs. Subsequently, the lowest concentration which gave activity as well as a higher concentration relative to the first one were selected. These experiments were performed nine times at these optimum concentrations. All results were normalised relative to the control and the standard deviation is calculated from the variability of the readings obtained for one compound at a particular concentration.

Sources of variability in cell work are usually due to several factors. The first one is the variability in the number of cells which occurs during the seeding process. Other

reasons are the unwanted dilution of DNA/transfection reagent or the unwanted dilution of the compound solutions which can happen during washing and treatment of cells. Cell lysis is handled one by one, hence differences may affect the results. Finally, pipetting errors can occur during the application of the cell lysates on the measurement plates. One last source of variability is due to the cell response itself. Indeed, cells may respond differently depending on the time they have been maintained in culture and how they have been handled. It is important to bear these factors in mind when analysing the data.

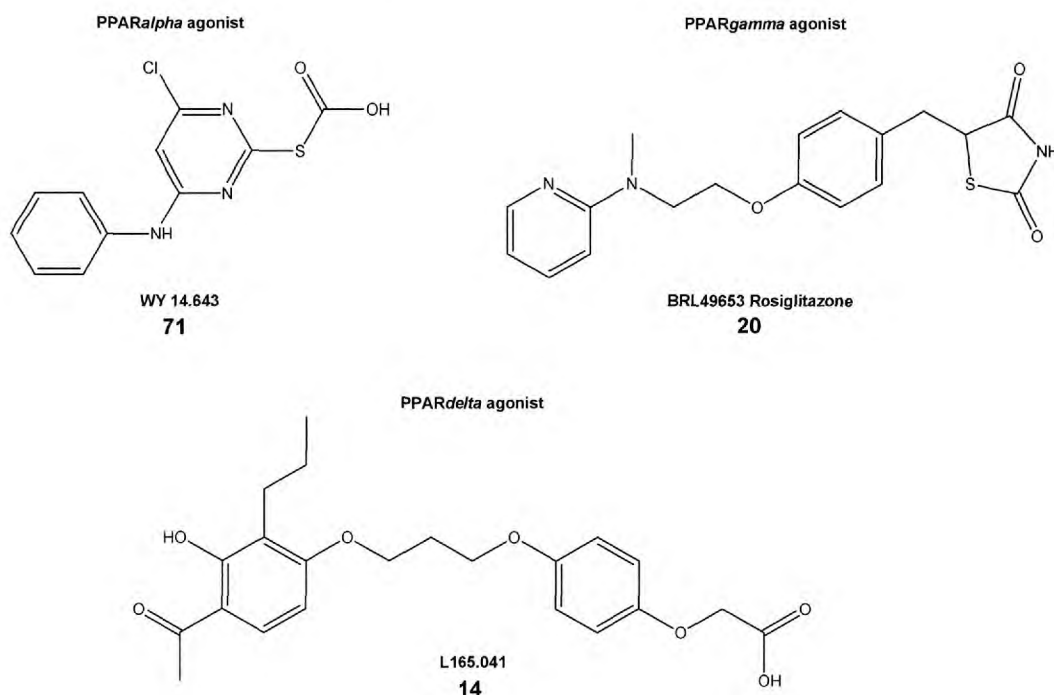


Figure 42 Specific PPAR agonists used as positive controls

The assays were carried out by Therese Røst under the supervision of Professor Rolf Berge at the Institute of Medicine, Bergen, in collaboration with Thia Medica AS.

If there is PPAR activation, a high expression of Luciferase relative to the control is expected. A high activity relative to the control at low concentrations indicates good potency. The lower the concentration, the better the compound since this means that a small dose of compound would be enough to activate the PPARs. This would reduce any toxicity problems or side-effects.

The preliminary PPAR activation results with *lyso* TTA-PC **34** and TTA-PG **36** are shown in **Figure 43**.

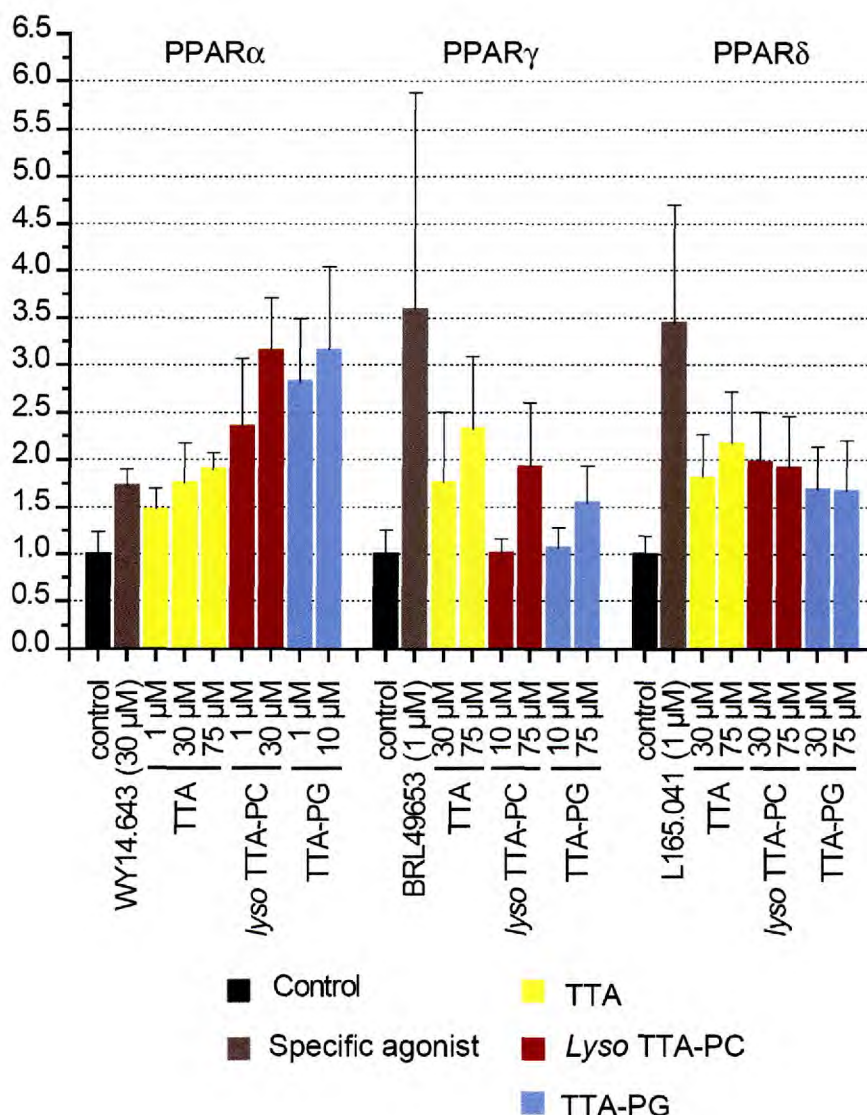


Figure 43 PPAR α , γ and δ activation results with *lyso* TTA-PC and TTA-PG

In the case of PPAR α , TTA's effect is more-or-less constant at the three different concentrations and close to the response induced by agonist WY14.643. *Lyso* TTA-PC dose dependently increased the activity, upto two-fold increase over the specific agonist WY14.643 at 30 μ M. TTA-PG increased PPAR α more than *lyso* TTA-PC at 1 and 10 μ M. A lower concentration of TTA-PG was enough to achieve the same effect on PPAR α compared to *lyso* TTA-PC. Overall, both new analogues activated PPAR α better than TTA itself, and TTA-PG was a better activator than *lyso* TTA-PC.

As can be expected, BRL49653 is a very potent agonist of PPAR γ and it leads to an increase of PPAR γ by three-fold relative to the control. The high variability in the response can be attributed to the factors previously discussed. The activation was dose-dependent with all the lipids and higher concentrations of 75 μ M had to be used to obtain significant activity. Neither *lyso* TTA-PC nor TTA-PG seemed to increase

the activity compared to TTA. In general, the lipids were not found to be potent activators of PPAR γ .

For PPAR δ , L165.041, the positive control, was found to increase PPAR δ activity by three-fold. *Lyso* TTA-PC and TTA-PG's effects on PPAR δ were comparable to that of TTA.

If we consider the whole set of results, we can conclude that *lyso* TTA-PC and TTA-PG activated the PPARs in the following order in human MCF-7 cells: $\alpha > \delta > \gamma$.

3.4 Summary

In order to improve the bioavailability of the PPAR activator, TTA **31**, two novel lipid analogues, TTA-PC **32** and TTA-TAG **33**, were synthesised as natural prodrugs. The release of the active compound, TTA, from the lipids is dependent on various hydrolytic enzymes present in the body: phospholipases A1, A2 and lipases. Preliminary *in vivo* experiments carried out with these two analogues showed an improvement in the beneficial effects in rats. In particular, the levels of plasma triacylglycerol, cholesterol and hepatic triacylglycerol levels were measured after treatment with the different compounds. TTA, TTA-PC and TTA-TAG showed a decrease in plasma triacylglycerol, cholesterol and hepatic triacylglycerol levels, with the largest decrease being affected by TTA-PC. Fatty acid oxidation and the activity of key mitochondrial enzymes involved in fatty acid oxidation and transport were also measured as these are very important dysfunctions in the metabolic syndrome and diabetes type II. Hence, the activities of fatty acid palmitoyl-CoA, carnitine palmitoyl transferase-II, 3-hydroxy-3-methylglutaryl-CoA synthase and fatty acyl-CoA were measured. In all cases, TTA and TTA-PC showed significant activity, whereas TTA-TAG was slightly less effective in general. It must be highlighted that TTA-PC considerably improved the activity of the key enzymes by nearly two-fold compared to TTA.

Having these promising results in hand, four further analogues were synthesised using enzymatic reactions. Starting from TTA-PC **32**, phospholipase A2 afforded *lyso* TTA-PC **34** in a good yield of 70% while transphosphatidylation with phospholipase D and serinol or glycerol yielded TTA-Pser **64** and TTA-PG **36** in good yields of 87% and 69% respectively. TTA-Chol **37** was obtained in 99% yield by the coupling between TTA **31** and cholesterol. The *in vitro* PPAR activation of the new lipid analogues was tested using a luciferase reporter gene assay at the Institute of

Medicine in Norway. Due to solubility and formulation issues, only lyso TTA-PC and TTA-PG could be tested *in vitro*. Preliminary results showed that both lyso TTA-PC and TTA-PG are promising compounds, displaying good activity relative to parent compound TTA. In human MCF-7 cells, the PPARs were activated in the following order by the two new lipids: $\alpha > \delta > \gamma$. Their effects *in vivo* now need to be assessed.

CHAPTER 4

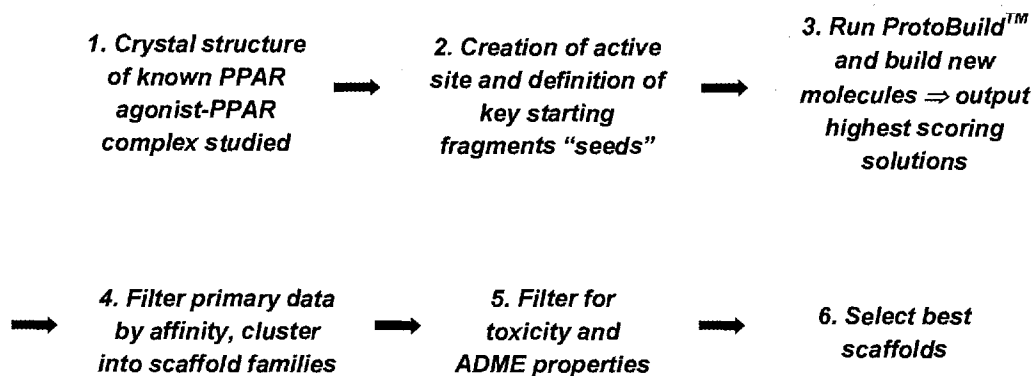
Synthesis of novel heterocyclic leads

4.1 Identification of leads by *de novo* design

Novel heterocyclic leads were designed as potential PPAR dual α/γ agonists using a *de novo* approach developed by Prosarix Ltd, an *in silico* screening company based in Cambridge, UK. ProtoBuild™ is proprietary software used to create novel drug-like chemical scaffolds and it provides an alternative method of developing lead-like hits. This technology offers the following advantages:

- engineering of novel scaffolds using chemical features present in known active compounds;
- better specificity than the screening of candidates; and
- design of higher affinity-compounds compared to the screening of pre-existing catalogues.

ProtoBuild™ is the only *de novo* design tool that incorporates a flexible binding site model, a pharmacophore-driven scaffold generation and a fast consensus scoring approach. It is outlined in **Flowchart 1**.



Flowchart 1 Prosarix Ltd's Protobuild™ approach

First of all, the crystal structure of a known dual PPAR α/γ agonist GI262570 complexed with PPAR γ was studied (**Figure 44**).¹⁹⁹ Two main interactions were found to be important: a carboxylic acid moiety maps well into the H-bond donor site whilst an aromatic ring fits well into the main hydrophobic site. Analysis of this LBD and also of the LBD of PPAR α enabled a hypothesis for a pharmacophore required to design dual agonists. The critical interactions with the LBDs were used to define the binding site for new structures' determination and this provides the starting "seeds" which are key fragments for the binding. Next, ProtoBuild™ was used to build novel molecules which fit into the defined binding site, growing the molecules from the starting "seeds" into the pharmacophore features defined. This consists of doing separate

ProtoBuild™ runs (containing a library of 93 fragments to grow into the pharmacophore features). Ten separate runs were conducted and the resulting output molecules (about 1000 per run) were ranked for affinity and clustered into scaffold families. Next, they were filtered for toxicity substructures and ADME properties (e.g. Lipinski descriptors²⁰⁰) in order to choose the molecules with the best drug-like properties. ADME properties are very important in drug design as they give a preliminary indication on the absorption, distribution, metabolism and elimination of the drug in the body. Even if a compound is very potent, it may not become a drug if it suffers from poor ADME. The filters used included the molecular weight, the solubility, the number of hydrogen bond acceptors and donors and the calculated log octanol/water partition coefficient predictions (clogP which is a measure for the lipophilicity of a compound).²⁰¹ The process resulted into two distinct drug-like chemical scaffolds as potential dual PPAR α/γ agonists.

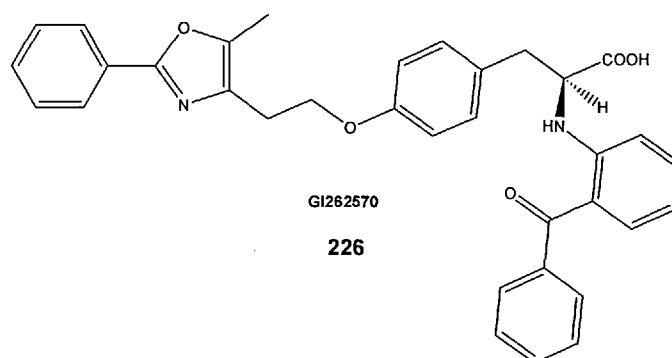


Figure 44 Structure of GI262570

The first scaffold consists of an indole core with different aromatic groups, R_1 , on the 2-position of the indole and an ethoxy propanoic side chain at the 5-position, with R_2 being a methyl or a trifluoro group (**Figure 45**). There is one chiral centre *alpha* to the carboxylic acid moiety. A racemic synthesis will be explored first to test for the activity of the indole leads. The screening study suggested the synthesis of molecules **38** to **43**, with $R_1 = \text{H}$, phenyl and naphthylmethyl groups (**Figure 46**). Indoles **38** and **39** would allow us to measure the importance of the aryl group for the binding to the receptor in the secondary hydrophobic site.

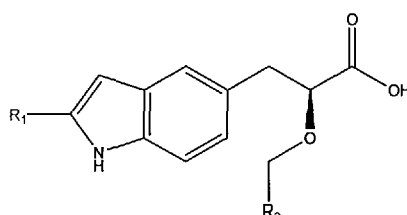


Figure 45 Indole scaffold

The ProtoBuild™ runs show that the indole ring can be tolerated in the ligand binding domains of both PPAR α and PPAR γ (Figure 47). The 2-naphthylmethyl group fits into the hydrophobic site at the entrance of the pocket; the indole ring fits into the main hydrophobic one while the carboxylic acid fits into the hydrogen bond donor site. As explained in Chapter 1, the ligand binding domains of PPAR α and PPAR γ are similar in size, allowing such type of agonists to be developed.

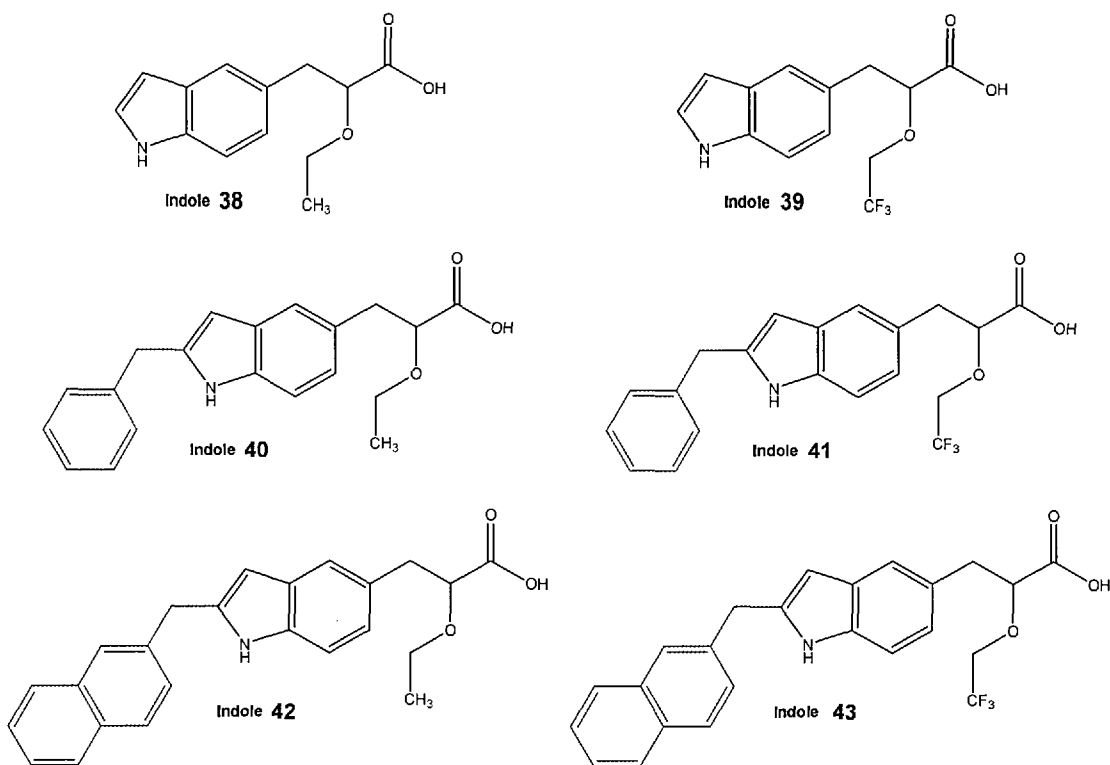


Figure 46 Indole leads 38 to 43

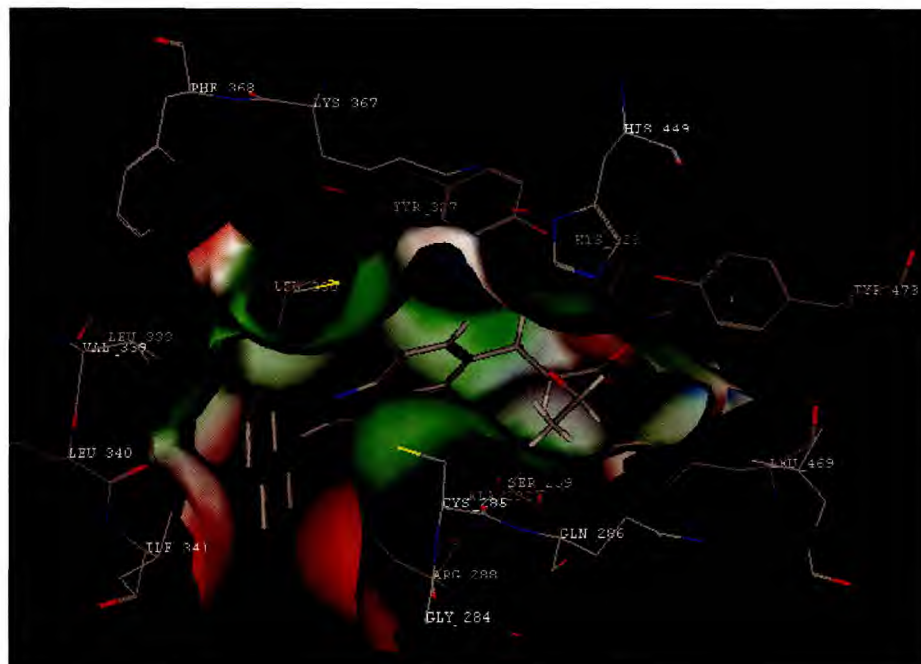


Figure 47 Proposed interaction of indole **42** with PPAR γ

The objective is to synthesise these indole-core molecules and test their potential *in vitro* and *in vivo* as PPAR α/γ dual agonists in the aim of developing new treatments for metabolic as well as neurological diseases.

4.2 Synthesis of the indole scaffold

4.2.1. Indole scaffold: retrosynthesis and envisaged strategy

The retrosynthesis envisaged for the indole leads is outlined in **Figure 48**. This convergent synthesis allows for the introduction of the aryl (R_1) group on the 2-position of the indole in the last step of the synthesis. Indeed, a linear strategy would be employed to prepare precursors **75** and **76** from *para*-nitrophenylpyruvic acid **77** and in the meantime, the different carbonyl compounds **72** to **74** would be prepared, allowing a convergent Fischer Indole synthesis in the last step to give the six different indole targets **38** to **43**.

Scheme 18 illustrates the proposed forward enantioselective synthesis. *Para*-nitrophenyl pyruvic acid **77** would have to be prepared first from *para*-nitrophenylacetic acid **78** using a methodology developed by Wasserman *et al.*²⁰² The next step consists of a stereoselective reduction of the α -keto acid **77** into the corresponding α -hydroxy acid **80** using the following enzyme, staphylococcus epidermis D-lactate dehydrogenase.^{203,204} The ethers **81** and **82** are to be synthesised using the corresponding halide and silver oxide.²⁰⁵ Reduction of the nitro group into the primary amine by hydrogenation over Pd/C would afford amines **78** and **84** which will be converted into the corresponding hydrazines **75** and **76** using concentrated hydrochloric acid, sodium nitrite and tin(II) chloride.²⁰⁶ This reaction goes through the formation of the diazonium salt which is subsequently reduced into the hydrazine with tin(II) chloride. The final step consists of a Fischer Indole synthesis with carbonyl compounds **72-74** using zinc(II) chloride as catalyst.¹⁷⁶

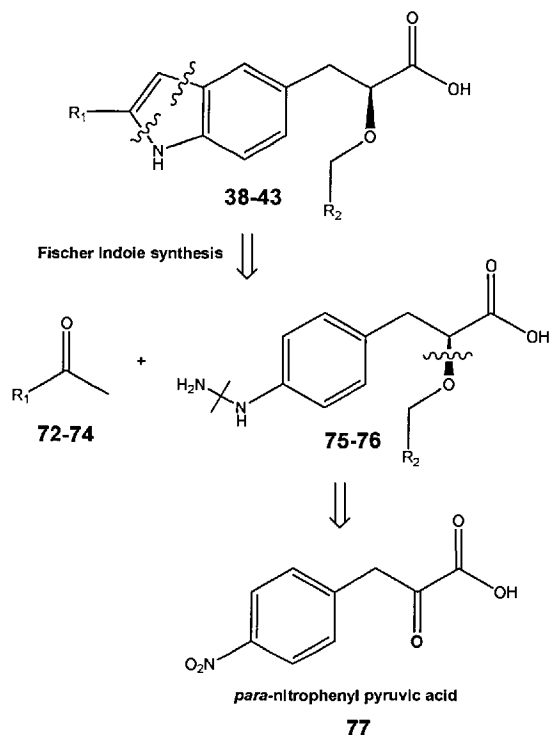
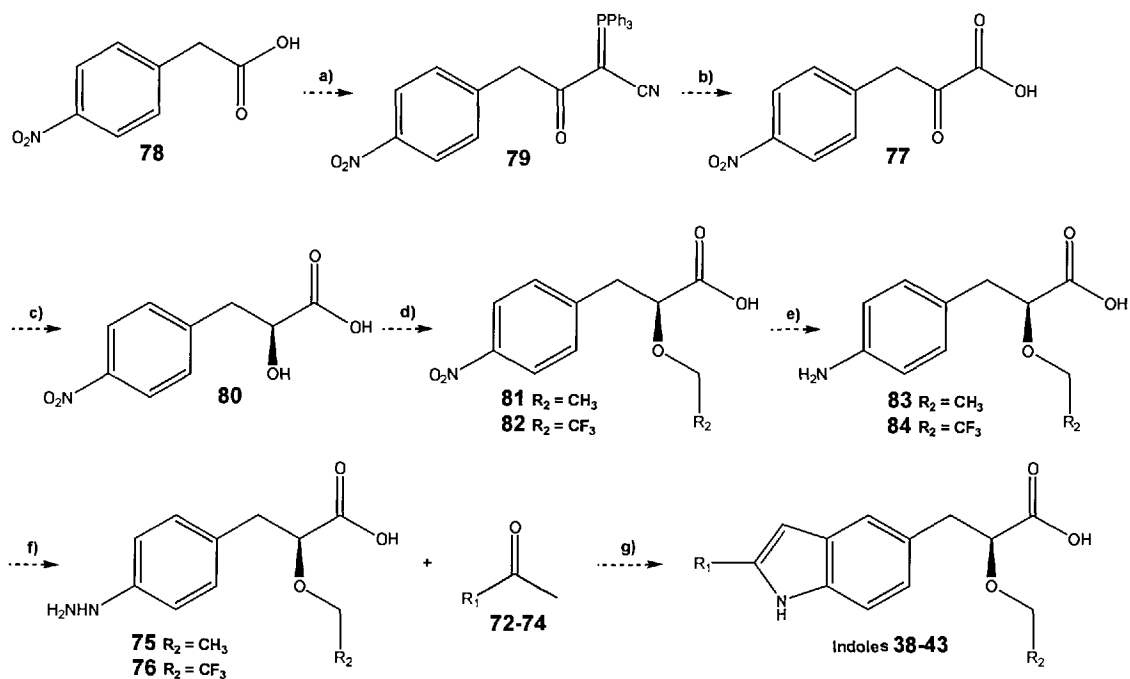


Figure 48 Retrosynthesis envisaged for the indole leads



a) PPh_3CHCN , EDCI, DMAP, dry DCM b) 1. O_3 , dry DCM 2. N_2 , THF/ H_2O c) *Staphylococcus epidermis* D-lactate dehydrogenase d) Ag_2O , R_2 e) H_2 , Pd/C f) 1. NaNO_2 , *conc.* HCl 2. SnCl_2 , g) ZnCl_2 , EtOH, reflux

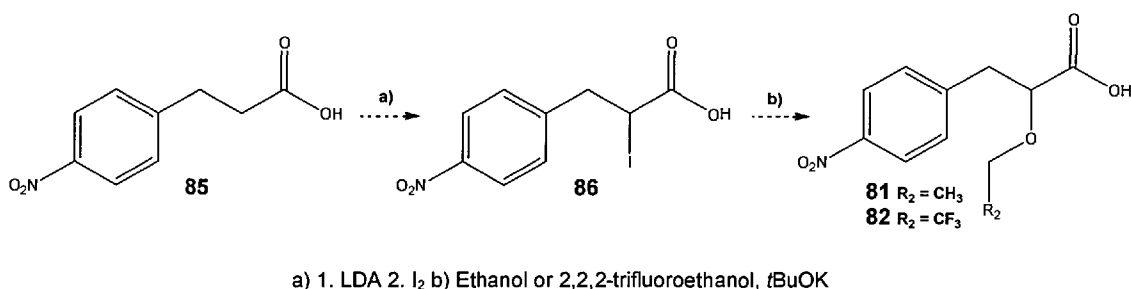
Scheme 18 Proposed forward enantioselective synthesis of indoles **38-43**

4.2.2. Synthesis of the indole leads: 1st synthetic approach

A racemic synthetic approach to the indole products was first explored since this would allow us to optimise the key steps of the synthesis and still provide a compound that could be tested for its pharmaceutical activity.

4.2.2.1. Racemic synthesis of the precursor to the Fischer indole synthesis

In the case of the racemic synthesis, we adopted a slight change of strategy to synthesise ethers **81** and **82** in order to reduce the total number of synthetic steps. Thus, we chose to start the synthesis with iodination of commercially available *para*-nitrophenylpropanoic acid **85** (Scheme 19).^{207,208} Transformation of the resultant iodide **86** to the corresponding ethers **81** and **82** can be effected by treatment with potassium *tert*butoxylate and ethanol or 2,2,2-trifluoroethanol respectively and the synthesis can be completed as proposed in Scheme 18.

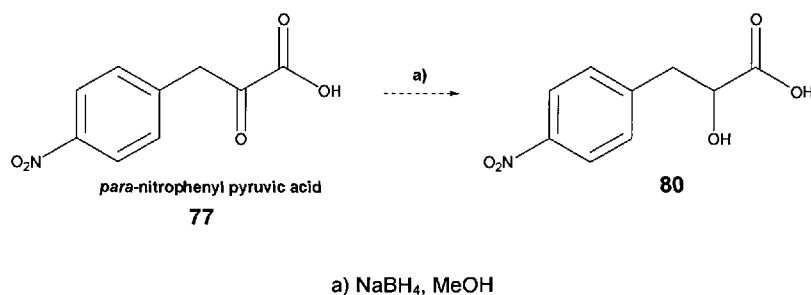


Scheme 19 Proposed route to the racemic synthesis of precursors **81** and **82**

The synthesis began by iodinating acid **85** with two equivalents of lithium diisopropylamine and iodine in dry THF, under anhydrous conditions. To a solution of LDA in THF at -78 °C, was added starting material **85**. The reaction mixture was allowed to warm up to room temperature and then added dropwise to a solution of iodine in THF at -78 °C. Initial experiments were carried out with commercially available LDA solution in heptane/THF/ethyl-benzene. The reaction was repeated with varying experimental conditions: the number of equivalents of LDA and the reaction time were increased. However, the reaction did not afford any product **86**. The use of *in situ* synthesised LDA from freshly distilled diisopropylamine and *n*-BuLi did not yield any product either.

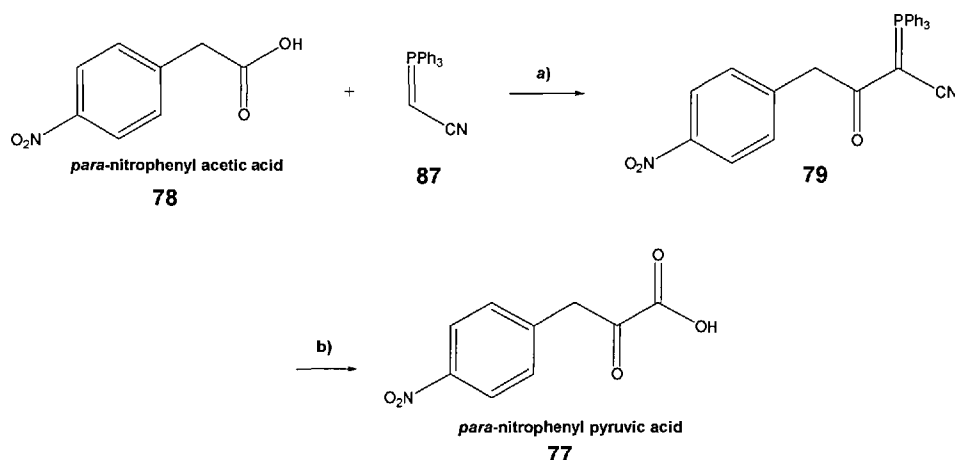
In view of this lack of success, it was decided to synthesise ethers **81** and **82** from *para*-nitrophenylpyruvic acid **77** as for the enantioselective synthesis shown in

Scheme 18. Reduction of α -keto acid **72** into the racemate α -hydroxy acid **80** can be done using sodium borohydride in methanol.



Scheme 20 Reduction into α -hydroxy acid **80** using NaBH_4

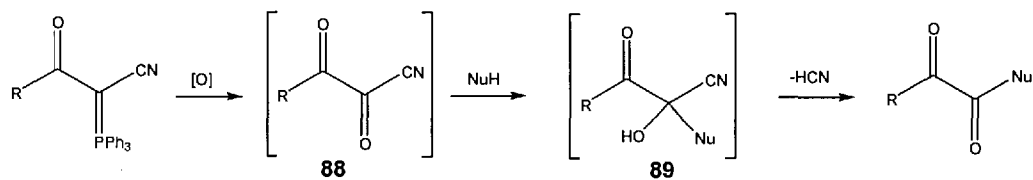
The first step required preparation of *para*-nitrophenylpyruvic acid **77** from commercially available *para*-nitrophenyl acetic acid **78** (**Scheme 21**). Thus, acid **78** was coupled to triphosphoranylidene acetonitrile **87**, using EDCI as coupling agent and a catalytic amount of DMAP affording the new phosphorane **79** in 82% yield.^{202,209} Ozonolysis of phosphorane **79** in dry DCM at -78°C , followed by quenching with THF/ H_2O yielded the desired product **77** with a yield of 60% on small scale reactions.



a) EDCI, DMAP, dry DCM, 0°C to RT, 22 hr, 82% b) 1. O_3 , dry DCM, -78°C , 20 min 2. N_2 , THF/ H_2O , -78°C to RT, 24 hr, 60%

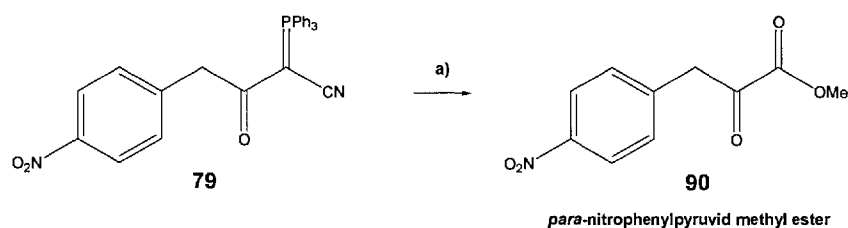
Scheme 21 Synthesis of *para*-nitrophenyl pyruvic acid **77**

Cyano keto phosphoranes undergo ready oxidation to the highly electrophilic vicinal diketo nitrile **88**, which can be trapped by reaction with nucleophiles to give transient cyanohydrin **89** (**Scheme 22**). These undergo facile elimination of HCN to form α -keto acids, esters and amides.



Scheme 22 Mechanism of ozonolysis

However, the purification of acid **77** proved tedious. Crystallisation was unsuccessful and chromatography on silica gel had to be employed. Hence, it was decided to synthesise methyl ester **90** by conducting the ozonolysis in DCM/methanol, in order to render the purification easier (**Scheme 23**). Furthermore, a protected ester moiety would be much easier to carry forward in the synthesis than a more reactive acid.



a) 1. O₃, DCM/MeOH, -78 °C, 30 min 2. N₂, -78 °C to RT, 16 hr, 35%

Scheme 23 Synthesis of the methyl ester **90**

Indeed, the methyl ester **90** was easier to purify by chromatography, however the yield from the ozonolysis was less good (35% compared to 60%). Only the enol form was observed by NMR. This could be explained by the excellent delocalisation as shown in **Figure 49**. This observation is in accordance with similar reports in the literature.²¹⁰

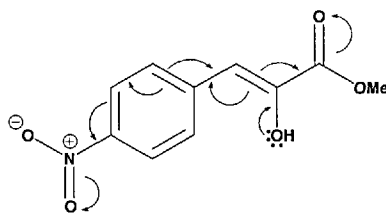
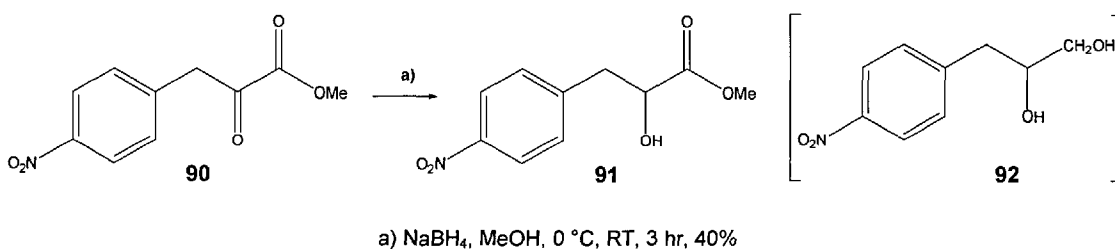


Figure 49 Stabilisation of the enol form by mesomeric effects

In order to improve the overall synthesis of *para*-nitrophenylpyruvic methyl ester **90**, solid phase chemistry was employed in the coupling reaction between *para*-nitrophenylacetic acid **78** and triphosphoranylidene acetonitrile **87**. This should help with the purification of the intermediate phosphorane **79**. Different reaction conditions were tested employing EDCI and DMAP resins. The use of DMAP resin greatly

improved the ease of crystallisation of the phosphorane **79** and pure white crystals were obtained in an excellent yield of 94%. The reaction time of the ozonolysis step was also reduced slightly and purification of α -keto ester **90** was made easier by utilising a silver nitrate work up which decomposes any cyanohydrin **89** left. A yield of 40% was obtained for the ozonolysis step.

The reduction of α -keto ester **90** into the corresponding α -hydroxy ester **91** was carried out using sodium borohydride in methanol, affording the product in a yield of 40% (**Scheme 24**).^{210,211,212} No diol **92** was obtained as observed in the literature.²¹³



Scheme 24 Reduction into the α -hydroxy ester **91**

Efforts to improve the yield of the reduction consisted firstly of the use of solid phase chemistry and secondly, of a one-pot ozonolysis-reduction. Two different resins (polystyrylmethyl)trimethylammonium cyanoborohydride (resin 1) and (polystyrylmethyl)trimethylammonium borohydride (resin 2) were tried but neither of them yielded the product in a satisfactory yield (**Figure 50**). Yields of less than 5% were obtained.

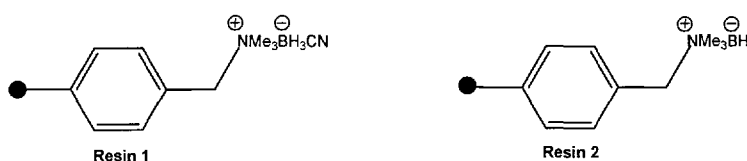
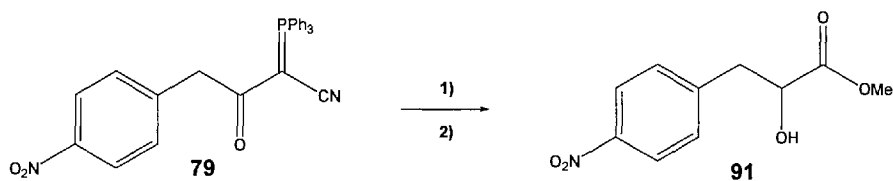


Figure 50 Resins used for solid phase reductions

In the case of the one pot ozonolysis-reduction (**Scheme 25**), one equivalent of sodium borohydride was added to the reaction mixture after the ozonolysis; however, α -hydroxy ester **91** was isolated in only 12% yield.

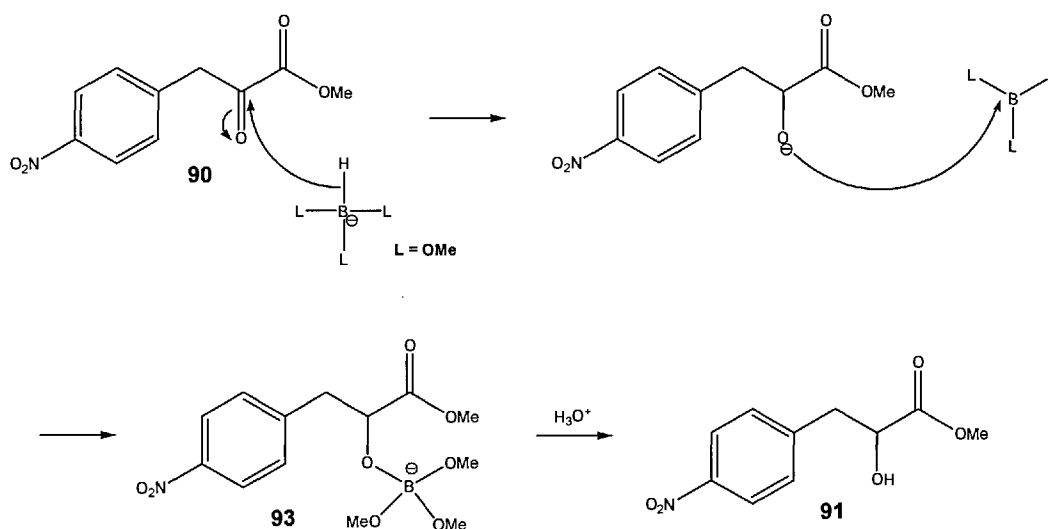


a) 1. O_3 , DCM/MeOH 7:3, -78°C , 30 min 2. N_2 , 3.5 hr b) NaBH_4 , -78°C to RT, 3 hr, 12%

Scheme 25 One pot ozonolysis-reduction

It was therefore decided to proceed with the two steps consecutively, *i.e.* to isolate *para*-nitrophenylpyruvic methyl ester **90** and subsequently carry out the reduction. Experiments to optimise the yield of the reduction focussed on changing the following conditions: number of equivalents of NaBH_4 , the temperature of the reaction, and the order of addition of the starting material and NaBH_4 to MeOH . Thus, the yield was greatly increased from 40 to 66% by adding 1.4 equivalents of sodium borohydride in one portion to the α -keto ester **90** in anhydrous methanol at 0°C and allowing the reaction to stir at 0°C for 2 hours.

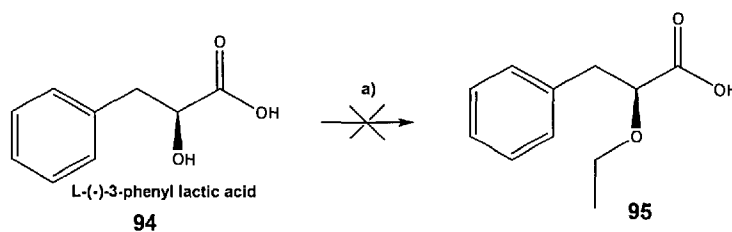
The proposed mechanism of the reduction is outlined in **Scheme 26**. The hydride atoms of sodium borohydride are displaced by the methoxy groups from methanol. The first step is a hydride transfer from the reducing agent to the carbonyl group. The oxyanion produced can help stabilise the electron-deficient BL_3 molecule, giving rise to alkoxyborate intermediate **93**, hydrolysis of which gives the α -hydroxy ester **91**.²¹⁰



Scheme 26 Reaction mechanism for the reduction using NaBH_4

The next step was the synthesis of the ether using the corresponding halide and silver(I) oxide.²⁰⁵ This reaction was first modelled on a commercially available analogue, L-(-)-3-phenyllactic acid **94**. The latter was refluxed with ethyl iodide and

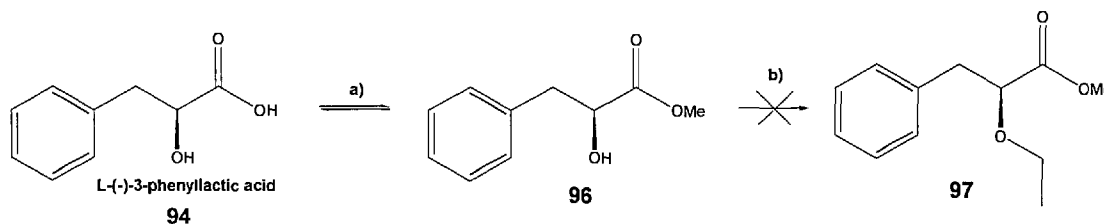
silver(I) oxide in dry DMF (**Scheme 27**). Silver(I) oxide weakens the C-I bond of ethyl iodide and leads to its fission. Silver(I) iodide thus precipitates, and the nucleophilic hydroxyl group of acid **94** reacts with the electrophile. Silver(I) hydroxide is produced and it forms a salt with the carboxylic acid. However, no product was obtained. The reaction was also unsuccessfully attempted in solvent free conditions.



a) Ethyl iodide, Ag₂O, anhydrous DMF, reflux at 100 °C, 5 hr

Scheme 27 Ether synthesis using silver oxide

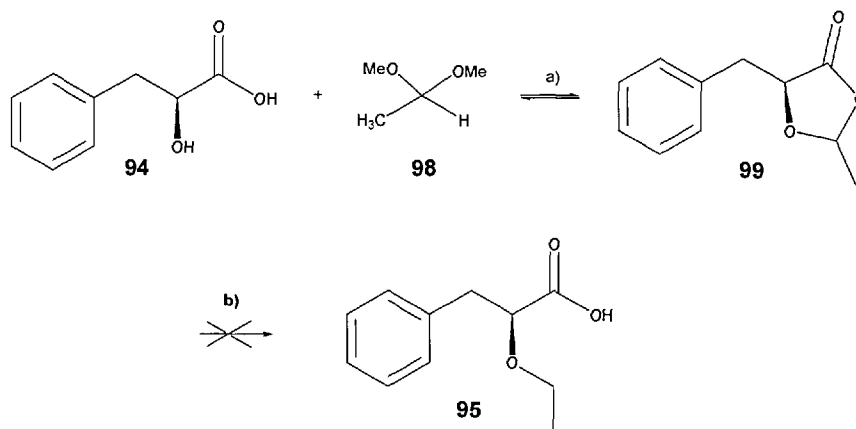
Next, the ether synthesis was attempted on the methyl ester **96**, readily prepared from acid **94** in 76% yield, in order to avoid any side reactions associated with the acid moiety.



a) MeOH, H⁺, RT, 18 hr, 76% b) Ethyl iodide, Ag₂O, anhydrous DMF, 60-65 °C, 6 hr

Scheme 28 Conversion into methyl ester **96**, followed by the synthesis of ether **97**

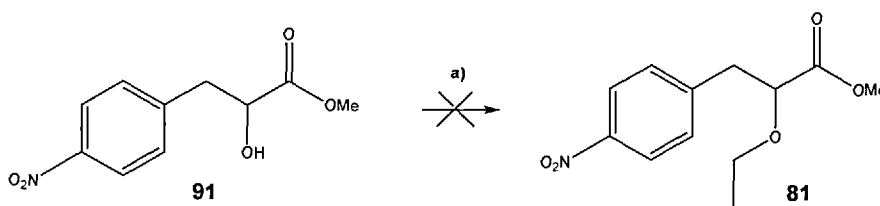
A trace amount of product was observed (mass spectrometry, ¹H NMR) but the yield could not be improved. One possible explanation for the poor success of this reaction could be due to loss of water from the ethoxypropanoate side-chain to give a fully conjugated system. It was therefore decided to attempt the ether formation through the synthesis of an acetal which would block prevent elimination of the alkoxy side chain, followed by opening of the acetal using a Grignard reagent as shown in **Scheme 29**.^{214,215} The starting material **94** was treated with acetaldehyde dimethyl acetal **98** and a catalytic amount of pyridinium *p*-toluene sulfonate using Dean Stark conditions. The crude product **99** was used directly in the second step where it was treated slowly with the Grignard reagent, *tert*-butylmagnesium chloride. However, NMR analysis of the crude did not reveal the presence of any product.



a) H^+ , anhydrous toluene, Dean Stark set-up, molecular sieves 4Å, reflux, 3.5 hr b) *t*-BuMgCl, anhydrous ether, molecular sieves 4Å, RT, 1 hr

Scheme 29 Ether synthesis by opening the acetal **99** with a Grignard reagent

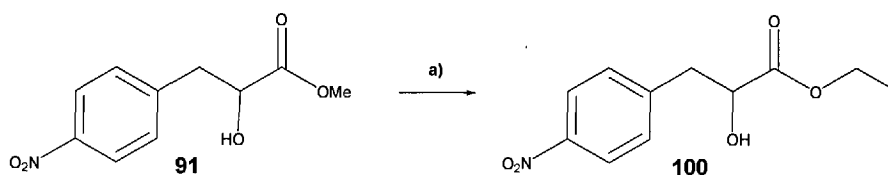
Finally we decided to synthesise ether **81** using a basic alkylation procedure with sodium hydride and ethyl iodide as outlined in **Scheme 30**. The main concern with this step is that the α -hydroxy ester **91** is prone to elimination under the basic alkylation conditions. Moreover, the presence of the electron withdrawing nitro group in *para* position would make the benzylic protons more acidic, further increasing the risk of elimination under basic conditions.



a) NaH, ethyl iodide, anhydrous DMF, 80 °C, 19 hr

Scheme 30 Ether synthesis using sodium hydride and ethyl iodide

After the reaction was carried out on α -hydroxy ester **91** and purification of the crude, the presence of a broad doublet integrating for one proton at 2.98 ppm by 1H NMR in $CDCl_3$ was observed. When the NMR was run in MeOD, this peak disappeared, confirming it was a hydroxyl group. The reaction had yielded the ethyl ester **100** as shown in **Scheme 31**.



a) NaH, ethyl iodide, anhydrous DMF, 80 °C, 19 hr, 34%

Scheme 31 Transesterification observed

The transesterification could be explained by the presence of traces of water in the solvent which could have reacted with sodium hydride to form sodium hydroxide *in situ*. The sodium hydroxide could have saponified the methyl ester to give the corresponding acid which would be susceptible to transesterification. The reaction was therefore repeated using rigorously dried, anhydrous DMF. In this case, the crude NMR indicated a complex mixture and no product could be identified or isolated after chromatography. The different side products possible could be due to deprotonation *alpha* to the carbonyl, followed by O- and/or C-alkylation with ethyl iodide or deprotonation of the benzylic proton, followed by elimination. The use of a milder base such as sodium *tert*-butoxide or of phase transfer alkylation conditions might have been better conditions to investigate. Other alternatives could have included a Horner Wadsworth Emmons coupling from aldehyde **101** and phosphonoacetate **102**, followed by reduction of the double bond or the insertion of a rhodium-generated carbenoid from diazo **103** into ethanol (**Figure 51**).

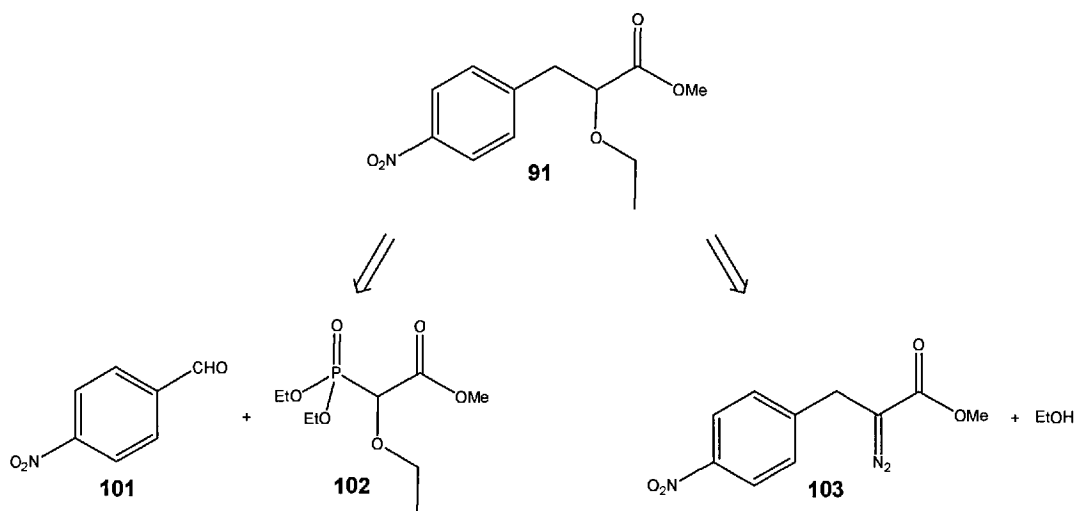
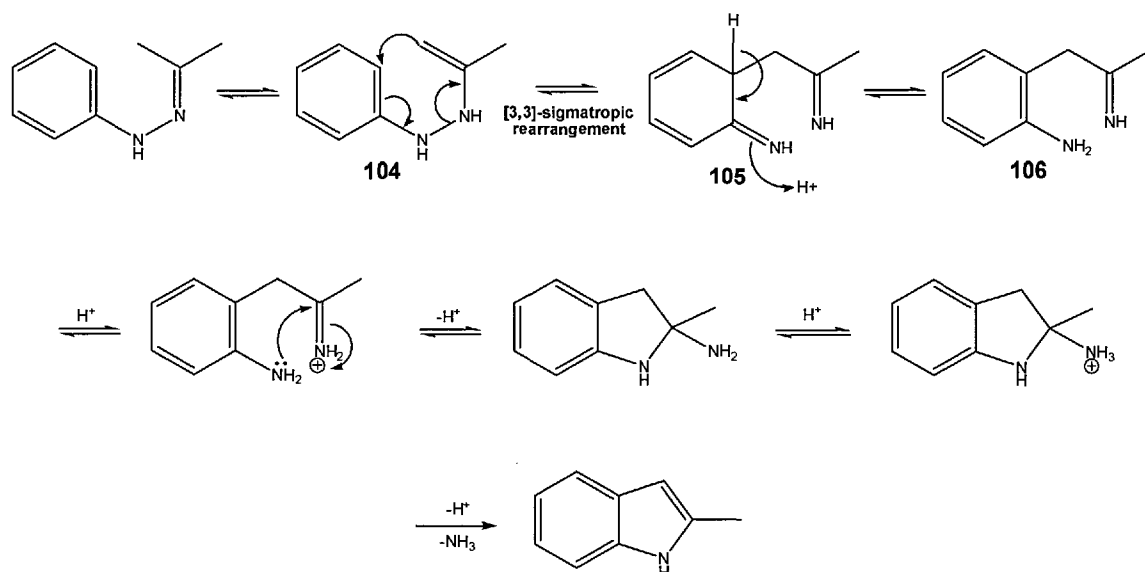


Figure 51 Other alternative routes for the synthesis of the ether **91**

4.2.2.2. Hydrazine formation and Fischer Indole synthesis

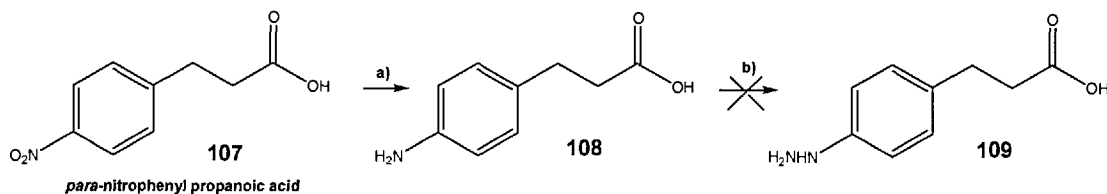
In parallel to the above efforts, some preliminary work was conducted on the Fischer indole reaction of the synthesis. The proposed mechanism for the Fischer Indole synthesis is shown in **Scheme 32**. The mechanism involves a [3,3]-sigmatropic rearrangement of an ene hydrazine tautomer **104** to give intermediate **105** which spontaneously cyclises by loss of ammonia, probably *via* indoline **106**. The reaction is driven forward by the loss of ammonia and the formation of an aromatic indole.



Scheme 32 Mechanism for the Fischer Indole synthesis

Initial model experiments were carried out on commercially available *para*-nitrophenylpropanoic acid **107** (**Scheme 32**). The first step was the preparation of the primary amine **108** by reduction of the nitro group by hydrogenation over Pd/C at room temperature over 15 hours. TLCs clearly indicated complete conversion of the starting material into the amine and the ninhydrin stain showed its presence by revealing a strong pink spot. Thus, amine **108** was afforded in an excellent yield of 99%.

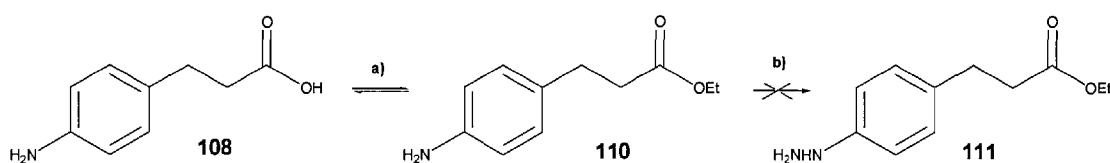
The next step was to prepare hydrazine **109**. This reaction proceeds through the formation of the diazonium salt which is next reduced into the hydrazine by tin(II) chloride.^{216,217,218} An NMR of the crude reaction in D₂O revealed the presence of a complex mixture of products which proved difficult to purify or to identify any desired product **109**. The strongly acidic conditions of the reaction lead to the formation of salts which makes it more difficult to purify the crude.



a) H_2 , Pd/C, RT, 15 hr, 99% b) 1. $\text{NaNO}_{2(\text{aq})}$, conc HCl, -5°C , 30 min 2. SnCl_2 , conc HCl, 0°C to RT, 3.5 hr

Scheme 33 Synthesis of hydrazine **109** *via* formation of the diazonium salt

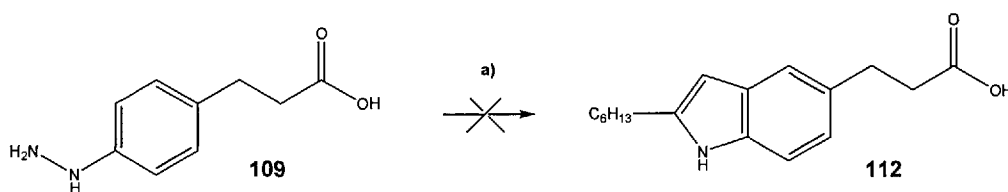
It was decided to synthesise ethyl ester **110** from amine **108** first in order to render the purification of the hydrazine easier (**Scheme 34**). However, the hydrazine formation on ester **110** led to a complex mixture of products and the desired hydrazine **111** could not be isolated.



a) EtOH, H^+ , RT, 21 hr, 30% b) 1. $\text{NaNO}_{2(\text{aq})}$, conc HCl, -5°C , 30 min 2. SnCl_2 , conc HCl, 0°C to RT, 3.5 hr

Scheme 34 Esterification of amine **96**

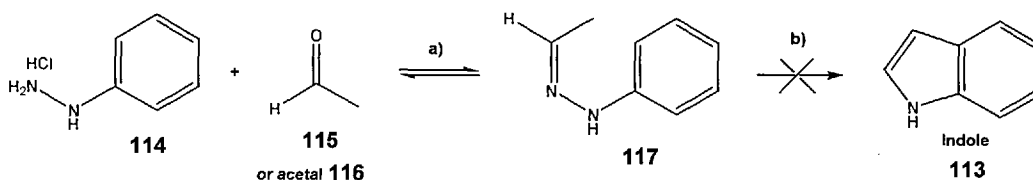
In further model studies, the Fischer Indole synthesis was attempted on the crude hydrazines **109** with octanal, with and without a Lewis acid catalyst (**Scheme 35**).²¹⁹ Both protic acids such as dilute sulphuric acid²²⁰ and acetic acid and a Lewis acid such as zinc chloride were employed. However, no indole product **112** was afforded in any of the various reactions attempted; complex mixtures were obtained, often giving a dark insoluble gum probably as a result of aldehyde polymerisation.



a) Octanal, H^+ , EtOH/ H_2O 5:1, reflux, 14 hr

Scheme 35 Fischer Indole synthesis with octanal

At this stage, it was decided to attempt the synthesis of unsubstituted indole **113** using the Fischer Indole synthesis and evaluate different reaction conditions (**Scheme 36**).



a) H^+ , 65 °C, 3 hr b) EtOH/H₂O 5:1, 80 °C, 14 hr

Scheme 36 Indole synthesis from phenyl hydrazine hydrochloride

The first step was to prepare hydrazone **117** from commercially available phenyl hydrazine hydrochloride **114** and acetaldehyde **115** or acetaldehyde dimethyl acetal **116**. The acetal is sometimes preferred as it is easier to handle (not volatile like acetaldehyde) and also to avoid self-condensation. The conditions used for the preparation of the hydrazone **117** are summarised in **Table 7**.²²¹

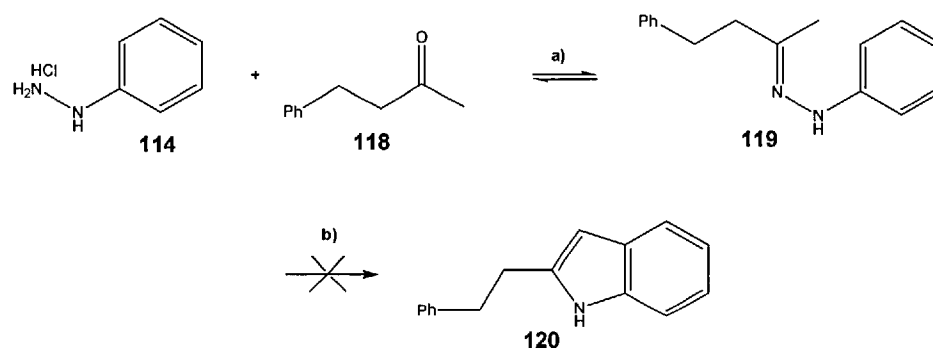
	<i>Reagent</i>	<i>Conditions</i>	<i>Solvent</i>	<i>Reaction time</i>
1	Acetal	35% aq. HCl, RT	MeOH/H ₂ O 1:1	15 hours
2	Acetal	Drops of glacial AcOH, 70-80 °C	EtOH	15 hours
3	Acetaldehyde	RT	ACN/H ₂ O 1:1	1 hour
4	Acetaldehyde	0.1% AcOH, RT	ACN/H ₂ O 1:1	1 hour
5	Acetaldehyde	RT	ACN/H ₂ O 1:1	15 hours
6	Acetaldehyde	0.1% AcOH, RT	ACN/H ₂ O 1:1	15 hours
7	Acetaldehyde	1. RT 2. 40 °C	<i>d</i> -CHCl ₃	5 hours
8	Acetaldehyde	1. <i>cat.</i> BF ₃ OEt ₂ , RT 2. 40 °C	<i>d</i> -CHCl ₃	5 hours

Table 7 Different experimental conditions for the synthesis of the hydrazone **117**

The product was seen in reactions 2, 3 and 4 by mass spectrometry. However, all these reactions gave complicated mixtures by ¹H-NMR. Unsubstituted hydrazones are very sensitive to oxidation and hydrolysis, making them difficult to handle in practice.²²² The Fischer Indole synthesis was attempted on the crude hydrazone **117** by refluxing the mixtures in ethanol/H₂O 5:1 with an acid catalyst. A few experiments were set up using the same catalysts as above, namely dilute sulphuric acid, acetic acid and zinc chloride. In all cases, a dark gum was obtained with no trace of indole product **113**, probably due to polymerisation.

We next decided to look at the Fischer Indole synthesis using substituted hydrazones. Benzylacetone **118** and phenylhydrazine hydrochloride **114** were employed to prepare hydrazone **119** (**Scheme 37**). The reaction was carried out in acetic acid at room temperature over one to two hours.

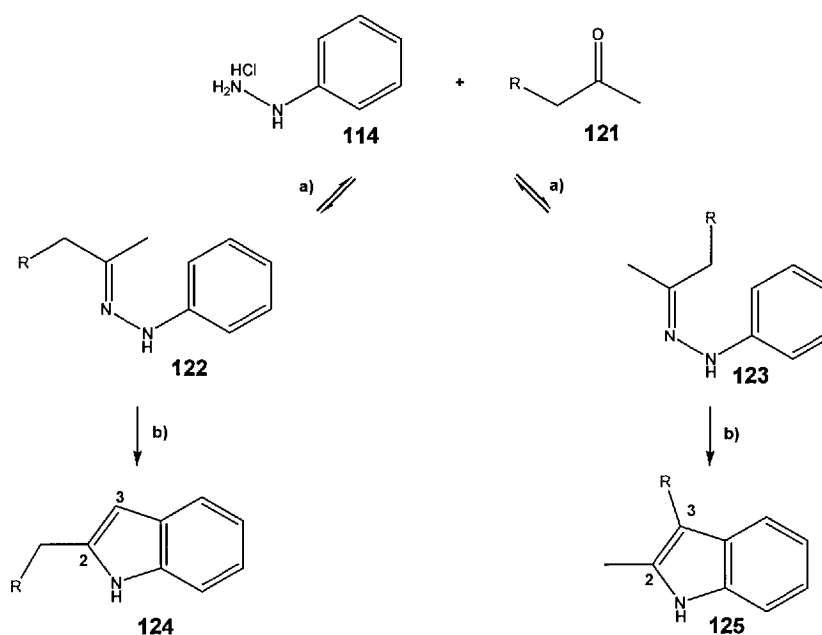
Cleaner TLCs were obtained from the hydrazone formation than in the case of unsubstituted hydrazone **117**, however NMR analysis was still complicated by impurities and no desired product **119** could be isolated. The Fischer Indole synthesis with the same acid catalysts as above was attempted on a small scale on the crude hydrazone **119**. However, a mixture of products was obtained, none of which corresponded to the desired indole product **120**.



a) AcOH, RT, 1-2 hr b) EtOH/H₂O 5:1, reflux, 15 hr

Scheme 37 Fischer Indole synthesis on substituted hydrazone **119**

It is known that the Fischer Indole synthesis can be very difficult, often leading to a mixture of products in the case where unsymmetrical ketones are used.²²² Indeed, two possible isomers of the hydrazone each lead to a different indole. For instance, with unsymmetrical ketone RCH₂COCH₃ **121**, the two possible isomers would lead to indole products **124** and **125** respectively (**Scheme 38**).



a) AcOH, RT b) EtOH/H₂O 5:1, reflux

Scheme 38 Regioselectivity of the cyclisation in the Fischer Indole synthesis

The regioselectivity issue makes this reaction difficult especially when the separation between the two different products is not facile. Many factors govern the direction of indolisation such as the size, strength and concentration of the Lewis acid, the alcoholic solvent and the temperature of the reaction.²²² Migration from the 3-position to the 2-position can be performed in the presence of a Lewis acid such as aluminium chloride at high temperature (130-150 °C).

In our synthesis, the different R groups are quite bulky (**Figure 52**) and we would expect that this would favour the formation of the desired product which is the 2-substituted indole.

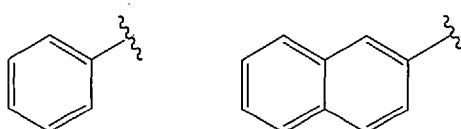


Figure 52 Different R groups for the 2-position of the indole

Given the failure of the indole synthesis from hydrazines and the difficulty to control the regioselectivity of the indolisation, we decided to focus on an alternate synthetic approach.

4.2.3. Synthesis of the indole leads: 2nd synthetic approach

The second approach to our racemic indole targets is given in **Figure 53**. The important aspect of this approach is that a suitably aldehyde-functionalised indole **128** provides an ideal template on which the aryl substituents and PPAR-binding carboxylic acid moiety can be built. This second strategy would also allow a convergent approach as the R₁ substituents would only be introduced after having carried out the Horner Wadsworth Emmons (HWE) coupling. The proposed forward racemic synthesis for indoles **38** and **39** where R₁ is a hydrogen atom is outlined in **Scheme 39**. Starting from commercially available indole-5-carboxaldehyde **128**, a HWE coupling with the two different phosphonoacetates **129** and **130** respectively, would give the corresponding *Z* and *E* isomers **131-134**. Reduction of the double bond can be carried out using magnesium turnings in dry methanol to afford precursors **126** and **127**. An asymmetric hydrogenation using a chiral rhodium-based catalyst could be used in the enantioselective synthesis. Finally, saponification of the ethyl ester would give the first two indole targets **38** and **39**.

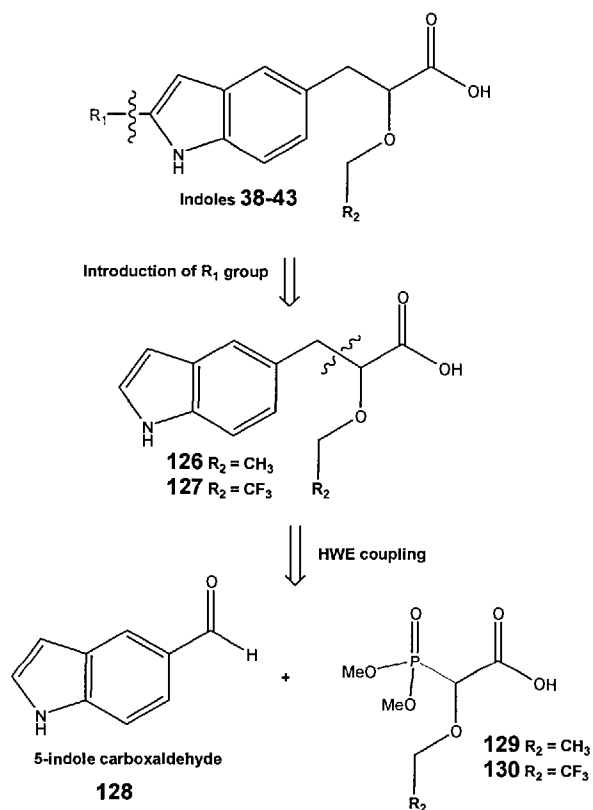
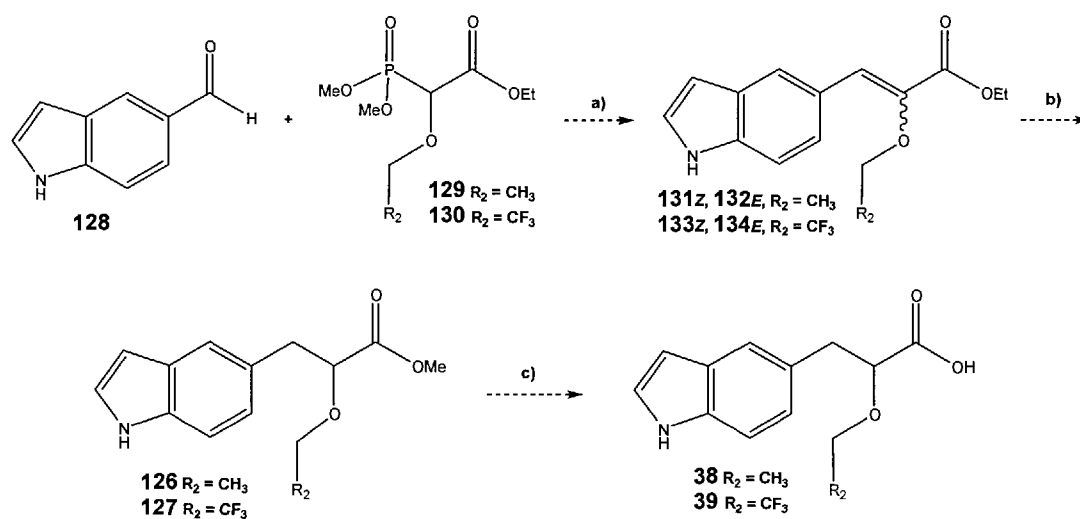


Figure 53 2nd retrosynthetic analysis of the indole leads

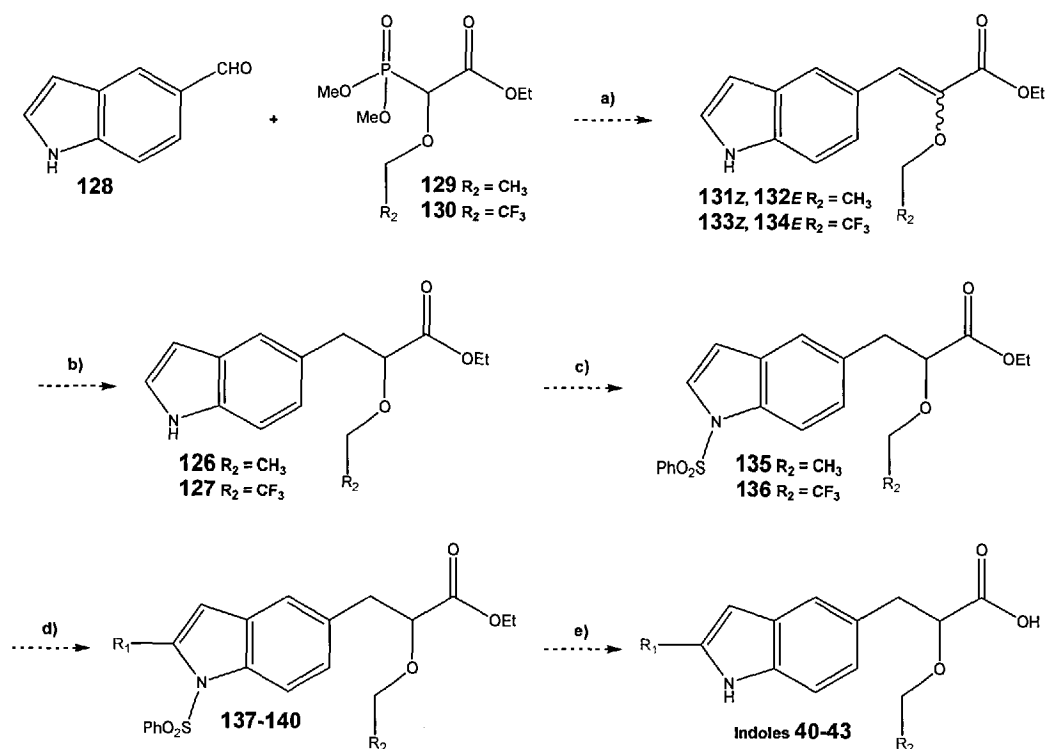


a) NaH, dry THF, 0 °C to RT b) Mg, dry MeOH c) KOH, EtOH/H₂O, reflux

Scheme 39 Forward racemic synthesis for indoles **38** and **39** ($R_1 = \text{H}$)

For indoles **40** to **43**, where R_1 is an aromatic group, the first two steps would be similar to the synthesis of targets **38** and **39** (**Scheme 40**). Then, the nitrogen of the indoles **135** and **136** would have to be protected using a benzenesulfonyl group for instance, followed by selective arylation on the 2-position of the indole to yield precursors **135-136**.²²³ The final step requires saponification of the ester and

deprotection of the benzenesulfonyl group in basic hydrolysis conditions to give the final indole targets **40** to **43**.



a) Phosphonoacetate, NaH, dry THF, 0 °C to RT b) Mg, dry MeOH c) 1. NaH, DMSO, 0 °C, 1 hr 2. PhSO₂Cl in THF, 0 °C to RT d) 1. LDA, -78 °C to 0 °C, 5 min 2. R₁Br, -78 °C to RT, 12 hr e) KOH(aq), heat to 100 °C

Scheme 40 Proposed forward synthesis for indoles **40-43** ($R_1 \neq \text{H}$)

Phosphonoacetate **129** can be synthesised from commercially available 2-chloro-2-ethoxyacetic ester **141**²²⁴ whereas phosphonoacetate **130** can be prepared from triethyl phosphonodiazooacetate **142** (Figure 54).^{225,226}

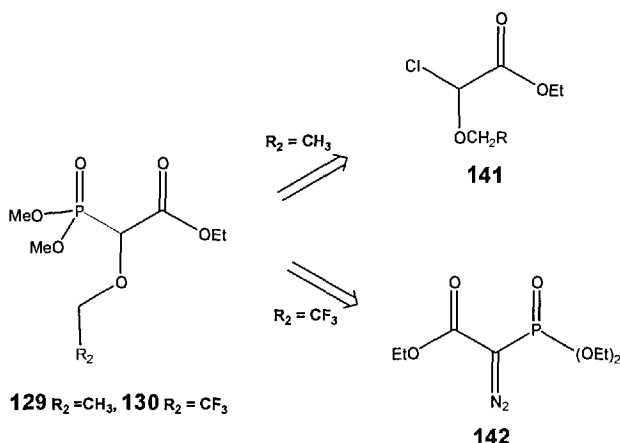
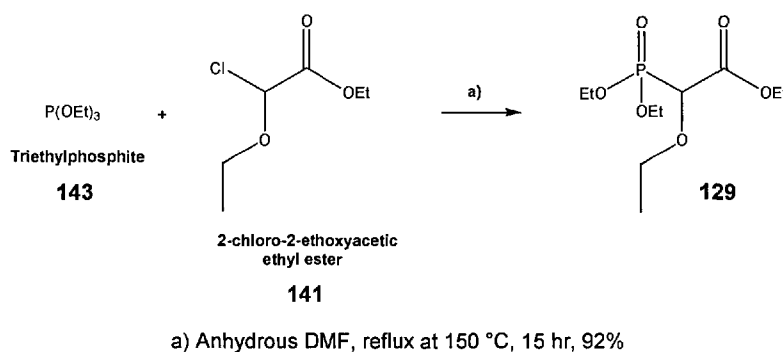


Figure 54 Retrosynthesis of the different phosphonoacetates **129** and **130**

4.2.3.1. Preliminary research on the 2nd synthetic approach

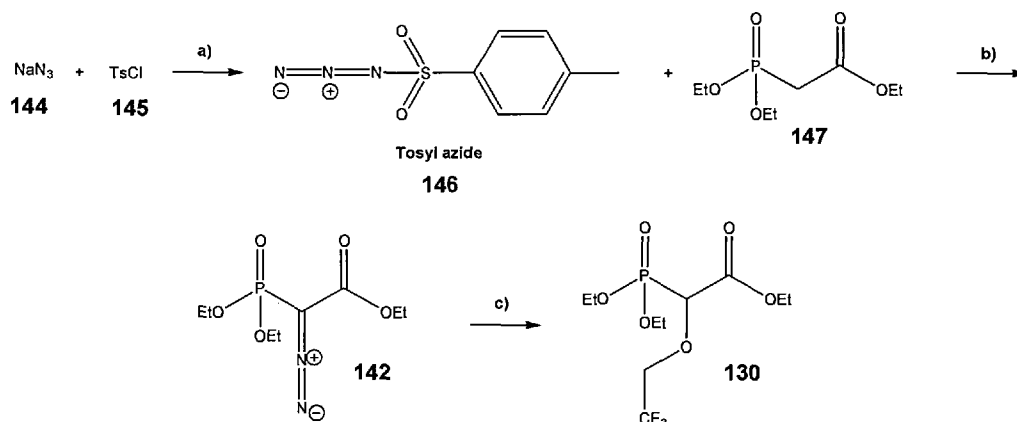
A number of model studies were carried out in order to test the major steps in this route. It was crucial to investigate the HWE coupling and test the feasibility of a convergent synthesis. The latter would be done by testing for any side reactions on the ethoxy ethylpropanoate side chain of compound **135** with the conditions required for the introduction of an aryl group on the 2-position of the indole. Before this could be done, we also had to also establish the ideal indole arylation conditions.

First of all, the HWE coupling reagents were prepared. For R₂ being a methyl group, triethylphosphite **143** and commercially available 2-chloro-2-ethoxyacetic acid **141** were coupled using Arbuzov chemistry as described by Grell *et al* (**Scheme 41**).²²⁴ This reaction proceeded smoothly, phosphonoacetate **129** was obtained in a quantitative yield of 92% and used without any purification.



Scheme 41 Preparation of the phosphonoacetate **129**

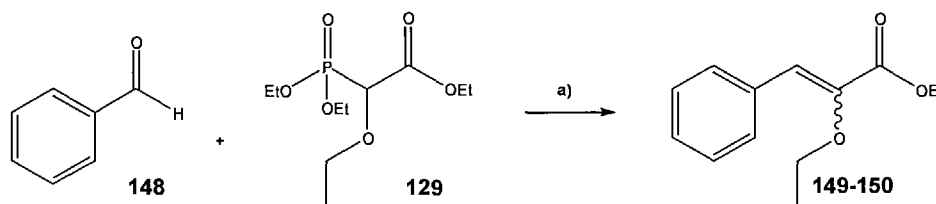
The synthesis of the 2,2,2-trifluoro phosphonoacetate **130** is shown in **Scheme 42**. Tosyl azide **146** which is the diazo transfer reagent was first prepared by coupling sodium azide **144** and tosyl chloride **145**.²²⁷ The diazo intermediate **142** was next synthesised from tosyl azide **146** and phosphonoacetate **147** using sodium hydride in dry THF.^{225,228} Finally, rhodium(II) acetate dimer was used to generate a carbenoid from the diazo compound **142** which was inserted into the O-H bond of 2,2,2-trifluoroethanol, as described by Haigh *et al*.²²⁶



a) EtOH, acetone, RT, 23 hr, 96% b) NaH, dry THF, 0 °C to RT, 5 hr, 70% c) 2,2,2-trifluoroethanol, $[\text{Rh}(\text{OAc})_2]_2$, benzene, reflux, 63%

Scheme 42 Synthesis of 2,2,2-trifluorophosphonoacetate 130

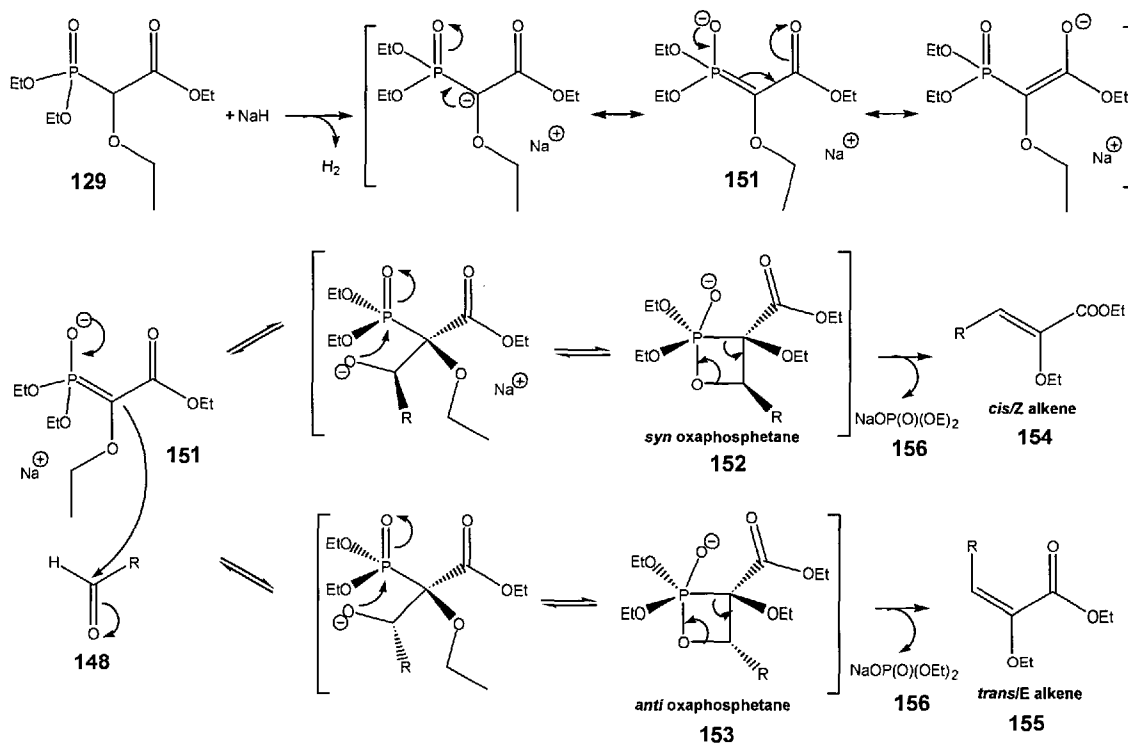
Having the two phosphonoacetates in hand, the HWE coupling was tested using commercially available benzaldehyde **148** and phosphonoacetate **129** as shown in **Scheme 43**. Briefly, sodium hydride was slowly added to a cooled solution of the phosphonoacetate **129** before dropwise addition of benzaldehyde **148**.^{229,230} After aqueous work up to remove the phosphate by-product, chromatography on silica gel yielded the *Z* and *E* isomers **149** and **150** in a 58% yield (Ratio *Z/E* = 86:14).



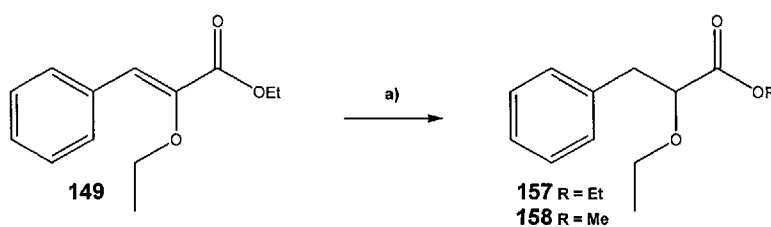
a) NaH, anhydrous THF, 0 °C to RT, 16 hr, 58%

Scheme 43 HWE coupling

The mechanism of the HWE coupling is outlined in **Scheme 44**. Sodium hydride first deprotonates the hydrogen *alpha* to the ester of phosphonoacetate **129** (*pK_a* about 10), the nucleophilic ylid **151** generated attacks the electrophilic carbonyl group of benzaldehyde **148** to form oxaphosphetanes **152-153**. The latter is subsequently cleaved to give the alkenes **154-155** and a phosphate byproduct **156** which is easily removed by aqueous work up. The ratio of olefin isomers depends on the stereochemical outcome of the initial addition.



The selective reduction of the double bond can be carried out with magnesium turnings in dry methanol. A test reaction on alkene **149** proceeded smoothly as described by Lohray *et al.*²²⁹ A mixture of methyl ester **157** and ethyl ester **158** was obtained due to transesterification (**Scheme 45**). The products were isolated in a yield of 83% (ratio of methyl ester **157** to ethyl ester **158** = 57:43). The complete conversion to the methyl ester can be achieved by increasing the reaction time.

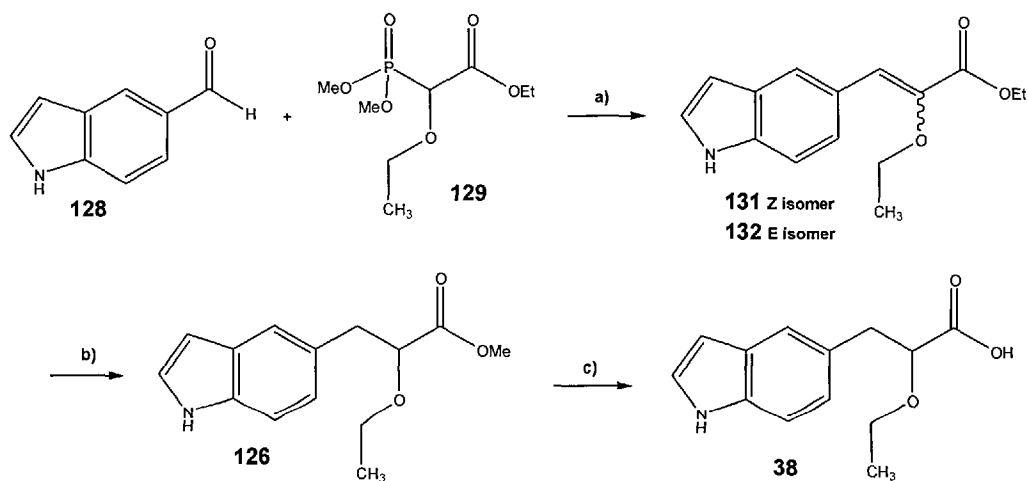


Scheme 45 Reduction of the double bond using magnesium

4.2.3.2. Synthesis of indole targets **38** and **39**

Having tested the HWE coupling and magnesium reduction conditions, indole leads **38** and **39** were next synthesised. **Scheme 46** shows the synthesis of indole lead **38**. Starting from commercially available indole-5-carboxaldehyde **128**, the HWE coupling was optimised using 2.2 eq of NaH and 2.0 eq of phosphonoacetate **129**. After purification, the *Z* and *E* isomers **131** and **132** were isolated in a ratio of 63:37 with an

overall yield of 93%. The reduction of the double bond proceeded smoothly at room temperature and the methyl ester **126** was isolated with a yield of 83%. Finally, saponification of the methyl ester with potassium hydroxide in a 1:1 mixture of ethanol/water gave the desired target **38** in a 92% yield.²³¹

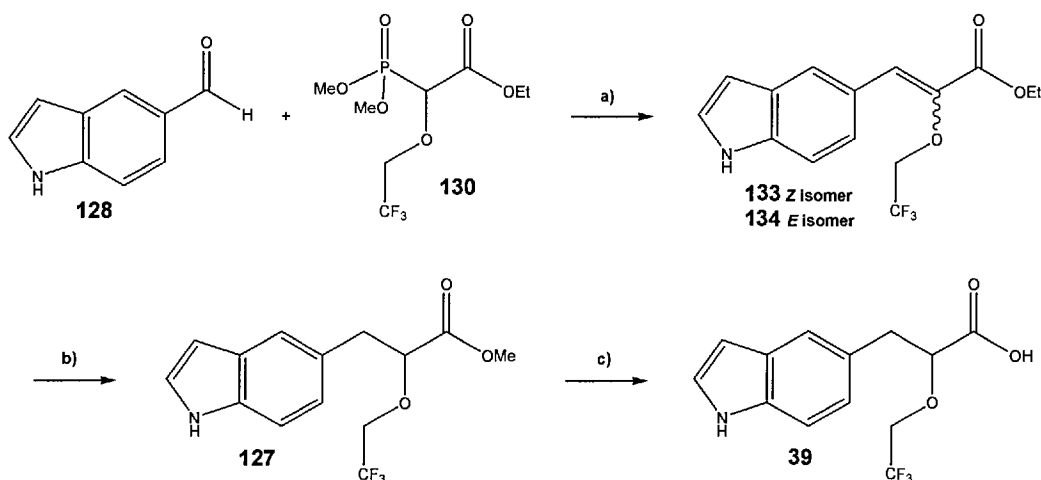


a) NaH, dry THF, 0 °C to RT, 93% b) Mg turnings, dry MeOH, RT, 83% c) KOH, EtOH/H₂O, reflux, 92%

Scheme 46 Synthesis of indole lead **38**

The synthesis of indole lead **39** was conducted in a similar fashion (**Figure 48**). Indole-5-carboxaldehyde **128** was coupled with the 2,2,2-trifluoro phosphonoacetate **130** to yield the *Z* and *E* isomers **133** and **134** in a 99% overall yield. The last two steps were carried out as for indole **38**. After the reduction of the double bond, indole precursor **127** was isolated in a 60% yield. The second indole lead **39** was isolated with a yield of 93% after saponification.

One concern about indoles **126** and **127** was the risk of elimination of the ethoxy side-chain to yield a fully conjugated system with the aromatic indole heterocycle. NMR analysis of the crude after the reduction of the double bond revealed only a trace amount of elimination (< 4-5%) compared to the yield of the desired products **126** and **127** (between 60 and 83%).



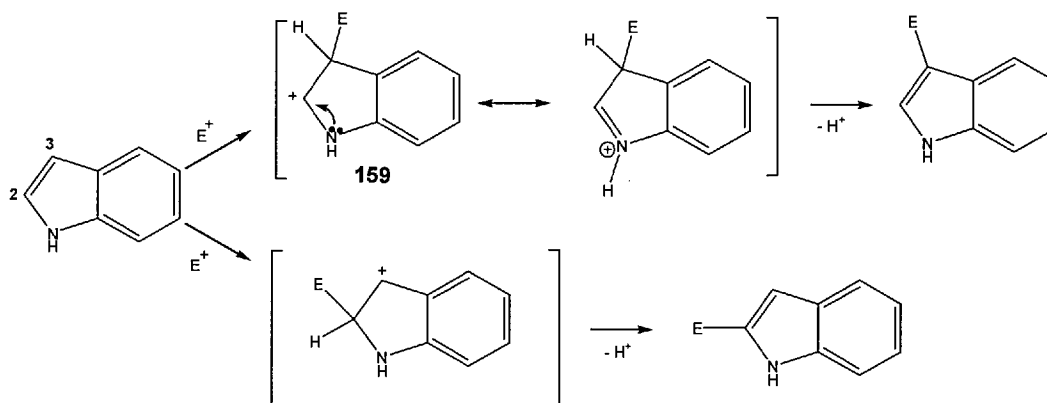
a) NaH, dry THF, 0 °C to RT, 99% b) Mg turnings, dry MeOH, RT, 60% c) KOH, EtOH/H₂O, reflux, 93%

Scheme 47 Synthesis of indole lead **39**

4.2.3.3. Feasibility of convergent synthesis

For the preparation of the 2-aryl indole products **40** to **43**, it was necessary to investigate the introduction of the R₁ group on the 2-position of the indole. The 3-position is the most reactive on an indole ring and is the most prone to electrophilic substitution. Indeed, the energy of activation of intermediate **159** is lowered because it is possible to delocalise the positive charge through resonance involving the nitrogen lone pair of electrons. This is not possible on the C2 position. Any attempt to delocalise the positive charge would disrupt the 6π-electron system of the benzene ring (

Scheme 48).



Scheme 48 Electrophilic substitution on an indole ring

In order to achieve C2 substitution, lithiation is used as it is selective for this position due to the influence of the nitrogen atom. For syntheses requiring *N*-unsubstituted

indoles, *N*-protecting groups are required. The benzenesulfonyl group was chosen as it allows chelation of lithium to the oxygen of the benzenesulfonyl group and enhances substitution on the C2 position (**Figure 55**). The lithiated intermediate, without isolation, can be reacted with an electrophile.

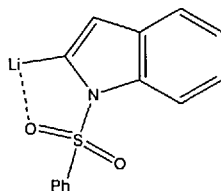
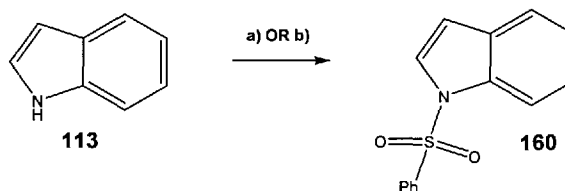


Figure 55 C2 lithiation

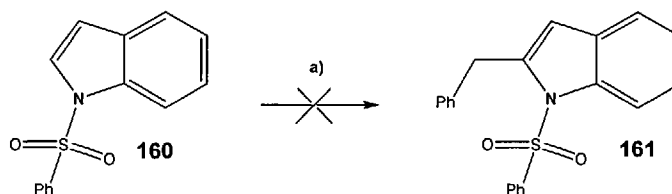
It was decided to find the optimum arylation conditions on 1-benzenesulfonyl indole **160**. Thus, the protection of commercially available indole **113** with the benzenesulfonyl group was carried out using sodium hydride, DMSO and benzenesulfonyl chloride in THF at room temperature (**Scheme 49**).²²³ Product **160** was obtained in a 72% yield after crystallisation from ethanol. A second procedure using a phase transfer catalyst was also used.²³² In this case, crystallisation from ethanol afforded the product **160** in a yield of 88%.



a) 1. NaH, DMSO, 0 °C, 1 hr 2. PhSO₂Cl in THF, 0 °C to RT, 72%
OR b) 1. NaOH 50%_(aq), H₂O, toluene, tetrabutylammonium bromide 2. PhSO₂Cl in toluene, RT, 88%

Scheme 49 Protection of indole **113** with a benzenesulfonyl group

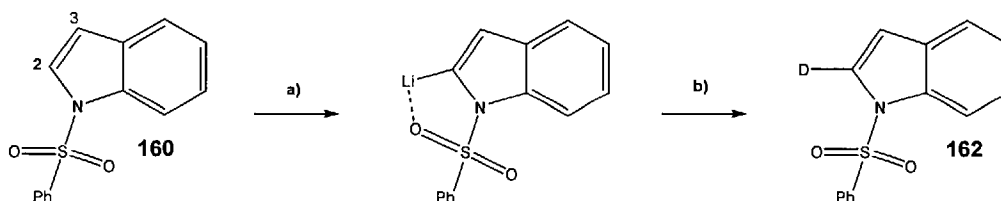
A number of bases were used for the lithiation step including LDA, *n*-BuLi and *t*-BuLi. Since one of the required R₁ groups (**Figure 46**) is a benzyl group, a model benzylation procedure was carried out on indole **160** using commercially available lithium diisopropylamide (LDA) in THF/heptane/ethyl benzene, 2.0M (**Scheme 50**), adapted from Iwanowicz *et al.* and Wenkert *et al.*^{223,233} However, no product **161** was isolated at all. LDA was therefore prepared *in situ* from *n*-BuLi and freshly distilled diisopropylamine and immediately used for the benzylation reaction under the same conditions, but still no product **161** was obtained.



a) 1. LDA, $-78\text{ }^{\circ}\text{C}$ to $0\text{ }^{\circ}\text{C}$, 5 min 2. PhCH_2Br , $-78\text{ }^{\circ}\text{C}$ to RT, 12 hr

Scheme 50 Benzylation on the 2-position of the indole **160** using LDA

Quenching the reaction with MeOD proved that deprotonation of the proton at the 2-position of indole was successful as deuterated indole **162** was seen by NMR (**Scheme 51**).



a) LDA, anhydrous THF, $-78\text{ }^{\circ}\text{C}$ to $0\text{ }^{\circ}\text{C}$, 2.5 hr b) MeOD, $0\text{ }^{\circ}\text{C}$, 1 hr, RT, 1 hr

Scheme 51 Deprotonation with LDA and quenching with MeOD

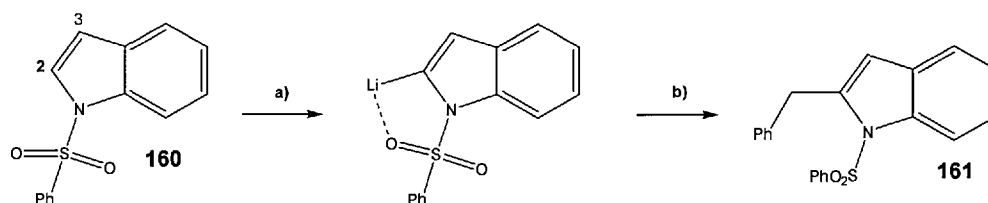
It was therefore decided to convert the bromide of benzyl bromide into an iodide which is a better leaving group. Benzyl iodide **164** was made from benzyl bromide **163** using the Finkelstein halogen exchange reaction using sodium iodide and acetone (**Scheme 52**).²³⁴ The equilibrium is driven to the right as NaBr formed is insoluble in acetone. This reaction proceeded smoothly and the product obtained was pure by NMR. However, the use of the more reactive benzyl iodide **163** still afforded no detectable product **161** in the benzylation reaction.



Scheme 52 Synthesis of benzyl iodide **164** by Finkelstein halogen exchange

The reaction was next tried with *n*-BuLi.^{235,236} Protected indole **160** was added to a solution of *n*-BuLi in a mixture of anhydrous ether and THF at $-50\text{ }^{\circ}\text{C}$, under nitrogen. Benzyl bromide was added after one hour and the reaction mixture was slowly allowed to warm up to RT. After work up and chromatography, a small amount of product (21%) was isolated.

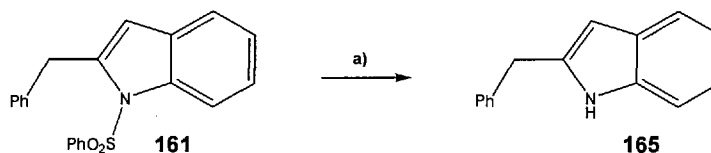
In an effort to improve the yield, it was decided to attempt the benzylation with *t*-BuLi as described by Hassan *et al.*²³⁷ The conditions described herein were unsuccessful in our hands. The conditions were then adapted from a method described by Sundberg *et al.* (**Scheme 53**).²³⁸ The reaction was optimised as follows: to the indole **160** in dry THF at -45 °C, was added *t*-BuLi dropwise. The solution turned yellow, then deep orange. After 50 minutes, benzyl bromide was added dropwise and the reaction mixture was allowed to warm up to room temperature over 16 hours. Chromatography on silica gel yielded 58% of product **161**. Hassan *et al.* reported the benzylic protons in ¹H NMR as a doublet (5.67 ppm and 4.24 ppm with a coupling constant of 14.1 Hz), yet we observed a singlet integrating for two protons at 4.27 ppm. Also, the chemical shift of the benzylic carbon was reported at 53.26 ppm in ¹³C NMR whereas we observed a chemical shift of 35.22 ppm.²³⁷



a) *t*-BuLi, -45 to -40 °C, 50 min b) PhCH₂Br, -45 °C to RT, 16 hr, 58%

Scheme 53 Benzylation of indole **160** using *t*-BuLi

The position of the benzyl group on C2 was confirmed by NMR after deprotecting the benzenesulfonyl group by refluxing with NaOH 2M and methanol at 110 °C (**Scheme 54**), furnishing indole product **165** in a 91% yield after chromatography.²³⁸ The NMR spectrum was in accordance with the literature.^{239,240}

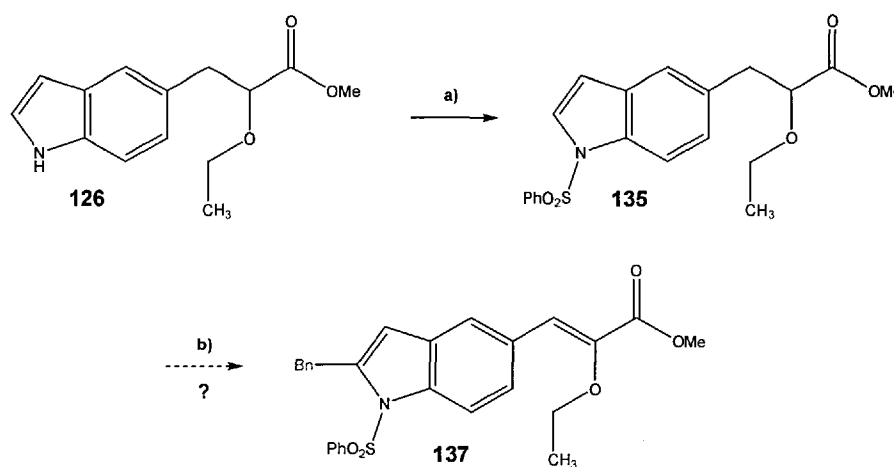


a) NaOH 2M/MeOH, reflux at 110 °C, 91%

Scheme 54 Hydrolysis of benzenesulfonyl group of indole **161**

Once the benzylation conditions were optimised, the feasibility of the convergent synthesis shown in **Scheme 40** (page 109) was investigated. The main concern was whether the ethoxy ethylpropanoate side chain would be stable to the arylation conditions. It was important to attempt the reaction on the following indole derivative **135** to evaluate the competition between the two reactive sites: the 2-position of the indole and the ethoxy ethylpropanoate side chain. Indole derivative **126**, previously

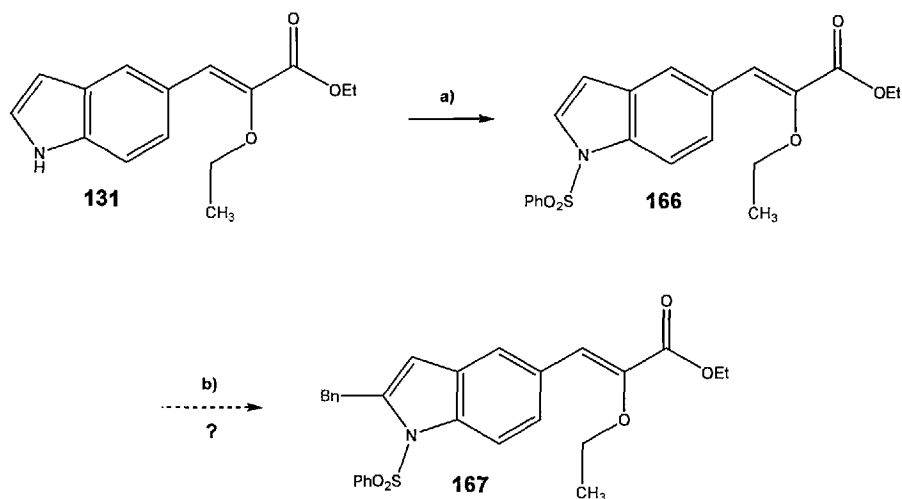
synthesised (**Scheme 46**), was protected using the phase transfer conditions to give compound **135**. The yield was of only 47% as some of the methyl ester had been saponified under the basic conditions of the reaction. One important consideration when using indole intermediate **135** is that it has a few acidic protons and an alkoxy group which could be a good leaving group. All this could lead to different side-products. One possibility is the formation of the lithium enolate of the ester which would lead to the introduction of the benzyl group on the carbon *alpha* to the carbonyl group. Another possibility could be the abstraction of the proton in the benzylic position, followed by elimination of the alkoxy group to give a fully conjugated system. Indeed, when indole **135** was subjected to the benzylation conditions, a mixture of side-products but no desired product **137** was obtained (**Scheme 55**).



- a) 1. NaOH 50%_(aq), H₂O, *n*Bu₄NBr, toluene 2. PhSO₂Cl in toluene, RT, 47%
 b) 1. *t*-BuLi, -45 °C, 55 min 2. BnBr, -45 °C to RT, 15 hr

Scheme 55 Feasibility of convergent synthesis with indole **135**

It was decided to attempt the benzylation on intermediate **166** which was first made by protecting previously synthesised indole intermediate **131** (**Scheme 46**). Compound **166** isolated in an 89% yield, was subsequently treated with the benzylation conditions (**Scheme 56**).



a) 1. NaOH 50%_(aq), H₂O, *n*Bu₄NBr, toluene 2. PhSO₂Cl in toluene, RT, 89%

b) 1. *t*-BuLi, -45 °C, 55 min 2. BnBr, -45 °C to RT, 15 hr

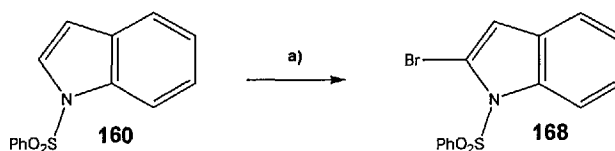
Scheme 56 Competition between reactive sites of indole **166** under arylation conditions

A number of different conditions were tried, as summarised in **Table 8**. Only entry 1 gave a trace amount of the desired compound. A mixture of side-products indicating that side-reactions had occurred preferentially on the ethoxy ethylpropanoate side chain was seen by proton NMR.

	<i>Reagents</i>	<i>Results</i>
1	<i>n</i> -BuLi, dry ether, BnBr, -50 °C to RT	Trace amount of product
2	LDA, dry ether/THF, BnBr, -78 °C to RT	No product
3	<i>t</i> -BuLi, dry THF, BnBr, -45 °C to RT	No product

Table 8 Arylation attempts on indole derivative **166**

In order to favour the reaction at the 2-position of the indole, a bromo group was introduced at this position to yield bromoindole **168** which was subsequently subjected to lithiation and benzylation. A number of bromination conditions tested on indole analogue **160** are summarised in **Table 9 (Scheme 57)**.²⁴¹



a) 1. Strong base 2. Br₂ or BrCN

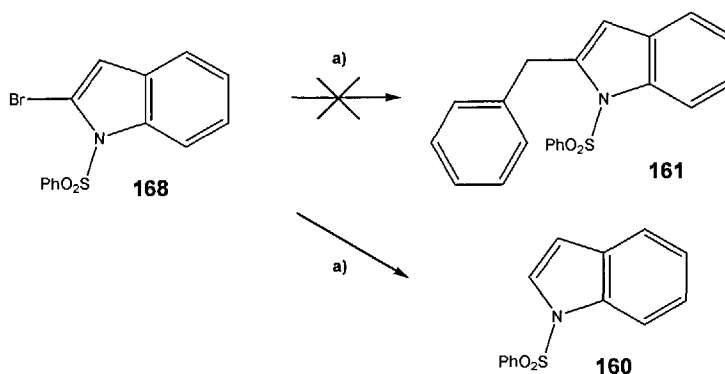
Scheme 57 Bromination of indole **160**

	Reagents	Conditions	Results
1	<i>t</i> -BuLi, Br ₂	Dropwise addition of base at -60 °C	25% product, 71% starting material
2	<i>t</i> -BuLi, BrCN	Dropwise addition of base at -50 °C	Very messy reaction, product 25%, no starting material
3	<i>t</i> -BuLi, BrCN	Dropwise addition of base at -55 °C Slight change in the temperatures	Only starting material
4	<i>t</i> -BuLi, BrCN	Dropwise addition of base at -55 °C Slight change in the temperatures	Only starting material
5	LDA, BrCN	Commercially available LDA used	Only starting material
6	LDA, BrCN	LDA prepared <i>in situ</i>	Clean reaction, 57% product

Table 9 Bromination attempts

The LDA conditions with cyanogen bromide gave the desired 2-bromo compound **168** in the best yield and the reaction proceeded cleanly (entry 6). The benzylation was attempted on the bromo derivative as shown in **Table 10**. However, no desired product was obtained at all. All of the reactions yielded back indole starting material **160** with no bromo group.

	Reagents	Conditions
1	<i>t</i> -BuLi, BnBr	Dropwise addition of base at -65 °C, BnBr added at -55 °C
2	<i>t</i> -BuLi, BnBr, TBAI	Dropwise addition of base to a mixture of SM, BnBr, TBAI at -60 °C
3	LDA, BnBr ²⁴²	SM added to commercially available base at -78 °C
4	LDA, BnBr ²⁴²	SM added to LDA prepared <i>in situ</i> at -78 °C

Table 10 Benzylation attempts on the bromo derivative **168**

a) 1. Lithium base, anhydrous THF 2. BnBr (conditions as *per table 10*)

Scheme 58 Benzylation on the bromo derivative **168**

Next, it was decided to use a Negishi coupling by making the zinc intermediate by transmetalation from the lithiated indole (**Table 11**).²⁴³ The introduction of a benzyl group was successful but gave a poor yield (entry 1). When the reaction was transposed to the cyano indole (entry 2), only a trace amount of product was obtained. Interestingly, the following side product was isolated (**Figure 56**), indicating a side-reaction on the cyano group. After thorough analysis of the reaction conditions, it was found that an excess of *n*-BuLi had been used by mistake for the *in situ* preparation of LDA in this case. The excess *n*-BuLi had reacted with the cyano group to yield side-product **169**.

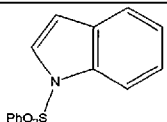
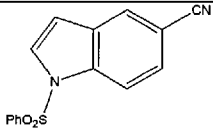
	Starting material	Reagents and conditions	Results
1		1. LDA, TBAI, THF, sieves 4Å, -78 °C to 0 °C 2. ZnCl ₂ , -78 °C to RT 3. BnBr, Pd(PPh ₃) ₄ , RT, then reflux 70 °C	16% product
2		1. LDA, TBAI, THF, sieves 4Å, -78 °C to 0 °C 2. ZnCl ₂ , -78 °C to RT 3. BnBr, Pd(PPh ₃) ₄ , RT, then reflux 70 °C	Trace amount product

Table 11 Arylation conditions through transmetalation using Zn

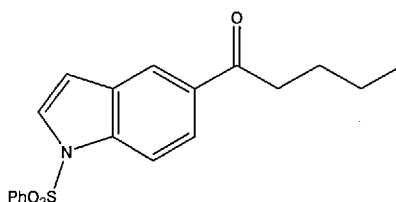
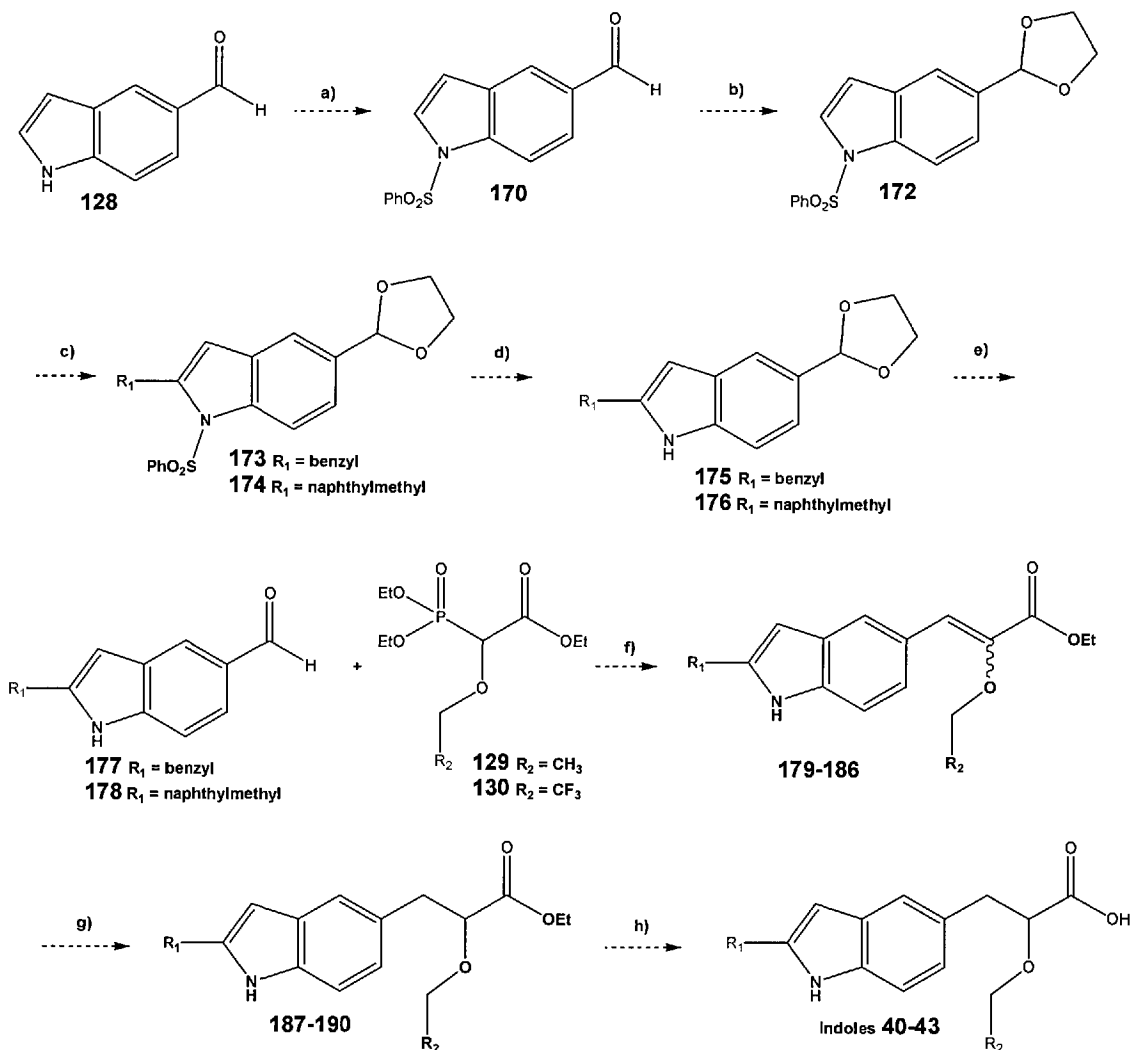


Figure 56 Side-product **169** isolated in entry 2 of Table 11

Having had no success with any of these conditions, the introduction of R₂ would have to be carried out before introducing the ethoxy ethylpropanoate side chain. This means that it will not be possible to carry out a convergent synthesis of the indole targets using this synthetic strategy and a less economic linear strategy would have to be followed.

The following route was chosen for the synthesis of the indole leads (**Scheme 59**). Starting from commercially available indole-5-carboxaldehyde **128**, the first step is to protect the nitrogen of the indole with a benzenesulfonyl group. The next step is protect the aldehyde **170** in the form of an acetal and introduce the appropriate R₁ groups on the 2-position of the indole. The benzenesulfonyl group would have to be cleaved before carrying out the HWE coupling. Indeed, some side reactions were

observed on the protecting group when a test reaction was carried on 1-benzenesulfonyl-5-indole carboxaldehyde **170** (Figure 57). After carrying out the Horner Wadsworth Emmons (HWE) coupling with the two different phosphonoacetates **129** and **130** respectively, the double bond of compounds **179** to **186** would be selectively reduced using magnesium turnings. The final step is saponification of the ester to yield indoles **40** to **43**.



Scheme 59 Route chosen for the synthesis of the indole leads

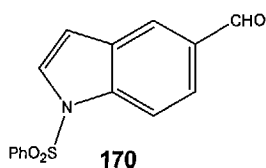


Figure 57 1-(phenylsulfonyl)-1*H*-indole-5-carbaldehyde

4.2.3.4. Synthesis of indole leads 40 and 41

The synthesis of indole target **40** (Figure 58) was therefore started using the route described above (Scheme 59).

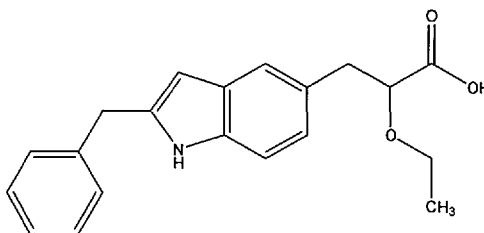
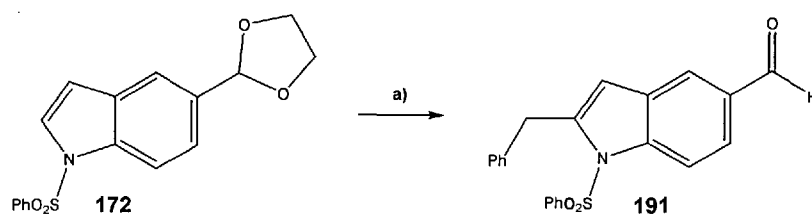


Figure 58 Indole lead 40

5-Indole carboxaldehyde **128** was protected with a benzenesulfonyl group using NaOH, H₂O, (*n*Bu)₄NBr and phenylsulfonyl chloride in toluene.²³² Purification by chromatography on silica gel yielded the desired product **170**. The acetalisation was first carried out with ethylene glycol and a catalytic amount of *para*-toluenesulfonic acid in toluene.²⁴⁴ The reaction mixture was refluxed using a Dean Stark apparatus and a dark insoluble gum was obtained. The reaction was therefore repeated using benzene as solvent. In this case, the reaction proceeded smoothly and an NMR of the crude showed the presence of acetal **172** and a tiny amount of starting material **170** which was removed by treatment with tosyl hydrazine resin in DCM. The product was obtained in a 99% yield. Due to the sensitivity of the indole to light, both protecting steps were conducted in the dark.

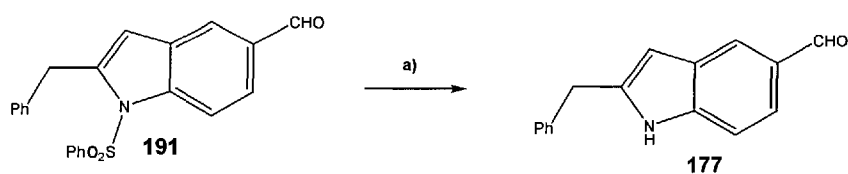
The acetal **172** was benzylated using the optimised conditions with *t*-BuLi and benzyl bromide described in Scheme 53. The benzylation reaction was successful, however ¹H NMR of the crude reaction mixture indicated that cleavage of the acetal had occurred. This was confirmed after isolation of aldehyde **191** after chromatography. This might have occurred due to a slightly acidic work up which had been carried out after the benzylation step in order to neutralise the excess base. The purification by chromatography proved to be quite tedious and a yield of 28% was obtained for aldehyde **191** (Scheme 60).



a) 1. *t*-BuLi, dry THF, -45 °C 2. BnBr, -45 °C to RT, 28%

Scheme 60 Benzylation of acetal **172**

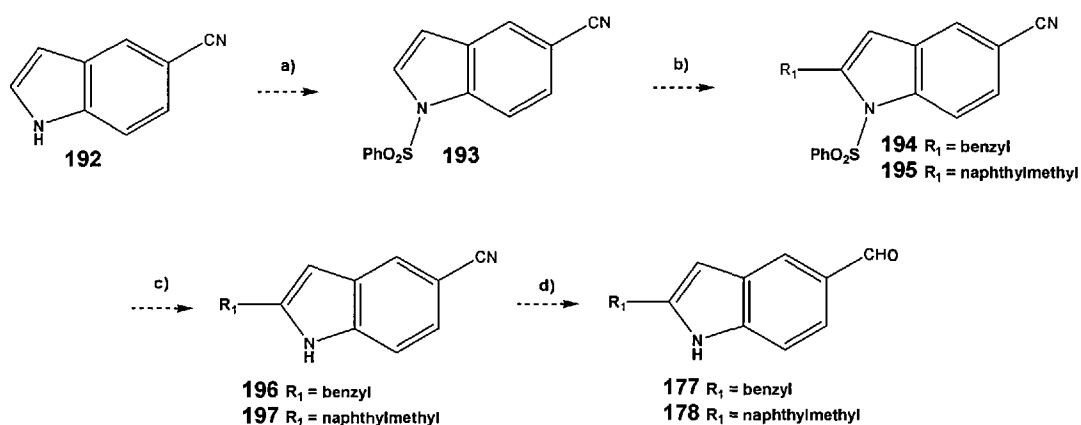
Aldehyde **191** was subjected to the basic hydrolysis of the benzenesulfonyl group (**Scheme 61**). Indole **177** was isolated, after work up and chromatography, in a yield of 39%.



a) MeOH/NaOH 2M 5:1, reflux at 110 °C, 39%

Scheme 61 Hydrolysis of benzenesulfonyl group of indole **191**

An alternate route was investigated in order to synthesise indole intermediate **177** in a better overall yield (**Scheme 62**).



a) 1. NaOH 50%_(aq), H₂O, (*n*Bu)₄NBr, toluene 2. PhSO₂Cl in toluene, RT b) 1. *t*-BuLi, -45 °C, 55 min 2. R₁Br, -45 °C to RT, 12 hr c) NaOH_(aq), heat to 100 °C d) DIBAL, dry THF, RT

Scheme 62 3rd alternate route towards indole aldehyde precursors **177** and **178**

Commercially available 5-cyanoindole **192** was first protected with a benzenesulfonyl group under phase transfer conditions.²³² The protected indole product **193** was purified by crystallisation from ethanol in a 96% yield. The next step was the

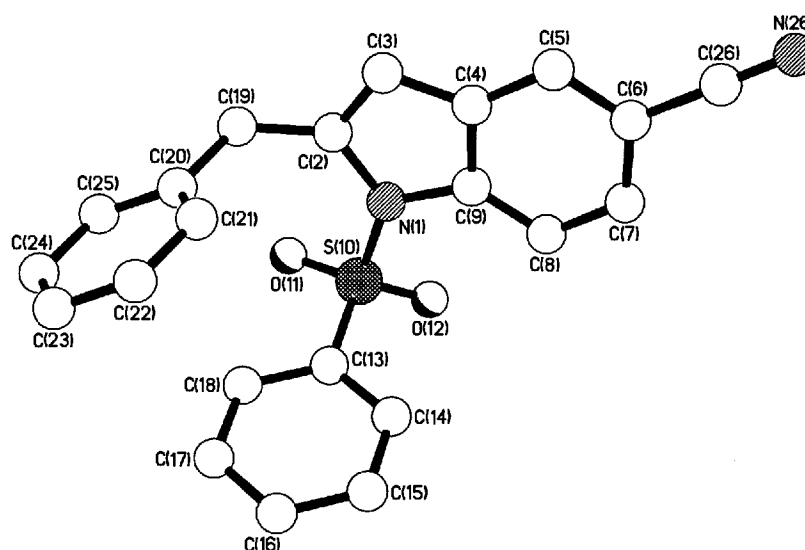
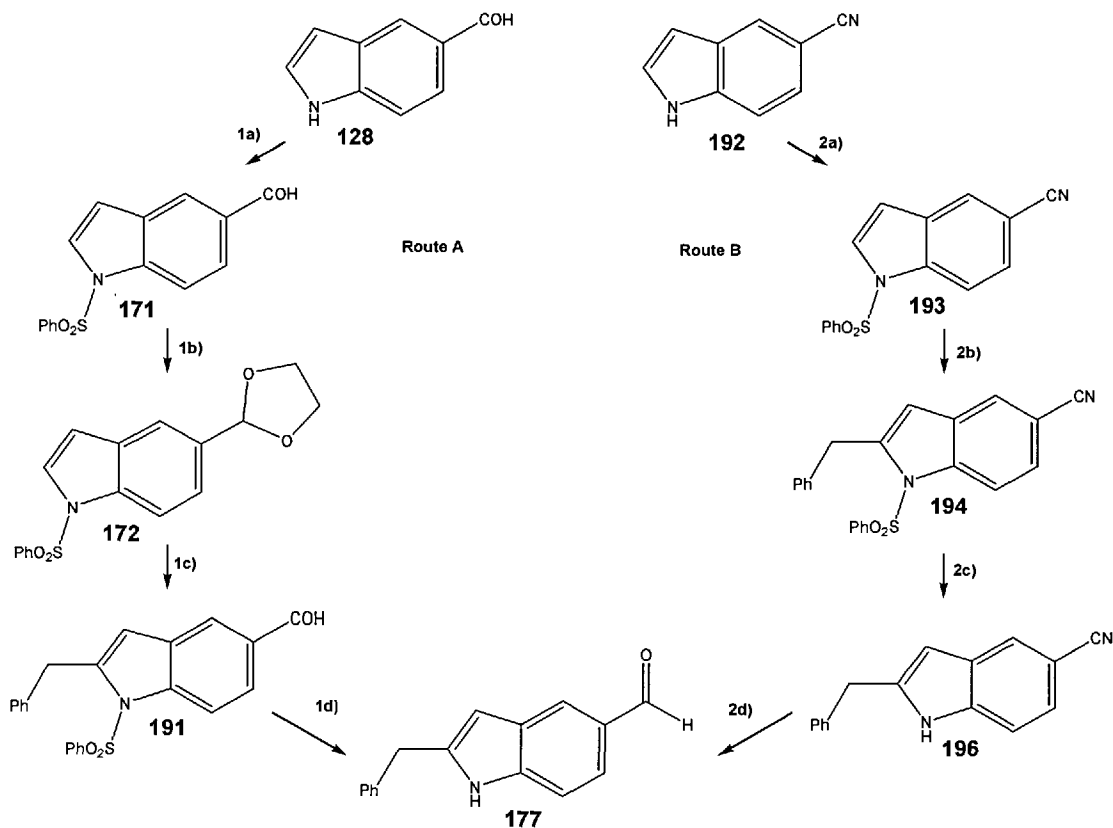


Figure 60 Crystal structure of 2-benzyl indole **194**

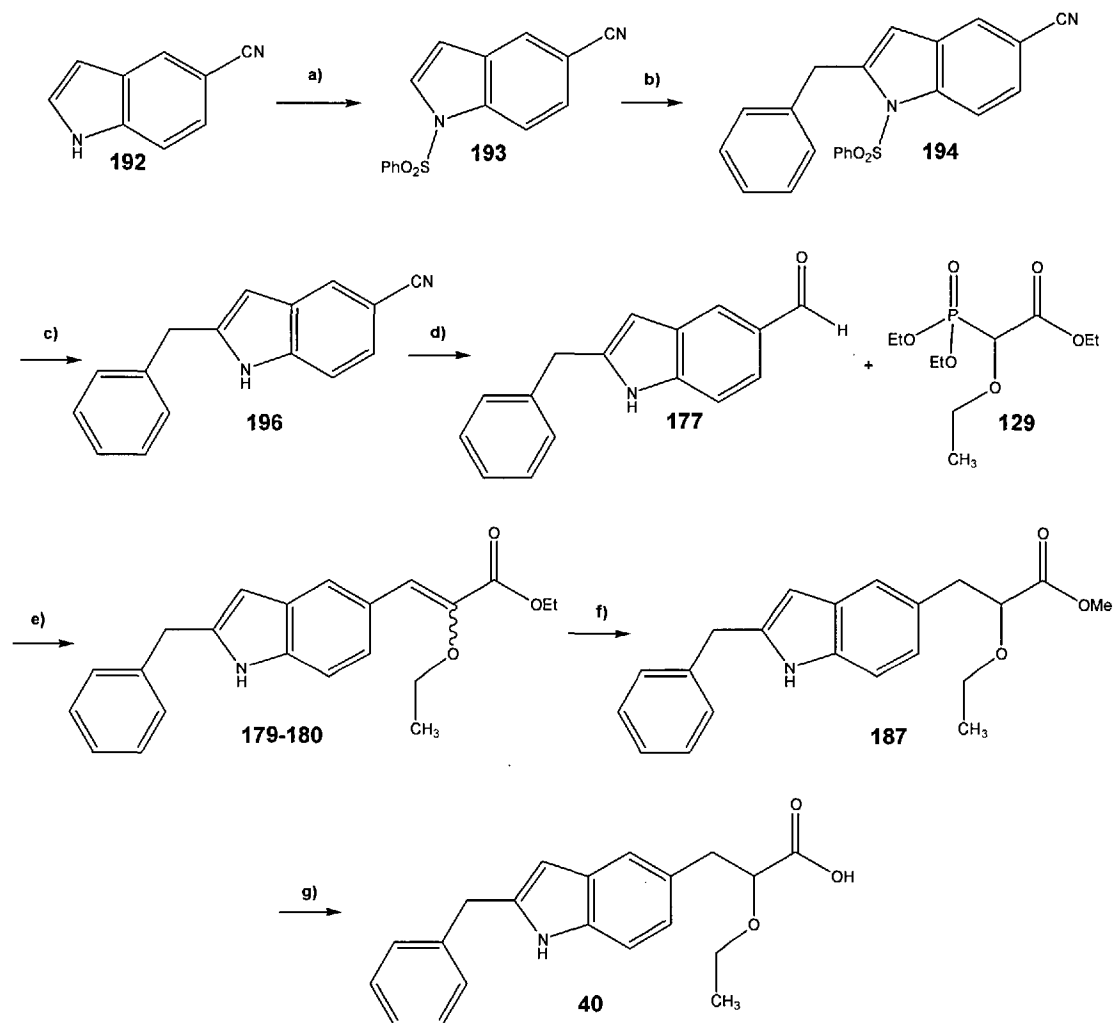
The benzenesulfonyl group was next hydrolysed under basic conditions by refluxing with aqueous sodium hydroxide 2M and methanol. After work up and column chromatography, indole **196** was isolated in a yield of 99%.²³⁸ It was subsequently reduced to the corresponding aldehyde **177** using diisobutyl aluminium hydride (DIBAL). The cyanide **196** was treated slowly with DIBAL in anhydrous THF at RT and the desired aldehyde **177** was obtained in a 59% yield after acidic work-up and chromatographic purification.²⁴⁵ Efforts to improve the yield of the DIBAL reduction consisted in attempting different experimental conditions with three different DIBAL solutions in the following three solvents: toluene, THF and DCM. The DIBAL reduction was optimised in dry DCM, followed by a Rochelle salt work up which afforded aldehyde **177** in 80% yield.²⁴⁶

A comparison of routes A and B towards indole **177** is shown in **Scheme 64**. Although both routes required the same number of synthetic steps, route B afforded a better overall yield (39% versus 9%) and rendered purification and isolation of the intermediate products easier. It was therefore validated for the synthesis of indole targets **40** to **43**.



Scheme 63 Comparison between routes A and B

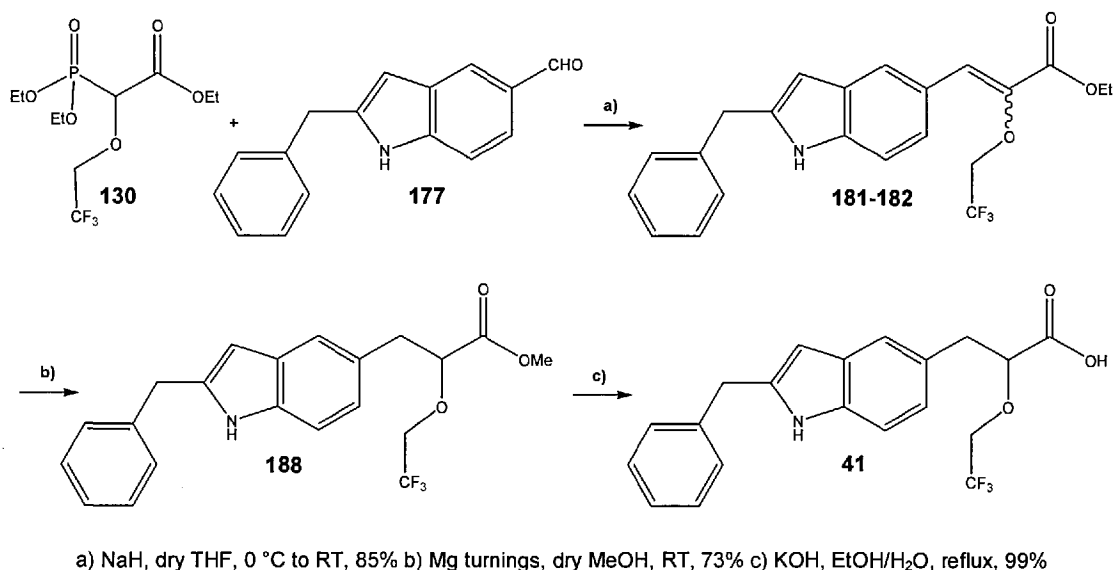
The overall synthesis of indole target **40**, using route B, is shown in **Scheme 64**. Continuing the synthesis towards indole analogue **40**, HWE coupling with phosphonoacetate **129** was performed on aldehyde **177**. The conditions were optimised with 1.80 eq of phosphonoacetate **129** and 2.2 eq of NaH. After an aqueous work up was carried out, chromatography on silica gel yielded the desired *Z* and *E* isomers **179** and **180** in a ratio of 63:37 in an excellent overall yield of 90%. After the selective reduction of the double bond of intermediate **187** using magnesium turnings in a 76% yield, saponification of the methyl ester yielded indole **40** in a 93% yield.



a) 1. *n*-C₄H₉NBr, NaOH_(aq), toluene, H₂O 2. PhSO₂Cl, RT, 96% b) 1. *t*-BuLi, -45 °C, 55 min 2. BnBr, -45 °C to RT, 15 hr 51% c) NaOH_(aq), MeOH 99% d) DIBAL, dry DCM, 80% e) NaH, dry THF, 0 °C to RT, 90% f) Mg turnings, dry MeOH, RT, 76% g) KOH, EtOH/H₂O, reflux, 93%

Scheme 64 Synthesis of indole lead 40

For the preparation of indole lead **41**, 2-benzyl aldehyde **177** was coupled with 2,2,2-trifluorophosphonoacetate **130**, affording the *Z* and *E* isomers **181** and **182** in a yield of 85%. Finally, reduction and saponification proceeded smoothly to give the final compound in a yield of 73% over the two steps.



Scheme 65 Synthesis of indole lead **41**

4.2.3.5. Synthesis of indole leads **42** and **43**

In the case of indole leads **42** and **43**, a naphthylmethyl group is found on the 2-position of the indole. The overall synthesis of indole **42**, shown in **Scheme 66**, was carried out similarly to that of indole target **40**. The introduction of the naphthylmethyl group was again found to be successful with the *t*-BuLi conditions albeit with a lower yield than in the case of the benzyl group. Different conditions were attempted in an unsuccessful effort to improve the yield (**Table 12**). One of the main side-products obtained in most cases was found to be indole **198**, **Figure 61**. This is thought to be due to the hydrolysis of the benzenesulfonyl group due to the basic conditions of the reaction. In order to try to minimise the formation of this side-product, a BOC protecting group was used instead of a benzenesulfonyl group, yielding indole **171** and the introduction of the naphthylmethyl group was then attempted on it (**Figure 62**).²⁴⁷ Yet, this did not improve the yield of the reaction. Also, 2-(bromomethyl)naphthalene was converted into the more reactive iodo analogue **225** (NaphI)²⁴⁸ using a Finkelstein exchange as described earlier (**Scheme 52**, page 116). This did not improve the yield of the reaction (entries 12 and 13). Entry 7 with the *t*-BuLi conditions gave the product in the best yield.

	Reagents	Results
1	1. <i>n</i> -BuLi, dry ether, -50 °C 2. NaphBr, -50 °C to RT	SM, trace amount of product
2	1. LDA, dry THF, -78 °C 2. NaphBr, -78 °C to RT ²⁴⁹	SM, some product
3	1. <i>t</i> -BuLi, dry THF, -60 °C 2. NaphBr, -60 °C to RT	SM, some product
4	1. <i>t</i> -BuLi, dry THF, -65 °C 2. NaphBr, -60 °C to RT	SM, some product
5	1. <i>t</i> -BuLi, dry THF, -78 °C 2. NaphBr, -78 °C to RT ²⁵⁰	SM (14%), product (21%)
6	1. <i>t</i> -BuLi, dry THF, -78 °C, 10 min 2. NaphBr, -78 °C to RT	SM (60%), product (23%)
7	1. <i>t</i> -BuLi, dry THF, -45 °C, 50 min 2. NaphBr, -45 °C to RT	SM, product (30%)
8	1. <i>t</i> -BuLi, dry THF, -100 °C, 10 min 2. NaphBr, -70 °C to RT	SM, product (19%)
9	1. <i>t</i> -BuLi, dry THF, <-100 °C, 10 min 2. NaphBr, -100 °C to RT	SM, trace amount of product
10	1. LDA, THF, sieves 4Å, -78 °C to 0 °C 2. ZnCl ₂ , -78 °C to -15 °C 3. NaphBr, -30 °C to RT	SM only, no product
11	1. LDA, TBAI, THF, sieves 4Å, -78 °C to 0 °C 2. ZnCl ₂ , -78 °C to RT 3. NaphBr, Pd(PPh ₃) ₄ , RT, then reflux 70 °C	SM recovered, no product
12	1. LDA, THF, sieves 4Å, -78 °C to 0 °C 2. ZnCl ₂ , -78 °C to RT 3. NaphI, Pd(PPh ₃) ₄ , RT 4. Reflux 70 °C	SM recovered, no product
13	1. LDA, THF, sieves 4Å, -78 °C to 0 °C 2. NaphI, -78 °C to RT	SM only

Table 12 Different conditions for the introduction of the naphthylmethyl group

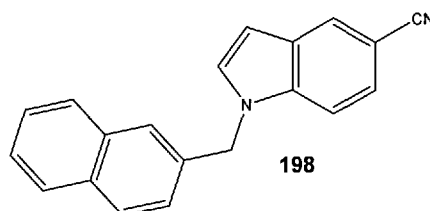


Figure 61 Indole side-product **198** isolated after arylation reaction

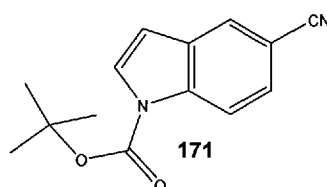
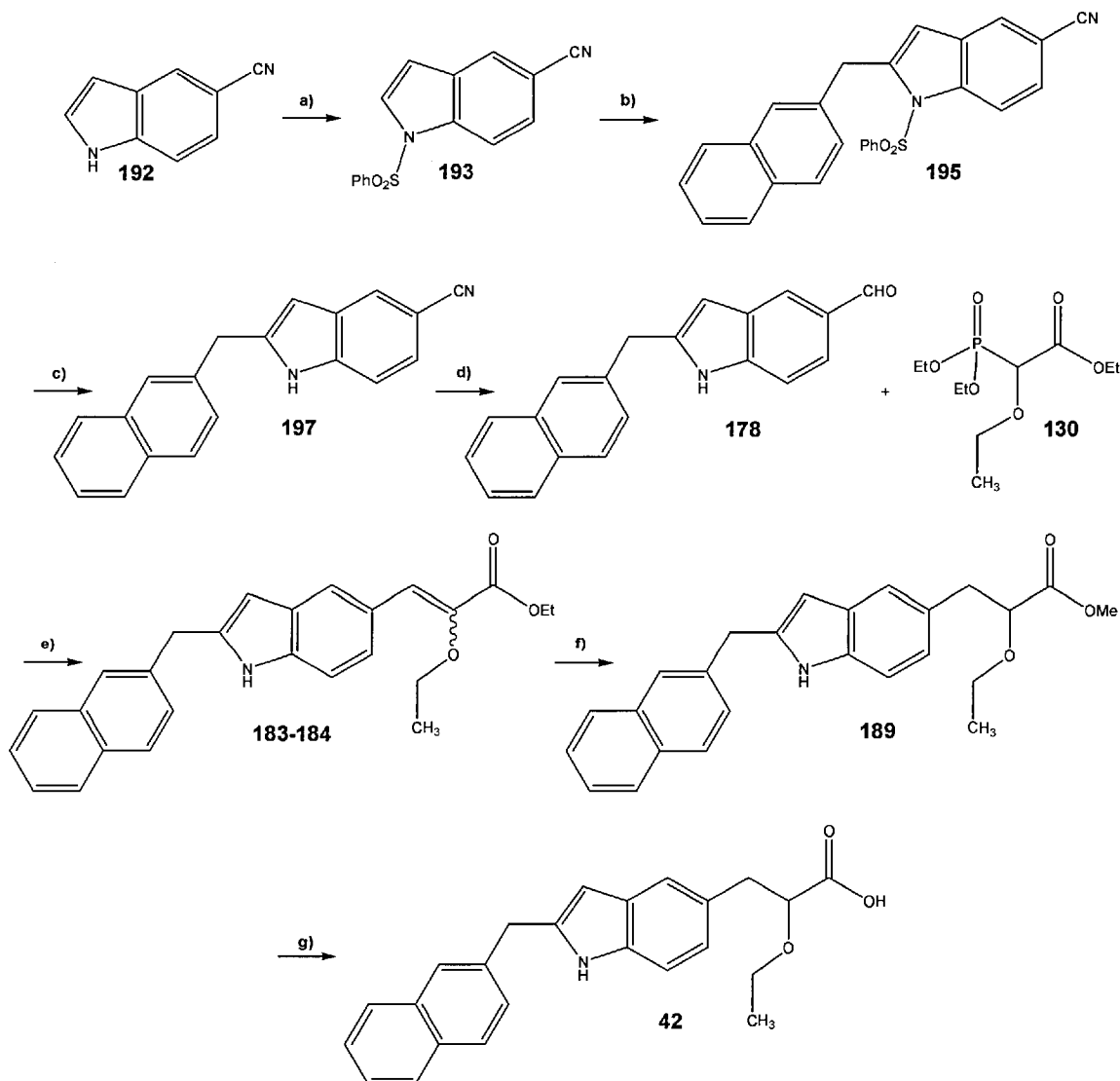


Figure 62 BOC protected cyano indole **171**



a) 1. $n\text{-C}_4\text{H}_9\text{NBr}$, $\text{NaOH}_{(\text{aq})}$, toluene, H_2O 2. PhSO_2Cl , RT, 96% b) 1. $t\text{-BuLi}$, $-45\text{ }^\circ\text{C}$, 55 min 2. NaphBr , $-45\text{ }^\circ\text{C}$ to RT, 15 hr, 30% c) $\text{NaOH}_{(\text{aq})}$, MeOH 99% d) DIBAL , dry DCM , 86% e) NaH , dry THF , $0\text{ }^\circ\text{C}$ to RT, 79% f) Mg turnings, dry MeOH , RT, 80% g) KOH , $\text{EtOH}/\text{H}_2\text{O}$, reflux, 97%

Scheme 66 Synthesis of indole lead 42

2-naphthylmethyl indole **195** was re-crystallised from hexane/ DCM 20:1. NOE difference experiments were carried out in order to show the presence of the naphthylmethyl group on the 2-position of the indole. Irradiation of the protons $\text{H}5'$ at 4.52 ppm showed strong interactions with protons $\text{H}3$, $\text{H}7'$, $\text{H}13'$ and a milder interaction with protons $\text{H}2'$. No interaction was seen with indole proton $\text{H}4$. Irradiation of the indole proton $\text{H}3$ at 6.19 ppm gave a strong signal with the indole proton $\text{H}4$, a reciprocal interaction with protons $\text{H}5'$ and a milder interaction with aromatic protons $\text{H}7'$ and $\text{H}13'$. This suggests the naphthylmethyl group is on the 2-position of the indole.

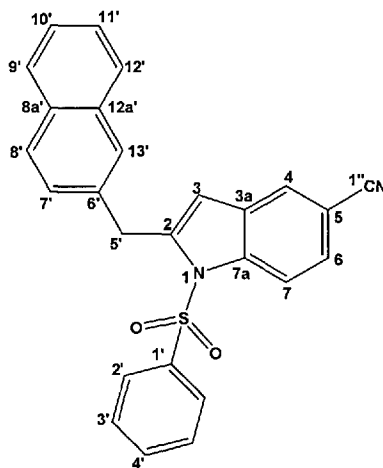


Figure 63 Structure of 2-naphthylmethyl indole **195**

The selective introduction of the aryl moiety on the 2-position was confirmed after the crystallographic structure was obtained by X-ray crystallography experiments conducted by Dr Andrew White. The full tables of crystallographic data are included in the appendix.

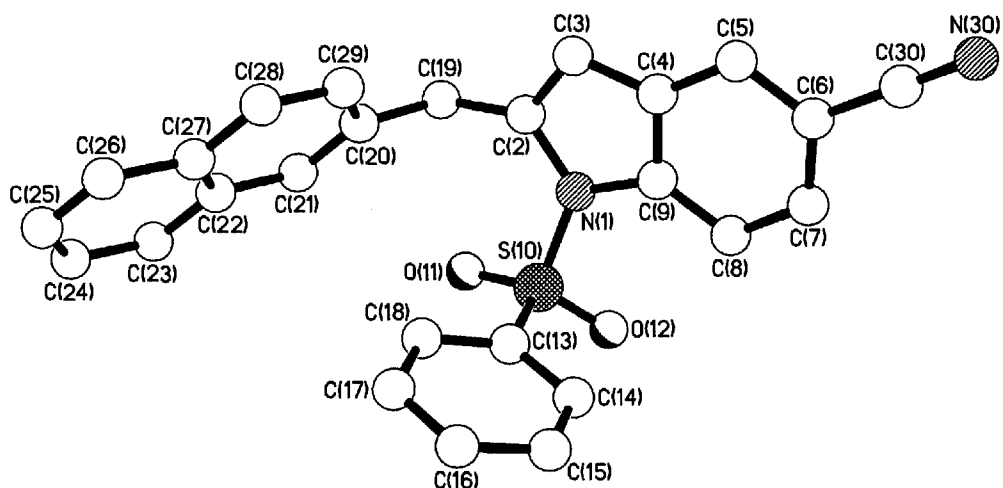
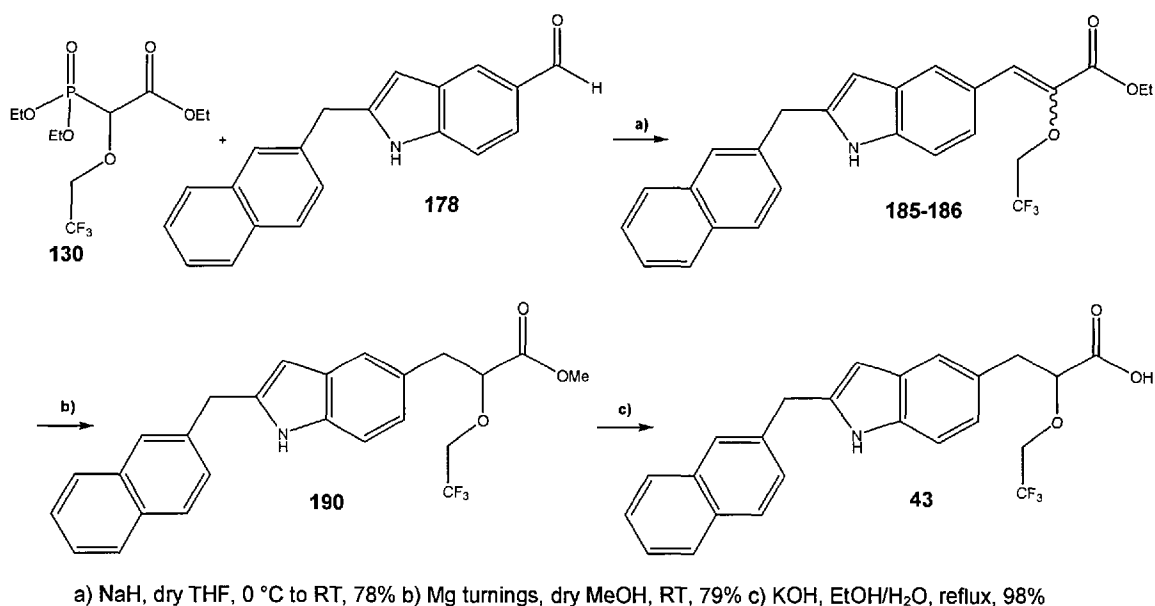


Figure 64 Crystal structure of 2-naphthylmethyl indole **195**

Continuing the synthesis towards indole **42** (Scheme 66), the deprotection of the benzenesulfonyl group, followed by the DIBAL reduction was carried out to give indole **178**. HWE coupling with phosphonoacetate **130** was next performed on aldehyde **178** and the *Z* and *E* isomers **183** and **184** were isolated in a ratio of 63:37 with an overall yield of 79%. After the selective reduction of the double bond of using magnesium turnings to afford indole precursor **189** in an 80% yield, saponification of the methyl ester **189** yielded indole lead **43** in a 97% yield.

In a similar fashion, aldehyde **178** was coupled with the 2,2,2-trifluorophosphonoacetate **130** to give the *Z* and *E* isomers **185** and **186** in a ratio of 38:62, with an overall yield of 78% (Scheme 67). Finally, reduction of the double bond afforded indole precursor **190** in 79% yield and saponification gave the final indole lead **43** in a 98% yield.



Scheme 67 Synthesis of indole lead **43**

The purity of all the indole compounds was assessed by elemental analysis and a minimum of 98% purity was targeted for each lead. This was important to us in order to have the highest purity possible before proceeding to the biological testing of the compounds. It was found that it was best to purify the intermediates at each step in order to ensure the maximum purity for the final compound. Thus, chromatography on silica gel, followed by crystallisation wherever possible, was carried out affording very high purities of at least 97% for the intermediates and final compounds. The compounds were kept at -20 °C, under argon. A routine NMR in the appropriate solvents showed that the compounds were stable; elimination of the ethoxy side-chain was not observed.

4.2.4. Indoles *in vitro* PPAR activation assay: results and discussions

Once the indole leads **38** to **43** were successfully synthesised, it was important to test their activity on the PPARs (Figure 65). A Luciferase gene reporter assay in human MCF-7 breast cancer cells was carried out by Therese Røst under the supervision of

Professor Rolf Berge at the Institute of Medicine of Bergen, in collaboration with Thia Medica AS, as previously described in Chapter 3.

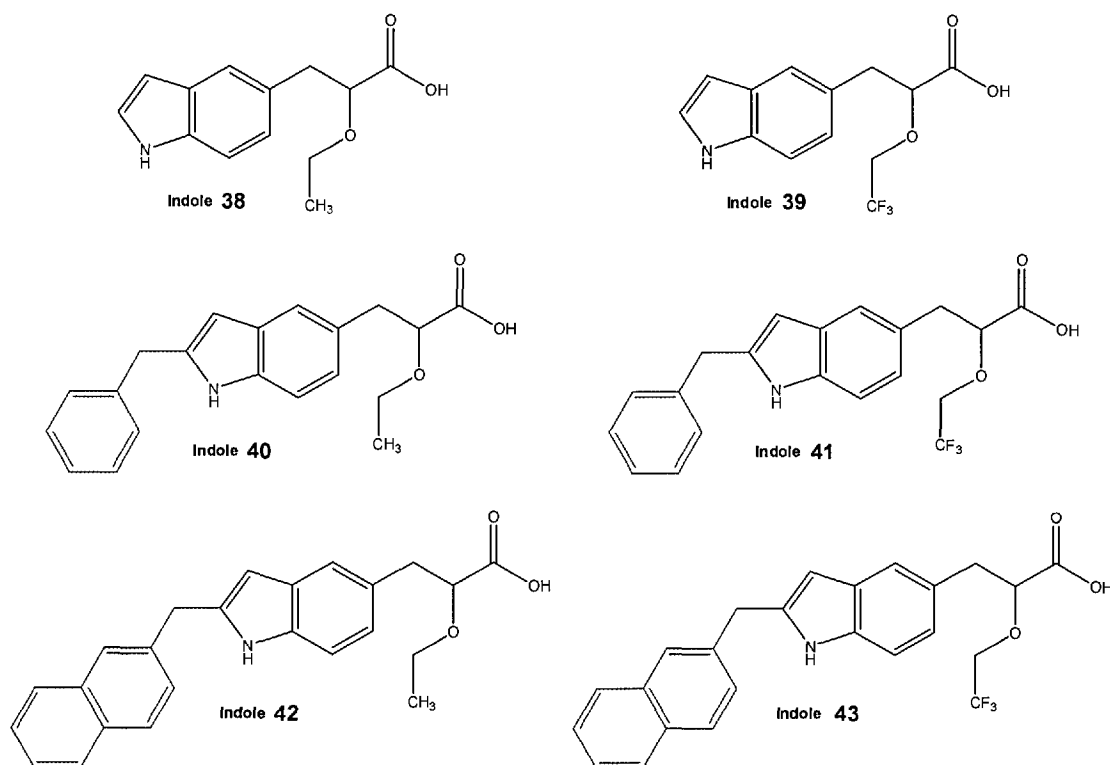


Figure 65 Indole leads tested *in vitro*

Again, the negative control consists of transfection without treatment with any of the compounds and the positive controls are the same selective potent PPAR agonists at concentrations of 30 μM and 75 μM : WY14.643 **71** for PPAR α , BRL49653 **20** for PPAR γ , and L165.041 **14** for PPAR δ (**Figure 42**, Chapter 3). Different concentrations of TTA (1 μM , 30 μM and 75 μM) were run in parallel as previously.

Five different concentrations between 1 μM and 75 μM of the indole leads **38** to **43** in DMSO were prepared. There were no solubility issues with the “druglike” designed indole leads except for indole **40** at 75 μM . The maximum concentration at which it was completely soluble was 50 μM , therefore this concentration was used. These five different concentrations of the compounds were used to get a preliminary indication of their effects on the activation. The lowest concentration which gave activity as well as a higher concentration relative to the first one were selected. These experiments were performed nine times at these optimum concentrations. All results were normalised relative to the negative control and the standard deviation is calculated

from the variability of the readings obtained for one compound at a particular concentration.

4.2.4.1 PPAR α activation assay with the indole leads

The PPAR α activation results are shown in **Figure 66**.

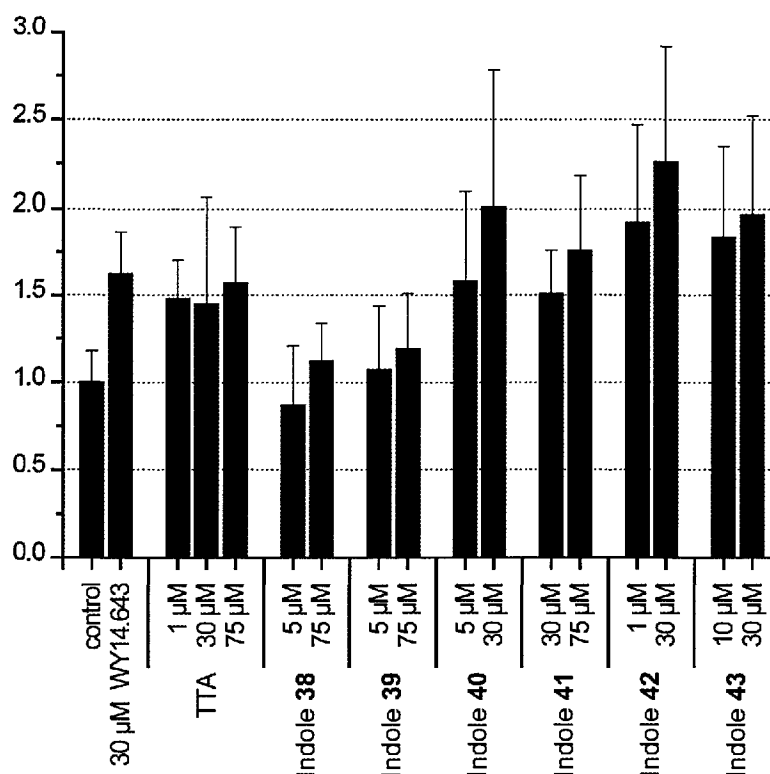


Figure 66 PPAR α activation results with the six indole leads **38** to **43**

It can be seen that, in general, indoles **38** and **39** were less potent than the other four targets. This supports the fact that the aryl group on the 2-position of the indole is important for activation of the receptor.

With indole **40**, the activation of PPAR α at 5 μM is comparable to that of WY14.643 at 30 μM , showing that it is a potent activator. Indole **41** is also a strong activator although a higher concentration is needed to see a comparable effect as with target **3**. Indole **42** is a very potent activator of PPAR α , in fact, the best activator out of the series. Its activity at a low concentration of 1 μM is already slightly better than that of WY14.643 at 30 μM . Indole **43**'s effect is very significant at low concentrations of 10 and 30 μM . If we compare indoles **40** and **42** to indoles **41** and **43**, it indicates that

the ethyl ether gives slightly better activation than the 2,2,2-trifluoro ether. Comparison of indole leads **40** and **41** with indoles **42** and **43** shows that the last two compounds with a 2-naphthylmethyl group activate PPAR α better than the first two leads **40** and **41** with a 2-benzyl group.

4.2.4.2 PPAR γ activation assay with the indole leads

Figure 67 shows the complete series of PPAR γ activation results.

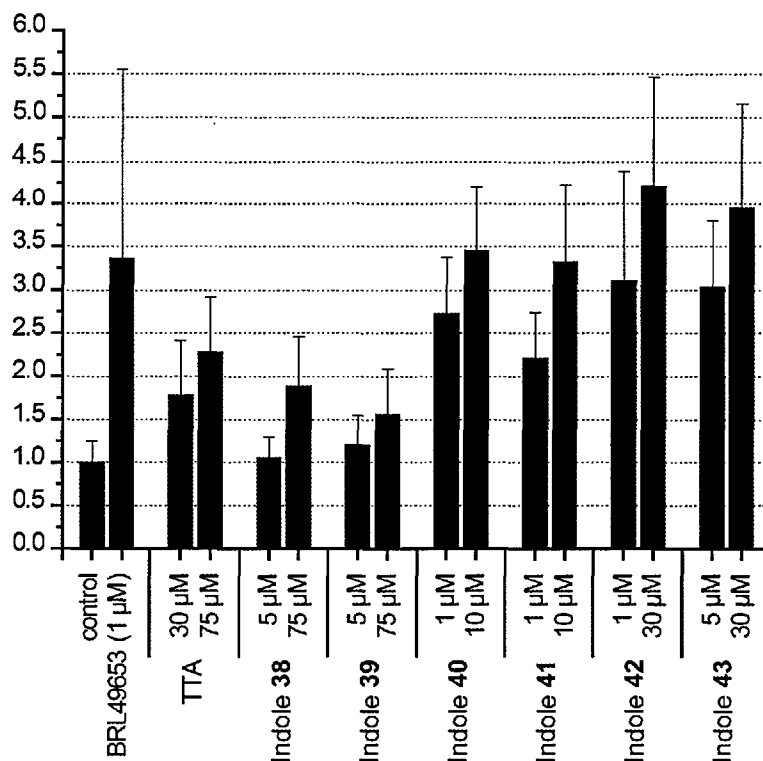


Figure 67 PPAR γ activation with the six indole leads **38** to **43**

Big variability was seen with the positive control's response. This has been discussed previously in Chapter 3. As with PPAR α , indoles **38** and **39** activated PPAR γ the least, confirming that the aryl group on the 2-position of the indole is necessary for strong activation of the receptor. Indole **40** is a potent activator of PPAR γ at low concentrations of 1 to 10 μ M. Indole **41** is as effective as indole **40**, although its activation is slightly less strong. Indoles **42** and **43** are both very potent agonists, with indole **42** being very potent at a low concentration of 1 μ M. If we compare indoles **38**, **40** and **42** to leads **39**, **41** and **43**, it seems that the ethyl ether gives better activation of PPAR γ than the 2,2,2-trifluoroethyl ether. Comparison between indoles **40** and **41**

and indoles **42** and **43** indicates that the naphthylmethyl group is favoured for PPAR γ activation.

4.2.4.3 PPAR δ activation assay with the indole leads

Figure 68 shows the full series of PPAR δ activation results. In general, the six compounds were not found to be as strong activators of PPAR δ as L165.041. Indeed, the indoles had been designed to be dual PPAR α/γ agonists and the data obtained seems to confirm that they are potent activators of PPAR α and PPAR γ , but less effective on PPAR δ .

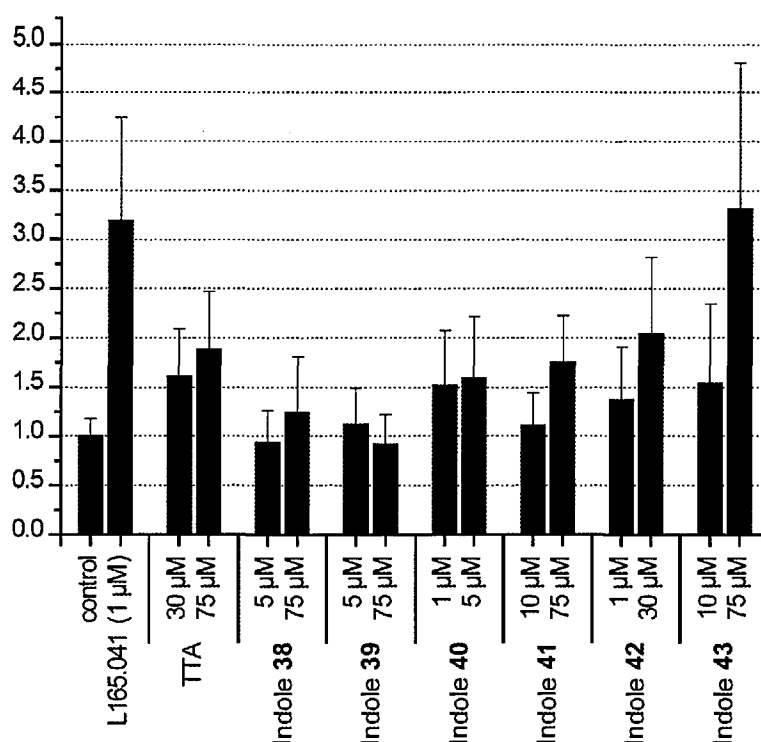


Figure 68 PPAR δ activation with the six indole targets **38** to **43**

Indoles **38** and **39** were statistically not different from the control. Indole **40**, at concentrations of 1 and 5 μ M, gives comparable activity to that of TTA at 30 μ M whereas a much higher concentration of indole **41** is needed to observe similar activity to that of TTA at 75 μ M. The activation with indole **42** was higher than with TTA at a concentration of 30 μ M, indicating that this compound is a more potent agonist than TTA. Indole **43** was also potent, however at high concentrations of 75 μ M. In the case of PPAR δ , it was not possible to conclude on whether the 2,2,2-trifluoro ether was better than the ethyl ether as there was no pattern from the data observed. Indole **40** seemed to show the best activation of PPAR δ at low

concentrations. Its effect at low concentrations of 1 and 5 μM was comparable to TTA's effect at 30 and 75 μM which has been proven to be a potent PPAR δ agonist.

If we consider the activation results of the three PPAR subtypes (**Figure 69**) by the most potent indoles **40** to **43**, it appears that indoles **42** and **43** are slightly better PPAR α/γ dual agonists than indoles **40** and **41**. In fact, the indoles activated the PPARs in the following order in human MCF-7 cells: $\gamma > \alpha > \delta$. The indoles had been designed to be dual PPAR α/γ agonists by Prosarix Ltd. and we obtained proof of concept of the ProtoBuild™ *de novo* approach.

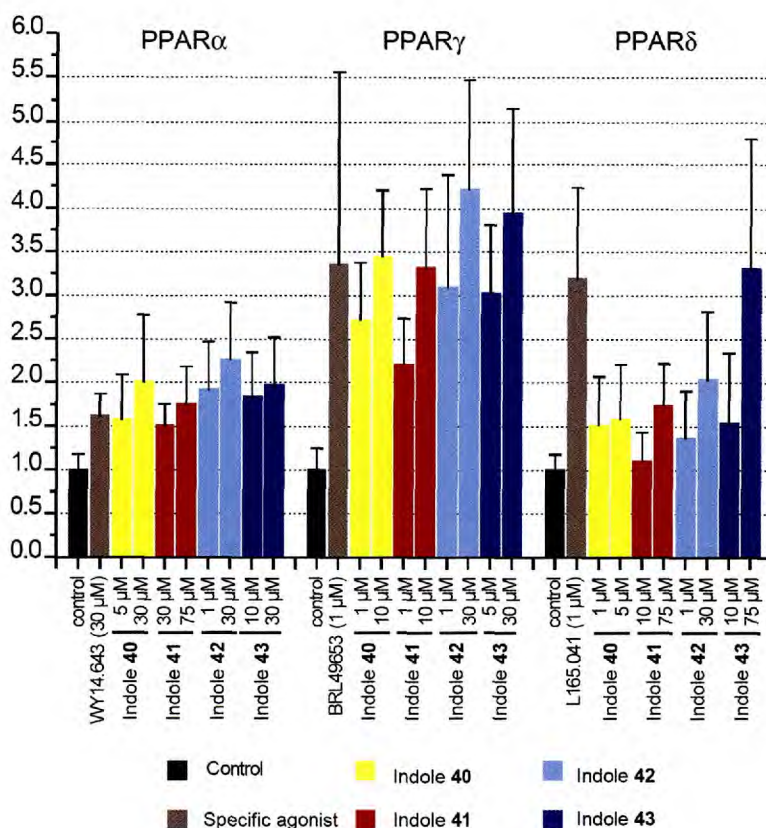


Figure 69 PPAR activation with indole targets **40** to **43**

Before choosing the most suitable candidate for further biology tests, it would be important to carry out some further *in vitro* assays to test the toxicity of the compounds and to measure some preliminary pharmacokinetic properties in order to see which compound would have the best druglike properties. Once the best candidate is chosen, the enantioselective synthesis can be carried out to give the desired enantiomer and to proceed to further testing of the compound as a potential treatment of metabolic diseases.

4.3 Work towards the pyrrolidine scaffold

4.3.1. Pyrrolidine scaffold: retrosynthetic analysis

A pyrrolidine scaffold was also designed as a potential PPAR α/γ dual agonist by Prosarix Ltd (**Figure 70**). The aim was to devise a synthetic approach to this new scaffold and proceed to the racemic synthesis.

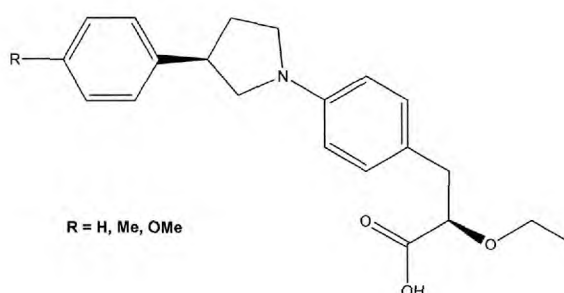


Figure 70 Pyrrolidine scaffold

Figure 71 shows the proposed interaction of the pyrrolidine lead with R being an OMe group with the PPAR γ active site. The aromatic ring fits in the hydrophobic site while the acidic head group fits into the hydrogen bond donor site.

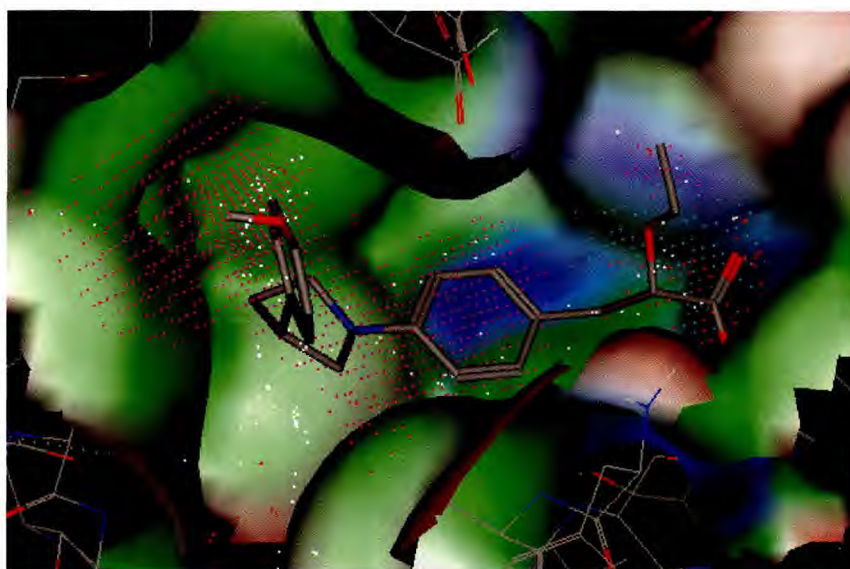


Figure 71 Proposed interaction of the pyrrolidine scaffold with the PPAR γ active site (R = OMe)

The racemic retrosynthetic analysis is shown in **Figure 72**. The key step involves a Buchwald-Hartwig synthesis of tertiary amines between precursors **201** and **202**.^{251,252}

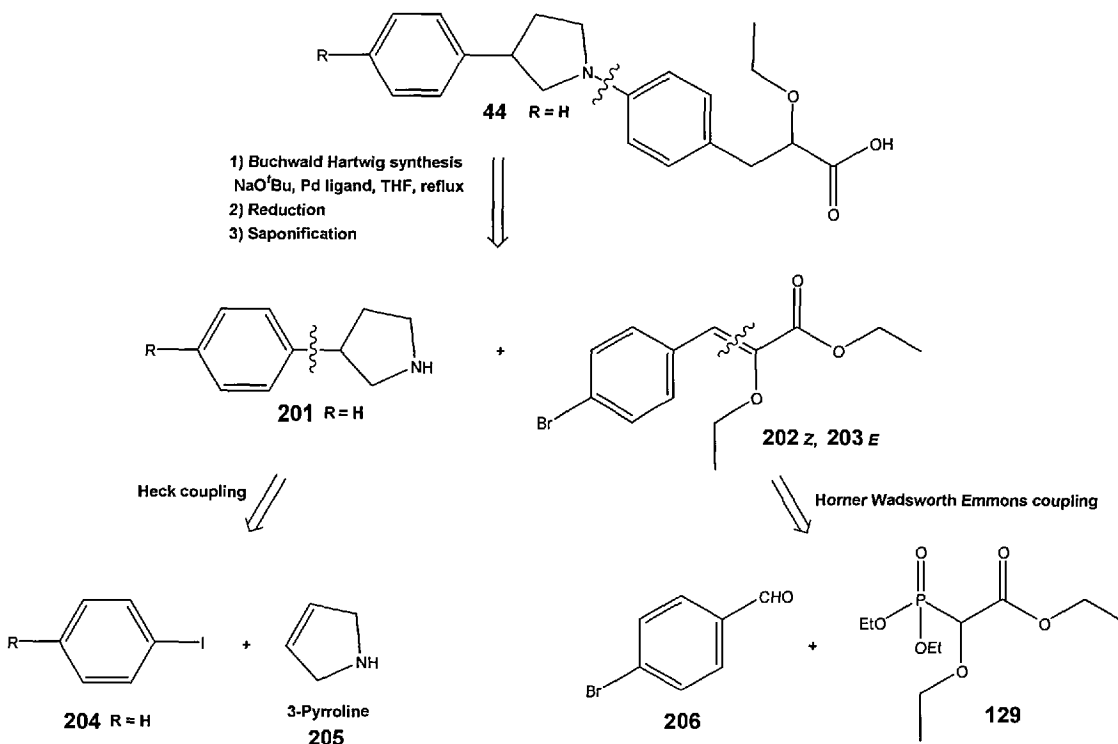
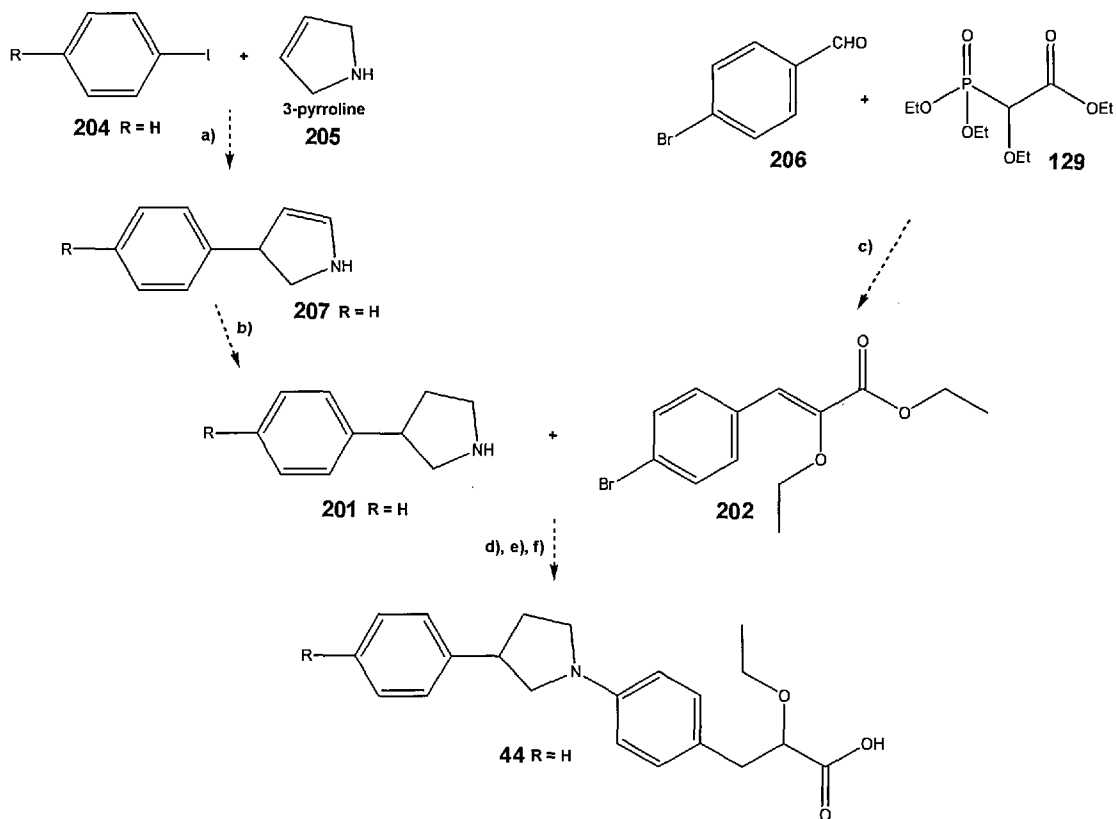


Figure 72 Retrosynthetic analysis of the pyrrolidine scaffold

Precursor **201** can be prepared by a Mizoroki-Heck coupling between the aryl halide **204** and 3-pyrroline **205**, followed by a reduction of the pyrroline **207** into the corresponding pyrrolidine **201** while precursor **202** can be made by a Horner Wadsworth Emmons coupling between 4-bromobenzaldehyde **206** and phosphonoacetate **129** which was made using Arbuzov chemistry as previously described in section 4.2.3.1 (**Scheme 41**). The proposed forward, convergent synthesis is shown in **Figure 73**. The Buchwald-Hartwig amination would bring together the two key precursors **201** and **202**. Finally, reduction of the double bond, followed by saponification would give the desired pyrrolidine lead **44**.



a) Pd(dba)₂ (3mol%), THF, ^tPr₂Net b) Pd/C, HCO₂NH₄ c) NaH, dry THF, 0 °C to RT
 d) NaO^tBu, 5mol% (DPPF)PdCl₂, THF, 100 °C e) Mg, dry MeOH, RT f) KOH, EtOH/H₂O

Figure 73 Proposed forward synthesis of the pyrrolidine scaffold

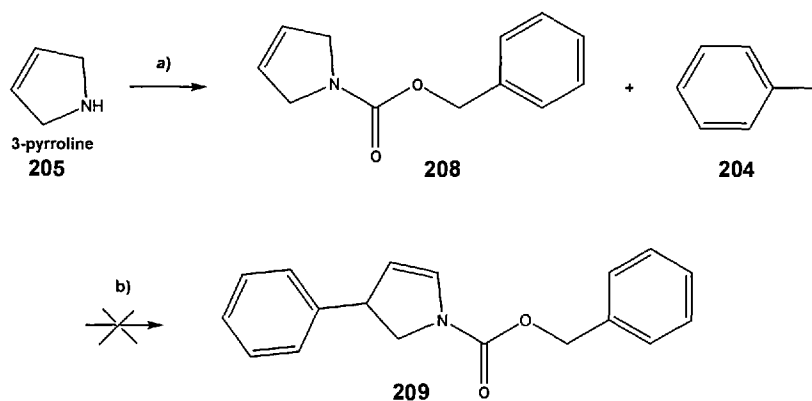
4.3.2. Synthesis of the pyrrolidine scaffold

The synthesis was attempted with R = H. In order to synthesise pyrroline precursor **207**, the Mizoroki-Heck reaction was attempted between phenyl iodide **204** and commercially available 3-pyrroline **205** using various conditions summarised in **Table 13**.^{253,254} Entry 1 involved the use of Pd(dba)₂, diisopropylethylamine in anhydrous toluene²⁵⁵ while entries 2 and 3 consisted of the use of Pd(OAc)₂, NaHCO₃, *n*Bu₄NHSO₄, molecular sieves 4Å, with and without triphenylphosphine, in either acetonitrile or DMF.²⁵⁶ However, none of the reactions were successful. The reactions led to a complex mixture of products which was difficult to analyse by NMR, even after purification by chromatography. It was therefore decided to protect the nitrogen atom of 3-pyrroline before attempting the Heck reaction in order to prevent any side-reactions occurring on the nitrogen atom.

	Reagents	Anhydrous solvent	Results
1	Pd(dba) ₂ , diisopropylethylamine, reflux	Toluene	No SM left, no product isolated
2	Pd(OAc) ₂ , NaHCO ₃ , nBu ₄ NHSO ₄ , PPh ₃ , molecular sieves 4Å, 60 °C	Acetonitrile	Iodobenzene recovered, no product isolated
3	Pd(OAc) ₂ , NaHCO ₃ , nBu ₄ NHSO ₄ , molecular sieves 4Å, 60 °C	DMF	No product isolated

Table 13 Heck coupling conditions on 3-pyrroline

A benzoate group was chosen as it requires the same cleavage conditions as those required for the reduction of the double bond after the Heck reaction, so both transformations could be done simultaneously in one pot. 3-pyrroline **205** was therefore treated with benzyl chloroformate and potassium carbonate in dry DCM and the desired protected pyrroline **208** was isolated after chromatography. Next, it was subjected to the Heck coupling conditions described by Sonesson *et al.* (**Scheme 68**).²⁵⁷ It was thus treated with phenyl iodide **204**, Pd(OAc)₂, *i*Pr₂Net, Ag₂CO₃ and P(*o*-tol)₃ in anhydrous DMF at 100 °C. However, the reaction was unsuccessful and no desired product **209** was obtained after purification of the crude. It was not possible to conclusively identify the side-products obtained but NMR seemed to indicate that there had been a side reaction on the protecting group which contains an aromatic phenyl ring.

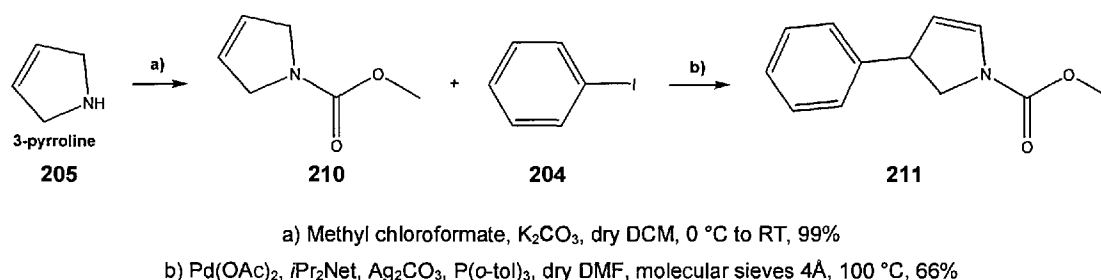


a) Benzyl chloroformate, K₂CO₃, dry DCM, 0 °C to RT, 54% b) Pd(OAc)₂, *i*Pr₂Net, Ag₂CO₃, P(*o*-tol)₃, dry DMF, 100 °C

Scheme 68 Protection of 3-pyrroline with benzyl chloroformate, followed by Heck reaction

Thus, it was decided to use a methyl carbamate protecting group as described by Sonesson *et al.*²⁵⁷ In this case, methyl chloroformate was used and once the desired pyrroline **210** was obtained, the Heck coupling was attempted using the same

conditions as above: phenyl iodide **204**, Pd(OAc)₂, *i*Pr₂Net, Ag₂CO₃ and P(*o*-tol)₃ in dry DMF at 100 °C.²⁵⁷



Scheme 69 Protection of 3-pyrroline with methyl chloroformate, followed by Heck reaction

The first issue to consider is the competition between arylation to give the desired C-3 arylated product **211** and double bond isomerisation of protected pyrroline **210** to the enamide **212** which would lead to the C-2 arylated product **213** (Figure 74). This regioselectivity problem can be overcome by choosing the right phosphine ligand. Monodentate ligands have been found to be a lot more effective than bidentate ones. Moreover, the use of silver additives controls the double bond migration. Sonesson *et al.* found that a minimum of 0.7 eq of silver carbonate when using phenyl iodide as arylating agent was necessary to fully suppress the formation of the 2-aryl pyrroline. The second issue is the undesired diarylation, which leads to the formation of compound **214**. An excess of the olefin with respect to the iodide (ratio 10:1) was required to considerably decrease the formation of the diarylated pyrroline. The Heck reaction was successful and the desired product **211** was isolated after chromatography in a 66% yield.

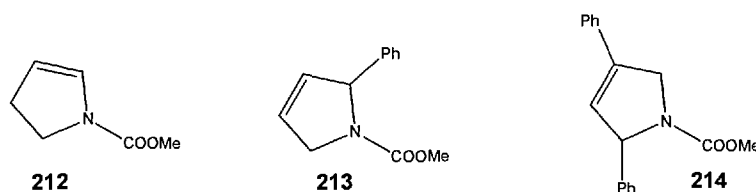
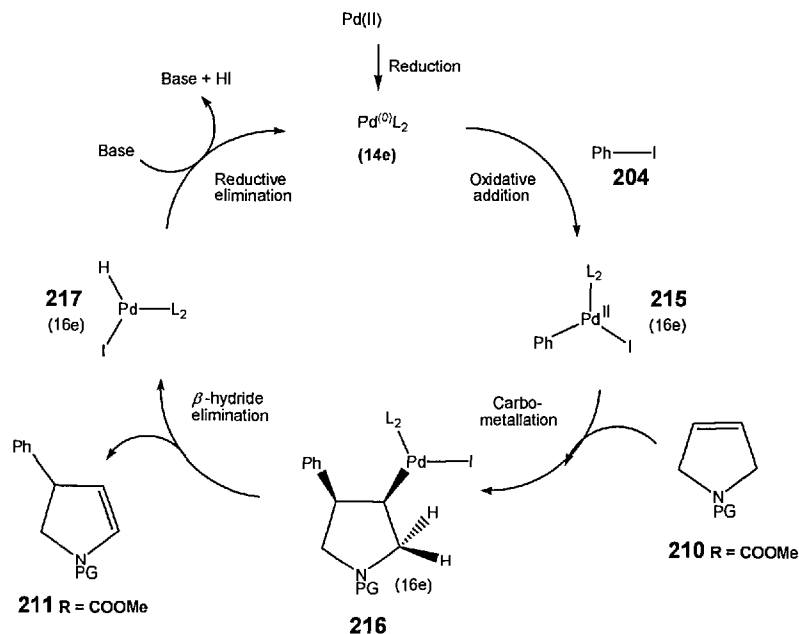


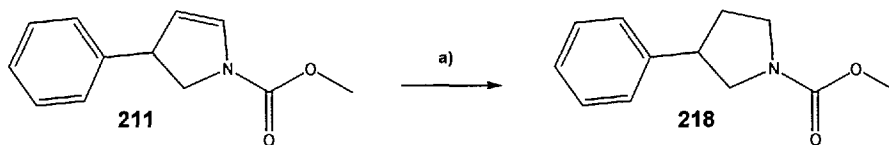
Figure 74 Possible side-products of the Heck reaction

The mechanism for the Heck reaction is outlined in **Scheme 70**. It involves reduction of palladium (II) into the active palladium (0) state, oxidative addition of the halide **204** to give the 16-electron species **215**, insertion of the olefin, and elimination of the product **211** by a β -hydride elimination process. Treatment with base regenerates the palladium (0) catalyst. The whole process is a catalytic cycle. Ag₂CO₃ effectively removes the hydrogen halide as soon as it is formed so that β -hydride elimination can take place.



Scheme 70 Mechanism of Heck coupling

Once we had the desired intermediate **211** in hand, we proceeded to the reduction of the double bond using a transfer hydrogenation as described by Sonesson *et al.*²⁵⁷ Pyrroline **211** was refluxed with ammonium formate in the presence of a catalytic amount of Pd/C in anhydrous methanol under an inert atmosphere. The starting material was still seen by NMR after 8 hours. The reaction was attempted several times but did not go to completion. It was decided to try the reduction with hydrogen gas and a catalytic amount of PtO₂ (**Scheme 71**).^{258,259} These conditions were successful and the desired pyrrolidine **218** was isolated with a yield of 65% after purification by chromatography.

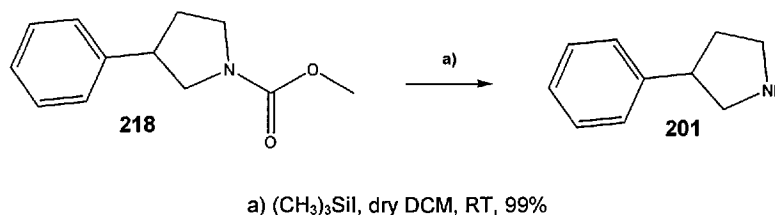


a) H₂, cat. PtO₂, anhydrous methanol, 65%

Scheme 71 Reduction of pyrroline **211** into pyrrolidine **218**

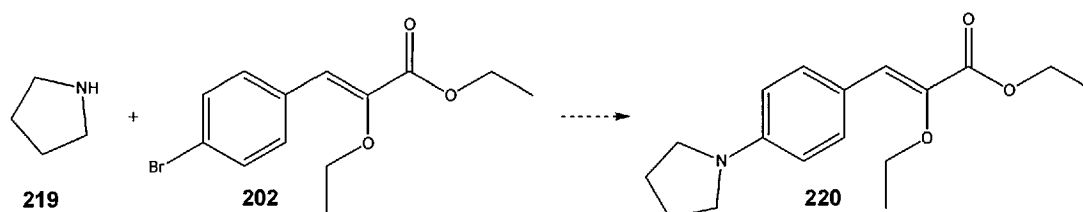
The deprotection of the carbamate of the protected pyrrolidine **218** was next carried out by refluxing with potassium hydroxide in ethanol (**Scheme 72**). The reaction did not go to completion under these conditions. The number of equivalents of potassium hydroxide and the reaction time were increased; however starting material was still present. Alternative conditions were investigated as described by Ablordeppey *et al.*

where the starting material was refluxed with potassium hydroxide in diethylene glycol and water.²⁶⁰ The purification of the crude mixture proved to be tedious due to the ethylene glycol, and still no desired product was isolated. At this stage, the reaction was attempted using iodotrimethylsilane in dry DCM.^{261, 262} These conditions were successful and the desired product was obtained with a 99% yield after purification.



Scheme 72 Cleavage of carbamate group of protected pyrrolidine **218**

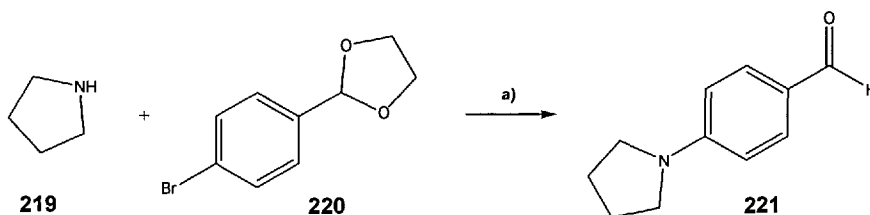
Next, the Buchwald-Hartwig amination conditions were investigated. Some model reactions were first carried out on commercially available pyrrolidine **219**. It was important to determine whether the reaction between the amine and intermediate **202** would be successful. 4-bromobenzaldehyde was coupled with phosphonoacetate **129** using the Horner Wadsworth Emmons coupling conditions previously investigated. The reaction proceeded smoothly and the bromo *Z* and *E* isomers **202** and **203** were isolated with a yield of 78%. The Buchwald-Hartwig amination was attempted using $\text{Pd}_2(\text{dba})_3$, (\pm)-BINAP and sodium *tert*-butoxide in toluene (**Scheme 73**) as it had been found to provide an excellent catalyst system for the cross coupling of amines with aryl bromides.^{263,264} However, the reaction yielded only a trace amount of the product.



Scheme 73 Buchwald-Hartwig synthesis of tertiary amine **220**

It was decided to try the reaction with the protected acetal derivative of 4-bromobenzaldehyde in order to avoid any side-reactions between the free nitrogen of pyrrolidine **219** and the carbonyl group of bromo compound **202**. Acetals have been found to be stable under these conditions by Buchwald *et al.*²⁶³ The acetal analogue **220** was synthesised from its corresponding aldehyde using ethylene glycol, catalytic *para*-toluenesulfonic acid and dry toluene with a Dean Stark set up.²⁶⁵ After isolation

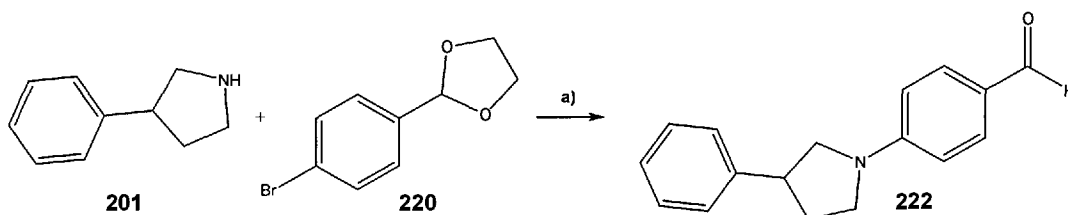
of the acetal, the Buchwald-Hartwig amination was carried out using the same conditions as above (**Scheme 74**). In this case, the reaction proceeded smoothly and only the aldehyde **221** was isolated after chromatography with a yield of 65%. The NMR of the crude reaction mixture had not shown the presence of the aldehyde, the acetal was therefore cleaved during the purification by chromatography.



a) NaO^tBu, (±)-BINAP, Pd₂(dba)₃, dry toluene, 70 °C, 65%

Scheme 74 Buchwald-Hartwig synthesis of tertiary amine using acetal **220**

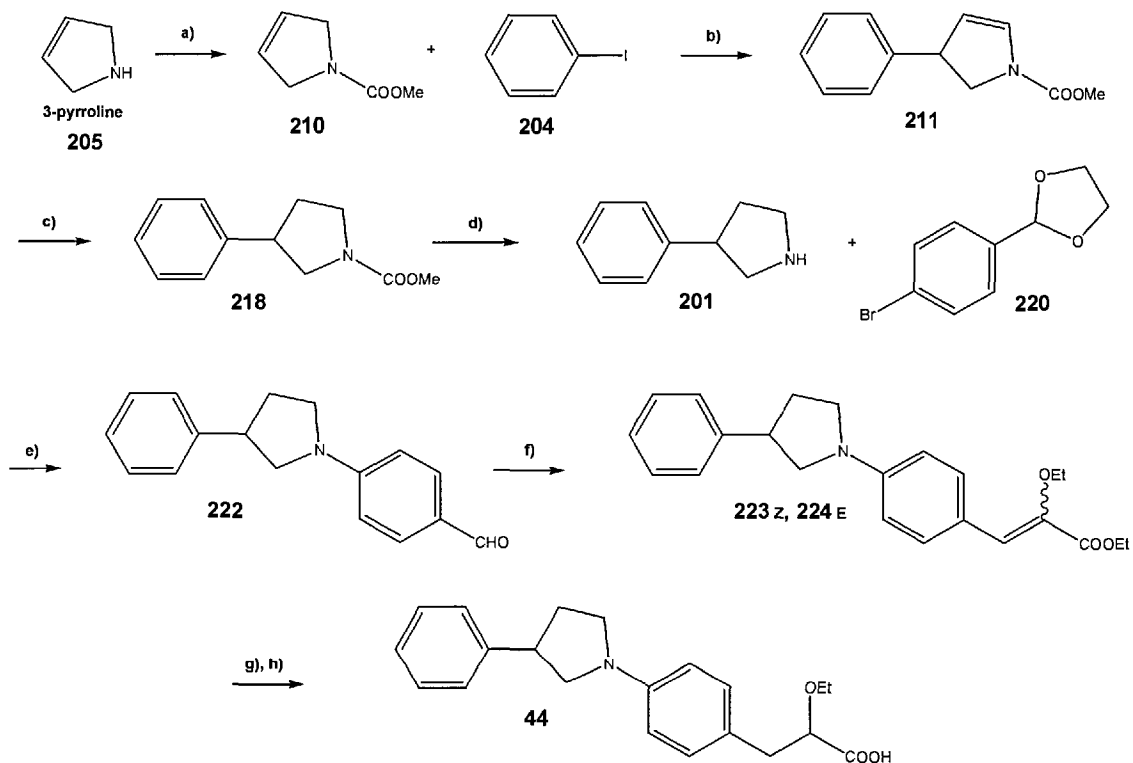
Having validated these conditions, the reaction was attempted on pyrrolidine **201** (**Scheme 75**). In this case, most of the acetal starting material was obtained after purification, together with a trace amount of product **222** (4%). The reaction was repeated and the number of equivalents of sodium *tert*-butoxide, Pd₂(dba)₃ and (±)-BINAP was increased. The yield of the reaction was significant improved to 25%. In future work, the Buchwald Hartwig amination conditions will have to be further optimised.



a) NaO^tBu, (±)-BINAP, Pd₂(dba)₃, dry toluene, 70 °C, 25%

Scheme 75 Buchwald-Hartwig amination on the desired pyrrolidine **201**

The last three steps of the synthesis involve a methodology used previously to build up the ethoxypropanoic acid side chain on the indole scaffold. The HWE coupling with phosphonoacetate **129** proceeded smoothly to give the *Z* and *E* isomers **223** and **224** in a ratio of 63:37, with an overall yield of 92%. Reduction of the double bond using magnesium turnings, followed by saponification with potassium hydroxide afforded the desired pyrrolidine **44** (**Scheme 76**).



- a) Methyl chloroformate, K_2CO_3 , dry DCM, 0 °C to RT, 99% b) $Pd(OAc)_2$, iPr_2Net , Ag_2CO_3 , $P(o-tol)_3$, dry DMF, sieves 4Å, 100 °C, 66% c) H_2 , PtO_2 , dry MeOH, 65% d) TMSI, dry DCM, RT, 99%
 e) NaO^tBu , (\pm)-BINAP, $Pd_2(dba)_3$, dry toluene, 70 °C, 25% f) Phosphonoacetate **129**, NaH, dry THF, 0 °C to RT, 92%
 g) Mg, dry MeOH, RT, 68% h) KOH, EtOH/ H_2O , 88%

Scheme 76 Synthesis of the pyrrolidine target **44**

4.4 Summary

Our objective is to design and synthesise new potent dual PPAR α/γ agonists as potential treatments for the metabolic syndrome and diabetes type II, as well as inflammatory neurological diseases. Prosarix Ltd, using its proprietary software, designed two novel heterocyclic scaffolds using a *de novo* approach.

The racemic synthesis of the six indole leads **38** to **43** derived from the first heterocyclic scaffold as well as the PPAR activation assay was described (**Figure 75**). A number of synthetic routes were explored before validating the one where the starting material is 5-cyano indole. We have obtained proof of concept for Prosarix Ltd's software as we showed activation of both PPAR α and PPAR γ using a luciferase reporter gene assay. Overall, the indoles activated the PPARs in the following order in human MCF-7 cells: $\gamma > \alpha > \delta$. The activation of PPAR δ was less significant. Indole leads **42** and **43** out of the series were the best activators of PPAR α and PPAR γ . We have thus synthesised a novel series of 2-aryl indole small molecules with a specific activation profile of the PPAR family of nuclear receptors.

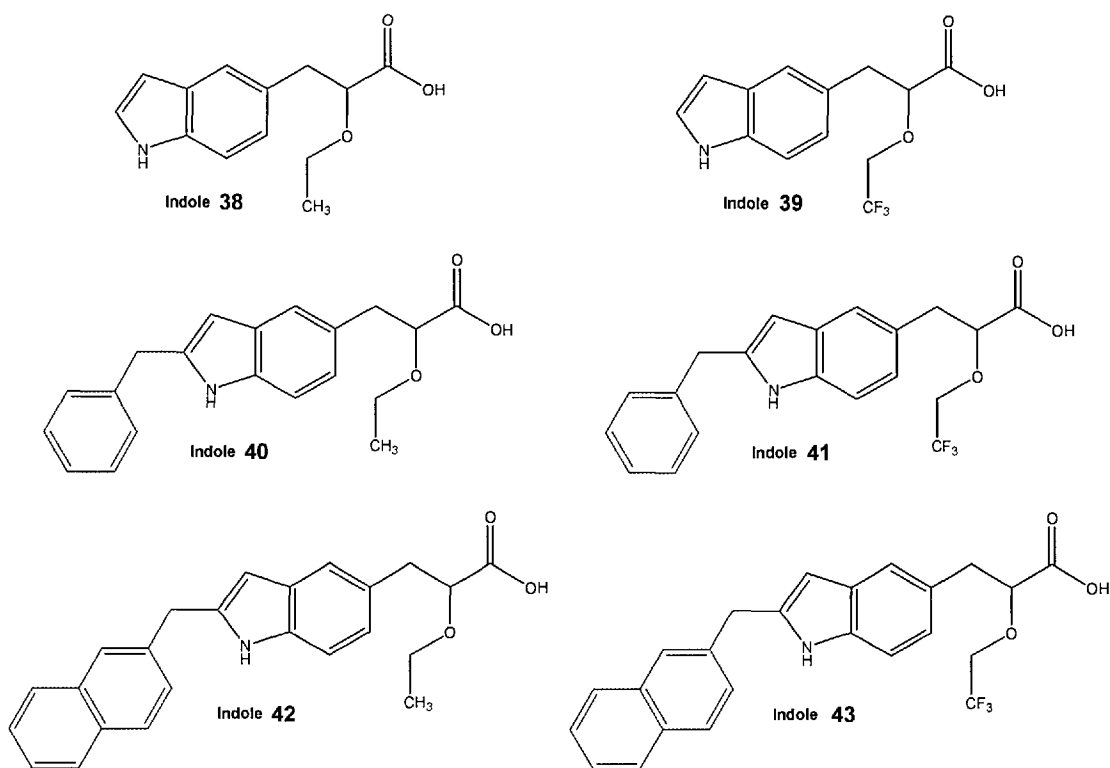
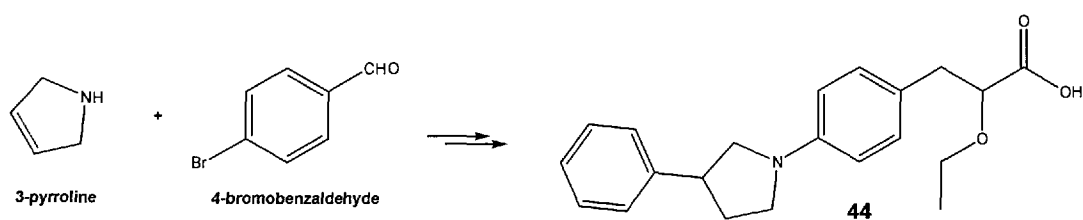


Figure 75 Indole leads 38-43

Work towards the second heterocyclic scaffold was also described and the synthesis route of the pyrrolidine lead **44** was successful from 3-pyrroline and 4-bromobenzaldehyde.



Scheme 77 Synthesis of the pyrrolidine lead **44**

CHAPTER 5

Conclusions and future directions

Given the importance of metabolic diseases such as the metabolic syndrome and diabetes type II today and the lack of adequate treatment which prevents the development of these diseases, there is an urgent need for new effective drugs. The peroxisome proliferators-activated receptors have been established as powerful targets because of their positive actions on insulin sensitivity, glucose and lipid metabolism. In fact, one current class of pharmaceutical drugs is the thiazolidinediones, which are peroxisome proliferator-activated receptor (PPAR) γ agonists. However, their side-effects include weight gain, oedema and liver toxicity. New effective drugs with an improved side-effect profile are needed.

PPARs are transcription factors which directly control gene expression by binding to specific response elements within promoters; there are three subtypes α , γ , and δ . Considering the critical physiological role of all the PPAR subtypes as lipid sensors and regulators of lipid metabolism, the aim of this project was to synthesise novel dual or pan PPAR agonists as potential drugs for the treatment of metabolic disorders.

The first part of the project consisted of the synthesis of lipid analogues in collaboration with Professor Rolf Berge at the Institute of Medicine of Bergen and ThiaMedica AS, Norway. Tetradecylthioacetic acid (TTA) **31**, a fatty acid analogue, developed by Thia Medica AS, was found to be a potent pan PPAR agonist. Although it is presently in clinical studies, TTA suffers from poor ADME characteristics. In order to improve the bioavailability of the PPAR activator, TTA **31**, two novel lipid analogues, TTA-PC **32** and TTA-TAG **33**, were synthesised as natural prodrugs (**Figure 76**). The mechanism of absorption and digestion of phospholipids and triglycerides is such that they are better absorbed in the gut.

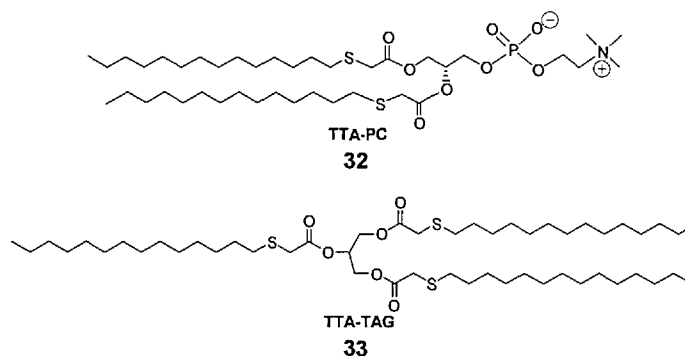


Figure 76 First two TTA analogues synthesised

In vivo experiments in male Wistar rats were conducted with TTA, TTA-PC and TTA-TAG by Professor Rolf Berge's team in Norway. Although all three compounds showed a decrease in plasma triacylglycerol, cholesterol and hepatic triacylglycerol levels, TTA-PC's effects were far better than TTA. Fatty acid oxidation and the activity of key mitochondrial enzymes involved in fatty acid oxidation and transport were also measured as these are very important dysfunctions in the metabolic diseases. It was found that the activities of fatty acid palmitoyl-CoA, carnitine palmitoyl transferase-II, 3-hydroxy-3-methylglutaryl-CoA synthase and fatty acyl-CoA were all significantly increased with TTA and TTA-PC whereas TTA-TAG was slightly less effective in general. Importantly, TTA-PC significantly improved the activity of the key enzymes by nearly two-fold compared to TTA.

These promising results motivated us to synthesise four further TTA analogues using a variety of enzymatic reactions (**Figure 77**). Starting from TTA-PC **32**, phospholipase A2 afforded *lyso* TTA-PC **34** in a 70% while transphosphatidylation with phospholipase D and serinol or glycerol yielded TTA-Pser **64** and TTA-PG **36** in 87% and 69% yields respectively. TTA-Chol **37** was obtained in 99% yield by the coupling between TTA **31** and cholesterol. The *in vitro* PPAR activation of the new lipid analogues was measured using a luciferase reporter gene assay at the Institute of Medicine of Bergen. Due to solubility and formulation issues, only *lyso* TTA-PC and TTA-PG could be tested *in vitro*. Preliminary results showed that both *lyso* TTA-PC and TTA-PG are promising compounds, displaying good activity relative to parent compound TTA. In human MCF-7 cells, the PPARs were activated in the following order by the two new lipids: $\alpha > \delta > \gamma$. Their effects *in vivo* now need to be assessed.

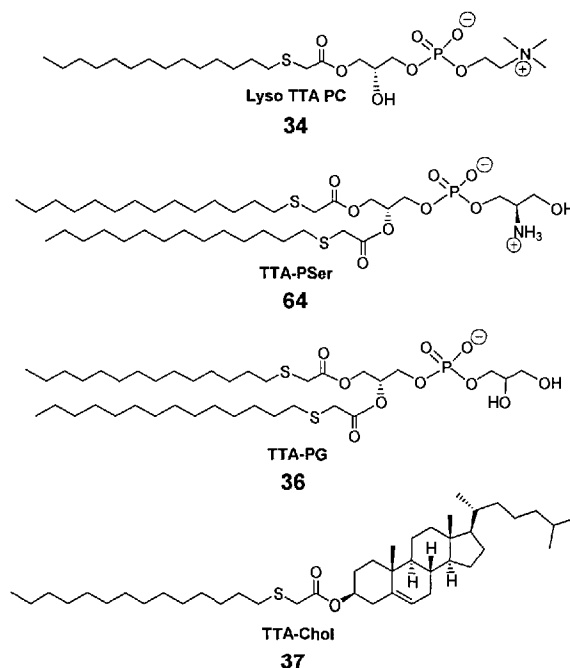
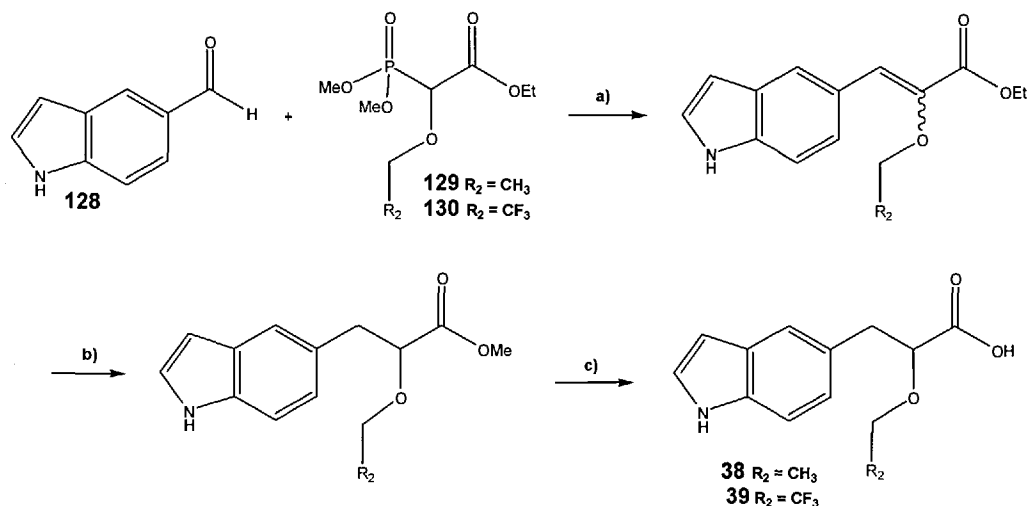


Figure 77 Structures of novel lipid analogues of TTA

The second part of the project consisted of the synthesis of novel indole leads, designed as potential PPAR α/γ dual agonists by Prosarix Ltd, using their proprietary *de novo* approach design ProtoBuild™. The first synthetic route envisaged, involving a final step Fischer Indole synthesis, was unsuccessful. Thus, the indole leads **38** to **43** targets were synthesised using another approach where the starting material is a suitably functionalised indole. **Scheme 78** shows the synthetic route employed for indoles **38** and **39** (where R₁ = H) whereas **Scheme 79** shows the methodology developed for the synthesis of indoles **40** to **43** (where R₁ = benzyl or a naphthylmethyl group). An important aspect of the second synthesis focussed on the selective introduction of the aryl group on the 2-position of the indole. This was achieved by protecting the indole nitrogen with benzenesulfonyl group, followed by lithiation and finally treatment with the corresponding bromide.

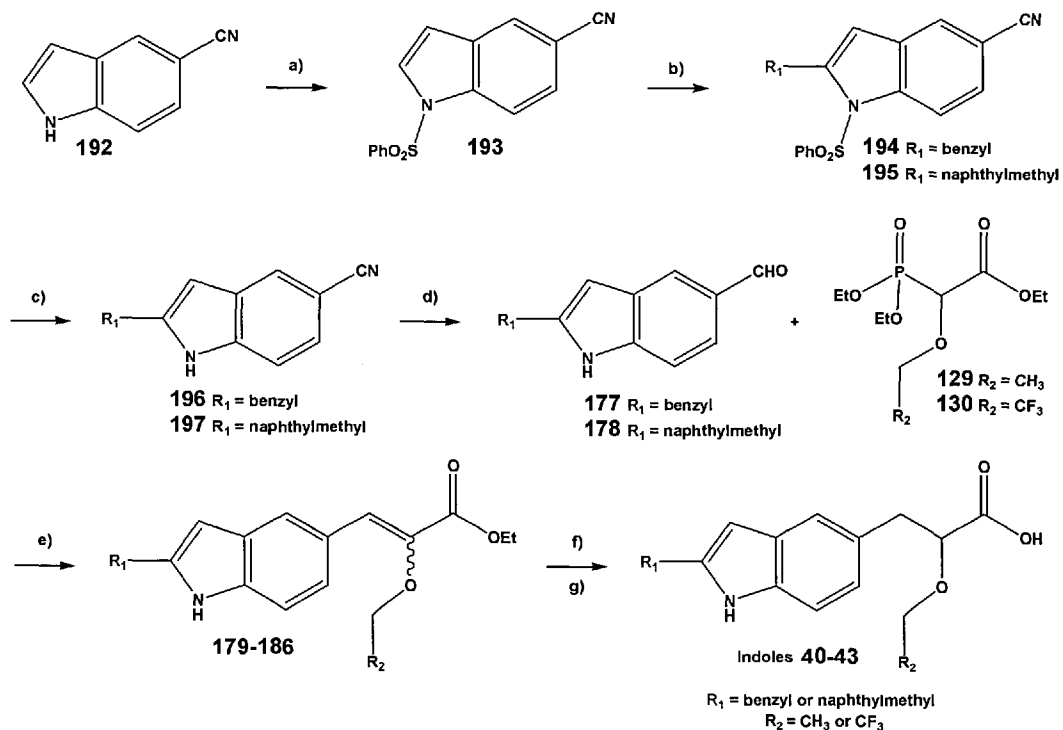


a) NaH, dry THF, 0°C to RT b) Mg turnings, dry MeOH, RT c) KOH, EtOH/H₂O, reflux

Scheme 78 Synthesis of indole leads 38 and 39

The six indole leads 38 to 43 were thus successfully synthesised. The degree of purity of the compounds was very important prior to their testing *in vitro*. A minimum of 97% purity of the indoles was achieved by careful purification of all the intermediates, followed by crystallisation wherever possible. Full characterisation of the indoles included ¹H and ¹³C NMR, HRMS, elemental analysis, IR and the measurement of melting points wherever applicable.

After the 6 indole leads were synthesised, their potential as PPAR activators was evaluated using a luciferase reporter gene assay by Professor Berge's research team based at the Institute of medicine of Bergen.



Scheme 79 Route chosen for the synthesis of the last four indole leads

The assay showed that the indoles **38** to **43** activated the PPARs in the following order in the human breast cancer cell line MCF-7: $\gamma > \alpha > \delta$. In terms of structure-activity relationship, indoles **38** and **39** were much less potent in general, confirming that the presence of the aryl group on the 2-position of the indole is important for the interaction in the hydrophobic site at the entrance (**Figure 47**, page 92). The full structures of indoles **40** to **43** and their PPAR activation results are summarised in **Figure 78** and **Figure 79**. Indoles **42** and **43** were found to be slightly more potent PPAR α/γ dual agonists than indoles **40** and **41** in the indole series. The activation assay thereby gave proof of concept for Prosarix Ltd's *de novo* design software which has allowed us to synthesise a novel class of 2-aryl indoles with an ethoxypropanoic acid side-chain at the 5-position. Further *in vitro* tests are to be carried out with this family of compounds in order to assess their ADME properties and choose the best candidate for future development and *in vivo* work.

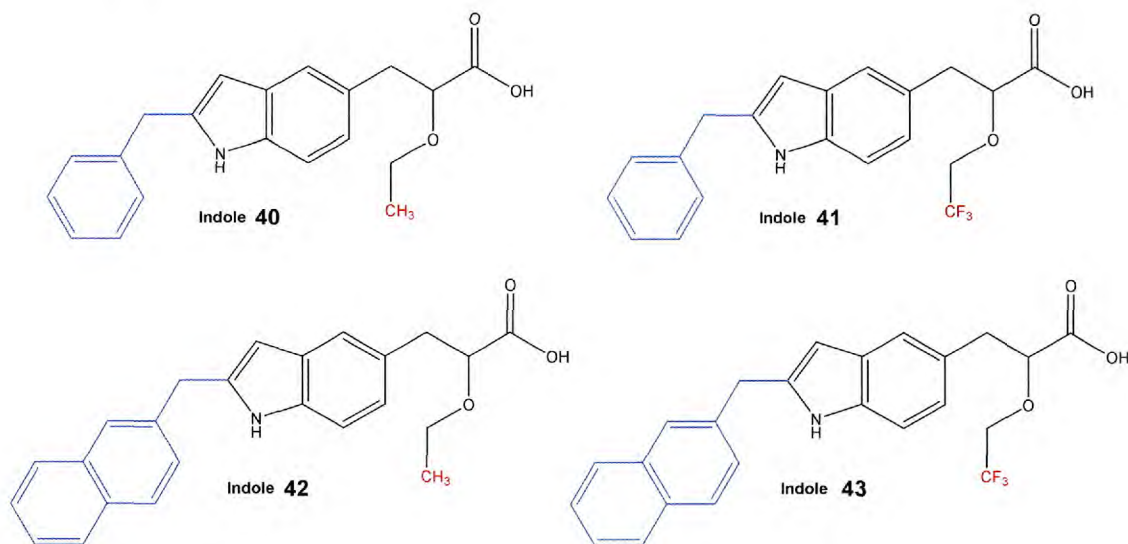


Figure 78 Novel class of indoles synthesised as PPAR agonists

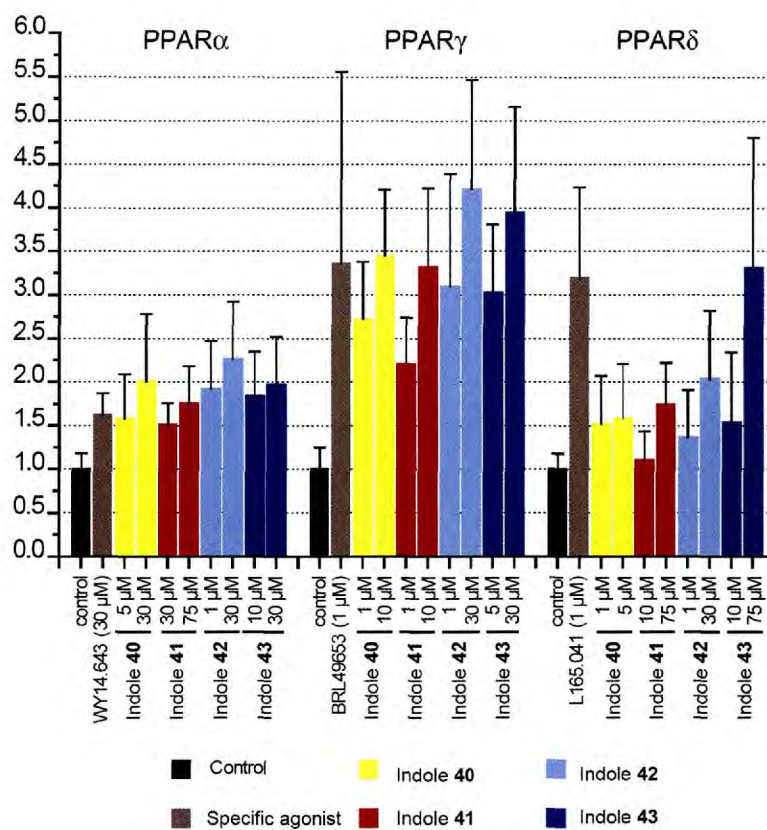
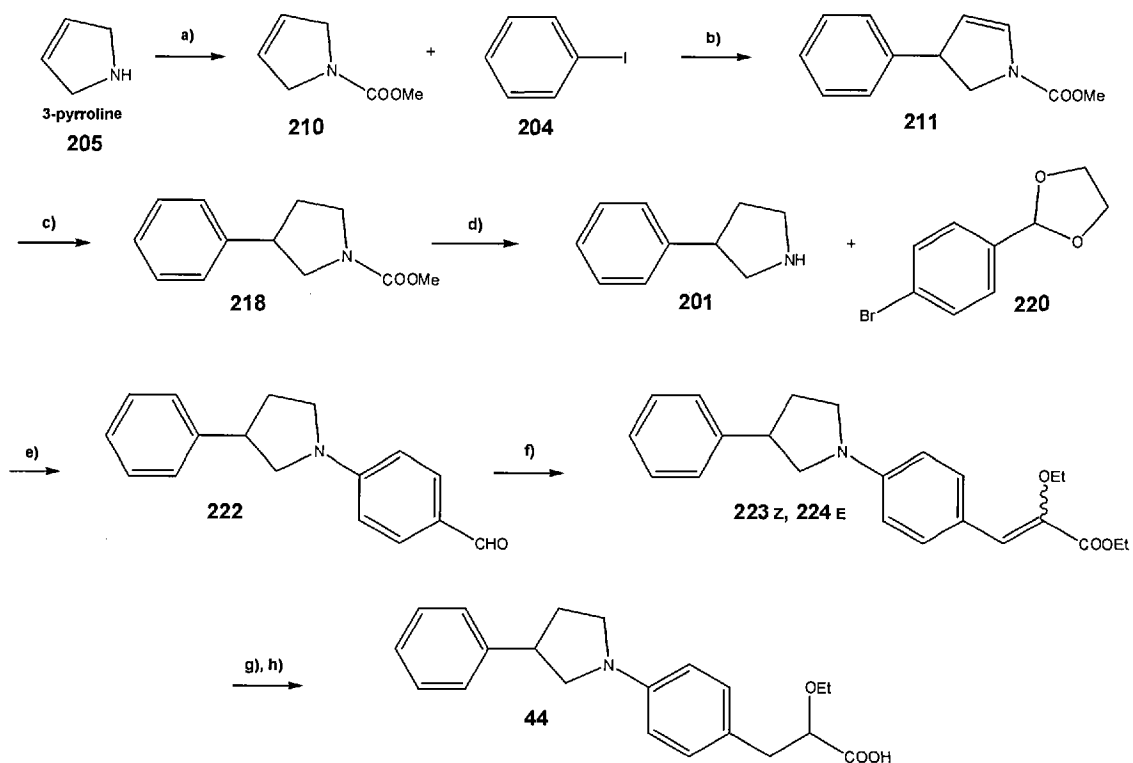


Figure 79 PPAR activation results with indoles 40 to 43

Furthermore, the synthesis of the second heterocyclic scaffold was also described in Chapter 4. The key pyrrolidine **222** was synthesised using a variety of palladium couplings involving a Mizoroki-Heck coupling and a Buchwald-Hartwig amination reaction (**Scheme 80**). The final steps included a Horner Wadsworth Emmons

coupling, followed by reduction of the double bond and saponification to give the first pyrrolidine target **44**. Its potential as a PPAR agonist is now to be evaluated.



- a) Methyl chloroformate, K_2CO_3 , dry DCM, 0 °C to RT, 99% b) $Pd(OAc)_2$, iPr_2Net , Ag_2CO_3 , $P(o-tol)_3$, dry DMF, sieves 4Å, 100 °C, 66% c) H_2 , PtO_2 , dry MeOH, 65% d) TMSI, dry DCM, RT, 99%
 e) NaO^tBu , (\pm)-BINAP, $Pd_2(dba)_3$, dry toluene, 70 °C, 25% f) Phosphonoacetate **129**, NaH, dry THF, 0 °C to RT, 92%
 g) Mg, dry MeOH, RT, 68%, h) KOH, EtOH/ H_2O 1:1, reflux, 88%

Scheme 80 Synthesis of the pyrrolidine lead **44**

To conclude, we have synthesised two series of orthogonal PPAR agonists which have very different PPAR activation profiles. A comparison between the PPAR activation of the lipids *lyso* TTA-PC and TTA-PG with respect to the indoles shows that the TTA analogues activate PPAR α better than the indoles whereas the indoles activate PPAR γ better with the exception of indole **40** which was found to be a potent activator of PPAR δ . The order of activation of the PPARs is as follows in human MCF-7 cells: $\alpha > \delta > \gamma$ for the lipids and $\gamma > \alpha > \delta$ for the indoles. The difference in these activation profiles means that the two families of compounds will have different effects in terms of potency, beneficial effects and side-effects.

The pyrrolidine offers the possibility of developing yet another family of PPAR agonists with its own activation profile.

CHAPTER 6

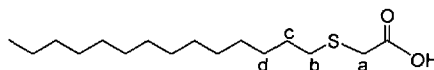
Experimental

6.1 General information

All reactions were carried out under an atmosphere of nitrogen or argon, in oven-dried glassware, unless otherwise stated. CH_2Cl_2 was distilled over P_2O_5 , and other solvents were bought and pre-dried as required. Hipersolv chloroform was used for some reactions. All chemicals were purchased from Sigma-Aldrich, Lancaster and Merck Biosciences. **Flash column chromatography** was performed on silica gel 60 (Merck Kieselgel 60 F₂₅₄ 230-240 mesh) according to the method of *W. C. Still*.²⁶⁶ TLC refers to thin layer chromatography performed on pre-coated Merck silica gel (0.2 mm, 60 F₂₅₄) aluminium-backed plates, and visualised with a UV lamp (254 nm) and/or stained with acidic ammonium molybdate (IV), basic potassium manganate (VII; KMnO_4), iodine and phosphomolybdic acid. Special chromatography solvent mixtures are: solvent A - $\text{CH}_2\text{Cl}_2/\text{MeOH}/\text{H}_2\text{O}$ 345:90:10, solvent B - $\text{CH}_2\text{Cl}_2/\text{MeOH}/\text{H}_2\text{O}$ 65:25:4, solvent C - $\text{CH}_2\text{Cl}_2/\text{MeOH}/\text{AcOH}$ 92:7:1. **Melting points** were measured on a Stuart Scientific SMP3 apparatus and are reported without correction. **Infra red spectra** (IR) were measured on a JASCO FT/IR-620 spectrometer. **¹H NMR, ¹³C NMR and ³¹P NMR spectra** were recorded on Bruker Avance 400. ¹H NMR was recorded at 400 MHz and chemical shifts, δ_{H} are quoted in parts per million (ppm), using residual isotopic solvent as internal reference (CDCl_3 , $\delta_{\text{H}} = 7.27$ ppm; CD_3OD , $\delta_{\text{H}} = 3.30$ ppm). Data is reported as follows: (integration; br = broad; s = singlet, d = doublet, t = triplet, q = quartet, m = multiplet; coupling constant(s) *J* in Hz to the nearest 0.5 Hz; assignment). Peaks split by the presence of a phosphorus atom are indicated with a superscript p. ¹³C NMR spectra were recorded at 100 MHz and chemical shifts, δ_{C} are quoted in parts per million (ppm), using residual isotopic solvent as internal reference (CDCl_3 , $\delta_{\text{C}} = 77.00$ ppm; CD_3OD , $\delta_{\text{C}} = 49.05$ ppm). Data is reported as follows: (C, CH, CH₂, CH₃; d = doublet, q = quadruplet; coupling constant(s) *J* in Hz to the nearest 0.5 Hz; assignment). ¹³C NMR has only been assigned when the latter was confirmed by correlation between ¹H and ¹³C NMR. Peaks split by the presence of a phosphorus atom are indicated with a superscript p. **Mass spectra** were recorded using VG Platform II, VG-070B, Joel SX-102 or Bruker Esquire 3000 ESI instruments. Mass accuracy is indicated to the nearest 0.1 ppm. **Elemental analysis** was carried out by Stephen Boyer using a Perkin Elmer 2400 CHN elemental analyser at the Science Technical Support unit, London Metropolitan University.

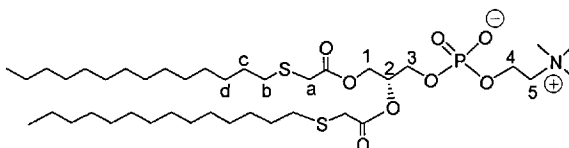
6.2 Chemistry

2-(Tetradecylthio)acetic acid **31**



Tetradecyl bromide (5.36 ml, 18.0 mmol, 1.00 eq) was added to a solution of thioglycolic acid (1.25 ml, 18.0 mmol, 1.00 eq) in 25% NaOH in MeOH (6.03 g in 24.0 ml) and the mixture was stirred vigorously at RT for 72 hr. After dilution with water, the mixture was acidified to pH 1 with concentrated HCl and the aqueous phase was extracted with diethyl ether. Drying with MgSO₄ and concentration *in vacuo* afforded a cloudy white solid which was purified by flash column chromatography on silica gel (hexane/EtOAc 3:1) to yield 4.73 g (91%) of TTA as a fluffy white amorphous solid: mp 69.0-71.0 °C (cyclohexane); R_f 0.50 [hexane/EtOAc 3:1]; ν_{\max} (nujol)/cm⁻¹ 2952, 2851, 1685 (C=O), 1461, 1377, 724; δ_{H} (CDCl₃) 3.27 (2H, s, Ha), 2.68-2.65 (2H, t, J 7.5, Hb), 1.66-1.58 (2H, m, Hc), 1.41-1.36 (2H, m, Hd), 1.27 (20H, s, 10xCH₂), 0.908-0.874 (3H, t, J 7.0, CH₃); δ_{C} (CDCl₃) 176.65 (C, C=O), 33.54 (CH₂, Ca), 32.87 (CH₂, Cb), 31.95 (CH₂, Cc), 29.67, 29.65, 29.63, 29.57, 29.48, 29.34, 29.16, 28.90, 28.72 (9xCH₂), 14.13 (CH₃); m/z (EI⁺) 287 ([M]⁺, 100); found [M+H]⁺, 798.5156, C₄₀H₈₁NO₈PS₂ requires [M+H]⁺, 798.5141; Δ = 1.9 ppm.

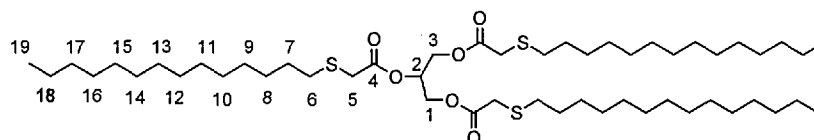
di-Tetradecylthioacetoyl-sn-glycero-3-phosphocholine **32**



To a solution of tetradecylthioacetic acid **31** (261 mg, 0.905 mmol, 1.00 eq) in DCM (5.00 ml), was added CDI (190 mg, 1.17 mmol, 1.30 eq) and the solution stirred for 2 hr and 45 mins at RT under argon. In the meantime, DBU (135 μ L, 0.905 mmol, 1.00 eq) was added to a solution of L- α -GPC (133 mg, 0.301 mmol, 0.33 eq) in DMSO (5.00 ml) and the solution was also stirred at RT, under argon for 2 hr and 45 min. The solution became turbid upon addition of DBU. The first solution was next transferred to the second one *via* cannula. The mixture was stirred vigorously at RT for 16 hr. A clear yellow solution was obtained. The mixture was acidified with acetic acid 0.1M (12.0 ml), and washed with CHCl₃/MeOH 2:1 (5x10.0 ml). The organic phase was washed with H₂O/MeOH 1:1 (5x50.0 ml) and the aqueous phase

extracted with $\text{CHCl}_3/\text{MeOH}$ 2:1 (3x100 ml). The organic phases were combined and concentrated *in vacuo* to give a brownish oil (2.78 g) which was purified by flash column chromatography on silica gel (DCM, solvent A in DCM: 10%, 20%, 80%, 90%, solvent A, solvent B, methanol) to yield 168 mg (70%) of TTA-PC as a white amorphous solid: R_f 0.40 [solvent B]; ν_{max} (nujol)/ cm^{-1} 3376, 2954-2851, 1733, 1467, 1248, 1091, 765; δ_{H} (CDCl_3) 5.25 (1H, br, H2), 4.45-4.41 (2H, dd, J 12.0, J 3.0, H1), 4.28-4.23 (2H, m, 2H3), 4.00-3.97 (2H, t, J 6.0, H4), 3.85-3.74 (2H, m, H5), 3.31-3.28 (13H, br, 3x NCH_3 , Ha), 2.63-2.58 (4H, m, Hb), 1.61-1.54 (4H, m, Hc), 1.38-1.35 (2H, m, Hd), 1.26 (40H, s, 20x CH_2), 0.85-0.82 (6H, t, J 7.0, 2x CH_3); δ_{C} (CDCl_3) 170.38, 170.13 ($\underline{\text{C}}$, 2x $\text{C}=\text{O}$), 71.50-71.43^P ($\underline{\text{C}}\text{H}$, d, J 7.0, C2), 66.34-66.27^P ($\underline{\text{C}}\text{H}_2$, d, J 7.0, C5), 63.50 ($\underline{\text{C}}\text{H}_2$, C1), 63.31-63.25^P ($\underline{\text{C}}\text{H}_2$, d, J 6.0, C3), 59.40-59.35^P ($\underline{\text{C}}\text{H}_2$, d, J 5.0, C4), 54.37 (NCH_3), 33.60, 33.45 ($\underline{\text{C}}\text{H}_2$, 2xCa), 32.76, 32.68 ($\underline{\text{C}}\text{H}_2$, 2xCb), 31.91 ($\underline{\text{C}}\text{H}_2$, 2xCc), 29.71, 29.66, 29.62, 29.60, 29.35, 29.32, 29.02, 29.01, 28.85, 28.82 (18x $\underline{\text{C}}\text{H}_2$), 22.66 (2x $\underline{\text{C}}\text{H}_2$), 14.09 (2x $\underline{\text{C}}\text{H}_3$); δ_{P} ($\text{CDCl}_3/\text{MeOD}$ 2:1) -0.68; m/z (FAB⁺) 798 ($[\text{M}]^+$, 5), 510 ($[\text{M}^+$ -one fatty acid chain], 2), 184 ($[(\text{HO})\text{OP}(\text{O})\text{OCH}_2\text{CH}_2\text{N}(\text{CH}_3)_3]^+$, 41), 86 ($[\text{CH}_2\text{CH}_2\text{N}(\text{CH}_3)_3]^+$, 100), 72 (53), 57 ($[\text{N}(\text{CH}_3)_3]^+$, 30); found $[\text{M}+\text{H}]^+$, 798.5156, $\text{C}_{40}\text{H}_{81}\text{NO}_8\text{PS}_2$ requires $[\text{M}+\text{H}]^+$, 798.5141; $\Delta = 1.9$ ppm.

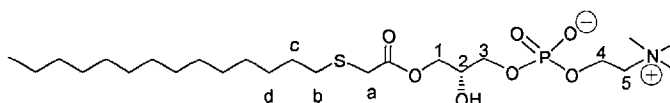
tri-Tetradecylthioacetoylglyceride 33



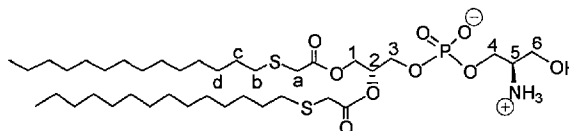
HBTU (1.16 g, 3.05 mmol, 3.28 eq) and DMAP (1.09 g, 8.95 mmol, 9.64 eq) were added to a solution of TTA (834.0 mg, 2.89 mmol, 3.11 eq) and glycerol (85.5 mg, 0.928 mmol, 1.00 eq) in dry DCM under argon. The mixture was stirred at RT, under argon, for 19 hr. The reaction had not gone to completion, thus some more TTA (93.1 mg, 0.323 mmol, 0.35 eq) was added and the reaction stirred for a further 4 hr. 15.0 ml of citric acid solution (7%) were added to the reaction mixture. The aqueous phase was separated from the organic phase and extracted with DCM (4x25.0 ml). The organic phases were combined, dried on MgSO_4 and concentrated *in vacuo* to give a white solid (2.49 g) which was purified by flash column chromatography on silica gel (hexane, hexane/EtOAc 9:1, 8:2, 6:4, EtOAc) to yield 698 mg (83%) of TTA-TAG **33** as a white amorphous powder: R_f 0.40 [hexane/EtOAc 8:2]; ν_{max} (nujol)/ cm^{-1} 3026-2852, 1737, 1722, 1493, 1377, 1262, 1170, 1028, 770; δ_{H} ($\text{CDCl}_3/\text{MeOD}$ 2:1) 5.32-5.26 (1H, m, H2), 4.39-4.35 (2H, dd, J 12.0, J 4.0, 2xH1), 4.26-4.21 (2H, dd, J 12.0, J

6.0, 2xH3), 3.20 (6H, s, 3x2H5), 2.61-2.57 (6H, m, 3x2H6), 1.59-1.52 (6H, m, 3x2H7), 1.36-1.31 (6H, m, 3x2H8), 1.22 (60H, br, 3x2(H9-H18), 0.86-0.82 (9H, t, J 7.0, 3x3H19); δ_C (CDCl₃/MeOD 2:1) 171.27, 170.83, 170.49 (C, 3xC=O), 70.26 (CH, 3xC2), 63.10 (CH₂, C1, C3), 33.80-33.68 (CH₂, 3xC5), 33.16, 33.13 (CH₂, 3xC6), 32.33 (CH₂, 3xC7), 30.09, 30.07, 30.02, 29.95, 29.76, 29.65, 29.64, 29.39, 29.19, 29.16 (33xCH₂, 3x(C8-C18)), 14.33 (CH₃, 3xC19); m/z (FAB⁺) 901 ([M]⁺, 59), 705 (21), 615 ([M-TTA]⁺, 69), 345 (19), 270 (49), 243 (80), 227 (11), 83 (41), 59 (66), 55 (94), 43(100); found [M+H]⁺, 901.5948, C₅₁H₉₈O₆S₃ requires [M+H]⁺, 901.5906; Δ = 4.7 ppm.

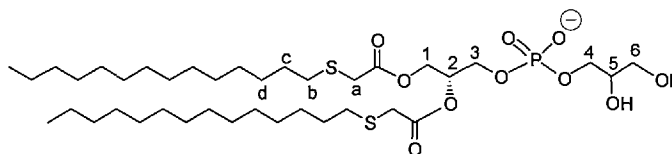
Lyso-di-tetradecylthioacetoyl-sn-glycero-3-phosphocholine 34



TTA-PC **32** (49.4 mg, 0.062 mmol, 1.00 eq) was dissolved in diethylether/methanol 99:1 (2.00 ml). Tris-Cl 50 mM (2.00 ml) and CaCl₂ 40 mM (1.00 ml) were added to the solution (pH adjusted to 8.4), followed by phospholipase A₂ from *crotalus adamenteus* venom (63 units). The mixture was stirred at 37 °C for 4 hr, after which the aqueous phase was separated from the organic one and extracted with CHCl₃/MeOH 2:1 (4x10.0 ml). The organic phases were combined and concentrated *in vacuo* to give a white solid (104 mg) which was purified by flash column chromatography on silica gel (DCM, solvent A in DCM: 20%, solvent A, solvent B) to yield 20.4 mg (62%) of lyso TTA PC as a sticky white powder: R_f 0.10 [solvent B]; ν_{\max} (nujol)/cm⁻¹ 3348, 2953-2852, 1732, 1463, 1249, 1135, 1054, 721; δ_H (CDCl₃/MeOD 2:1) 4.28-4.11 (3H, m, 2xH1, H2, 1xH3), 3.95-3.86 (3H, m, 2xH4, 1xH3), 3.59 (2H, b, 2xH5), 3.23-3.12 (11H, m, 2xHa, 3xNCH₃), 2.60-2.56 (2H, t, J 7.5, 2xHb), 1.58-1.51 (2H, m, 2xHc), 1.34-1.32 (2H, m, 2xHd), 1.21 (20H, s, 10xCH₂), 0.85-0.81 (3H, t, J 7.0, CH₃); δ_C (CDCl₃/MeOD 2:1) 171.52 (C, C=O), 69.05-68.99^P (CH, d, J 6.0, C2), 67.22-67.17^P (CH₂, d, J 5.0, C5), 66.88 (CH₂, C3), 66.28 (CH₂, C1), 59.63-59.58^P (CH₂, d, J 5.0, C4), 54.52 (NCH₃), 33.99, 33.87 (CH₂, 2xCa), 33.12 (CH₂, 2xCb), 32.33 (CH₂, 2xCc), 30.05, 30.01, 29.94, 29.75, 29.64, 29.57, 29.42, 29.16 (9xCH₂), 23.06 (2xCH₂), 14.30 (CH₃); δ_P (CDCl₃/MeOD 2:1) -0.17; m/z (FAB⁺) 528 ([M+H]⁺, 1), 510 ([M-OH]⁺, 0.5), 458 (1), 243 ([HO(CH₂)₃(O)-PO(O)(CH₂)₂NMe₃]⁺, 7), 104 ([HO(CH₂)₂-NMe₃]⁺, 61), 86 ([CH₂CH₂N-(CH₃)₃]⁺, 60), 72 (40), 55 ([N(CH₃)₃]⁺, 95); found [M+H]⁺, 528.3106, C₂₄H₅₁NO₇PS requires [M+H]⁺, 528.3124; Δ = -3.4 ppm.

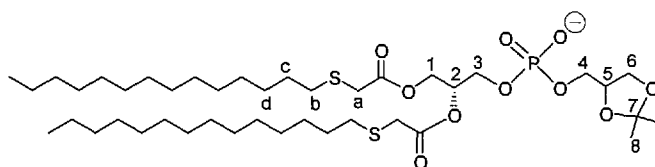
di-Tetradecylthioacetoyl-sn-glycero-3-phosphoserinol 64

A 5.5M solution of serinol (1.00 g, 11.0 mmol) in NaOAc 100 mM (1.00 ml) and CaCl₂ 50 mM (1.00 ml) was prepared and the pH adjusted to 6.2 with acetic acid. Phospholipase D from *streptomyces species* (63 units, 2.00 eq) was added to serinol (0.040 ml, 0.241 mmol, 6.00 eq) solution in a flask. TTA-PC **32** (32.0 mg, 0.040 mmol, 1.00 eq) dissolved in hipersolv chloroform (1.50 ml) was added to the mixture and the latter was stirred at 30 °C for 3 hr and 15 min. The organic phase was separated from the aqueous one and washed with water (2x20.0 ml). The aqueous phase was extracted with DCM (4x20.0 ml). The organic phases were combined and concentrated *in vacuo* to give a white solid (37.4 mg) which was purified by flash column chromatography on silica gel (DCM, solvent A in DCM: 20%, 40%, 60%, 80%, solvent A, solvent B, methanol) to yield 27.3 mg (87%) of TTA-PSer as a white sticky powder: R_f 0.60 [solvent B]; ν_{max} (nujol)/cm⁻¹ 3420, 2953-2852, 2110, 1732, 1463, 1279, 1064, 721; δ_H (CDCl₃/MeOD 2:1) 5.23 (1H, br, H₂), 4.44-4.41 (1H, dd, J 12.0, J 3.0, H₁), 4.27-4.00 (8H, m, 2xH₃, 2xH₄, NH₂, 2xH₆), 3.74-3.67 (1H, m, OH), 3.38 (1H, br, H₅), 3.23-3.22 (4H, m, Ha), 2.62-2.57 (4H, m, Hb), 1.56-1.53 (4H, m, Hc), 1.35-1.33 (4H, m, Hd), 1.23 (40H, br, 20xCH₂), 0.86-0.82 (6H, t, J 6.5, 2xCH₃); δ_C (CDCl₃/MeOD 2:1) 170.47, 170.21 (C, 2xC=O), 71.24-71.16^p (CH, J 8.0, C₂), 63.45-63.40^p (CH, J 5.0, C₅), 63.03 (CH₂, C₁), 62.76-62.71^p (CH₂, J 5.0, C₄), 58.83 (CH₂, C₆), 53.55 (NCH), 33.31, 33.19 (CH₂, 2xCa), 32.58, 32.54 (CH₂, 2xCb), 31.63 (CH₂, 2xCc), 29.37, 29.33, 29.27, 29.03, 28.98, 28.80, 28.51, 22.33 (20xCH₂), 13.49 (2xCH₃); δ_P (CDCl₃/MeOD 2:1) -0.93; m/z (FAB⁺) 784 ([M-H]⁺, 26), 514 (7), 287 (TTA⁺, 17), 229 (21), 170 ([[(HO)(O)PO(O)(CH₂)-CH(NH₂)-CH₂OH]⁺, 16), 153 ([[(O₂)PO(CH₂)-CH(NH₂)CH₂OH]⁺, 59), 79 (100); m/z (ESI⁻) 784 (100), 191 (32); found [M+H]⁺, 784.4651, C₃₈H₇₅NO₉PS₂⁻ requires [M+H]⁺, 784.4621; Δ = 3.8 ppm.

di-Tetradecylthioacetoyl-sn-glycero-3-phosphoglycerol 36

A 16M solution of glycerol (1.00 ml, 1.47 mmol) in NaOAc 100 mM (0.500 ml) and CaCl₂ 50 mM (0.500 ml) was prepared and the pH adjusted to 6.1 with acetic acid. Phospholipase D from *streptomyces species* (76 units, 2.00 eq) was added to glycerol 16 M (0.100 ml, 1.60 mmol, 42.3 eq) in a flask. TTA-PC 32 (30.2 mg, 0.038 mmol, 1.00 eq) dissolved in hipersolv chloroform (1.50 ml) was added to the mixture and the latter was stirred at 30 °C for 5 hr. The organic phase was separated from the aqueous one and washed with water (2x20.0 ml). The aqueous phase was next extracted with DCM (4x20.0 ml). The organic phases were combined and concentrated in vacuo to give a white solid (57.5 mg) which was purified by flash column chromatography on silica gel (DCM, solvent A in DCM: 20%, 40%, 60%, 80%, solvent A, methanol) to yield 18.7 mg (63%) of TTA-PG as a white amorphous solid: R_f 0.55 [solvent B]; ν_{\max} (nujol)/cm⁻¹ 3567, 2953-2853, 1730, 1462, 1377, 1232, 1072; δ_{H} (CDCl₃/MeOD 2:1) 5.22 (1H, br, H2), 4.44-4.40 (1H, dd, *J* 12.0, *J* 3.0, H1), 4.27-4.22 (1H, dd, *J* 12.0, *J* 7.0, H1), 4.11-3.89 (4H, m, 2xH3, 2xH4), 3.77 (1H, m, H5), 3.23-3.19 (4H, m, Ha), 2.61-2.56 (4H, m, Hb), 1.59-1.52 (4H, m, Hc), 1.36-1.33 (4H, m, Hd), 1.28-1.18 (40H, br, 20xCH₂), 0.86-0.82 (6H, t, *J* 7.0, 2xCH₃); δ_{C} (CDCl₃/MeOD 2:1) 171.24, 170.97 (C, 2xC=O), 72.00-71.93^P (CH, *J* 7.0, C2), 71.57-71.52^P (CH, *J* 5.0, C5), 67.20-67.15^P (CH₂, *J* 5.0, C3), 64.10-64.05^P (CH₂, *J* 5.0, C4), 63.82 (CH₂, C1), 62.99 (CH₂, C6), 34.05, 33.93 (CH₂, 2xCa), 33.33, 33.29 (CH₂, 2xCb), 32.37 (CH₂, 2xCc), 30.12, 30.08, 30.02, 30.00, 29.77, 29.73, 29.70, 29.54, 29.26, 29.24 (10xCH₂), 23.07 (2xCH₂), 14.23 (2xCH₃); δ_{P} (CDCl₃/MeOD 2:1) -1.41; m/z (FAB) 786 ([M]⁺, 24), 650 (11), 514 (5), 325 (25), 287 ([TTA]⁺, 15), 229 (22), 153 ([[(O₂)PO-(CH₂)CH(OH)CH₂OH]⁺, 75), 92 (15), 79 (57), 46 (49), 16 (100); m/z (ESI-) 785 (100), 279 (56); found [M+H]⁺, 785.4470, C₃₈H₇₄O₁₀PS₂⁻ requires [M+H]⁺, 785.4170; Δ = 3.8 ppm.

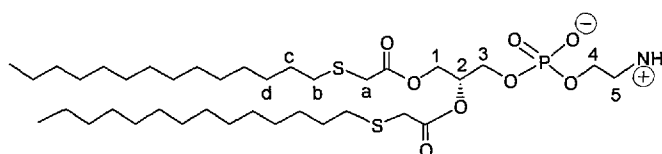
di-Tetradecylthioacetoyl-sn-glycero-3-phospho(2,2-dimethyl)-1,3-dioxolane-4-methanol **69**



A 7M solution of (S)-(+)-2,2-dimethyl-1,3-dioxolane-4-methanol solketal (0.900 ml, 7.29 mmol) in NaOAc 100 mM (0.500 ml) and CaCl₂ 50 mM (0.500 ml) was prepared and the pH adjusted to 6.4 with acetic acid. Phospholipase D from *streptomyces species* (250 units, 6.60 eq) was added to solketal 7M (0.050 ml, 0.356 mmol, 6.00

eq) in a flask. TTA-PC **32** (47.4 mg, 0.059 mmol, 1.00 eq) dissolved in hipersolv chloroform (1.50 ml) was added to the mixture and the latter was stirred at 30 °C for 5 hr. The organic phase was separated from the aqueous one and washed with water (2x20.0 ml). The aqueous phase was extracted with DCM (4x20.0 ml). The organic phases were combined and concentrated in vacuo to give a colourless oil which was purified by flash column chromatography on silica gel (DCM, solvent A in DCM: 10%, 20%, 30%, 40%, solvent A, solvent B, MeOH) to yield 50.9 mg (97%) of TTA-Pdioxolane as a white solid: R_f 0.55 [solvent B]; ν_{\max} (DCM film)/ cm^{-1} 3398, 3054, 2987, 1717, 1422, 1265, 740; δ_{H} ($\text{CDCl}_3/\text{MeOD}$ 2:1) 5.24-5.22 (1H, br, H2), 4.44-4.40 (2H, dd, J 12.0, J 3.0, H1), 4.27-4.22 (2H, m, 2xH3), 4.05-3.96 (3H, m, 2xH4, H5), 3.86-3.76 (2H, m, 2xH6), 3.22-3.20 (4H, m, Ha), 2.61-2.56 (4H, m, Hb), 1.59-1.51 (4H, m, Hc), 1.42-1.17 (50H, m, 6xH8, 4xHd, 20xCH₂), 0.86-0.82 (6H, t, J 7.0, CH₃); δ_{C} ($\text{CDCl}_3/\text{MeOD}$ 2:1) 171.13, 170.83 (C, 2xC=O), 110.09 (C, C7), 75.23-75.14^p (CH, J 9.0, C2), 71.84-71.76^p (CH, J 8.0, C5), 66.71 (CH₂, C1), 66.53-66.48^p (CH₂, J 9.0, C3), 63.95-63.90^p (CH₂, J 5.0, C4), 63.72 (CH₂, C6), 33.90, 33.78 (CH₂, 2xCa), 33.20, 33.16 (CH₂, 2xCb), 32.36 (CH₂, 2xCc), 30.11, 30.08, 30.01, 30.00, 29.78, 29.71, 29.70, 29.44, 29.24, 29.22 (10xCH₂), 26.94, 25.52 (CH₃, 2xC8), 23.08 (2xCH₂), 14.31 (2xCH₃); δ_{P} ($\text{CDCl}_3/\text{MeOD}$ 2:1) -3.20; m/z (ESI-) 825 ([M-1]⁺, 85), 555 (39), 507 (100), 329 (38), 30 (42).

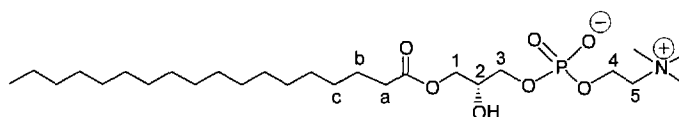
di-Tetradecylthioacetoyl-sn-glycero-3-phosphoethanolamine 67



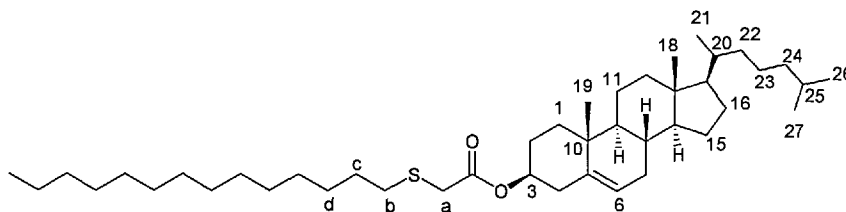
Ethanolamine (21.8 μL , 0.351 mmol) was added to NaOAc 100 mM (0.500 ml) and CaCl_2 50 mM (0.500 ml) and the pH was adjusted to 6.4 with acetic acid. Phospholipase D from *streptomyces species* (58.5 units, 1.00 eq) was added to the solution which was transferred to a flask containing TTA-PC **32** (46.6 mg, 0.059 mmol, 1.00 eq) dissolved in chloroform (1.50 ml). The mixture was stirred at 30 °C for 6 hr after which the organic phase was separated from the aqueous one and washed with water (2x15.0 ml). The aqueous phase was extracted with $\text{CHCl}_3/\text{MeOH}$ 2:1 (4x15.0 ml). The organic phases were combined and concentrated in vacuo to give a white solid (57.5 mg) which was purified by flash column chromatography on silica gel (DCM, solvent A in DCM: 20%, 40%, 60%, 80%, solvent A, solvent B, methanol) to yield 42.3 mg (95%) of TTA-PE as a white amorphous powder: R_f 0.35 [solvent A];

ν_{\max} (nujol)/ cm^{-1} 2953-2853, 1730, 1462, 1377, 1232, 1072; δ_{H} ($\text{CDCl}_3/\text{MeOD}$ 2:1) 5.23 (1H, br, H2), 4.43-4.22 (4H, 2xH1, 2xH3), 4.04-3.99 (4H, 2xH4, 2xH5), 3.22-3.19 (4H, m, 4Ha), 3.10 (br, NH), 2.61-2.56 (4H, m, Hb), 1.58-1.51 (4H, m, 4xHc), 1.37-1.22 (44H, m, 4xHd, 20xCH₂), 0.90-0.87 (6H, t, J 7.0, 2xCH₃); δ_{C} ($\text{CDCl}_3/\text{MeOD}$ 2:1) 171.14, 170.86 (C, 2xC=O), 71.78-71.70^P (CH, J 8.0, C2), 64.07-63.98^P (CH₂, J 5.0, C3), 63.64 (CH₂, C1), 62.13-62.08^P (CH₂, J 5.0, C4), 41.01-40.96 (CH₂, J 5.0, C5), 33.89-33.78 (CH₂, 2xCa), 33.18-33.13 (CH₂, 2xCb), 32.34 (CH₂, 2xCc), 30.10, 30.07, 29.98, 29.77, 29.69, 29.68, 29.42, 29.21, 29.19, 23.07 (20xCH₂), 14.09 (2xCH₃); δ_{P} (CDCl_3) -0.31; m/z (ESI⁺): 755 ([M+H]⁺, 90), 469 (100), 342 (34); found [M+H]⁺, 756.4678, C₃₇H₇₅NO₈PS₂ requires [M+H]⁺, 756.4672; Δ = 0.8 ppm.

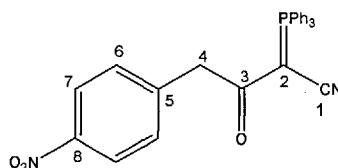
Lyso-1,2-distearoyl-sn-glycero-3-phosphocholine 58



DSPC **57** (99.4 mg, 0.126 mmol, 1.00 eq) was dissolved in diethylether/methanol 99:1 (3.00 ml). Tris-Cl 50 mM (1.00 ml) and CaCl₂ 40 mM (1.00 ml) were added to the solution (pH adjusted to 8.4), followed by phospholipase A₂ from *crotalus adamanteus* venom (126 units, 1.00 eq). The mixture was stirred at 37 °C for 1.5 hr, after which the aqueous phase was separated from the organic one and extracted with DCM (3x20.0 ml). The organic phases were combined and concentrated in vacuo to give a white solid (104 mg) which was purified by flash column chromatography on silica gel (DCM, solvent A in DCM: 20%, solvent A, solvent B) to yield 57.2 mg (87%) of *lyso* DSPC as a sticky white solid: R_f 0.10 [solvent B]; ν_{\max} (nujol)/ cm^{-1} 3376, 2953-2851, 1735, 1466, 1377, 1233, 1087, 970; δ_{H} ($\text{CDCl}_3/\text{MeOD}$ 2:1) 4.28 (2H, m, H2, H1), 4.03-3.97 (2H, m, H4), 3.92-3.83 (2H, m, H3), 3.73-3.60 (3H, m, H), 3.35-3.33 (2H, m, H5), 2.95 (9H, s, 3xNCH₃), 2.10-2.06 (2H, t, J 7.5, Ha), 1.37-1.34 (2H, m, Hc), 1.05-0.95 (28H, br, 14xCH₂), 0.63-0.60 (3H, t, J 7.0, CH₃); δ_{C} ($\text{CDCl}_3/\text{MeOD}$ 2:1) 174.81 (C, C=O), 69.39-69.33^P (CH, J 6.0, C2), 67.46-67.41^P (CH₂, J 5.0, C5), 67.08 (CH₂, C3), 65.52 (CH₂, C1), 59.66-59.61^P (CH₂, J 5.0, C4), 54.66, 54.63, 54.59 (3xNCH₃), 34.72 (2xCH₂, Ca, Cb), 32.33 (CH₂, Cc), 30.08, 29.96, 29.90, 29.81, 29.73, 29.71, 29.60, 25.34, 23.04 (13xCH₂), 14.22 (CH₃); δ_{P} ($\text{CDCl}_3/\text{MeOD}$ 2:1) -0.18; m/z (ESI⁺) 546 ([M+Na]⁺, 100), 524 ([M+H]⁺, 26), 487 (11), 184 (6), 104 (25); found [M+H]⁺, 524.3716, C₂₆H₅₅NO₇P requires [M+H]⁺, 524.3716; Δ = 0.0 ppm.

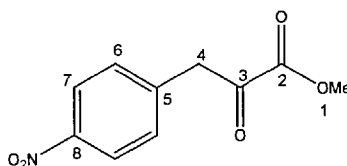
Cholesteroltetradecylthioacetate 37

HBTU (50.1 mg, 0.130 mmol, 1.09 eq) and DMAP (47.7 mg, 0.390 mmol, 3.30 eq) were added to a solution of TTA **31** (34.0 mg, 0.118 mmol, 1.00 eq) and cholesterol (47.1 mg, 0.122 mmol, 1.03 eq) in dry DCM under argon. The mixture was stirred at RT, under argon, for 18 hr. 5.00 ml of citric acid solution (7%) were added to the reaction mixture. The aqueous phase was separated from the organic phase and extracted with DCM (4x10.0 ml). The organic phases were combined and concentrated in vacuo to give a yellowish oil (160 mg) which was purified by flash column chromatography on silica gel (hexane, hexane/EtOAc 8:2, 7:3, EtOAc) to yield 76.0 mg (99%) of TTA-Chol as a sticky white powder: R_f 0.65 [hexane/EtOAc 8:2]; ν_{\max} (nujol)/ cm^{-1} 2924-2854, 1700, 1462, 1377; δ_H (CDCl_3) 5.39 (1H, d, J 4.0, H6), 4.67-4.65 (1H, m, H3), 3.19 (2H, s, 2xHa), 2.66-2.62 (2H, t, J 7.0, 2xHb), 2.37-2.35 (2H, d, J 7.5, 2xH4), 2.04-1.86 (2H, m, H25, H14), 1.69-0.69 (66H, m, 2xHc, 2xHd, 2xH11, 2xH13, 2xH16, 2xH15, H20, H9, H8, H17, 10x CH_2 , 2xH24, 2xH1, 2xH2, 2xH4, 2xH22, 2xH23, 3xH19, 3xH21, 3xH27, 3xH26, 3xH18, 3xH27, CH_3); δ_C (CDCl_3) 170.00 ($\underline{\text{C}}$, C=O), 139.44 ($\underline{\text{C}}$, C5), 122.82 ($\underline{\text{CH}}$, C6), 74.91 ($\underline{\text{CH}}$, C3), 56.68 ($\underline{\text{CH}}$, C14), 56.15 ($\underline{\text{CH}}$, C17), 50.03 ($\underline{\text{CH}}$, C9), 42.31 ($\underline{\text{C}}$, C13), 39.73 ($\underline{\text{CH}_2}$, C12), 39.52 ($\underline{\text{CH}_2}$, C24), 38.01 ($\underline{\text{CH}_2}$, C4), 36.96 ($\underline{\text{CH}_2}$, C1), 36.58 ($\underline{\text{C}}$, C10), 36.19 ($\underline{\text{CH}_2}$, C22), 35.78 ($\underline{\text{CH}}$, C20), 33.99 ($\underline{\text{CH}_2}$, Ca), 33.72 ($\underline{\text{CH}_2}$, Cb), 32.64 ($\underline{\text{CH}_2}$, Cc), 31.92 ($\underline{\text{CH}_2}$, C7), 31.86 ($\underline{\text{CH}}$, C8), 29.70, 29.66, 29.61, 29.52, 29.36, 29.19, 29.05, 28.76 (10x $\underline{\text{CH}_2}$), 28.21 ($\underline{\text{CH}_2}$, C16), 28.00 ($\underline{\text{CH}}$, C25), 27.71 ($\underline{\text{CH}_2}$, C2), 24.27 ($\underline{\text{CH}_2}$, C15), 23.83 ($\underline{\text{CH}_2}$, C23), 22.80 ($\underline{\text{CH}_3}$, C27), 22.54 ($\underline{\text{CH}_3}$, C26), 21.03 ($\underline{\text{CH}_2}$, C11), 19.29 ($\underline{\text{CH}_3}$, C19), 18.71 ($\underline{\text{CH}_3}$, C21), 14.15 ($\underline{\text{CH}_3}$), 14.10 ($\underline{\text{CH}_3}$), 11.84 ($\underline{\text{CH}_3}$, C18); m/z (FAB^+) 658 ($[\text{M}+\text{H}]^+$, 2), 504 (2), 369 ($[\text{M}-\text{TTA}]^+$, 53), 243 (11), 154 (62), 133 (88), 91 (77), 55 (100).

4-(4-Nitrophenyl)-3-oxo-2-(triphenyl- λ^5 -phosphanylidene)-butyronitrile 79

The syringe to be used for the reaction was first washed with DCM a few times. The DMAP resin (1.76 g, 2.88 mmol, 0.20 eq), *para*-nitrophenylacetic acid (2.63 g, 14.5 mmol, 1.01 eq), (cyanomethylene)triphenylphosphorane (4.32 g, 14.4 mmol, 1.00 eq), and *N*-(3-dimethylaminopropyl)-*N*-ethylcarbodiimide hydrochloride (3.68 g, 19.2 mmol, 1.34 eq) were added to the syringe as well as DCM (20.0 ml). The orange mixture was stirred on the solid phase shaker at RT for 15 hr. The solution turned greenish after 15 hr. The reaction mixture was transferred to a separating funnel and washed with 7% citric acid solution (100 ml). The aqueous phase was separated from the organic phase and extracted with DCM (3x40.0 ml). The organic phase was washed with water (2x100 ml) and the aqueous phase was extracted with DCM (4x80.0 ml). The organic phases were combined and concentrated *in vacuo* to give a greenish solid (7.83 g) which was purified by crystallisation from hexane/DCM 20:1 to yield 6.24 g (94%) of the product as shiny white crystals: R_f 0.50 [EtOAc]; ν_{\max} (nujol)/ cm^{-1} 3026-2854, 2170, 1737, 1582, 1493, 1262, 1028, 759; δ_H (CDCl_3) 8.18-8.16 (2H, d, J 8.0, H7), 7.64-7.62 (2H, d, J 8.0, H6), 7.57-7.32 (15H, m, Har), 4.06 (2H, s, H4); δ_C (CDCl_3) 192.04-192.00^P (\underline{C} , d, J 16.0, C3), 146.73 (\underline{C} , C8), 144.16 (\underline{C} , C5), 133.50-133.40^P (\underline{CH} , d, J 40.0, 6xPh_{meta}), 133.29-133.26^P (\underline{CH} , d, J 12.0, 3xPh_{para}), 130.28 (\underline{CH} , 2xC6), 129.23-129.10^P (\underline{CH} , d, J 52.0, 6xPh_{ortho}), 123.47 (\underline{CH} , 2xC7), 123.10-122.17^P (\underline{C} , d, J 372.0, C1), 122.44-122.28^P (\underline{CH} , d, J 64.0, 3xPh), 48.85 (\underline{CH}_2 , C4), 46.25-46.17^P (\underline{C} , d, J 32.0, C2); m/z (EI^+) 464 ($[\text{M}]^+$, 3), 328 (100), 262 (8), 201 (6), 184 (3), 183 (15), 165 (5), 108 (6), 77 (4); found $[\text{M}+\text{H}]^+$, 464.1309, $\text{C}_{21}\text{H}_{28}\text{N}_2\text{O}_3\text{P}$ requires $[\text{M}+\text{H}]^+$, 464.1290; $\Delta = 4.1$ ppm.

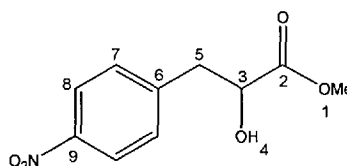
Methyl 3-(4-nitrophenyl)-2-oxopropanoate **90**



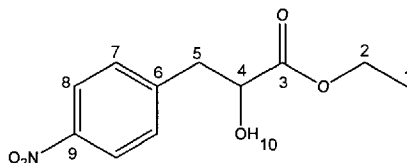
Ozone was bubbled for 30 mins into a solution of phosphorane **79** (4.89 g, 10.5 mmol, 1.00 eq) in DCM/MeOH 7:3 (100 ml) at -78 °C. The clear pale yellow solution turned lilac blue after 20 mins. N_2 was then bubbled for 23 mins. The solution turned colourless. It was stirred at -78 °C to -70 °C for 30 mins, at -50 °C to -45 °C for 45 mins, at -10 °C to 0 °C for 40 min, and finally at RT for 14.5 hr. The solution which had turned bright yellow was concentrated *in vacuo* to give a yellow oil (6.42 g). The yellow oil was re-dissolved in DCM (50.0 ml) and washed with 0.1M $\text{AgNO}_3(\text{aq})$

(2x50.0 ml). The aqueous phase was extracted with DCM (5x50.0 ml), the organic phases were combined and concentrated *in vacuo* to give a brownish oil (4.68 g). The crude was purified by flash column chromatography on silica gel (hexane/EtOAc 9:1, 8:2, 7:3, EtOAc) to yield 760.8 mg (37%) of **90** as a yellow amorphous powder: R_f 0.40 [hexane/EtOAc 1:1]; ν_{\max} (nujol)/ cm^{-1} 3422, 2924-2854, 1749, 1684, 1594, 1507, 1473, 1339, 1234, 1069; δ_H (CDCl_3) 8.23-8.21 (2H, d, J 9.0, H7), 7.91-7.89 (2H, d, J 9.0, H6), 6.79 (1H, s, OH_{enol}), 6.56 (1H, s, H4), 3.97 (3H, s, H1); δ_C (CDCl_3) 165.95 ($\underline{\text{C}}$, C2), 146.61 ($\underline{\text{C}}$, C8), 141.65 ($\underline{\text{C}}$, C5), 140.61 ($\underline{\text{C}}$, C3), 130.24 ($\underline{\text{CH}}$, 2xC6), 123.71 ($\underline{\text{CH}}$, 2xC7), 108.33 ($\underline{\text{CH}_2}$, C4), 53.71 ($\underline{\text{CH}_3}$, C1); m/z (EI^+) 223 ($[\text{M}]^+$, 39), 164 (45), 163 ($[\text{M}-\text{COOMe}]^+$, 100), 136 ($[\text{M}-\text{COCOOMe}]^+$, 95), 133 (28), 106 (18), 90 (33), 89 (59), 78 (30), 63 (24), 59 (21), 51 (11), 43 (4); found $[\text{M}+\text{H}]^+$, 223.0475, $\text{C}_{10}\text{H}_9\text{NO}_5$ requires $[\text{M}+\text{H}]^+$, 223.0481; $\Delta = -2.7$ ppm.

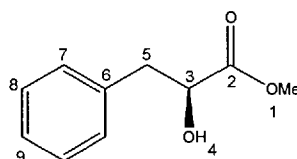
Methyl 2-hydroxy-3-(4-nitrophenyl)propanoate **91**



To a stirred yellow solution of α -keto ester **90** (718 mg, 3.22 mmol, 1.00 eq) in anhydrous methanol (20.0 ml) at 0 °C, under argon, was added sodium borohydride (174 mg, 4.60 mmol, 1.43 eq) in one portion. The solution first turned bright orange, then bright fluorescent red. It was stirred for 2 hr at 0 °C, then washed with saturated NH_4Cl (50.0 ml) and water (40.0 ml). The aqueous phase was separated from the organic phase and extracted with DCM (4x50.0 ml). The organic phases were combined and concentrated *in vacuo* to give a brownish oil (702 mg) which was purified by flash column chromatography on silica gel (1% NEt_3 , hexane/EtOAc 8:2, 6.5:3.5, 6:4, 1:1, EtOAc) to yield 476.3 mg (66%) of **91** as a yellow oil: R_f 0.30 [hexane/EtOAc 1:1]; ν_{\max} (DCM film)/ cm^{-1} 3560, 3025, 2924, 1734, 1602, 1473, 1374, 1154, 1028, 759; δ_H (CDCl_3) 8.18-8.16 (2H, d, J 8.0, H8), 7.43-7.40 (2H, d, J 8.5, H7), 4.52-4.48 (1H, m, H3), 3.81 (3H, s, H1), 3.27-3.23 (1H, dd, J 14.0, J 4.0, H5), 3.09-3.04 (1H, dd, J 14.0, J 7.0, H5), 2.89-2.88 (1H, d, J 5.0, H4); δ_C (CDCl_3) 174.00 ($\underline{\text{C}}$, C2), 146.94 ($\underline{\text{C}}$, C6), 144.32 ($\underline{\text{C}}$, C9), 130.33 ($\underline{\text{CH}}$, 2xC7), 123.41 ($\underline{\text{CH}}$, 2xC8), 70.50 ($\underline{\text{CH}}$, C3), 52.69 ($\underline{\text{CH}_3}$, C1), 39.90 ($\underline{\text{CH}_2}$, C5); m/z (EI^+) 207 ($[\text{M}-\text{OH}]^+$, 100), 176 (29), 166 (49), 137 (52), 120 (30), 107 (25), 91 (81), 78 (13), 65 (17).

Ethyl 2-hydroxy-3-(4-nitrophenyl)propanoate 100

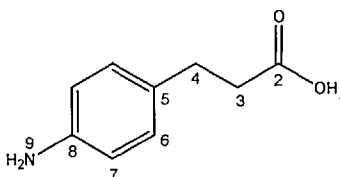
To a stirred solution of α -hydroxy ester **91** (74.6 mg, 0.331 mmol, 1.00 eq) and iodoethane (0.040 ml, 0.497 mmol, 1.50 eq) in anhydrous DMF (2.50 ml), was added sodium hydride (14.2 mg, 0.592 mmol, 1.79 eq). The mixture was stirred at 80 °C, under argon, for 19 hr before being concentrated in vacuo. It was re-dissolved in DCM (25.0 ml) and washed with water (2x25.0 ml). The aqueous phase was separated from the organic phase and extracted with DCM (2x30.0 ml) and chloroform (2x30.0 ml). The organic phases were combined and concentrated in vacuo to give a brown oil (86.7 mg) which was purified by flash column chromatography on silica gel (hexane/EtOAc 8:2, 7:3) to yield 27.0 mg (34%) of **100** as a yellow oil: R_f 0.60 [hexane/EtOAc 1:1]; ν_{\max} (nujol)/ cm^{-1} 3649, 3059-2849, 1733, 1493, 1265, 1181, 1028, 758; δ_H (CDCl_3) 8.16-8.14 (2H, d, J 9.0, H8), 7.43-7.41 (2H, d, J 9.0, H7), 4.48-4.44 (1H, m, H4), 4.27-4.22 (2H, dd, J 14.5, J 7.0, H2), 3.26-3.21 (1H, dd, J 14.0, J 4.0, H5), 3.08-3.03 (1H, dd, J 14.0, J 7.0, H5), 2.99-2.98 (1H, d, J 5.0, H10), 1.31-1.28 (3H, t, J 7.0, H1); δ_C (CDCl_3) 173.55 ($\underline{\text{C}}$, C3), 146.93 ($\underline{\text{C}}$, C6), 144.33 ($\underline{\text{C}}$, C9), 130.35 ($\underline{\text{CH}}$, 2xC7), 123.36 ($\underline{\text{CH}}$, 2xC8), 70.41 ($\underline{\text{CH}}$, C4), 62.07 ($\underline{\text{CH}_2}$, C2), 39.88 ($\underline{\text{CH}_2}$, C5), 14.08 ($\underline{\text{CH}_3}$, C1); m/z (EI^+) 221 (77), 193 (46), 166 (85), 137 (68), 120 (41), 107 (26), 91 (100), 75 (24).

(S)-Methyl 2-hydroxy-3-phenylpropanoate 96

Sulphuric acid (24.1 μL , 0.451 mmol, 0.10 eq) in anhydrous methanol (0.900 ml) was added to a stirred solution of L-(-)-3-phenyllactic acid (759 mg, 4.51 mmol, 1.00 eq) in methanol (2.00 ml). After stirring the mixture for 18 hr, under argon, at RT, it was concentrated in vacuo to give a white solid which was purified by flash column chromatography on silica gel (hexane, hexane/EtOAc 8:2, 7:3, 6:4, EtOAc) to yield 621 mg (76%) of the ester **96** as a white crystalline solid: R_f 0.55 [EtOAc]; ν_{\max} (nujol)/ cm^{-1} 3567, 3060-2924, 1734, 1602, 1452, 1375, 1181, 1029, 756; δ_H (CDCl_3)

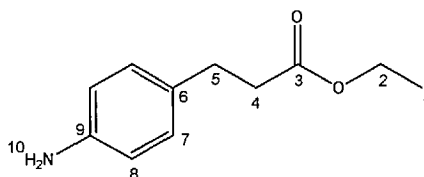
7.34-7.23 (5H, m, H_{ar}), 4.48-4.45 (1H, dd, *J* 7.0, *J* 4.5, H3), 3.77 (3H, s, H1), 3.16-3.12 (1H, dd, *J* 14.0, *J* 4.5, H5), 3.01-2.96 (1H, dd, *J* 14.0, *J* 7.0, H5), 2.92 (1H, br, H4); δ_c (CDCl₃) 175.08 (C, C2), 137.29 (C, C6), 129.78 (CH, C9), 128.72, 127.09 (CH, C7, C8), 72.17 (CH, C3), 52.35 (CH₃, C1), 41.03 (CH₂, C5); *m/z* (EI⁺) 180 ([M]⁺, 24), 162 ([M-OH]⁺, 52), 131 (15), 121 (25), 103 (24), 92 (23), 91 ([C₆H₅CH₂]⁺, 100), 77 (10); found [M+H]⁺, 180.0794, C₁₀H₁₂O₃ requires [M+H]⁺, 180.0786; Δ = 4.4 ppm.

3-(4-Aminophenyl)propanoic acid **108**



Para-nitrophenyl propanoic acid (2.72 g, 13.9 mmol, 1.00 eq) was dissolved in a mixture of EtOAc/EtOH 1:1 (40.0 ml). The flask was thoroughly flushed with hydrogen gas. Pd/C (276 mg, 10% in mass) was added and the mixture stirred at RT, under hydrogen, for 15 hr. It was filtered over celite, and the filtrate concentrated in vacuo to yield a white solid (2.42 g) which was purified by flash column chromatography on silica gel (DCM, DCM/solvent C 1:1, solvent C, methanol) to yield 2.27 g (98%) of **108** as an off-white powder: *R_f* 0.15 [solvent C]; ν_{\max} (nujol)/cm⁻¹ 3348, 3050-2854, 1696, 1435, 1283; δ_H (CDCl₃/MeOD 2:1) 6.96 (2H, d, *J* 8.5, H6), 6.64-6.62 (2H, d, *J* 8.5, H7), 2.80-2.76 (2H, t, *J* 8.0, H4), 2.52-2.48 (2H, t, *J* 8.0, H3); δ_c (CDCl₃/MeOD 2:1) 176.36 (C, C2), 144.80 (C, C8), 131.64 (C, C5), 129.42 (CH, 2xC6), 116.41 (CH, 2xC7), 36.60 (CH₂, C3), 30.61 (CH₂, C4); *m/z* (EI⁺) 165 ([M]⁺, 25), 120 (3), 119 (4), 106 ([M-CH₂COOH]⁺, 100), 91 (5), 77 (7), 65 (5); found [M+H]⁺, 165.0782, C₉H₁₁NO₂ requires [M+H]⁺, 165.0790; Δ = -1.1 ppm.

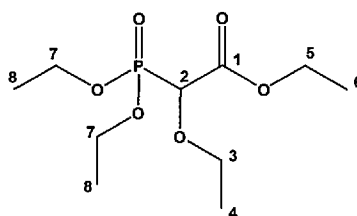
Ethyl 3-(4-aminophenyl)propanoate **110**



To a stirred solution of amine **108** (246 mg, 0.130 mmol, 1.00 eq) in ethanol (5.00 ml) were added two drops of concentrated sulphuric acid. A creamy ppt was seen. A few drops of concentrated sulphuric acid were added and the solution turned clear pale

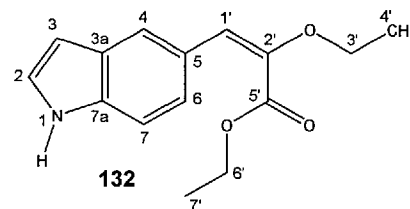
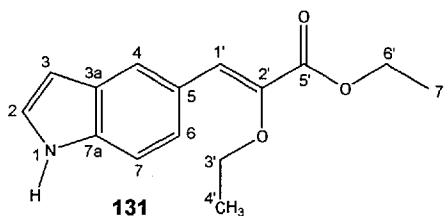
yellow. The mixture was stirred at RT for 21 hr and was then concentrated *in vacuo* to give a yellow oil (937 mg) which was purified by flash column chromatography on silica gel (hexane, hexane/EtOAc 9:1, 8:2, EtOAc) to yield 88.0 mg (30%) of amine **110** as a yellow oil: R_f 0.65 [EtOAc]; ν_{\max} (DCM film)/ cm^{-1} 3567, 1749, 1540, 1521, 1044; δ_H (CDCl_3) 7.01-6.99 (2H, d, J 8.5, H7), 6.63-6.61 (2H, d, J 8.5, H8), 4.16-4.10 (2H, dd, J 14.5, J 7.0, H2), 3.52 (2H, br, H10), 2.87-2.83 (2H, t, J 8.0, H5), 2.59-2.55 (2H, t, J 8.0, H4), 1.26-1.23 (3H, t, J 7.0, H1); δ_C (CDCl_3) 173.06 (\underline{C} , C3), 144.57 (\underline{C} , C9), 130.48 (\underline{C} , C6), 129.02 (\underline{CH} , 2xC7), 115.19 (\underline{CH} , 2xC8), 60.22 (\underline{CH}_2 , C2), 36.31 (\underline{CH}_2 , C4), 30.13 (\underline{CH}_2 , C5), 14.14 (\underline{CH}_3 , C1); m/z (EI^+) 193 ($[\text{M}]^+$, 36), 119 (17), 106 ($[\text{H}_2\text{NC}_6\text{H}_5\text{CH}_2]^+$, 100); found $[\text{M}+\text{H}]^+$, 193.1107, $\text{C}_{11}\text{H}_{15}\text{NO}_2$ requires $[\text{M}+\text{H}]^+$, 193.1103; $\Delta = 2.1$ ppm.

Ethyl 2-(diethoxyphosphoryl)-2-ethoxyacetate **129**²²⁴



To a colourless solution of 2-chloro-2-ethoxyacetic acid ethyl ester (1.41 g, 8.49 mmol, 1.00 eq) in anhydrous DMF (10.0 ml) was added triethylphosphite (1.46 ml, 8.49 mmol, 1.00 eq) and the reaction mixture was refluxed at 145 °C for 15 hr and at 152 °C for 30 min. The solution which had turned yellow was allowed to cool down to RT and water (40.0 ml) was poured onto the reaction mixture. The aqueous phase was extracted with DCM (3x40.0 ml). After drying the organic phase over MgSO_4 , concentration *in vacuo* yielded 2.11 g of **129** as a yellowish oil (92%) which was used as such for the HWE couplings: R_f 0.25 [hexane/EtOAc 1:1]; ν_{\max} (film)/ cm^{-1} 1746, 1265, 1145, 1039; δ_H (CDCl_3) 4.24-4.09 (5H, m, 4xH7, 2xH5), 3.68-3.61 (1H, m, H3), 3.54-3.47 (1H, m, H3), 1.29-1.21 (9H, m, 6xH8, 3xH4 or 3xH6), 1.19-1.16 (3H, m, 3xH4 or 3xH6); δ_C (CDCl_3) 167.34-167.32^P (\underline{C} , J 2.0, C1), 77.34-75.77^P (\underline{CH} , J 157.0, C2), 68.35-68.23^P (\underline{CH}_2 , J 12.0, C3), 63.46-63.39^P (\underline{CH}_2 , J 7.0, 1xC7), 63.37-63.30 (\underline{CH}_2 , J 7.0, 1xC7), 61.45 (\underline{CH}_2 , C5), 16.15-16.09^P (\underline{CH}_3 , J 6.0, 2xC8), 14.70 (\underline{CH}_3 , C4 or C6), 13.88 (\underline{CH}_3 , C4 or C6); m/z (ESI^+) 291 ($[\text{M}+\text{Na}]^+$, 100), 269 ($[\text{M}+\text{H}]^+$, 69); found $[\text{M}+\text{H}]^+$, 269.1162, $\text{C}_{10}\text{H}_{22}\text{O}_6\text{P}$ requires $[\text{M}+\text{H}]^+$, 269.1154; Found: C, 44.6; H, 7.9. Required: C, 44.8; H, 7.9; $\Delta = 3.0$ ppm.

(*Z*)-Ethyl 2-ethoxy-3-(1*H*-indol-5-yl)acrylate **131** and (*E*)-ethyl 2-ethoxy-3-(1*H*-indol-5-yl)acrylate **132**¹⁷⁷



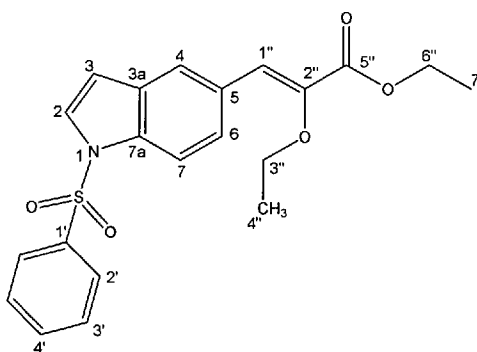
To a milky suspension of sodium hydride, 60% in oil (310 mg, 7.75 mmol, 2.23 eq) and molecular sieves 4Å in anhydrous THF (40.0 ml) at 0 °C, under a constant flow of N₂, was added dropwise *via* syringe pump, phosphonoacetate **129** (1.87 g, 6.97 mmol, 2.00 eq) in THF (2.00 ml) over 29 min. The suspension turned into a clear pale yellow solution. The latter was stirred at 0 °C for 1 hr before the dropwise addition of 5-indole-carbaldehyde **128** (506 mg, 3.48 mmol, 1.00 eq) in dry THF (4.00 ml) *via* syringe pump over 38 min. The solution turned orange, it was stirred at 0 °C for 1 hr and at RT for 44 hrs. The reddish solution was concentrated *in vacuo*, then re-dissolved in EtOAc (40.0 ml) and washed with water (2x45.0 ml). Some NaCl was added to aid the separation of the two phases. The aqueous phase was extracted with EtOAc (4x90.0 ml). After drying the organic phase over MgSO₄, concentration *in vacuo* of the organic phase gave a brown liquid which was purified by flash column chromatography on silica gel (hexane/EtOAc 20:1, 15:1, 10:1, 9:1, 8:2) to yield 844 mg (93%) of the product. Ratio *Z*:*E* = 63:37.

Z isomer **131**: amorphous white powder; mp 77.5-78.5 °C (hexane/DCM 20:1); R_f 0.35 [hexane/EtOAc 6:4]; ν_{max} (nujol)/cm⁻¹ 3267, 2923-2850, 1731, 1687, 1550, 1378; δ_H (CDCl₃) 8.32 (1H, br, H1), 8.13 (1H, s, H4), 7.74-7.72 (1H, dd, *J* 8.5, *J* 1.5, H6), 7.40-7.38 (1H, d, *J* 9.0, H7), 7.23-7.22 (1H, t, *J* 3.0, H2), 7.20 (1H, s, H1'), 6.60-6.58 (1H, m, H3), 4.35-4.30 (2H, q, *J* 14.5, *J* 7.0, H3'), 4.06-4.00 (2H, q, *J* 14.0, *J* 7.0, H6'), 1.44-1.38 (6H, m, H4', H7'); δ_C (CDCl₃) 165.30 (C, C5'), 142.56, 136.03, 127.98 (3xC), 126.19 (CH, C1'), 125.60 (C, C3a), 124.90 (CH, C6), 124.56 (CH, C2), 123.46 (CH, C4), 111.00 (CH, C7), 103.36 (CH, C3), 67.46 (CH₂, C6'), 60.92 (CH₂, C3'), 15.55, 14.35 (CH₃, C4', C7'); m/z (EI⁺) 259 ([M]⁺, 100), 202 ([M-CH₂CH₃-CH₂CH₃]⁺, 39), 157 (75), 129 (51), 118 ([Indole]⁺, 13); found [M+H]⁺, 259.1199, C₁₅H₁₇NO₃ requires [M+H]⁺, 259.1208; Found: C, 69.6; H, 6.7; N, 5.3. Required: C, 69.5; H, 6.6; N, 5.4; Δ = -3.5 ppm.

E isomer **132**: amorphous white powder; mp 98.5-100.5 °C (hexane/DCM 20:1); R_f 0.28 [hexane/EtOAc 6:4]; ν_{max} (nujol)/cm⁻¹ 3330, 2923-2850, 1702, 1621, 1379, 1227,

1176; δ_{H} (CDCl₃) 8.23 (1H, br, H1), 7.51-7.50 (1H, d, *J* 0.5, H4), 7.30-7.28 (1H, d, *J* 8.5, H7), 7.17-7.16 (1H, t, *J* 3.0, H2), 7.08-7.06 (1H, dd, *J* 8.5, *J* 1.5, H6), 6.50-6.49 (1H, m, H3), 6.32 (1H, s, H1'), 4.18-4.13 (2H, q, *J* 14.0, *J* 7.0, H3'), 3.99-3.94 (2H, q, *J* 14.0, *J* 7.0, H6'), 1.45-1.42 (3H, t, *J* 7.0, H7'), 1.09-1.06 (3H, *J* 7.0, H4'); δ_{C} (CDCl₃) 165.24 (C, C5'), 146.23, 134.93, 127.82, 126.17 (4xC, C2', C7a, C5, C3a), 124.54 (CH, C2), 122.99 (CH, C6), 120.54 (CH, C4), 111.47 (CH, C1'), 110.58 (CH, C7), 102.57 (CH, C3), 64.62 (CH₂, C6'), 61.07 (CH₂, C3'), 14.53 (CH₃, C4'), 13.68 (CH₃, C7'); *m/z* (EI⁺) 259 ([M]⁺, 100), 202 ([M-CH₂CH₃-CH₂CH₃]⁺, 37), 157 (68), 129 (49); found [M+H]⁺, 259.1199, C₁₅H₁₇NO₃ requires [M+H]⁺, 259.1208; Found: C, 69.6; H, 6.5; N, 5.5. Required: C, 69.5; H, 6.6; N, 5.4; Δ = -3.5 ppm.

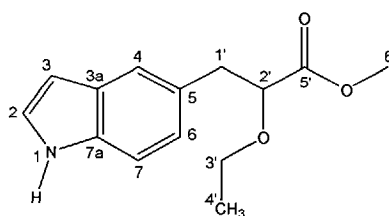
(Z)-Ethyl 2-ethoxy-3-(1-(phenylsulfonyl)-1H-indol-5-yl)acrylate **166**



To a vigorously stirred mixture of indole **131** (475 mg, 1.83 mmol, 1.00 eq) and *n*-tetrabutylammonium bromide (59.5 mg, 0.185 mmol, 0.10 eq) in 50% aqueous NaOH (1.80 ml), toluene (2.30 ml) and water (2.70 ml) was added dropwise, over 10 min, benzenesulfonyl chloride (0.240 ml, 1.89 mmol, 1.03 eq) in toluene (0.900 ml) *via* syringe pump. The reaction mixture turned from yellow to green, then brown and finally violet upon addition of the chloride. It was stirred at RT for 18 hr. A yellow organic layer on top of a colourless aqueous layer was observed. After removal of the aqueous phase, the organic phase was washed with 0.1M NaHCO₃ (30.0 ml), water (40.0 ml) and saturated brine (40.0 ml). After extractions of the aqueous phases with EtOAc (4x25.0 ml, 1x50.0 ml, 1x50.0 ml), the organic phase was dried over MgSO₄ and concentrated *in vacuo* to give a pale orange oil (798 mg) which was purified by flash column chromatography on silica gel (hexane/EtOAc 15:1, 10:1) to give 648 mg (89%) of the product as an amorphous white solid; mp 109.5-110.5 °C (hexane/DCM 20:1); *R_f* 0.20 [hexane/EtOAc 8:2]; ν_{max} (nujol)/cm⁻¹ 2954-2850, 1709, 1460, 1373, 1176, 1089, 723; δ_{H} (CDCl₃) 8.01 (1H, d, *J* 1.5, H4), 7.99-7.97 (1H, d, *J* 9.0, H7), 7.92-7.89 (2H, m, 2xH4'), 7.78-7.75 (1H, dd, *J* 9.0, *J* 1.5, H6), 7.58-7.57 (1H, d, *J* 3.5,

H2), 7.56-7.53 (1H, m, H4'), 7.48-7.44 (2H, m, 2xH3'), 7.05 (1H, s, H1''), 6.68-6.67 (1H, dd, J 3.5, H3), 4.34-4.28 (2H, q, J 14.5, J 7.0, 2xH3''), 4.04-3.99 (2H, q, J 14.0, J 7.0, 2xH6''), 1.40-1.36 (6H, m, 3xH4', 3xH7'); δ_c (CDCl₃) 164.71 (C, C5''), 144.12 (C), 138.15 (C), 134.67 (C), 133.92 (CH, C4'), 130.89 (CH, C3a), 129.31 (CH, 2xC3'), 129.13 (C, C5), 126.88 (CH), 126.74 (CH), 123.91 (C1''), 123.27 (C4), 113.37 (CH, C7), 109.46 (CH, C3), 67.62 (CH₂, C6''), 61.13 (CH₂, C3''), 15.55 (CH₃), 14.29 (CH₃); m/z (EI⁺) 399 ([M]⁺, 100), 342 (11), 297 (55), 156 (90); found [M+H]⁺, 399.1146, C₂₁H₂₁NO₅S requires [M+H]⁺, 399.1140; Found: C, 63.1; H, 5.4; N, 3.5. Required: C, 63.1; H, 5.3; N, 3.5; Δ = 1.5 ppm.

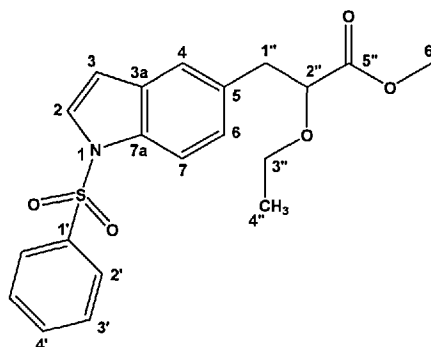
Methyl 2-ethoxy-3-(1H-indol-5-yl)propanoate 126



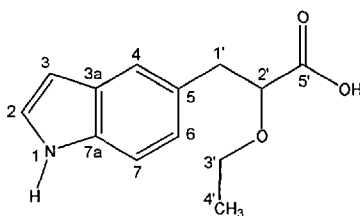
To a yellow solution of the starting material **131** (380 mg, 1.47 mmol, 1.00 eq) in anhydrous methanol (13.0 ml) at RT, under a constant flow of N₂, were added the magnesium turnings (648 mg, 26.7 mmol, 18.2 eq) in one portion and the reaction mixture was stirred at RT for 3 hr. Effervescence was seen as hydrogen gas was evolved. The reaction mixture was poured onto water (60.0 ml) and the two phases were separated. The aqueous phase was extracted with DCM (4x60.0 ml) and the organic extracts were washed with brine (60.0 ml). After extraction with DCM (4x60.0 ml) and drying over MgSO₄, concentration *in vacuo* gave a brownish oil which was purified by flash column chromatography on silica gel (hexane/EtOAc 9:1, 8:2, EtOAc) to yield 300 mg (83%) of the product as a yellow oil: R_f 0.20 [hexane/EtOAc 7.5:2.5]; ν_{\max} (film)/cm⁻¹ 3408, 2977-2850, 1741, 1444, 1209, 1110; δ_H (CDCl₃) 8.25 (1H, br, H1), 7.51 (1H, s, H4), 7.32-7.30 (1H, d, J 8.0, H7), 7.18-7.17 (1H, t, J 3.0, H2), 7.11-7.08 (1H, dd, J 8.5, J 1.5, H6), 6.51-6.50 (1H, m, H3), 4.14-4.11 (1H, dd, J 7.5, J 1.5, H2'), 3.71 (3H, s, H4''), 3.65-3.58 (1H, m, H3'), 3.42-3.35 (1H, m, H3'), 3.15 (1H, s, H1'), 3.13-3.12 (1H, d, J 3.0, H1'), 1.20-1.16 (3H, t, J 7.0, H4'); δ_c (CDCl₃) 173.30 (C, C5'), 134.80 (C), 128.19 (C), 127.98 (C), 124.38 (CH, C2), 123.54 (CH, C6), 121.04 (CH, C4), 110.74 (CH, C7), 102.23 (CH, C3), 80.98 (CH, C2'), 66.21 (CH₂, C3'), 51.73 (CH₃, C6'), 39.51 (CH₂, C1'), 15.02 (CH₃, C4'); m/z (EI⁺) 247 ([M]⁺, 16), 130 (100), 117 (3); found [M+H]⁺, 247.1205, C₁₄H₁₇NO₃ requires [M+H]⁺,

247.1208; Found: C, 68.2; H, 6.9; N, 5.8. Required: C, 68.0; H, 6.9; N, 5.7; $\Delta = -1.2$ ppm.

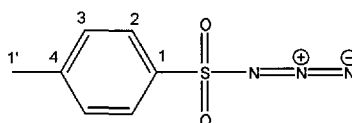
Methyl 2-ethoxy-3-(1-(phenylsulfonyl)-1H-indol-5-yl)propanoate 135



To a vigorously stirred mixture of indole **126** (237 mg, 0.960 mmol, 1.00 eq) and *n*-tetrabutylammonium bromide (32.0 mg, 0.099 mmol, 0.10 eq) in 50% aqueous NaOH (0.900 ml), toluene (0.600 ml) and water (1.40 ml) was added dropwise, over 16 min, benzenesulfonyl chloride (0.140 ml, 1.06 mmol, 1.10 eq) in toluene (0.800 ml) *via* syringe pump. The reaction mixture turned from yellow to orange. It was stirred at RT for 18.5 hr. After removal of the aqueous phase, the organic phase was washed with 0.1M NaHCO₃ (20.0 ml), water (60.0 ml) and saturated brine (60.0 ml). After extractions of the aqueous phases with EtOAc (2x10.0 ml, 4x100 ml), the organic phase was dried over MgSO₄ and concentrated *in vacuo* to give an off-white oil which was purified by flash column chromatography on silica gel (hexane/EtOAc 9:1, 8:2, EtOAc) to give 175 mg (47%) of the product as a colourless oil: *R_f* 0.15 [hexane/EtOAc 7.5:2.5]; ν_{\max} (DCM film)/cm⁻¹ 3062-2975, 1743, 1531, 1269, 1178, 1043; δ_{H} (CDCl₃) 7.92-7.90 (1H, d, *J* 8.5, H7), 7.88-7.86 (2H, m, H3'), 7.55-7.51 (2H, m, H2, H4'), 7.45-7.40 (3H, m, H2', H4), 7.21-7.19 (1H, dd, *J* 8.5, *J* 1.5, H6), 6.62-6.61 (1H, d, *J* 3.0, H3), 4.05-4.02 (1H, dd, *J* 7.5, *J* 5.5, H2''), 3.67 (3H, s, H4''), 3.61-3.55 (1H, m, H3''), 3.36-3.29 (1H, m, H3''), 3.08-3.06 (2H, dd, *J* 7.5, *J* 5.5, H1''), 1.15-1.11 (3H, t, *J* 7.0, H4''); δ_{C} (CDCl₃) 172.86 (C, C5''), 138.29 (C), 133.82 (C), 133.73 (CH, C4'), 132.35 (C), 130.89 (C), 129.19 (CH, 2xC2'), 126.72 (CH, 2xC3'), 126.48 (CH), 126.19 (CH), 121.97 (CH, C4), 113.21 (CH, C7), 109.18 (CH, C3), 80.28 (CH, C2''), 66.19 (CH₂, C3''), 51.81 (CH₃, C6''), 39.12 (CH₂, C1''), 14.98 (CH₃, C4''); *m/z* (EI⁺) 387 ([M]⁺, 15), 274 (20), 270 ([M-ethoxypropanoic side chain]⁺, 100), 129 (27); found [M+H]⁺, 387.1141, C₂₀H₂₁NO₅S requires [M+H]⁺, 387.1140; $\Delta = 0.3$ ppm.

2-Ethoxy-3-(1H-indol-5-yl)propanoic acid **38**

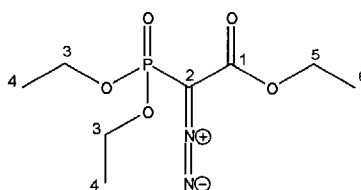
To a pale yellow solution of the starting material **126** (53.4 mg, 0.216 mmol, 1.00 eq) in a mixture of ethanol/water 1:1 (1.60 ml), were added the potassium hydroxide pellets (15.1 mg, 0.269 mmol, 1.25 eq) and the solution was stirred at 78 °C for 15 hr. The yellow solution was allowed to cool down to RT and concentrated *in vacuo*. With vigorous stirring in ice, was added 1M HCl (~8 drops) until a pH of 1 was reached. The desired acid crashed out as a brown ppt. It was dissolved in DCM and washed with water (2x30.0 ml). The aqueous phase was extracted with DCM (4x50.0 ml). After drying over MgSO₄, concentration *in vacuo* gave 46.2 mg (92%) of the product as a pale yellow oil: R_f 0.45 [Solvent B]; ν_{\max} (DCM film)/cm⁻¹ 3411, 2978-2929, 1724, 1265, 1105; δ_{H} (CDCl₃) 10.8 (1H, br, OH), 8.47 (1H, br, H1), 7.57 (1H, s, H4), 7.30-7.28 (1H, d, *J* 8.5, H7), 7.15-7.13 (2H, m, H2, H6), 6.52 (1H, br, H3), 4.23-4.20 (1H, dd, *J* 8.0, *J* 4.5, H2'), 3.70-3.62 (1H, m, 1xH3'), 3.49-3.41 (1H, m, 1xH3'), 3.31-3.26 (1H, dd, *J* 14.0, *J* 4.0, H1'), 3.21-3.16 (1H, dd, *J* 14.0, *J* 7.5, H1'), 1.21-1.17 (3H, t, *J* 7.0, H4'); δ_{C} (CDCl₃) 177.33 (C, C5'), 134.76 (C), 127.84 (C), 127.49 (C), 124.63 (CH), 123.25 (CH), 120.95 (CH, C4), 110.93 (CH, C7), 101.80 (CH, C3), 80.27 (CH, C2'), 66.52 (CH₂, C3'), 38.91 (CH₂, C1'), 14.82 (CH₃, C4'); m/z (EI⁺) 233 ([M]⁺, 22), 130 (M-(ethoxypropanoic acid side chain))⁺, 100; found [M+H]⁺, 233.1047, C₁₃H₁₅NO₃ requires [M+H]⁺, 233.1052; Found: C, 67.0; H, 6.4; N, 5.9. Required: C, 66.9; H, 6.5; N, 6.0; Δ = -2.1 ppm.

4-Methyl-benzenesulfonyl azide **146**²²⁷

To a solution of sodium azide (5.10 g, 78.4 mmol, 1.00 eq) in ethanol (25.0 ml) was added a colourless solution of *p*-toluene sulfonyl chloride (14.9 g, 78.2 mmol, 1.00 eq) in acetone (70.0 ml). A precipitate of NaCl formed immediately. The reaction mixture was stirred at RT for 17 hr. It was then filtered and the acetone was removed by rotary evaporation. The organic phase was diluted with DCM (40.0 ml), and

washed with water (3x40 ml). The aqueous phase was extracted with DCM (4x90.0 ml). After drying the organic phase over Na_2SO_4 , concentration *in vacuo* yielded 15.1 g of **146** as a colourless liquid (98%): R_f 0.40 [hexane/EtOAc 8:2]; ν_{max} (film)/ cm^{-1} 2129, 1369, 1171; δ_{H} (CDCl_3) 7.85-7.83 (2H, m, H2), 7.42-7.40 (2H, m, H3), 2.48 (3H, br, H1'); δ_{C} (CDCl_3) 146.17 (C, C4), 135.42 (C, C1), 130.21 (CH, 2xC3), 127.43 (CH, 2xC2), 21.65 (CH₃, C1'); m/z (EI^+) 197 ($[\text{M}]^+$, 8), 155 ($[\text{M-azide}]^+$, 70), 91 ($[\text{methylbenzene}]^+$, 100); found $[\text{M+H}]^+$, 197.0256, $\text{C}_7\text{H}_7\text{N}_3\text{O}_2\text{S}$ requires $[\text{M+H}]^+$, 197.0259; Found: C, 42.7; H, 3.6; N, 21.3. Required: C, 42.6; H, 3.6; N, 21.3; $\Delta = -1.5$ ppm.

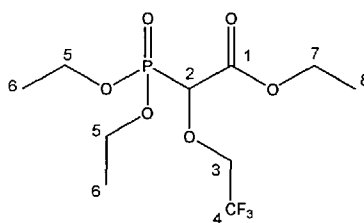
Ethyl 2-diazo-2-(diethoxyphosphoryl)acetate **147**²²⁸



To a suspension of sodium hydride (157 mg, 3.92 mmol, 1.23 eq) in dry THF (8.00 ml) under nitrogen at 0 °C, was added dropwise, over 3 min, triethylphosphonoacetate (0.630 ml, 3.20 mmol, 1.00 eq). The suspension turned into a clear colourless solution. After stirring at 0 °C for 47 min, was added, a solution of tosyl azide **146** (630 mg, 3.20 mmol, 1.00 eq) in dry THF (2x1.00 ml). The reaction mixture turned yellow, it was left to stir in the ice bath overnight. Ether (14.0 ml) and water (14.0 ml) were added and the 2 layers were separated. The aqueous phase was extracted with ether (4x20.0 ml). The combined ethereal extracts were washed with aq NaOH 0.5M (50.0 ml), water (90.0 ml) and brine (80.0 ml). The aqueous phases were extracted with ether respectively (4x50.0 ml, 3x80.0 ml, 2x100 ml). After drying the organic phase over MgSO_4 , concentration *in vacuo* yielded a colourless liquid which was purified by flash column chromatography on silica gel (hexane, hexane/EtOAc 8:2, 6:4) to yield 586 mg (73%) of the product as a pale yellow liquid: R_f 0.20 [hexane/EtOAc 1:1]; ν_{max} (film)/ cm^{-1} 2987, 2131, 1707, 1284, 1026; δ_{H} (CDCl_3) 4.28-4.22 (2H, q, J 14.5, J 7.0, 2xH5), 4.23-4.10 (4H, m, 2xH3), 1.36-1.33 (6H, dt, J 7.0, J 0.5, 2xH4), 1.30-1.27 (3H, J 7.0, H6); δ_{C} (CDCl_3) 163.40-163.28^p (C, d, J 12.0, C1), 129.48-126.32^p (C, d, J 316.0, C2), 63.59-63.53^p (CH₂, d, J 6.0, C3), 61.61 (CH₂, C5), 16.09-16.02 (CH₃, d, J 7.0, C4), 14.25 (CH₃, C6); m/z (EI^+) 250 ($[\text{M}]^+$, 16), 121 (100), 109 (98), 93 (73), 81 (68), 65 (87); found $[\text{M+H}]^+$, 250.0711, $\text{C}_8\text{H}_{15}\text{N}_2\text{O}_5\text{P}$ requires

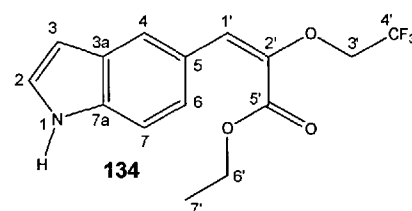
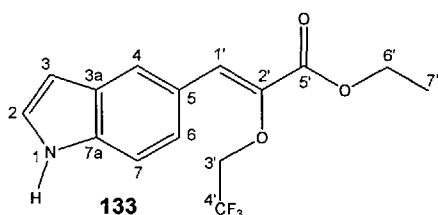
$[M+H]^+$, 250.0719; Found: C, 38.5; H, 6.0; N, 11.1. Required: C, 38.4; H, 6.0; N, 11.2;
 $\Delta = -3.2$ ppm.

Ethyl 2-(diethoxyphosphoryl)-2-(2,2,2-trifluoroethoxy)acetate **130**²³⁰



A mixture of diazo ester **147** (586 mg, 2.34 mmol, 1.00 eq), trifluoroethanol (0.340 ml, 4.68 mmol, 2.00 eq) and Rh(II) acetate dimer (10.5 mg, 0.024 mmol, 0.01 eq) in benzene (7.00 ml) was heated at 85 °C for 22 hr. The green solution was concentrated *in vacuo* to give a greenish oil which was purified by flash column chromatography on silica gel (hexane/EtOAc 8:2, 7:3, 6:4, 1:1) to yield 474 mg (63%) of the product as a colourless liquid: R_f 0.21 [hexane/EtOAc 4:6]; ν_{max} (film)/ cm^{-1} 1743, 1265, 1041; δ_H (CDCl₃) 4.52-4.47^p (1H, d, J 14.5, H2), 4.37-4.08 (7H, m, 2xH5, H7, 1xH3), 3.98-3.89 (1H, m, 1xH3), 1.36-1.30 (9H, m, 2xH6, H8); δ_C (CDCl₃) 166.09 (C, C1), 127.51-119.19 (C, q, J 277.5, C4), 77.89-76.33^p (CH, d, J 156.0, C2), 69.09-67.94^p (CH₂, dq, J 35.0, J 11.5, C3), 64.05-63.93^p (CH₂, t, J 6.0, C5), 62.21 (CH₂, C7), 16.26-16.20^p (CH₃, d, J 6.0, C6), 13.99 (CH₃, C8); m/z (EI⁺) 322 ([M]⁺, 1), 249 ([M-ethyl]⁺, 20), 183 ([M-(trifluoroether + 2 ethyl groups)]⁺, 61), 155 ([M-(trifluoroether + 3 ethyl groups)]⁺, 100), 65 (64); found $[M+H]^+$, 322.0787, C₁₀H₁₈F₃O₆P requires $[M+H]^+$, 322.0793; Found: C, 37.3; H, 5.6. Required: C, 37.3; H, 5.6; $\Delta = -1.9$ ppm.

(Z)-Ethyl 3-(1H-indol-5-yl)-2-(2,2,2-trifluoroethoxy)acrylate **133** and **(E)-ethyl 3-(1H-indol-5-yl)-2-(2,2,2-trifluoroethoxy)acrylate **134****



To a milky suspension of sodium hydride (9.8 mg, 0.245 mmol, 1.40 eq) in anhydrous THF (0.800 ml) at 0 °C, was added dropwise *via* syringe pump, phosphonoacetate **130** (60.0 mg, 0.186 mmol, 1.06 eq) in THF (0.600 ml) over 7 min, under a constant flow of N₂. The suspension turned into a clear pale yellow solution. The latter was

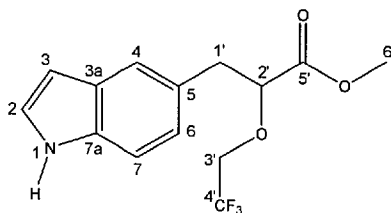
stirred at 0 °C for 24 min before the dropwise addition of 5-indole-carbaldehyde (25.4 mg, 0.175 mmol, 1.00 eq) in dry THF (0.900 ml) *via* syringe pump over 34 min. The solution which had turned orange was left stirring in the ice bath over 15 hr, and then at RT for 25.5 hr. The yellowish solution was concentrated *in vacuo*, re-dissolved in EtOAc (15.0 ml) and washed with water (15.0 ml). The aqueous phase was extracted with EtOAc (4x15.0 ml) and the organic extracts were washed with brine (50.0 ml). The aqueous phase was extracted with EtOAc (4x50.0 ml). After drying the organic phase over MgSO₄, concentration *in vacuo* of the organic phase gave a yellowish slurry which was purified by flash column chromatography on silica gel (hexane/EtOAc 20:1, 15:1, 10:1, 8:2) to yield 54.3 mg (99%) of the products. Ratio Z:E = 59:41.

Z isomer: amorphous white powder; mp 98.0-99.0 °C (hexane/DCM); R_f 0.20 [hexane/EtOAc 7.5:2.5]; ν_{\max} (nujol)/cm⁻¹ 3343, 2977-2850, 1691, 1459, 1371, 1261, 1056; δ_{H} (CDCl₃) 8.26 (1H, br, H1), 8.11 (1H, s, H4), 7.70-7.67 (1H, dd, *J* 8.5, *J* 1.5, H6), 7.42-7.40 (1H, d, *J* 9.0, H7), 7.27 (1H, br, H1'), 7.25-7.24 (1H, t, *J* 3.0, H2), 6.61-6.60 (1H, m, H3), 4.41-4.31 (4H, m, H3', H6'), 1.42-1.38 (3H, t, *J* 7.0, H7'); δ_{C} (CDCl₃) 164.05 (C, C5'), 140.54 (C, C2'), 136.37 (C, C7a), 128.08 (C, C5), 127.58-119.27 (C, q, *J* 277.0, C4"), 127.34 (CH, C2), 125.06 (CH), 124.84 (CH), 124.84 (C, C3a), 124.19 (CH, C4), 111.16 (CH, C7), 103.62 (CH, C3), 68.38-67.34 (CH₂, q, *J* 34.5, C3'), 61.34 (CH₂, C6'), 14.29 (CH₃, C7'); m/z (EI⁺) 313 ([M]⁺, 100), 230 ([M-CH₂CF₃]⁺, 6), 202 ([M-CH₂CH₃-CH₂CF₃]⁺, 39), 157 (33), 129 (44), 118 ([Indole]⁺, 13); found [M+H]⁺, 313.0925, C₁₅H₁₄F₃NO₃ requires [M+H]⁺, 313.0926; Found: C, 57.6; H, 4.6; N, 4.5. Required: C, 57.7; H, 4.5; N, 4.5; Δ = -0.3 ppm.

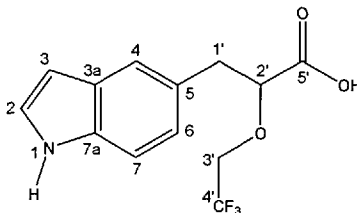
E isomer: amorphous pale yellow powder; mp 88.0-89.0 °C (hexane/DCM); R_f 0.16 [hexane/EtOAc 7.5:2.5]; ν_{\max} (nujol)/cm⁻¹ 3372, 2950-2850, 1711, 1461, 1378, 1269, 1157; δ_{H} (CDCl₃) 8.19 (1H, br, H1), 7.63-7.62 (1H, d, *J* 1.0, H4), 7.35-7.33 (1H, d, *J* 8.5, H7), 7.22-7.21 (1H, t, *J* 3.0, H2), 7.18-7.15 (1H, dd, *J* 8.5, *J* 1.5, H6), 6.74 (1H, s, H1'), 6.55-6.53 (1H, m, H3), 4.31-4.25 (2H, q, *J* 16.5, *J* 8.5, H3'), 4.23-4.17 (2H, q, *J* 14.0, *J* 7.0, H6'), 1.16-1.12 (3H, t, *J* 7.0, H7'); δ_{C} (CDCl₃) 163.51(C, C5'), 143.55 (C, C2'), 135.52 (C, C7a), 127.76 (C, C5), 124.77 (CH, C2), 124.54 (C, C3a), 123.42 (CH, C6), 127.40-119.08 (C, q, *J* 277.0, C4'), 121.67 (CH, C4), 121.56 (CH, C1'), 110.62 (CH, C7), 103.00 (CH, C3), 68.19-67.14 (CH₂, q, *J* 35.0, C3'), 61.29 (CH₂, C6'), 13.75 (CH₃, C7'); m/z (EI⁺) 313 ([M]⁺, 100), 230 ([M-CH₂CF₃]⁺, 6), 202 ([M-CH₂CH₃-CH₂CF₃]⁺, 38), 157 (34), 129 (48), 118 ([Indole]⁺, 15); found [M+H]⁺,

313.0926, C₁₅H₁₄F₃NO₃ requires [M+H]⁺, 313.0926; Found: C, 57.8; H, 4.6; N, 4.4. Required: C, 57.7; H, 4.5; N, 4.5; Δ = 0.0 ppm.

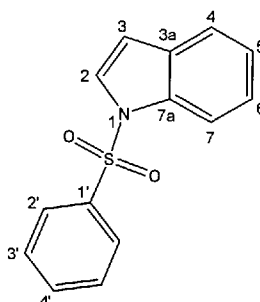
Methyl 3-(1H-indol-5-yl)-2-(2,2,2-trifluoroethoxy)propanoate 127



To a mixture of the starting material **133** and **134** (1.12 g, 3.59 mmol, 1.00 eq) and the magnesium turnings (1.31 g, 53.8 mmol, 15.0 eq) at 0 °C, under a constant flow of N₂, was added the anhydrous methanol (15.0 ml). Effervescence was seen after a few mins and the RM turned darker yellow. The reaction mixture was left in the ice bath for 14.5 hr. A white agglomerate was seen, some dry methanol (10.0 ml) was added and the reaction mixture was stirred at RT for another 45 min. The RM was cooled to 0 °C and water (22.0 ml) was added, followed by 2M HCl (14.0 ml). The mixture was filtered and brine (100 ml) was added. The 2 phases were separated and the aqueous phase was extracted with DCM (3x100 ml, 1x150 ml). After drying over MgSO₄, concentration *in vacuo* gave an almost colourless oil which was purified by flash column chromatography on silica gel (hexane/EtOAc 20:1, 10:1, 9:1, 8:2) to yield 653 mg (60%) of the product as a pale yellow oil: R_f 0.20 [hexane/EtOAc 7.5:2.5]; ν_{max} (DCM film)/cm⁻¹ 3377, 2933, 1741, 1513, 1278, 1164; δ_H (CDCl₃) 8.13 (1H, br, H1), 7.51 (1H, s, H4), 7.34-7.32 (1H, d, J 8.5, H7), 7.21-7.20 (1H, t, J 3.0, H2), 7.10-7.08 (1H, dd, J 8.5, J 1.5, H6), 6.52-6.51 (1H, m, H3), 4.28-4.25 (1H, dd, J 7.5, J 5.0, H2'), 4.02-3.93 (1H, m, H3'), 3.75 (3H, s, H6'), 3.73-3.66 (1H, m, H3'), 3.26-3.21 (1H, dd, J 14.0, J 5.0, H1'), 3.19-3.14 (1H, dd, J 14.0, J 8.0, H1'); δ_C (CDCl₃) 171.50 (C, C5'), 134.91 (C), 128.05 (C), 127.72-119.40 (C, q, J 277.0, C4'), 127.42 (C), 124.43 (CH, C2), 123.62 (CH, C6), 121.25 (CH, C4), 110.84 (CH, C7), 102.47 (CH, C3), 82.02 (CH, C2'), 68.40-67.38 (CH₂, q, J 34.0, C3'), 52.11 (CH₂, C6'), 39.17 (CH₂, C1'); m/z (EI⁺) 301 ([M]⁺, 100), 242 (65), 201 ([M-CH₂CH₃-CH₂CF₃]⁺, 39), 131 (80); found [M+H]⁺, 301.0923, C₁₄H₁₄F₃NO₃ requires [M+H]⁺, 301.0926; Found: C, 55.9; H, 4.7; N, 4.6. Required: C, 55.8; H, 4.7; N, 4.7; Δ = -1.0 ppm.

3-(1H-Indol-5-yl)-2-(2,2,2-trifluoroethoxy)propanoic acid **39**

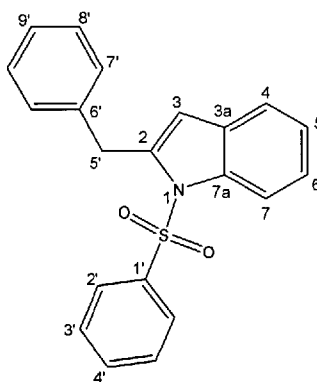
To a very pale yellow solution of the starting material **127** (40.4 mg, 0.134 mmol, 1.00 eq) in a mixture of ethanol/water 1:1 (1.60 ml), were added the potassium hydroxide pellets (9.6 mg, 0.171 mmol, 1.30 eq) and the solution was stirred at 78 °C for 15 hr. The solution was allowed to cool down to RT and concentrated *in vacuo*. With vigorous stirring in ice, was added 1M HCl (~5 drops) until a pH of 1 was reached. The desired acid crashed out. It was dissolved in DCM and washed with water (2x30.0 ml). The aqueous phase was extracted with DCM/MeOH 99:1 (4x50.0 ml). After drying over MgSO₄ and filtration, concentration *in vacuo* gave 38.1 mg (93%) of the product as a pale yellow oil: R_f 0.25 [Solvent B]; ν_{max} (DCM film)/cm⁻¹ 3415, 2933, 1726, 1279, 1167; δ_H (CDCl₃/MeOD 2:1) 9.85 (1H, br, OH), 7.45 (1H, s, H4), 7.29-7.27 (1H, d, *J* 8.0, H7), 7.14-7.13 (1H, m, H2), 7.04-7.01 (1H, dd, *J* 8.5, *J* 1.5, H6), 6.38-6.37 (1H, m, H3), 4.20-4.17 (1H, dd, *J* 8.5, *J* 4.0, H2'), 3.97-3.87 (1H, m, 1xH3'), 3.70-3.60 (1H, m, 1xH3'), 3.21-3.16 (1H, dd, *J* 14.0, *J* 4.0, H1'), 3.09-3.04 (1H, dd, *J* 14.0, *J* 8.0, H1'); δ_C (CDCl₃/MeOD 2:1) 173.97 (C, C5'), 135.68 (C), 128.53 (C), 128.33-120.02 (C, q, *J* 277.0, C4'), 127.67 (CH, C3a), 125.20 (CH, C2), 123.52 (CH, C6), 121.31 (CH, C4), 111.40 (CH, C7), 101.73 (CH, C3), 82.44 (CH, C2'), 68.69-67.66 (CH₂, q, *J* 68.5, *J* 34.5, C3'), 39.63 (CH₂, C1'); m/z (EI⁺) 287 ([M]⁺, 18), 130 ([M-(ethoxypropanoic acid side chain)]⁺, 100); found [M+H]⁺, 287.0763, C₁₃H₁₂NO₃F₃ requires [M+H]⁺, 287.0769; Found: C, 54.7; H, 4.2; N, 4.8. Required: C, 54.4; H, 4.2; N, 4.9; Δ = -2.0 ppm.

1-(Phenylsulfonyl)-1H-indole **160**²³⁸

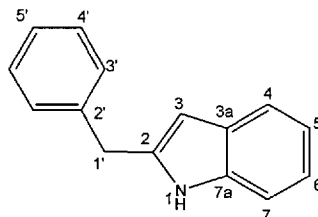
To a solution of sodium hydride (159 mg, 6.46 mmol, 1.57 eq) in anhydrous DMSO (1.60 ml) was added a solution of 1*H*-indole **113** (34.0 mg, 0.118 mmol, 1.00 eq) in dry THF (2.40 ml) at 0°C under argon. The milky reaction mixture was stirred at RT, under Ar, for 1 hour. It turned into a clear yellow solution, to which benzenesulfonyl chloride (0.551 ml, 4.32 mmol, 1.05 eq) was added at 0 °C. After stirring at RT for 19 hr, the mixture was poured onto water and extracted with EtOAc (4x25.0 ml). Concentration *in vacuo* gave a whitish solid which was purified by crystallisation from ethanol to yield 0.765 g (72%) of the product as white needles.

2nd experimental procedure using phase transfer conditions:

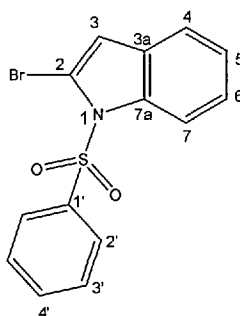
To a vigorously stirred mixture of 1*H*-indole **113** (3.02 g, 25.7 mmol, 1.00 eq) and *n*-tetrabutylammonium bromide (0.833 g, 7.58 mmol, 0.10 eq) in 50% aqueous NaOH (25.0 ml), toluene (18.0 ml) and water (38.0 ml) was added dropwise, over 30 min, benzenesulfonyl chloride (3.61 ml, 28.3 mmol, 1.10 eq) in toluene (20.0 ml) *via* a syringe pump. The mixture turned pink upon addition of benzenesulfonyl chloride. The reaction flask was covered with aluminium foil and the mixture stirred at RT for 18 hr. The solution turned green. After removal of the aqueous phase, the organic phase was washed with 0.1M NaHCO₃ (30.0 ml), water (40.0 ml) and saturated brine (40.0 ml). After extractions with EtOAc, the organic phase was dried over Na₂SO₄ and concentrated *in vacuo* to give a pinkish oil (6.70 g) which was purified by crystallisation from ethanol to yield 5.81 g (88%) of the product as white needles: mp 79.5-80.0 °C (ethanol) [lit.,²³⁸ mp 77.5-79 °C (DCM/hexane)]; R_f 0.25 [hexane/EtOAc 8:2]; ν_{\max} (nujol)/cm⁻¹ 2925-2854, 1919, 1771, 1576, 1497, 1396, 1339, 1263, 1069; δ_{H} (CDCl₃) 8.02-8.00 (1H, d, *J* 8.5, H7), 7.90-7.88 (2H, d, *J* 7.5, 2xH2'), 7.59-7.58 (1H, d, *J* 4.0, H2), 7.55-7.52 (2H, m, H4, H4'), 7.46-7.42 (2H, t, *J* 8.0, 2xH3'), 7.35-7.31 (1H, dt, *J* 8.0, *J* 1.0, H6), 7.26-7.22 (1H, dt, *J* 7.5, H5), 6.68-6.67 (1H, d, *J* 3.5, H3); δ_{C} (CDCl₃) 138.30 (C, C1'), 134.85 (C, C7a), 133.76 (CH, C4'), 130.74 (C, C3a), 129.23 (CH, 2xC3'), 126.73 (CH, 2xC2'), 126.29 (CH, C2), 124.63 (CH, C5), 123.35 (CH, C6), 121.39 (CH, C4), 113.52 (CH, C7), 109.21 (CH, C3); *m/z* (EI⁺) 257 ([M]⁺, 93), 141 (27), 116 ([indole]⁺, 100), 89 (28), 77 (54), 63 (11), 51 (15); found [M+H]⁺, 257.0509, C₁₄H₁₁NO₂S requires [M+H]⁺, 257.0511; Found: C, 63.9; H, 4.4; N, 5.7. Required: C, 65.4; H, 4.3; N, 5.4; Δ = -0.8 ppm.

2-Benzyl-1-(phenylsulfonyl)-1H-indole 161

To a colourless solution of 1-(phenylsulfonyl)-1H-indole **160** (210 mg, 0.817 mmol, 1.00 eq) in anhydrous THF (3.00 ml), was added dropwise a 1.7M *t*-BuLi solution in pentane (0.580 ml, 0.980 mmol, 1.20 eq) over 8 min, at -45 °C, under a constant flow of N₂. The solution which had turned yellow, then bright orange, was stirred at -45 °C to -40 °C over 55 min, before the dropwise addition of benzyl bromide (116 μL, 0.975 mmol, 1.19 eq) diluted in dry THF (1.00 ml) over 6 min, at -45 °C. The reaction mixture was allowed to warm up to -10 °C over 1 hour, then put in an ice bath for another hour, before being allowed to warm up to RT over 22 hr. The reaction mixture was poured over 5% citric acid (2x40.0 ml) and the aqueous phase was extracted with DCM (4x50.0 ml). The organic phase was dried over MgSO₄ and concentrated *in vacuo* to give a brownish gum (245 mg) which was purified by flash column chromatography on silica gel (hexane/EtOAc 20:1, 18:1) to yield 165 mg (58%) of the product as a white crystalline solid: mp 98.0-100.0 °C (hexane/DCM 20:1); R_f 0.25 [hexane/EtOAc 10:1]; ν_{\max} (nujol)/cm⁻¹ 2854, 1460, 1369, 1142, 746, 730, 708; δ_{H} (CDCl₃) 8.09-8.07 (1H, d, *J* 8.5, H7), 7.56-7.54 (2H, d, *J* 7.5, 2xH2'), 7.41-7.37 (1H, t, *J* 7.5, H7), 7.28-7.09 (10H, m, H9', 2xH8', 2xH7', 2xH3', H4', H6, H5), 6.04 (1H, br, H3), 4.27 (2H, s, H5'); δ_{C} (CDCl₃) 140.96 (C, C2), 139.05 (C, C1'), 137.90 (C, C3a), 137.24 (C, C6'), 133.53 (CH, C4'), 129.41 (C, C7a), 129.34 (CH, 2xC3'), 129.11 (CH, 2xC2'), 128.47 (CH, 2xC7'), 126.66 (CH, C9'), 126.27 (CH, 2xC8'), 124.13 (CH, C5), 123.54 (CH, C6), 120.32 (CH, C4), 114.66 (CH, C7), 111.05 (CH, C3), 35.22 (CH₂, C5'); *m/z* (EI⁺) 348 ([M+H]⁺, 21), 347 ([M]⁺, 75), 206 (72), 205 ([M-Bzsulfonyl group], 100), 77 (21), 51 (6); found [M+H]⁺, 347.0970, C₂₁H₁₇NO₂S requires [M+H]⁺, 347.0980; Found: C, 72.7; H, 4.9; N, 4.0. Required: C, 72.6; H, 4.9; N, 4.0; Δ = -2.9 ppm.

2-Benzyl-1H-indole 165^{239, 240}

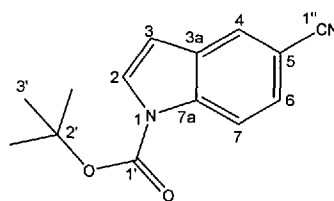
To a solution of MeOH/NaOH 2M 5:1 (18.0 ml) was added the 2-benzyl indole **161** (94.9 mg, 0.273 mmol, 1.00 eq) and the reaction mixture was refluxed at 110 °C for 48 hr. After allowing the reaction mixture to cool down to RT, it was treated with 0.1M HCl to a pH of 2 and the aqueous phase was extracted with ether (3x50.0 ml) and DCM (3x50.0 ml). Concentration *in vacuo* of the organic phase gave the crude which was purified by flash column chromatography on silica gel (hexane/EtOAc 20:1, 12:1, 1:1) to yield 51.4 mg (91%) of the product as a yellowish brown oil: R_f 0.20 [hexane/EtOAc 9:1]; ν_{\max} (DCM film)/ cm^{-1} 3733, 3055, 1422, 1265, 895, 740, 705; δ_H (CDCl_3) 7.79 (1H, br, H1), 7.62-7.60 (1H, dd, J 7.5, J 1.0, H4), 7.41-7.37 (2H, m, 2xH4'), 7.34-7.28 (4H, m, H5', 2xH3', H7), 7.19-7.11 (2H, m, H5, H6), 6.39-6.38 (1H, br, H3), 4.18 (2H, s, H1'); δ_C (CDCl_3) 138.49 (\underline{C} , C2'), 137.75 (2x \underline{C}), 136.26 (\underline{C} , C3a), 128.81 (\underline{CH} , 2xC3'), 128.71 (\underline{CH} , 2xC4'), 126.72 (\underline{CH} , C5'), 121.29 (\underline{CH}), 119.98 (\underline{CH} , C4), 119.70 (\underline{CH}), 34.70 (\underline{CH}_2 , C1'); m/z (EI^+) 208 ($[\text{M}+\text{H}]^+$, 15), 207 ($[\text{M}]^+$, 100), 206 (50), 130 ($[\text{M}-\text{Ph}]^+$, 62); found $[\text{M}+\text{H}]^+$, 207.1057, $\text{C}_{13}\text{H}_{15}\text{N}$ requires $[\text{M}+\text{H}]^+$, 207.1048; Found: C, 86.9; H, 6.2; N, 6.8. Required: C, 86.9; H, 6.3; N, 6.8; $\Delta = 4.3$ ppm.

1-Benzenesulfonyl-2-bromo-1H-indole 168^{241, 250}

To a clear colourless solution of diisopropylamine (0.110 ml, 0.778 mmol, 1.09 eq) in anhydrous THF (1.50 ml) at -78 °C, under a constant flow of N_2 , was added dropwise, *n*-BuLi, 2.5M in hexanes (0.290 ml, 0.725 mmol, 1.02 eq) over 4 min. The almost colourless solution was stirred at a temperature below -75 °C for 34 min before the dropwise addition of 1-(phenylsulfonyl)-1H-indole **160** (183 mg, 0.710 mmol, 1.00 eq)

in anhydrous THF (1.80 ml) *via* syringe pump, over 9 min. The reaction mixture turned yellowish. After stirring at a temperature below $-70\text{ }^{\circ}\text{C}$ for 1.5 hr, it was allowed to warm up to $0\text{ }^{\circ}\text{C}$ over 1 hr. The reaction mixture turned orangish. It was cooled down to $-78\text{ }^{\circ}\text{C}$ again before cyanogen bromide (96.6 mg, 0.912 mmol, 1.28 eq) dissolved in dry THF (0.700 ml) was added dropwise, over 2 min. The solution which turned brown was allowed to warm up to RT over 18.5 hr before being poured onto 0.1M NaHCO_3 (12.0 ml). After extraction with DCM (4x12.0 ml), the organic extracts were washed with water (40.0 ml) and brine (2x50.0 ml). The aqueous phases were extracted with DCM (4x40.0 ml and 4x90.0 ml respectively) and the organic extracts were dried over anhydrous K_2CO_3 . Concentration *in vacuo* of the organic phase gave a brownish solid which was purified by flash column chromatography on silica gel (hexane, hexane/DCM 8:2, 1:1) to yield 136 mg (57%) of the product as a white powder: mp $45.0\text{-}47.0\text{ }^{\circ}\text{C}$ (hexane/DCM 20:1) [lit.,²⁵⁰ mp $50\text{-}51\text{ }^{\circ}\text{C}$]; R_f 0.30 [hexane/DCM 1:1]; ν_{max} (DCM film)/ cm^{-1} 2923-2850, 1460, 1375, 1186, 1081, 728, 662; δ_{H} (CDCl_3) 8.30-8.28 (1H, d, J 8.5, H4), 7.91-7.89 (2H, m, H2'), 7.59-7.55 (1H, m, 3J 7.5, H7), 7.47-7.42 (3H, m, H3', H4'), 7.36-7.32 (1H, dt, J 8.0, J 1.5, H6), 7.27-7.22 (1H, m, H5), 6.74 (1H, s, H3); δ_{C} (CDCl_3) 138.29 (C, C1'), 137.57 (C, C7a), 134.09 (CH, C4'), 129.71 (C, C3a), 129.17 (CH, 2xC3'), 127.06 (CH, 2xC2'), 124.92 (CH), 124.05 (CH), 119.96 (CH, C7), 115.26 (CH), 115.23 (CH), 109.98 (CH, C2); m/z (EI^+); 337 (79), 194 ([M-(benzenesulfonyl group)]⁺, 79), 141 (74), 115 ([Indole]⁺, 42), 77 ([benzene]⁺, 100); found [M+H]⁺, 334.9608, $\text{C}_{14}\text{H}_{10}^{79}\text{BrNO}_2\text{S}$ requires [M+H]⁺, 334.9616; found [M+H]⁺, 336.9587, $\text{C}_{14}\text{H}_{10}^{81}\text{BrNO}_2\text{S}$ requires [M+H]⁺, 336.9595; $\Delta^{79}\text{Br} = -2.4\text{ ppm}$, $\Delta^{81}\text{Br} = -2.4\text{ ppm}$.

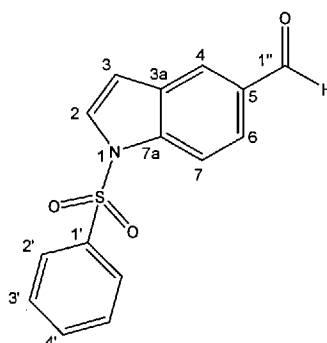
tert-Butyl 5-cyano-1*H*-indole-1-carboxylate **171**²⁴⁷



To an orange solution of 5-cyanoindole (1.00 g, 7.03 mmol, 1.00 eq) and DMAP (17.6 mg, 0.144 mmol, 0.02 eq) in anhydrous DCM (5.00 ml) at RT, under a constant flow of N_2 , was added BOC anhydride (1.69 g, 7.75 mmol, 1.10 eq) in one portion. The reaction mixture turned brownish, it was covered with Al foil and stirred at RT for 15.5 hr. The reaction was quenched with HCl 1M (5.00 ml). The 2 phases were separated, the organic phase was washed with water (25.0 ml). The aqueous phase was

extracted with DCM (4x25.0 ml). After drying over MgSO_4 , concentration *in vacuo* gave an off-white solid which was dissolved in hot methanol (50-60 °C) and cooled to RT. Water (2.40 ml) was added to the crystallised product, the flask was put in an ice bath for 10 min. Filtration yielded 1.28 g (75%) of the product as shiny white needles: mp 127.0-128.0 °C (methanol); R_f 0.35 [hexane/EtOAc 7.5:2.5]; ν_{max} (DCM film)/ cm^{-1} 2950-2800, 2212, 1743, 1460, 1371, 1072, 727; δ_{H} (CDCl_3) 8.27-8.25 (1H, d, J 8.5, H7), 7.91-7.90 (1H, d, J 1.0, H4), 7.72-7.71 (1H, d, J 3.5, H2), 7.58-7.55 (1H, dd, J 8.5, J 1.5, H6), 6.64-6.63 (1H, d, J 4.0, H3), 1.69 (9H, s, 3xH3'); δ_{C} (CDCl_3) 149.03 (C, C1'), 137.06 (C, C7a), 130.49 (C, C3a), 128.05 (CH, C2), 127.31 (CH, C6), 125.78 (CH, C4), 119.77 (C, C1''), 116.00 (CH, C3), 106.92 (CH, C7), 106.08 (CH, C5), 84.91 (C, C2'), 28.10 (CH₃, C3'); m/z (EI^+) 242 ($[\text{M}]^+$, 24), 186 ($[\text{M-tert butyl group}]^+$, 31), 169 (19), 142 ($[\text{M-BOC group}]^+$, 41), 57 (100); found $[\text{M+H}]^+$, 242.1051, $\text{C}_{14}\text{H}_{14}\text{N}_2\text{O}_2$ requires $[\text{M+H}]^+$, 242.1055; Found: C, 69.4; H, 5.7; N, 11.5. Required: C, 69.4; H, 5.8; N, 11.6; $\Delta = -1.7$ ppm.

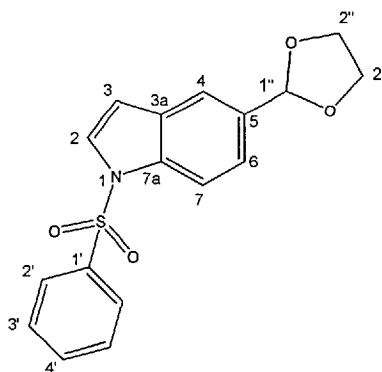
1-(Phenylsulfonyl)-1H-indole-5-carbaldehyde **170**



To a vigorously stirred mixture of 1H-indole-5-carbaldehyde **128** (282 mg, 1.94 mmol, 1.00 eq) and *n*-tetrabutylammonium bromide (0.646 g, 0.200 mmol, 0.10 eq) in 50% aqueous NaOH (1.90 ml), toluene (1.40 ml) and water (2.90 ml) was added dropwise, over 30 min, benzenesulfonyl chloride (0.272 ml, 2.14 mmol, 1.10 eq) in toluene (1.50 ml) *via* a syringe pump. The reaction flask was covered with aluminium foil and the mixture stirred at RT for 18 hr. The solution was orange. After removal of the aqueous phase, the organic phase was washed with 0.1M NaHCO_3 (10.0 ml), water (10.0 ml) and saturated brine (20.0 ml). After extractions with EtOAc (4x25.0 ml), the organic phase was dried over MgSO_4 and concentrated *in vacuo* to give an orange oil (0.629 g) which was purified by flash column chromatography (hexane, hexane/EtOAc 9:1, 8:2, 6:4) to yield 0.447 g (81%) of the product as a pale pink crystalline solid: R_f 0.10 [hexane/EtOAc 8:2]; ν_{max} (DCM film)/ cm^{-1} 2958, 1695, 1442,

1375, 1274, 1118, 727; δ_{H} (CDCl₃) 10.05 (H1''), 8.15-8.12 (1H, d, *J* 9.0, 1xH2'), 8.08-8.08 (1H, d, *J* 1.0, H7), 7.93-7.86 (3H, m, 1xH2', H6, H4), 7.70-7.69 (1H, d, *J* 3.5, H2), 7.61-7.57 (1H, tt, *J* 7.5, *J* 1.0, H4'), 7.51-7.47 (2H, m, 2xH3'), 6.81-6.80 (1H, d, *J* 3.5, H3); δ_{C} (CDCl₃) 191.71 (C=O), 138.10 (C, C7a), 137.95 (C, C1'), 134.29 (CH, C4'), 132.34 (CH, C5), 130.87 (C, C3a), 129.50 (2xCH), 128.00 (CH, C2), 126.83 (2xCH), 125.37 (CH, C4), 124.77 (CH, C6), 113.94 (CH, C7), 109.56 (CH, C3); *m/z* (EI⁺) 286 ([M+H]⁺, 21), 285 ([M]⁺, 80), 141 (63), 116 ([indole]⁺, 22), 77 (100), 51 (19); found [M+H]⁺, 285.0460, C₁₅H₁₁NO₃S requires [M+H]⁺, 285.0460; Δ = 0.0 ppm.

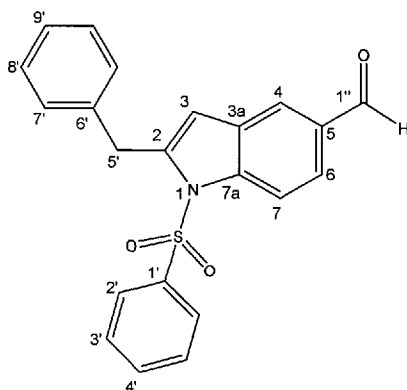
5-(1,3-Dioxolan-2-yl)-1-(phenylsulfonyl)-1H-indole **172**



To a clear colourless solution of 1-(phenylsulfonyl)-1H-indole-5-carbaldehyde **170** (155 mg, 0.542 mmol, 1.00 eq) and ethylene glycol (59.0 mg, 0.951 mmol, 1.75 eq) in benzene (60.0 ml) was added a catalytic amount of *para*-toluenesulfonic acid monohydrate (10.8 mg, 0.057 mmol, 0.10 eq) and the reaction mixture was refluxed at 105 °C for 14 hr using a Dean Stark set up. The set up was covered with aluminium foil. The reaction mixture which had turned brown was allowed to cool down to RT, and poured onto sat. NaHCO₃ (20.0 ml). The organic phase turned dark green. After extracting the aqueous phase with ether (3x20.0 ml), and DCM (3x30.0 ml), the organic phase was dried over anhydrous K₂CO₃ and concentrated *in vacuo* to give a dark green oil (162 mg). The crude was treated with polystyrene sulfonyl hydrazide resin loading 2.67 mmol/g (245 mg, 0.654 mmol) in DCM (35.0 ml) for 2 hr, next the resin was filtered off and the filtrate was concentrated *in vacuo* to yield 180 mg (99%) of the product as a dark green oil: *R_f* 0.15 [hexane/EtOAc 7:3]; ν_{max} (DCM film)/cm⁻¹ 3055, 2982, 1418, 1265, 738, 705; δ_{H} (CDCl₃) 8.04-8.01 (1H, d, *J* 8.5, H7), 7.87-7.85 (2H, d, *J* 8.0, 2xH2'), 7.67 (1H, s, H4), 7.60-7.59 (1H, d, *J* 3.0, H2), 7.54-7.51 (1H, t, *J* 7.0, H4'), 7.47-7.41 (3H, m, H6, 2xH3'), 6.68-6.67 (1H, d, *J* 3.0, H3), 5.87 (1H, s, H1''), 4.17-4.11 (2H, m, 2xH2''), 4.06-4.03 (2H, m, 2xH2''); δ_{C} (CDCl₃) 138.15 (C, C1'), 135.35 (C, C7a), 133.83 (CH, C4'), 133.18 (CH, C5), 130.68 (C,

C3a), 129.24 ($\underline{\text{CH}}$, 2xC3'), 126.89 ($\underline{\text{CH}}$, C2), 126.67 ($\underline{\text{CH}}$, 2xC2'), 123.11 ($\underline{\text{CH}}$, C6), 119.69 ($\underline{\text{CH}}$, C4), 113.54 ($\underline{\text{CH}}$, C7), 109.39 ($\underline{\text{CH}}$, C3), 103.83 ($\underline{\text{CH}}$, C1''), 65.34 ($\underline{\text{CH}}_2$, 2xC2''); m/z (EI⁺) 329 ([M]⁺, 3), 328 (3), 285 ([M-acetal]⁺, 82), 144 ([M-benzenesulfonyl group]⁺, 13), 141 (55), 116 ([indole]⁺, 19), 77 (100); found [M+H]⁺, 329.0712, C₁₇H₁₅NO₄S requires [M+H]⁺, 329.0722; Δ = -3.0 ppm.

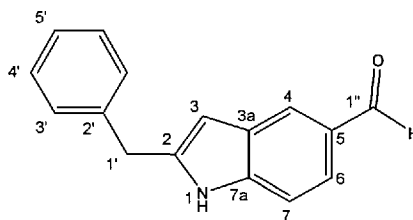
2-Benzyl-1-(phenylsulfonyl)-1H-indole-5-carbaldehyde 191



To a dark green solution of dioxolanindole **170** (104 mg, 0.315 mmol, 1.00 eq) in anhydrous THF (1.25 ml), was added dropwise a 1.7M *t*-BuLi solution in pentane (0.230 ml, 0.393 mmol, 1.25 eq) over 4 min, at -45 °C, under a constant flow of N₂. The solution which had turned dark brown, then reddish brown was stirred at -45 °C to -20 °C over 20-25 min, then at -45 °C for another 20 min, before the dropwise addition of benzyl bromide (47 μL , 0.393 mmol, 1.25 eq) diluted in dry THF (0.250 ml) over 6 min, at -45 °C. The reaction mixture was allowed to warm up to -5 °C over 50 min, then put in an ice bath for one hour, before being allowed to warm up to RT over 18 hr. The reaction mixture was poured over 5% citric acid (2x25.0 ml) and the organic phase was washed with water (25.0 ml). The aqueous phase was extracted with DCM (4x25.0 ml). The organic phase was dried over MgSO₄ and concentrated *in vacuo* to give a brownish oil (245 mg) which was purified by flash column chromatography on silica gel (hexane, hexane/EtOAc 10:1, 9:1, 8:2) to yield 33.5 mg (28%) of the product as an off-white solid: R_f 0.20 [hexane/EtOAc 7.5:2.5]; ν_{max} (DCM film)/cm⁻¹ 3055, 2987, 1693, 1417, 1265, 898, 740; δ_{H} (CDCl₃) 10.03 (1H, s, H1''), 8.34-8.31 (1H, d, J 9.5, H7), 7.92-7.91 (1H, d, J 1.0, H4), 7.85-7.82 (1H, dd, J 9.0, J 1.5, H6), 7.68-7.66 (2H, dd, J 7.5, J 1.0, 2xH2'), 7.58-7.54 (1H, dt, J 7.5, H4'), 7.43-7.39 (2H, t, J 8.0, 2xH3'), 7.32-7.29 (3H, dt, J 7.0, J 1.0, 2xH8', H9'), 7.22-7.18 (2H, m, 2xH7'), 6.24 (1H, s, H3), 4.38 (2H, s, 2xH5'); δ_{C} (CDCl₃) 191.79 ($\underline{\text{C}}$, C1''), 143.07 ($\underline{\text{C}}$, C7a), 140.61 ($\underline{\text{C}}$, C1'), 138.71 ($\underline{\text{C}}$, C6'), 137.26 ($\underline{\text{CH}}$, C2), 134.03 ($\underline{\text{CH}}$, C4'), 132.40 ($\underline{\text{CH}}$, C5), 129.51 ($\underline{\text{C}}$, C3a), 129.36 (2x $\underline{\text{CH}}$), 129.32 (2x $\underline{\text{CH}}$), 128.62 ($\underline{\text{CH}}$,

2xC8'), 126.92 (CH, C9'), 126.37 (CH, 2xC2'), 125.03 (CH, C6), 123.24 (CH, C4), 114.99 (CH, C7), 110.99 (CH, C3); m/z (EI⁺) 375 ([M]⁺, 100), 233 ([M-Bzsulfonyl group]⁺, 65), 204 ([M-Bzsulfonyl group and aldehyde]⁺, 95), 77 (34); found [M+H]⁺, 375.0930, C₂₂H₁₇NO₃S requires [M+H]⁺, 375.0929; Δ = 0.3 ppm.

2-Benzyl-1H-indole-5-carbaldehyde **177**



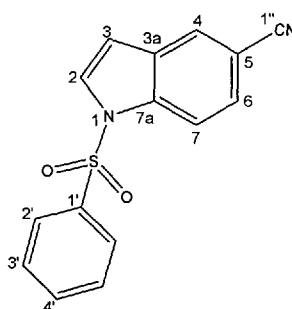
To a solution of MeOH/NaOH 2M 5:1 (7.90 ml) was added the 2-benzyl indole **191** (44.6 mg, 0.119 mmol, 1.00 eq) and the reaction mixture was refluxed at 110 °C for 16 hr. After allowing the reaction mixture to cool down to RT, it was treated with 0.1M HCl to a pH of 1 and the aqueous phase was extracted with DCM (5x15.0 ml). Concentration *in vacuo* of the organic phase afforded a pink oil which was purified by flash column chromatography on silica gel (hexane, hexane/EtOAc 9:1, 8:2, EtOAc) to yield 8.7 mg (39%) of the product as a pale orange amorphous powder.

2nd experimental procedure using DIBAL:

To a clear colourless solution of 2-benzyl-1H-indole-5-carbonitrile **145** (411 mg, 1.77 mmol, 1.00 eq) in anhydrous DCM (8.00 ml) under a constant flow of N₂, at 0 °C, was added dropwise the DIBAL-H solution, 1.0M in DCM (2.20 ml, 2.20 mmol, 1.24 eq) over 7 min. The reaction mixture which turned pale yellow was allowed to warm up to RT over 16 hrs. To the bright yellowish orange solution was added 1.0M Rochelle solution (17.0 ml) at 0 °C. Caution: evolution of gas. The reaction mixture was stirred at RT for 4.5 hr. The two phases were separated and the aqueous phase extracted with DCM (4x20.0 ml). The solvent was removed *in vacuo*, and the orange slurry was dissolved in DCM (10.0 ml) and stirred with 1M HCl (2.90 ml) at RT for 1 hr 40 min. Water (13.0 ml) was added, and the pH adjusted to 14 using 2M NaOH (2.90 ml). The produce was extracted with DCM (4x20.0 ml) and the organic phase was washed with water (60.0 ml) and brine (60.0 ml). After extraction of the aqueous phase with DCM (4x60.0 ml), drying over MgSO₄ and concentration *in vacuo*, an orange powder was obtained. It was purified by flash column chromatography on silica gel (hexane/EtOAc 10:1, 9:1) to yield 332 mg (80%) of the product as a pale

orange amorphous powder: mp 126.5-127.5 °C (hexane/DCM 20:1); R_f 0.20 [hexane/EtOAc 7.5:2.5]; ν_{\max} (nujol)/ cm^{-1} 3324, 3056-2850, 1671, 1373, 1056, 739; δ_H (CDCl_3) 10.01 (1H, s, H1''), 8.08 (2H, br, H1, H4), 7.71-7.69 (1H, dd, J 8.5, J 1.5, H6), 7.38-7.28 (6H, m, 2xH4', H7, H5', 2xH3'), 6.49 (1H, br, H3), 4.17 (2H, s, H5'); δ_C (CDCl_3) 192.47 ($\underline{\text{C}}\text{H}$, C1''), 139.95 ($\underline{\text{C}}$), 139.88 ($\underline{\text{C}}$), 137.76 ($\underline{\text{C}}$, C2'), 129.67 ($\underline{\text{C}}\text{H}$, C5), 128.87 (2x $\underline{\text{C}}\text{H}$), 128.81 (2x $\underline{\text{C}}\text{H}$), 128.54 ($\underline{\text{C}}$, C3a), 127.00 ($\underline{\text{C}}\text{H}$, C5'), 125.05 ($\underline{\text{C}}\text{H}$, C4), 122.10 ($\underline{\text{C}}\text{H}$, C6), 111.04 ($\underline{\text{C}}\text{H}$, C7), 102.58 ($\underline{\text{C}}\text{H}$, C3), 34.65 ($\underline{\text{C}}\text{H}_2$, C1'); m/z (EI^+) 235 ($[\text{M}]^+$, 100), 206 ($[\text{M-aldehyde}]^+$, 27), 167 (30), 158 (42), 149 (30), 91 (14); found $[\text{M+H}]^+$, 235.0997, $\text{C}_{16}\text{H}_{13}\text{NO}$ requires $[\text{M+H}]^+$, 235.0997; Found: C, 81.6; H, 5.5; N, 5.9. Required: C, 81.7; H, 5.6; N, 6.0; $\Delta = 0.0$ ppm.

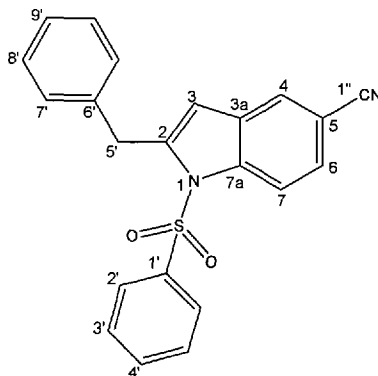
1-Benzenesulfonyl-1H-indole-5-carbonitrile **193**²²³



To a vigorously stirred mixture of indole-5-carbonitrile **192** (864 mg, 6.08 mmol, 1.00 eq) and *n*-tetrabutylammonium bromide (197 mg, 0.609 mmol, 0.10 eq) in 50% aqueous NaOH (5.90 ml), toluene (5.00 ml) and water (9.00 ml) was added dropwise, over 30 min, benzenesulfonyl chloride (0.850 ml, 0.688 mmol, 1.10 eq) in toluene (4.00 ml) *via* a syringe pump. The reaction flask was covered with aluminium foil and the mixture stirred at RT for 25 hr. The solution was yellow. After removal of the aqueous phase, the organic phase was washed with 0.1M NaHCO_3 (20.0 ml), water (75.0 ml) and saturated brine (75.0 ml). After extractions with EtOAc (3x70.0 ml), the organic phase was dried over MgSO_4 and concentrated *in vacuo* to give an off-white powder (1.69 g) which was purified by crystallisation from hexane/DCM 20:1 to yield 1.65 g (96%) of the product as white needles: mp 131.0-133.5 °C (hexane/DCM 20:1); R_f 0.35 [hexane/EtOAc 6:4]; ν_{\max} (nujol)/ cm^{-1} 2222, 1458, 1375, 1080, 721; δ_H (CDCl_3) 8.10-8.08 (1H, d, J 8.5, 1xH2'), 7.90-7.89 (3H, m, 1xH2', H4, H7), 7.71-7.70 (1H, d, J 3.5, H2), 7.62-7.56 (2H, m, 2xH3'), 7.51-7.47 (2H, t, J 8.0, H4', H6), 6.74-6.73 (1H, d, J 3.5, H3); δ_C (CDCl_3) 137.73 ($\underline{\text{C}}$, C7a), 136.43 ($\underline{\text{C}}$, C1'), 134.42 ($\underline{\text{C}}\text{H}$, C4'), 130.65 ($\underline{\text{C}}$, C3a), 129.54 ($\underline{\text{C}}\text{H}$, 2xC3'), 128.37 ($\underline{\text{C}}\text{H}$), 127.59 ($\underline{\text{C}}\text{H}$), 126.77 ($\underline{\text{C}}\text{H}$, 2xC2'), 126.36 ($\underline{\text{C}}\text{H}$, C4), 119.18 ($\underline{\text{C}}$, C1''), 114.27 ($\underline{\text{C}}\text{H}$, C7), 108.65 ($\underline{\text{C}}\text{H}$, C3), 107.03

(C, C5); m/z (EI^+) 282 ($[M]^+$, 50), 141 ($[M-BzSulfonyl\ group]^+$, 66), 114 ($[unsubstituted\ indole]^+$, 12), 77 (100); found $[M+H]^+$, 282.0474, $C_{15}H_{10}N_2O_2S$ requires $[M+H]^+$, 282.0463; Found: C, 63.7; H, 3.5; N, 9.9. Required: C, 63.8; H, 3.6; N, 9.9; $\Delta = 3.9$ ppm.

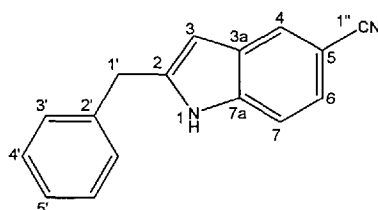
2-Benzyl-1-(phenylsulfonyl)-1H-indole-5-carbonitrile 194^{223}



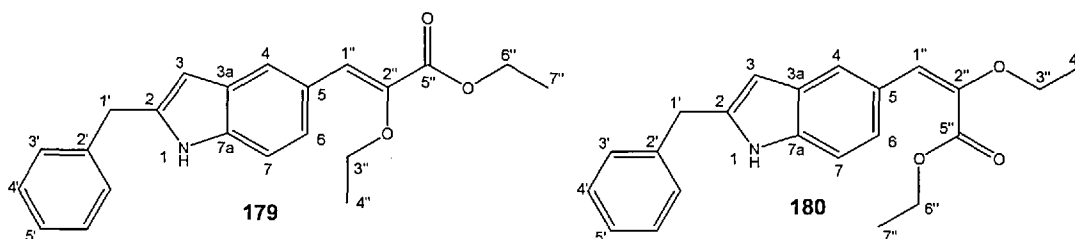
To a pale yellow solution of benzenesulfonyl indole **193** (210 mg, 0.743 mmol, 1.00 eq) in anhydrous THF (2.10 ml), was added dropwise a 1.7M *t*-BuLi solution in pentane (0.520 ml, 0.891 mmol, 1.20 eq) over 8 min, at $-45\text{ }^\circ\text{C}$, under a constant flow of N_2 . The solution which had turned dark yellow, then dark green was stirred at $-45\text{ }^\circ\text{C}$ to $-30\text{ }^\circ\text{C}$ over 55 min, cooled down to $-45\text{ }^\circ\text{C}$ before the dropwise addition of benzyl bromide (108 μL , 0.906 mmol, 1.22 eq) diluted in dry THF (1.50 ml) over 8 min. The reaction mixture was allowed to warm up to $-10\text{ }^\circ\text{C}$ over 55 min. The reaction mixture turned brown and finally orange. It was put in an ice bath for 55 min, before being allowed to warm up to RT over 15 hr. The reddish brown reaction mixture was poured over 5% citric acid (30.0 ml) and the organic phase was washed with water (30.0 ml). The aqueous phase was extracted with DCM (4x30.0 ml). The organic phase was dried over $MgSO_4$ and concentrated *in vacuo* to give an off-white solid (1.02 g) which was purified by flash column chromatography on silica gel (hexane/EtOAc 20:1, 15:1, 10:1) to yield 55.0 mg (51%) of the product as a yellow oil. Crystallisation from hexane/DCM 20:1 yielded the product as white needles: mp $130.5\text{-}131.5\text{ }^\circ\text{C}$ (hexane/DCM 20:1); R_f 0.20 [hexane/EtOAc 8:2]; ν_{max} (nujol)/ cm^{-1} 2220, 1460, 1371, 1053; δ_H ($CDCl_3$) 8.29-8.27 (1H, d, J 9.0, H7), 7.71 (1H, s, H4), 7.67-7.65 (2H, d, J 7.5, H2'), 7.60-7.56 (1H, t, J 7.5, H4'), 7.55-7.53 (1H, dd, J 9.0, J 1.0, H6), 7.44-7.40 (2H, t, J 9.0, H3'), 7.34-7.29 (3H, m, H8', H9'), 7.20-7.18 (2H, m, H7'), 6.16 (1H, s, H3), 4.37 (2H, s, 2xH5'); δ_C ($CDCl_3$) 143.63 (C, C6'), 138.98 (C, C7a), 138.59 (C, C2), 136.99 (C, C1'), 134.19 (CH, C4'), 129.46 (CH, 2xC3'), 129.38 (C, C3a), 129.33 (CH, 2xC7'), 128.69 (CH, 2xC8'), 127.18 (CH, C6), 127.03 (CH,

C9'), 126.39 (CH, 2xC2'), 125.04 (CH, C4), 119.32 (C, C1''), 115.35 (CH, C7), 110.07 (CH, C3), 107.10 (C, C5), 35.12 (CH₂, C5'); m/z (EI⁺) 372 ([M]⁺, 57), 284 ([M-Bn group]⁺, 30), 230 ([M-Bzsulfonyl group]⁺, 100), 141 (11), 115 ([indole]⁺, 5), 91 (12), 77 (47); found [M+H]⁺, 372.0934, C₂₂H₁₆N₂O₂S requires [M+H]⁺, 372.0932; Found: C, 71.0; H, 4.2; N, 7.6. Required: C, 71.0; H, 4.3; N, 7.5; Δ = 0.5 ppm.

2-Benzyl-1H-indole-5-carbonitrile **196**²²³



To a solution of MeOH/NaOH 2M 5:1 (25.0 ml) was added the 2-benzyl indole **194** (141 mg, 0.379 mmol, 1.00 eq) and the reaction mixture was refluxed at 110 °C for 18 hr. After allowing the reaction mixture to cool down to RT, it was treated with 0.1M HCl to a pH of 2 and the aqueous phase was extracted with DCM (4x25.0 ml). Concentration *in vacuo* of the organic phase gave a greenish oil (96 mg) which was purified by flash column chromatography on silica gel (hexane, hexane/EtOAc 10:1, 9:1, 8:2) to yield 87.0 mg (99%) of the product as an off-white solid: mp 119.5-120.5 °C (hexane/DCM 20:1); R_f 0.25 [hexane/EtOAc 7:3]; ν_{max} (nujol)/cm⁻¹ 3300, 3056-2850, 2229, 1373, 1056, 740; δ_H (CDCl₃) 8.12 (1H, br, H1), 7.88 (1H, s, H4), 7.38-7.25 (6H, m, H4', H7, H5', H6, H3'), 6.41 (1H, s, H3), 4.16 (2H, s, H5'); δ_C (CDCl₃) 140.38 (C, C2'), 137.94 (C, C7a), 137.53 (C, C2), 128.94 (2xCH), 128.82 (2xCH), 128.49 (C, C3a), 127.10 (CH, C5'), 125.40 (CH, C4), 124.49 (CH, C6), 120.82 (C, C1''), 111.26 (CH, C7), 102.84 (C, C5), 101.66 (CH, C3), 34.59 (CH₂, C5'); m/z (EI⁺) 232 ([M]⁺, 100), 231 (64), 155 (71), 91 (16), 84 (21), 49 (23), 43 (25); found [M+H]⁺, 232.1002, C₁₆H₁₂N₂ requires [M+H]⁺, 232.1000; Found: C, 82.9; H, 5.1; N, 11.9. Required: C, 82.7; H, 5.2; N, 12.1; Δ = 0.9 ppm.

(Z)-Ethyl 3-(2-benzyl-1H-indol-5-yl)-2-ethoxyacrylate 179 and **(E)-ethyl 3-(2-benzyl-1H-indol-5-yl)-2-ethoxyacrylate 180**

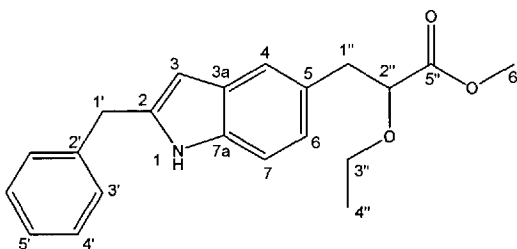
To a milky suspension of sodium hydride (19.5 mg, 0.488 mmol, 2.31 eq) in anhydrous THF (0.400 ml) at 0 °C, was added dropwise, phosphonoacetate **129** (123 mg, 0.459 mmol, 2.17 eq) in THF (1.00 ml) over 10 min, under a constant flow of N₂. The pale yellowish solution was stirred at 0 °C for 40 min before the dropwise addition of aldehyde **177** (49.7 mg, 0.211 mmol, 1.00 eq) in dry THF (1.00 ml) *via* syringe pump over 37 min. The solution which had turned orange was left stirring in the ice bath over 42 hr. The dark yellow solution was concentrated *in vacuo*, then dissolved in EtOAc (30.0 ml) and washed with water (35.0 ml). An emulsion was observed, thus some NaCl was added. The aqueous phase was extracted with EtOAc (4x45.0 ml). After drying the organic extract over MgSO₄, concentration *in vacuo* of the organic phase gave a deep orange slurry which was purified by flash column chromatography on silica gel (hexane/EtOAc 15:1, 12:1) to yield 66.0 mg (90%) of the product. Ratio Z:E = 63:37.

Z isomer **179**: colourless oil: R_f 0.20 [hexane/EtOAc 8:2]; ν_{\max} (DCM film)/cm⁻¹ 3441, 3055, 1743, 1646, 1051, 740; δ_{H} (CDCl₃) 8.03 (1H, br, H4), 7.89 (1H, br, H1), 7.65-7.62 (1H, dd, *J* 8.5, *J* 1.5, H6), 7.37-7.33 (2H, m, H4'), 7.30-7.22 (4H, m, H3', H7, H5'), 7.17 (1H, s, H1''), 6.36-6.35 (1H, d, *J* 1.0, H3), 4.34-4.29 (2H, q, *J* 14.5, *J* 7.0, H6''), 4.14 (2H, s, H1'), 4.04-3.98 (2H, q, *J* 14.0, *J* 7.0, H3''), 1.42-1.37 (6H, m, H7'', H4''); δ_{C} (CDCl₃) 165.31 (C, C5''), 142.43 (C, C2''), 138.67 (C, C2'), 138.21 (C, C2), 136.56 (C, C7a), 128.81 (2xCH), 128.77 (2xCH), 126.82 (CH, C5'), 126.30 (CH, C1''), 125.53 (2xC, C3a, C5), 124.08 (CH, C6), 122.71 (CH, C4), 110.43 (CH, C7), 101.73 (CH, C3), 67.41 (CH₂, C3''), 60.87 (CH₂, C6''), 34.69 (CH₂, C1'), 15.56 (CH₃, C4''), 14.36 (CH₃, C7''); *m/z* (EI⁺) 349 ([M]⁺, 100), 292 ([M-ethyl]⁺, 17), 292 (32), 247 (36), 219 (26), 91 (50); found [M+H]⁺, 349.1672, C₂₂H₂₃NO₃ requires [M+H]⁺, 349.1678; Found: C, 75.6; H, 6.5; N, 3.9. Required: C, 75.6; H, 6.6; N, 4.0; Δ = -1.7 ppm.

E isomer **180**: pale yellow oil: R_f 0.15 [hexane/EtOAc 8:2]; ν_{\max} (DCM film)/cm⁻¹ 3441, 3055-2850, 1725, 1644, 1548, 1266, 1043, 738; δ_{H} (CDCl₃) 7.75 (1H, br, H1), 7.40

(1H, s, H4), 7.36-7.32 (2H, m, 2xH4'), 7.28-7.25 (3H, m, 2xH3', H5'), 7.16-7.14 (1H, d, J 8.5, H7), 7.00-6.97 (1H, dd, J 8.5, J 1.0, H6), 6.29 (1H, s, H1''), 6.27 (1H, br, H3), 4.18-4.12 (4H, m, 2xH6'', 2xH1'), 3.98-3.93 (2H, q, J 14.0, J 7.0, 2xH3''), 1.44-1.41 (3H, t, J 7.0, 3xH4''), 1.11-1.08 (3H, t, J 7.0, 3xH7''); δ_c (CDCl₃) 165.20 (C, C5''), 146.16 (C, C2''), 138.41 (C, C2'), 138.16 (C, C2), 135.44 (C, C7a), 128.81 (2xCH), 128.74 (2xCH), 126.76 (CH, C5'), 126.26 (2xC, C3a, C5), 122.40 (CH, C6), 119.96 (CH, C4), 111.60 (CH, C1''), 110.00 (CH, C7), 101.20 (CH, C3), 64.63 (CH₂, C3''), 61.05 (CH₂, C6''), 34.73 (CH₂, C1'), 14.58 (CH₃, C4''), 13.77 (CH₃, C7''); m/z (EI⁺) 349 ([M]⁺, 16), 232 ([M-(benzyl+ethyl)]⁺, 100), 155 (77), 84 (42), 49 (56); found [M+H]⁺, 349.1671, C₂₂H₂₃NO₃ requires [M+H]⁺, 349.1678; Found: C, 75.7; H, 6.8; N, 3.9. Required: C, 75.6; H, 6.6; N, 4.0; Δ = -2.0 ppm.

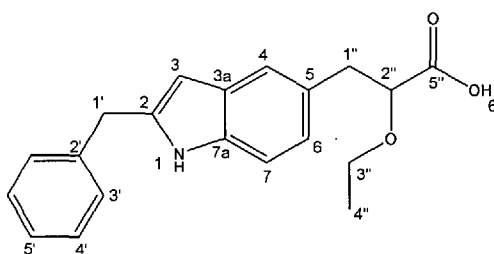
Methyl 3-(2-benzyl-1H-indol-5-yl)-2-ethoxypropanoate 187



To a yellow solution of the starting material **179** and **180** (55.2 mg, 0.158 mmol, 1.00 eq) in anhydrous methanol (2.00 ml) at RT, under a constant flow of N₂, were added the magnesium turnings (20.6 mg, 0.847 mmol, 5.36 eq) in one portion and the reaction mixture was stirred at RT for 7 hr. A few more magnesium turnings were added as well as some dry methanol (1.00 ml) and the reaction mixture was stirred at RT for another 12 hr before being poured onto water (35.0 ml). The aqueous phase was extracted with DCM (4x30.0 ml) and the organic extracts were washed with brine (70.0 ml). After extraction with DCM (4x100 ml) and drying over MgSO₄, concentration *in vacuo* gave a yellowish oil which was purified by flash column chromatography on silica gel (hexane/EtOAc 15:1, 10:1) to yield 40.6 mg (76%) of the product as a pale yellow oil: R_f 0.25 [hexane/EtOAc 7.5:2.5]; ν_{max} (DCM film)/cm⁻¹ 3392, 3027-2900, 1741, 1644, 1446, 1115, 705; δ_H (CDCl₃) 7.77 (1H, br, H1), 7.41 (1H, br, H4), 7.36-7.32 (2H, m, H4'), 7.29-7.26 (3H, m, H3', H5'), 7.17-7.15 (1H, d, J 8.5, H7), 7.02-7.00 (1H, dd, J 8.5, H6), 6.28 (1H, s, H3), 4.12 (2H, s, H1'), 4.11-4.07 (1H, t, J 6.5, H2''), 3.71 (3H, s, 3xH6''), 3.64-3.56 (1H, m, 1xH3''), 3.41-3.34 (1H, m, 1xH3''), 3.11-3.09 (2H, m, 2xH1''), 1.20-1.16 (3H, t, J 7.0, H6''); δ_c (CDCl₃) 173.28 (C, C5''), 138.51 (C, C2'), 138.03 (C, C2), 135.28 (C, C7a), 128.83 (C, C5), 128.80

(2x $\underline{\text{C}}\text{H}$), 128.68 (2x $\underline{\text{C}}\text{H}$), 128.24 ($\underline{\text{C}}$, C3a), 126.69 ($\underline{\text{C}}\text{H}$, C5'), 122.91 ($\underline{\text{C}}\text{H}$, C6), 120.44 ($\underline{\text{C}}\text{H}$, C4), 110.16 ($\underline{\text{C}}\text{H}$, C7), 100.86 ($\underline{\text{C}}\text{H}$, C3), 81.04 ($\underline{\text{C}}\text{H}$, C2''), 66.19 ($\underline{\text{C}}\text{H}_2$, C3''), 51.73 ($\underline{\text{C}}\text{H}_2$, C6''), 39.55 ($\underline{\text{C}}\text{H}_2$, C1''), 34.72 ($\underline{\text{C}}\text{H}_2$, C1'), 15.06 ($\underline{\text{C}}\text{H}_3$, C4''); m/z (EI⁺) 337 ([M]⁺, 37), 234 ([M-(benzyl + methyl groups)]⁺, 81), 220 ([M-(benzyl+2 methyl groups)]⁺, 100), 91 (29); found [M+H]⁺, 337.1664, C₂₁H₂₃NO₃ requires [M+H]⁺, 337.1678; Found: C, 74.8, H, 6.8; N, 4.1. Required: C, 74.8; H, 6.9; N, 4.2; Δ = -4.1 ppm.

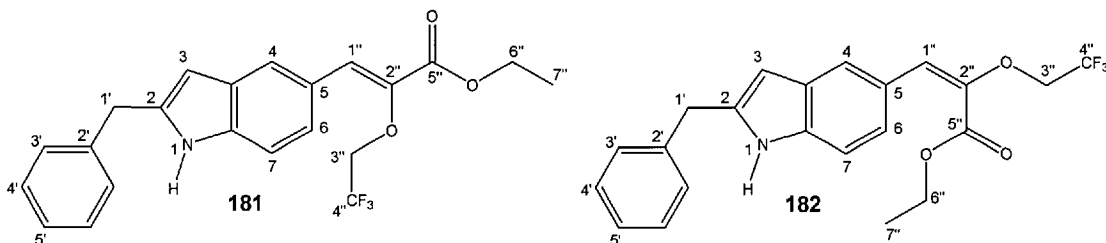
3-(2-Benzyl-1H-indol-5-yl)-2-ethoxy-propanoic acid **40**



To a yellow solution of the starting material **187** (33.4 mg, 0.099 mmol, 1.00 eq) in a mixture of ethanol/water 1:1 (1.00 ml), were added the potassium hydroxide pellets (10.0 mg, 0.178 mmol, 1.80 eq) and the yellow solution was stirred at 82 °C for 14 hr. The yellow solution was allowed to cool down to RT and concentrated *in vacuo*. With vigorous stirring in ice, was added 1M HCl (~10 drops) until a pH of 1 was reached. The desired acid crashed out as a brown ppt. It was dissolved in DCM and washed with water (35.0 ml). The aqueous phase was extracted with DCM (4x30.0 ml). After drying over MgSO₄, concentration *in vacuo* gave 29.8 mg (93%) of the product as a yellowish oil: R_f 0.20 [hexane/EtOAc 1:1]; ν_{max} (DCM film)/cm⁻¹ 3620, 3398, 1710, 1646, 1461, 1108; δ_{H} (CDCl₃) 7.77 (1H, br, H1), 7.42 (1H, s, H4), 7.36-7.32 (2H, m, H4'), 7.29-7.25 (3H, m, H3', H5'), 7.18-7.16 (1H, d, J 8.5, H7), 7.03-7.00 (1H, dd, J 8.0, J 1.5, H6), 6.28 (1H, s, H3), 4.14-4.12 (3H, m, 1xH2'', 2xH1'), 3.63-3.56 (1H, m, 1xH3''), 3.49-3.42 (1H, m, 1xH3''), 3.25-3.20 (1H, dd, J 14.0, J 4.0, H1''), 3.11-3.09 (1H, dd, J 14.0, J 8.0, H1''), 1.20-1.16 (3H, t, J 7.0, H4''); δ_{C} (CDCl₃) 175.40 ($\underline{\text{C}}$, C5''), 138.45 ($\underline{\text{C}}$), 138.15 ($\underline{\text{C}}$), 135.35 ($\underline{\text{C}}$, C7a), 128.86 ($\underline{\text{C}}$, C5), 128.81 and 128.70 (2x $\underline{\text{C}}\text{H}$ each, 2xC4', 2xC3'), 127.69 ($\underline{\text{C}}$, C3a), 126.71 ($\underline{\text{C}}\text{H}$, C5'), 122.95 ($\underline{\text{C}}\text{H}$, C6), 120.63 ($\underline{\text{C}}\text{H}$, C4), 110.27 ($\underline{\text{C}}\text{H}$, C7), 100.89 ($\underline{\text{C}}\text{H}$, C3), 80.36 ($\underline{\text{C}}\text{H}$, C2''), 66.82 ($\underline{\text{C}}\text{H}_2$, C3''), 38.85 ($\underline{\text{C}}\text{H}_2$, C1''), 34.71 ($\underline{\text{C}}\text{H}_2$, C1'), 15.05 ($\underline{\text{C}}\text{H}_3$, C4''); m/z (EI⁺) 323 ([M]⁺, 16), 220 ([M-(benzyl+methyl group)]⁺, 88), 199 (M-(benzyl + ether side chain + OH)]⁺, 100), 127 (51), 57 (53); found [M+H]⁺, 323.1520, C₂₀H₂₁NO₃ requires [M+H]⁺,

323.1521; Found: C, 74.2; H, 6.5; N, 4.4. Required: C, 74.3; H, 6.6; N, 4.3; $\Delta = -0.3$ ppm.

(Z)-Ethyl 3-(2-benzyl-1H-indol-5-yl)-2-(2,2,2-trifluoroethoxy)acrylate **181** and (E)-ethyl 3-(2-benzyl-1H-indol-5-yl)-2-(2,2,2-trifluoroethoxy)acrylate **182**



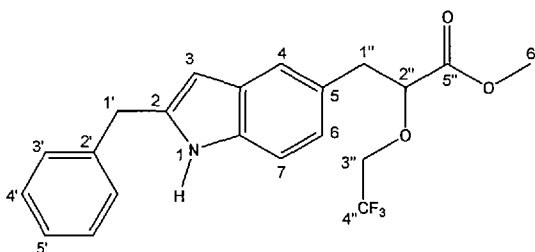
To a milky suspension of sodium hydride (17.0 mg, 0.425 mmol, 1.37 eq) and molecular sieves 4Å in anhydrous THF (1.40 ml) at 0 °C, under a constant flow of N₂, was added dropwise *via* syringe pump, phosphonoacetate **130** (112 mg, 0.347 mmol, 1.12 eq) in THF (1.20 ml) over 12 min. The suspension turned into a clear pale yellow solution. The latter was stirred at 0 °C for 29 min before the dropwise addition of aldehyde **177** (73 mg, 0.310 mmol, 1.00 eq) in dry THF (1.60 ml) *via* syringe pump over 38 min. The solution turned dark yellow. It was left to stir in the ice bath over 24 hr and at RT for another 16 hr, before being concentrated *in vacuo*. It was re-dissolved in EtOAc (30.0 ml) and washed with water (35.0 ml). Some NaCl was added. The 2 phases were separated and the aqueous phase was extracted with EtOAc (4x50.0 ml). After drying the organic extracts over MgSO₄, concentration *in vacuo* of the organic phase gave a yellowish slurry which was purified by flash column chromatography on silica gel (hexane/EtOAc 15:1, 10:1) to yield 107 mg (85%) of the product. Ratio Z:E = 39:61.

Z isomer **181**: yellow amorphous powder; mp 120.5-121.5 °C (hexane/DCM 20:1); R_f 0.30 [hexane/EtOAc 7.5:2.5]; ν_{\max} (DCM film)/cm⁻¹ 3441, 1743, 1548, 1371, 1265, 1055; δ_{H} (CDCl₃) 8.02 (1H, s, H4), 7.90 (1H, br, H1), 7.60-7.58 (1H, dd, *J* 8.5, *J* 1.5, H6), 7.37-7.34 (2H, m, 2xH4'), 7.30-7.24 (5H, m, 2xH3', H5', H1'', H7), 6.38-6.37 (1H, d, *J* 1.0, H3), 4.40-4.30 (4H, m, 2xH3'', 2xH6''), 4.14 (2H, s, 2xH1'), 1.42-1.38 (3H, t, *J* 7.0, 3xH7''); δ_{C} (CDCl₃) 164.08 (C, C5''), 140.33 (C, C2''), 138.91 (C), 138.10 (C), 136.91 (C, C7a), 128.88 (C, C5), 128.81 (2xC_H), 128.80 (2xC_H), 127.57-119.27 (C, q, *J* 277.0, C4''), 127.52 (C_H, C5'), 126.87 (C_H, C1''), 124.33 (C_H, C6), 124.24 (C, C3a), 123.36 (C_H, C4), 110.61 (C_H, C7), 101.85 (C_H, C3), 68.32-67.28 (C_H₂, q, *J* 35.0, C3''), 61.30 (C_H₂, C6''), 34.66 (C_H₂, C1'), 14.28 (C_H₃, C7'); m/z (EI⁺) 403 ([M]⁺, 45), 252 (25), 221 ([M-propanoic acid side chain]⁺, 100), 91 (27); found [M+H]⁺,

403.1392, $C_{22}H_{20}F_3NO_3$ requires $[M+H]^+$, 403.1395; Found: C, 65.4; H, 4.9; N, 3.5. Required: C, 65.5; H, 5.0; N, 3.5; $\Delta = -0.7$ ppm.

E isomer **182**: pale yellow oil: R_f 0.25 [hexane/EtOAc 7.5:2.5]; ν_{max} (DCM film)/ cm^{-1} 3441, 1743, 1548, 1265, 1053; δ_H ($CDCl_3$) 7.84 (1H, br, H1), 7.53 (1H, s, H4), 7.37-7.33 (2H, m, 2xH3'), 7.30-7.25 (3H, m, 2xH4', H5'), 7.19-7.16 (1H, d, J 8.5, H7), 7.10-7.07 (1H, dd, J 8.5, J 1.5, H6), 6.71 (1H, s, H1''), 3.61 (1H, br, H3), 4.30-4.23 (2H, q, J 17.0, J 8.5, 2xH3''), 4.23-4.18 (2H, q, J 14.5, J 7.0, 2xH6''), 4.12 (2H, s, 2xH1'), 1.18-1.15 (3H, t, J 7.0, 3xH7''); δ_C ($CDCl_3$) 163.53 (C, C5''), 143.28 (C, C2''), 138.55 (C), 138.26 (C), 136.03 (C, C7a), 128.79 (2xC_H), 128.74 (2xC_H), 128.54 (C, C5), 127.38-119.08 (C, q, J 277.0, C4''), 126.79 (C_H, C5'), 124.31 (C, C3a), 122.75 (C_H, C6), 121.76 (C_H, C1''), 120.95 (C_H, C4), 110.08 (C_H, C7), 101.32 (C_H, C3), 68.16-67.11 (C_H₂, q, J 35.0, C3''), 61.26 (C_H₂, C6''), 34.65 (C_H₂, C1'), 13.78 (C_H₃, C7'); m/z (EI⁺) 403 ($[M]^+$, 45), 252 (25), 221 ($[M\text{-propanoic acid side chain}]^+$, 100), 91 (27); found $[M+H]^+$, 403.1392, $C_{22}H_{20}F_3NO_3$ requires $[M+H]^+$, 403.1395; Found: C, 65.5; H, 5.0; N, 3.4. Required: C, 65.5; H, 5.0; N, 3.5; $\Delta = -0.7$ ppm.

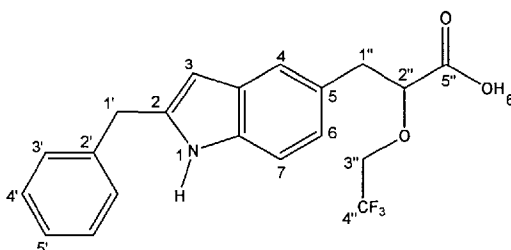
Methyl 3-(2-benzyl-1H-indol-5-yl)-2-(2,2,2-trifluoroethoxy)propanoate **188**



To a mixture of the starting material **181** and **182** (67.6 mg, 0.168 mmol, 1.00 eq) and the magnesium turnings (61.9 mg, 2.55 mmol, 15.2 eq) at RT, under a constant flow of N_2 , was added the anhydrous methanol (2.50 ml). After stirring at RT for 4 hr, the yellowish orange solution turned into a pale yellowish slurry. It was poured onto water (20.0 ml). The 2 phases were separated and the aqueous phase was extracted with DCM (4x25.0 ml). The organic extracts were washed with brine (80.0 ml). The aqueous phase was extracted with DCM (4x65.0 ml). After drying over $MgSO_4$, concentration *in vacuo* gave an orangish slurry which was purified by flash column chromatography on silica gel (hexane/EtOAc 15:1, 10:1, 9:1, 8:2) to yield 48 mg (73%) of the product as a very pale yellow oil: R_f 0.15 [hexane/EtOAc 8:2]; ν_{max} (DCM film)/ cm^{-1} 3361, 2920-2846, 1741, 1448, 1275, 1157, 790; δ_H ($CDCl_3$) 7.76 (1H, br, H1), 7.40 (1H, s, H4), 7.36-7.32 (2H, m, 2xH4'), 7.28-7.25 (3H, m, 2xH3', H5'), 7.18-7.16 (1H, d, J 8.5, H7), 7.01-6.98 (1H, dd, J 8.0, J 1.5, H6), 6.28 (1H, br, H3), 4.26-

4.23 (1H, m, H2''), 4.128 (2H, s, 2xH1'), 3.99-3.93 (1H, m, H3''), 3.74-3.66 (4H, m, 3xH6'', H3''), 3.21-3.11 (2H, m, 2xH1''); δ_c (CDCl₃) 171.50 (C, C5''), 138.43 (C), 138.16 (C), 135.37 (C, C7a), 128.86 (C, C5), 128.81 (2xCH), 128.70 (2xCH), 128.08-119.39 (C, q, *J* 278.0, C4''), 127.28 (C, C3a), 126.72 (CH, C5'), 122.85 (CH, C6), 120.54 (CH, C4), 110.29 (CH, C7), 100.88 (CH, C3), 82.02 (CH, C2''), 68.36-67.34 (CH₂, q, *J* 34.5, C3''), 52.08 (CH₃, C6''), 39.17 (CH₂, C1''), 34.69 (CH₂, C1'); *m/z* (EI⁺) 391 ([M]⁺, 27), 220 ([M-propanoic acid side chain]⁺, 100), 49 (23); found [M+H]⁺, 391.1394, C₂₁H₂₀F₃NO₃ requires [M+H]⁺, 391.1395; Found: C, 64.5; H, 5.1; N, 3.5. Required: C, 64.4; H, 5.2; N, 3.6; Δ = -0.3 ppm.

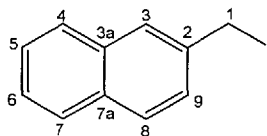
3-(2-Benzyl-1H-indol-5-yl)-2-(2,2,2-trifluoroethoxy)propanoic acid 41



Indole **188** (14.6 mg, 0.037 mmol, 1.00 eq) was refluxed with potassium hydroxide pellets (4.9 mg, 0.087 mmol, 2.34 eq) in a mixture of ethanol/water 1:1 (1.60 ml) at 82 °C for 15 hr. The pale yellow solution was allowed to cool down to RT and concentrated *in vacuo*. With vigorous stirring in ice, was added 1M HCl (~5 drops) until a pH of 1 was reached. The desired acid crashed out as a brown ppt. DCM was added and the 2 phases were separated. The aqueous phase was extracted with DCM (4x20.0 ml). After drying over MgSO₄, concentration *in vacuo* gave 14.0 mg (99%) of the product as a pale yellow oil: *R_f* 0.20 [hexane/EtOAc 1:9]; ν_{\max} (DCM film)/cm⁻¹ 3289, 2950-2850, 1702, 1651, 1425, 1053; δ_H (CDCl₃) 7.76 (1H, br, H1), 7.43 (1H, s, H4), 7.34-7.32 (2H, m, 2xH4'), 7.28-7.25 (3H, m, 2xH3', H5'), 7.19-7.17 (1H, d, *J* 8.5, H7), 7.03-7.01 (1H, dd, *J* 8.0, *J* 1.5, H6), 6.29 (1H, d, *J* 1.0, H3), 4.31-4.27 (1H, dd, *J* 8.0, *J* 4.5, H2''), 4.13 (2H, s, 2xH1'), 3.96-3.87 (1H, m, 1xH3''), 3.77-3.70 (1H, m, 1xH3''), 3.30-3.26 (1H, *J* 14.0, *J* 4.0, 1xH1''), 3.18-3.13 (1H, *J* 14.0, *J* 8.0, 1xH1''); δ_c (CDCl₃) 174.74 (C, C5''), 138.37 (C), 138.31 (C), 135.46 (C, C7a), 128.93 (C, C5), 128.83 (2xCH), 128.74 (2xCH), 127.57-119.26 (C, q, *J* 277.0, C4''), 126.92 (C, C3a), 126.77 (CH, C5'), 122.86 (CH, C6), 120.67 (CH, C4), 110.43 (CH, C7), 100.93 (CH, C3), 81.63 (CH, C2''), 68.64-67.61 (CH₂, q, *J* 34.5, C3''), 38.98 (CH₂, C1''), 34.72 (CH₂, C1'); *m/z* (EI⁺) 377 ([M]⁺, 30), 220 ([M-propanoic acid side chain]⁺, 100), 142 (9), 91 (12); found [M+H]⁺, 377.1244, C₂₀H₁₈F₃NO₃ requires

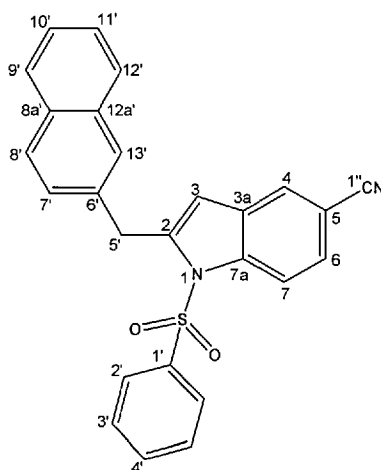
$[M+H]^+$, 377.1239; Found: C, 63.5; H, 4.7; N, 3.7. Required: C, 63.7; H, 4.8; N, 3.7; Δ = 1.3 ppm.

2-(Iodomethyl)naphthalene 225²⁴⁸



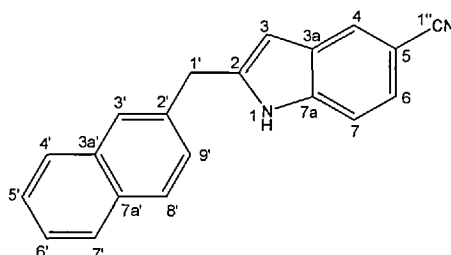
To a clear pale yellow solution of 2-(bromomethyl)naphthalene (1.17 g, 5.30 mmol, 1.00 eq) in acetone (15.0 ml) at RT, was added sodium iodide (795 mg, 5.30 mmol, 1.00 eq) in one portion. A creamy ppt immediately crashed out. The reaction mixture was stirred at RT for 16-17 hr. The reaction mixture was filtered, the yellow filtrate was concentrated *in vacuo* to give an off-white solid which was re-dissolved in DCM (25.0 ml) and washed with water (2x25.0 ml). The aqueous phase was extracted with DCM (4x50.0 ml). After drying over $MgSO_4$, concentration *in vacuo* gave a pale orangish powder. A progressive colour darkening was observed as soon as the product was isolated. The crude solid was purified by flash column chromatography on silica gel (hexane/DCM 99:1, hexane/EtOAc 1:1) to yield 1.07 g (75%) of the product as a pale orange powder: R_f 0.40 [hexane/EtOAc 10:1]; δ_H ($CDCl_3$) 7.85-7.80 (4H, m), 7.52-7.47 (3H, m), 4.65 (2H, s, 2xH1'); δ_C ($CDCl_3$) 136.54 (C), 133.22 (C), 132.75 (C), 128.72 (CH), 127.77 (CH), 127.70 (CH), 127.00 (CH), 126.90 (CH), 126.44 (CH), 126.35 (CH), 6.49 (CH₂, C1). The product decomposed into a black tar before any further characterisation could be carried out, as described in the literature.²⁶⁷

2-(Naphthalen-2-ylmethyl)-1-(phenylsulfonyl)-1H-indole-5-carbonitrile 195



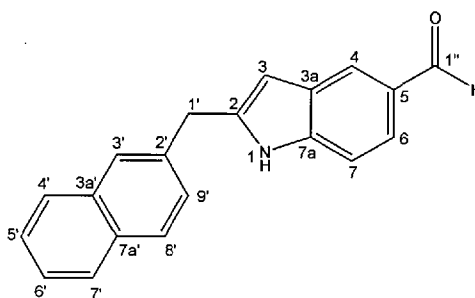
To a very pale yellow solution of indole-carbonitrile **193** (905 mg, 3.20 mmol, 1.00 eq) in anhydrous THF (10.0 ml), was added dropwise a 1.7M *t*-BuLi solution in pentane (2.30 ml, 3.91 mmol, 1.22 eq) over 8 min, at -48 to -45 °C, under a constant flow of N₂. The solution which had turned dark yellow, then dark green was stirred at -45 °C to -30 °C over 55 min, cooled down to -45 °C before the dropwise addition of 2-(bromomethyl)naphthalene (887 mg, 4.01 mmol, 1.25 eq) diluted in dry THF (2.00 ml) over 7 min. The reaction mixture was allowed to warm up to -10 °C over 50 min whereupon it turned brown. It was next put in an ice bath for 50 min, before being allowed to warm up to RT over 25 hr. The brown reaction mixture was poured over 5% citric acid (10.0 ml) and the organic phase was washed with brine (50.0 ml). The aqueous phase was extracted with DCM (4x50.0 ml). The organic phase was dried over anhydrous K₂CO₃ and concentrated *in vacuo* to give a brown oil (1.73 g) which was purified by flash column chromatography on silica gel (hexane/EtOAc 25:1, 20:1, 15:1) to yield 406 mg (30%) of the product as a yellow oil. Crystallisation from hexane/DCM 20:1 afforded shiny white needles: mp 142.0-143.0 °C (hexane/DCM 20:1); R_f 0.30 [hexane/EtOAc 7:3]; ν_{\max} (nujol)/cm⁻¹ 2950-2850, 2222, 1651, 1548, 1379, 1055; δ_{H} (CDCl₃) 8.32-8.30 (1H, d, *J* 9.0, H7), 7.86-7.83 (1H, m), 7.81-7.87 (1H, d, *J* 8.5), 7.73-7.71 (2H, m), 7.64-7.62 (2H, dd, *J* 8.5, *J* 1.0), 7.59 (1H, br, H4), 7.57-7.54 (1H, dd, *J* 9.0, *J* 1.5, H6), 7.50-7.46 (3H, m, 2xH3'), 7.32-7.28 (3H, m), 6.21 (1H, br, H3), 4.53 (2H, s, 2xH5'); δ_{C} (CDCl₃) 143.41 (C), 139.07 (C), 138.57 (C, C7a), 134.41 (C, C1'), 134.09 (CH, 2xC4'), 133.47 (C, C12a'), 132.44 (C, C8a'), 129.34 (CH, 2xC3'), 128.36 and 127.95 (2xCH, C2 and C4), 127.65, 127.61, 127.45, 127.25, 126.29, 126.25, 125.92, 125.08 (8xCH), 119.32 (C, C1''), 115.38 (CH, C7), 110.30 (CH, C3), 107.14 (C, C5), 35.24 (CH₂, C5'); *m/z* (EI⁺) 422 ([M]⁺, 61), 280 ([M-methyl naphthyl group]⁺, 100), 141 (34), 77 (34); found [M+H]⁺, 422.1087, C₂₆H₁₈N₂O₂S requires [M+H]⁺, 422.1089; Found: C, 74.0; H, 4.2; N, 6.6. Required: C, 73.9; H, 4.3; N, 6.6; Δ = -0.5 ppm.

2-(Naphthalen-2-ylmethyl)-1H-indole-5-carbonitrile 197



To a solution of MeOH (65.0 ml), NaOH 2M (12.5 ml) was added the indole **195** (503 mg, 1.19 mmol, 1.00 eq) and the reaction mixture was refluxed at 76 °C for 17 hr. After allowing the reaction mixture to cool down to RT, the clear colourless solution was poured onto 2M HCl (14.0 ml) to a pH of 3 and the aqueous phase was extracted with DCM (5x70.0 ml). Concentration *in vacuo* of the organic phase gave a white solid which was washed with water to yield 335 mg (99%) of the product as an amorphous white powder: mp 152.0-153.0 °C (hexane/DCM 20:1); R_f 0.25 [hexane/EtOAc 7:3]; ν_{\max} (nujol)/ cm^{-1} 3206, 2980-2850, 2215, 1461, 1371, 1053; δ_H (CDCl_3) 8.13 (1H, br, H1), 7.89 (1H, s), 7.86-7.80 (3H, m), 7.73 (1H, s, H4), 7.54-7.47 (2H, m), 7.37-7.34 (2H, m, H6), 7.28-7.26 (1H, d, J 8.5, H7), 6.46 (1H, d, J 1.0, H3), 4.33 (2H, s, H1'); δ_C (CDCl_3) 140.25 (\underline{C} , C2'), 137.95 (\underline{C} , C7a), 134.96 (\underline{C} , C2), 133.54 (\underline{C} , C3a'), 132.47 (\underline{C} , C7a'), 128.76 (\underline{CH}), 128.51 (\underline{C} , C3a), 127.74, 127.54, 127.30, 127.23, 126.99, 126.47, 125.99, 125.44, 124.53 (11x \underline{CH}), 120.81 (\underline{C} , C1''), 111.28 (\underline{CH} , C7), 102.88 (\underline{C} , C5), 101.77 (\underline{CH} , C3), 34.79 (\underline{CH}_2 , C1'); m/z (EI^+) 282 ($[\text{M}]^+$, 100), 155 (52); found $[\text{M}+\text{H}]^+$, 282.1142, $\text{C}_{20}\text{H}_{14}\text{N}_2$ requires $[\text{M}+\text{H}]^+$, 282.1157; Found: C, 85.1; H, 4.9; N, 9.9. Required: C, 85.1; H, 5.0; N, 9.9; Δ = -5.3 ppm.

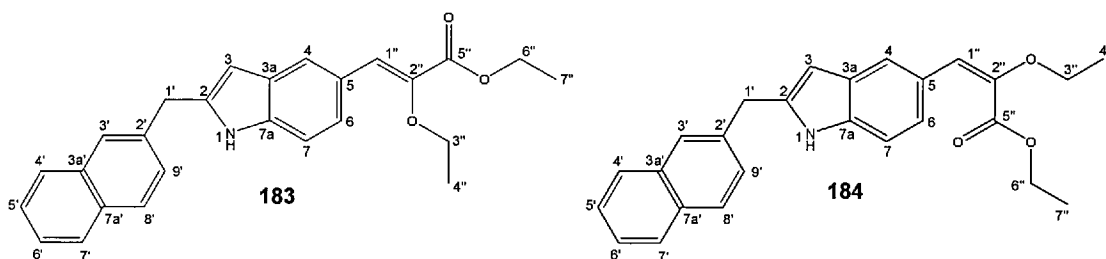
2-(Naphthalen-2-ylmethyl)-1H-indole-5-carbaldehyde **178**



To a clear colourless solution of indole **197** (312 mg, 1.10 mmol, 1.00 eq) in anhydrous DCM (5.50 ml) under a constant flow of N_2 , at 0 °C, was added dropwise the DIBAL-H solution, 1.0M in DCM (1.50 ml, 1.50 mmol, 1.36 eq). The reaction mixture turned pale yellow, it was allowed to warm up to RT over 14 hr. To the bright yellow solution was added a 1.0M Rochelle solution (10.2 ml) at 0 °C. Caution: evolution of gas. The reaction mixture was stirred at RT for 5 hr. The two phases were separated and the aqueous phase extracted with DCM (4x25.0 ml). The solvent was removed *in vacuo*, and the yellowish orange slurry was dissolved in DCM (10.0 ml) and stirred with 1M HCl (1.70 ml) at RT for 2 hr 20 min. Water (7.70 ml) was added, and the pH adjusted to 13 using 2M NaOH (1.10 ml). The two phases were extracted with separated, the aqueous phase was extracted with DCM (4x20.0 ml) and the organic extracts washed with water (40.0 ml) and brine (40.0 ml). After

extraction of the aqueous phase with DCM (4x40.0 ml), drying over MgSO₄ and concentration *in vacuo*, the off-white solid isolated was purified by flash column chromatography on silica gel (hexane/EtOAc 12:1, 10:1, 9:1, 7:3) to yield 272 mg (86%) of the product as an amorphous pale yellow powder: mp 162.5-163.5 °C (hexane/DCM 20:1); R_f 0.20 [hexane/EtOAc 7.5:2.5]; ν_{max} (nujol)/cm⁻¹ 3221, 2980-2850, 1660, 1306, 796; δ_H (CDCl₃/MeOD 1:2) 9.86 (1H, s, H1^{''}), 8.00 (1H, s, H4), 7.78-7.73 (3H, m), 7.69 (1H, s, H1), 7.61-7.59 (1H, d, J 8.5, H6), 7.44-7.33 (4H, m, H7), 6.36 (1H, br, H3), 4.25 (2H, s, 2xH1'); δ_C (CDCl₃/MeOD 1:2) 194.21 (C_H, C1^{''}), 141.47 (C), 141.20 (C), 136.49 (C, C5), 134.11 (C), 132.84 (C), 129.29 (C), 129.08 (C), 128.65, 128.03, 127.96, 127.63, 127.51, 126.54, 126.02 (7xCH), 125.93 (CH, C4), 121.94 (CH, C6), 111.83 (CH, C7), 102.50 (CH, C3), 35.13 (CH₂, C1'); m/z (EI⁺) 285 ([M]⁺, 100), 254 ([M-aldehyde]⁺, 38), 158 (50), 158 (42); found [M+H]⁺, 285.1146, C₂₀H₁₅NO requires [M+H]⁺, 285.1154; Found: C, 84.1; H, 5.3; N, 4.9. Required: C, 84.2; H, 5.3; N, 4.9; Δ = -2.8 ppm.

(*Z*)-Ethyl 2-ethoxy-3-(2-(naphthalen-2-ylmethyl)-1H-indol-5-yl)acrylate **183** and (*E*)-ethyl 2-ethoxy-3-(2-(naphthalen-2-ylmethyl)-1H-indol-5-yl)acrylate **184**

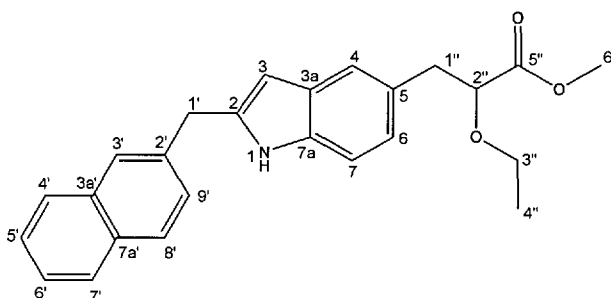


To a milky suspension of sodium hydride, 60% in oil (31.0 mg, 0.775 mmol, 2.18 eq) and molecular sieves 4Å in anhydrous THF (4.00 ml) at 0 °C, under a constant flow of N₂, was added dropwise, phosphonoacetate **129** (173 mg, 0.644 mmol, 1.81 eq) in THF (1.20 ml) over 12 min. The pale yellowish solution was stirred at 0 °C for 52 min before the dropwise addition of aldehyde **178** (102 mg, 0.356 mmol, 1.00 eq) in dry THF (2.00 ml) *via* syringe pump over 58 min. The solution which turned dark yellow was left to stir in the ice bath over 42 hr. The yellowish orange solution was concentrated *in vacuo*, re-dissolved in EtOAc (25.0 ml) and washed with water (30.0 ml). An emulsion was observed, thus some NaCl was added. The aqueous phase was extracted with EtOAc (4x40.0 ml). After drying the organic extracts over MgSO₄, concentration *in vacuo* of the organic phase gave an orange slurry which was purified by flash column chromatography on silica gel (hexane/EtOAc 12:1, 9:1, 8:2, EtOAc) to yield 112 mg (79%) of the product. Ratio *Z*:*E* = 63:37.

Z isomer **183**: colourless oil: R_f 0.30 [hexane/EtOAc 7:3]; ν_{\max} (DCM film)/ cm^{-1} 3352, 3053-2900, 1701, 1620, 1252, 1095, 740; δ_H (CDCl_3) 8.06 (1H, s, H4), 7.98 (1H, br, H1), 7.86-7.78 (3H, m), 7.72 (1H, s), 7.66-7.64 (1H, dd, J 8.5, J 1.0, H6), 7.52-7.47 (2H, m), 7.39-7.37 (1H, dd, J 8.5, J 1.0), 7.23-7.21 (1H, d, J 8.5, H7), 7.19 (1H, s), 6.41 (1H, br, H3), 4.34-4.29 (4H, m, 2xH6", 2xH1'), 4.05-4.00 (2H, q, J 14.0, J 7.0, 2xH3"), 1.43-1.37 (6H, m, 3xH4", 3xH7"); δ_C (CDCl_3) 165.32 (\underline{C} , C5"), 142.39, 138.60, 136.60, 135.70, 133.52, 132.36, 128.81 (7x \underline{C} , C7a, C2', C5, C2, C3a', C7a', C3a), 128.45, 127.67, 127.53, 127.16, 127.12, 126.34, 126.26, 125.74 (8x \underline{CH}), 125.48 (\underline{C}), 124.07 (\underline{CH} , C6), 122.70 (\underline{CH} , C4), 110.50 (\underline{CH} , C7), 101.81 (\underline{CH} , C3), 67.40 (\underline{CH}_2 , C3"), 60.87 (\underline{CH}_2 , C6"), 34.83 (\underline{CH}_2 , C1'), 15.54 (\underline{CH}_3), 14.32 (\underline{CH}_3); m/z (EI^+) 399 ($[\text{M}]^+$, 78), 342 ($[\text{M}-\text{both ethyl groups}]^+$, 25), 297 (24), 141 (100); found $[\text{M}+\text{H}]^+$, 399.1830, $\text{C}_{26}\text{H}_{25}\text{NO}_3$ requires $[\text{M}+\text{H}]^+$, 399.1834; Found: C, 78.3; H, 6.2; N, 3.6. Required: C, 78.2; H, 6.3; N, 3.5; $\Delta = -1.0$ ppm.

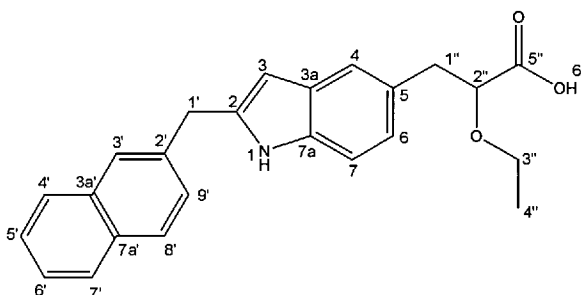
E isomer **184**: colourless oil: R_f 0.30 [hexane/EtOAc 7:3]; ν_{\max} (DCM film)/ cm^{-1} 3392, 3050-2900, 1712, 1635, 1228, 1153, 740; δ_H (CDCl_3) 7.85-7.79 (4H, m), 7.71 (1H, s), 7.52-7.45 (2H, m), 7.42 (1H, s, H4), 7.38-7.36 (1H, dd, J 8.5, J 1.5), 7.14-7.12 (1H, d, J 8.5, H7), 7.00-6.98 (1H, dd, J 8.5, J 1.5, H6), 6.33-6.32 (1H, d, J 1.0, H3), 6.29 (1H, s, H1"), 4.28 (2H, s, H1'), 4.18-4.11 (2H, q, J 14.5, J 7.0, 2xH6"), 3.98-3.93 (2H, q, J 14.0, J 7.0, 2xH3"), 1.44-1.41 (3H, t, J 7.0, 3xH4"), 1.11-1.08 (3H, t, J 7.0, 3xH7"); δ_C (CDCl_3) 165.19 (\underline{C} , C5"), 146.09, 138.06, 135.90, 135.46, 133.52, 132.33, 128.67 (7x \underline{C} , C7a, C2', C5, C2, C3a', C7a', C3a), 128.39, 127.66, 127.52, 127.19, 127.07, 126.23 (6x \underline{CH}), 126.20 (\underline{C}), 125.69 (\underline{CH}), 122.37 (\underline{CH} , C6), 119.92 (\underline{CH} , C4), 111.61 (\underline{CH} , C1"), 110.05 (\underline{CH} , C7), 101.25 (\underline{CH} , C3), 64.60 (\underline{CH}_2 , C3"), 61.04 (\underline{CH}_2 , C6"), 34.70 (\underline{CH}_2 , C1'), 14.53 (\underline{CH}_3 , C4"), 13.73 (\underline{CH}_3 , C7"); m/z (EI^+) 399 ($[\text{M}]^+$, 72), 342 ($[\text{M}-\text{both ethyl groups}]^+$, 24), 282 (34), 141 (100); found $[\text{M}+\text{H}]^+$, 399.1832, $\text{C}_{26}\text{H}_{25}\text{NO}_3$ requires $[\text{M}+\text{H}]^+$, 399.1834; Found: C, 78.3; H, 6.2; N, 3.6. Required: C, 78.2; H, 6.3; N, 3.5; $\Delta = -0.5$ ppm.

Methyl 2-ethoxy-3-(2-(naphthalen-2-ylmethyl)-1H-indol-5-yl)propanoate 189



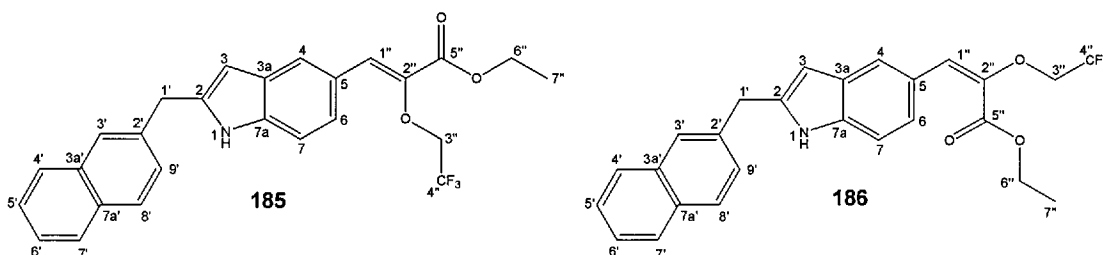
To a clear orange-brown solution of the starting material **183** and **184** (110 mg, 0.275 mmol, 1.00 eq) in anhydrous methanol (4.00 ml) at RT, under a constant flow of N₂, were added the magnesium turnings (68.5 mg, 2.82 mmol, 10.3 eq) in one portion. After stirring at RT for 4.5 hr, some starting material was still seen by MS. Therefore, were added, more magnesium turnings (46.7 mg, 1.92 mmol, 7.00 eq) and the reaction mixture was stirred for another 18 hr. The pale orangish suspension was poured onto water (30.0 ml). The 2 phases were separated and the aqueous phase was extracted with DCM (4x25.0 ml). The organic extracts were washed with brine (50.0 ml). The aqueous phase was extracted with DCM (4x45.0 ml). After drying over MgSO₄, concentration *in vacuo* gave a pale yellow oil which was purified by flash column chromatography on silica gel (hexane/EtOAc 10:1, 9:1, 8:2) to yield 85 mg (80%) of the product as a yellowish oil: R_f 0.15 [hexane/EtOAc 8:2]; ν_{\max} (DCM film)/cm⁻¹ 3392, 3050-2900, 1741, 1643, 1273, 1114, 740; δ_{H} (CDCl₃) 7.84-7.79 (4H, m), 7.71 (1H, s, H1), 7.51-7.45 (2H, m), 7.42 (1H, s, H4), 7.39-7.36 (1H, dd, *J* 8.5, *J* 1.5), 7.16-7.13 (1H, d, *J* 8.5, H7), 7.01-6.99 (1H, dd, *J* 8.0, *J* 1.5, H6), 6.33-6.32 (1H, d, *J* 1.0, H3), 4.28 (2H, s, H1'), 4.10-4.07 (1H, dd, *J* 7.0, *J* 6.0, 2xH2''), 3.71 (3H, s, H6''), 3.63-3.58 (1H, m, 1xH3''), 3.40-3.33 (1H, m, 1xH3''), 3.11 (1H, s, 1xH1''), 3.09-3.08 (1H, d, *J* 1.5, 1xH1''), 1.19-1.16 (3H, t, *J* 7.0, 3xH4''); δ_{C} (CDCl₃) 173.30 (C, C5''), 137.89, 135.97, 135.30, 133.53, 133.18, 132.33, 128.90 (7xC, C7a, C2', C5, C2, C3a', C7a'), 128.41 (CH), 128.26 (C, C3a), 127.72, 127.52, 127.24, 127.09, 126.35, 125.69 (6xCH), 122.95 (CH, C6), 120.47 (CH, C4), 110.19 (CH, C7), 101.02 (CH, C3), 81.02 (CH, C2''), 66.20 (CH₂, C3''), 51.77 (CH₃, C6''), 39.53 (CH₂, C1''), 34.92 (CH₂, C1'), 15.07 (CH₃, C4''); *m/z* (EI⁺) 387 ([M]⁺, 27), 270 ([M-side chain on 5-position]⁺, 100), 146 (67); found [M+H]⁺, 387.1835, C₂₅H₂₅NO₃ requires [M+H]⁺, 387.1834; Found: C, 77.5; H, 6.4; N, 3.7. Required: C, 77.5; H, 6.5; N, 3.6; Δ = 0.3 ppm.

2-Ethoxy-3-(2-(naphthalen-2-ylmethyl)-1H-indol-5-yl)propanoic acid **42**



The starting material **189** (62.1 mg, 0.160 mmol, 1.00 eq) was refluxed with potassium hydroxide pellets (18.0 mg, 0.321 mmol, 2.00 eq) in a mixture of ethanol/water 1:1 (1.60 ml) at 75 °C for 15 hr and at 90 °C for a further 2.5 hr. Some starting material was still seen by MS, thus more potassium hydroxide (31.0 mg, 0.552 mmol, 3.40 eq) was added and the RM was stirred for a further 4 hr. The light orange solution was allowed to cool down to RT and concentrated *in vacuo*. With vigorous stirring in ice, was added 1M HCl (~30 drops) until a pH of 1 was reached. The desired acid crashed out as an off-white ppt. DCM was added and the 2 phases were separated. The aqueous phase was extracted with DCM (4x10.0 ml). The extracts were washed with water (2x25.0 ml). The aqueous phase was extracted with DCM (4x45.0 ml, 3x20.0 ml, 2x50.0 ml). After drying over MgSO₄, concentration *in vacuo* gave 58.5 mg (98%) of the product as a yellowish oil: R_f 0.25 [hexane/EtOAc 1:9]; ν_{max} (DCM film)/cm⁻¹ 3403, 3053-2900, 1720, 1644, 1267, 1110, 739; δ_H (CDCl₃) 7.85-7.79 (4H, m), 7.71 (1H, s), 7.51-7.45 (2H, m), 7.43 (1H, s, H4), 7.39-7.36 (1H, dd, *J* 8.5, *J* 1.5), 7.16-7.14 (1H, d, *J* 8.5, H7), 7.02-7.00 (1H, dd, *J* 8.0, *J* 1.5, H6), 6.34 (1H, br, H3), 4.28 (2H, s, H1'), 4.14-4.11 (1H, dd, *J* 7.5, *J* 4.5, 2xH2''), 3.62-3.54 (1H, m, 1xH3''), 3.50-3.42 (1H, m, 1xH3''), 3.25-3.21 (1H, dd, *J* 14.0, *J* 4.0, 1xH1''), 3.11-3.06 (1H, dd, *J* 14.0, *J* 8.0, 1xH1''), 1.19-1.16 (3H, t, *J* 7.0, 3xH4''); δ_C (CDCl₃) 174.59 (C, C5''), 138.03, 135.90, 135.39, 133.53, 132.35, 128.87 (6xC, C7a, C2', C5, C2, C3a', C7a'), 128.44 (CH), 127.68 (CH), 127.65 (C, C3a), 127.53, 127.24, 127.12, 126.25, 125.72 (5xCH), 123.01 (CH, C6), 120.69 (CH, C4), 110.32 (CH, C7), 101.04 (CH, C3), 80.31 (CH, C2''), 66.89 (CH₂, C3''), 38.75 (CH₂, C1''), 34.93 (CH₂, C1'), 15.07 (CH₃, C4''); m/z (EI⁺) 373 ([M]⁺, 33), 270 ([M-side chain on 5-position]⁺, 100), 142 (36); found [M+H]⁺, 373.1676, C₂₄H₂₃NO₃ requires [M+H]⁺, 373.1678; Found: C, 77.1; H, 6.1; N, 3.6. Required: C, 77.2; H, 6.2; N, 3.8; Δ = 0.9 ppm.

(*Z*)-Ethyl 3-(2-(naphthalen-2-ylmethyl)-1H-indol-5-yl)-2-(2,2,2-trifluoroethoxy)acrylate **185** and (*E*)-ethyl 3-(2-(naphthalen-2-ylmethyl)-1H-indol-5-yl)-2-(2,2,2-trifluoroethoxy)-acrylate **186**



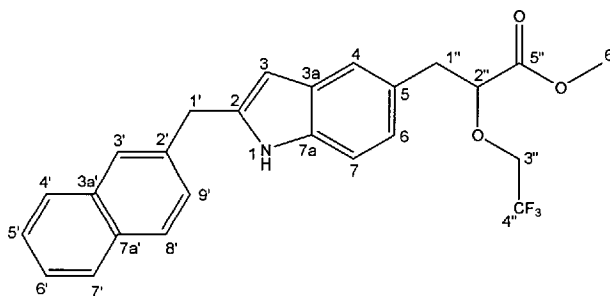
To a milky suspension of sodium hydride, 60% in oil (29.4 mg, 0.735 mmol, 1.41 eq) and molecular sieves 4Å in anhydrous THF (3.60 ml) at 0 °C, under a constant flow of N₂, was added dropwise, phosphonoacetate **130** (180 mg, 0.560 mmol, 1.08 eq) in THF (1.20 ml) over 12 min. The pale yellowish solution was stirred at 0 °C for 35 min before the dropwise addition of aldehyde **178** (148 mg, 0.520 mmol, 1.00 eq) in dry THF (1.60 ml) *via* syringe pump over 42 min. The solution which had turned bright yellow was left to stir in the ice bath over 39 hr. The light yellow solution was concentrated *in vacuo*, re-dissolved in EtOAc (30.0 ml) and washed with water (30.0 ml). An emulsion was observed, thus some NaCl was added. The aqueous phase was extracted with EtOAc (4x30.0 ml). After drying the organic extracts over MgSO₄, concentration *in vacuo* of the organic phase gave a very pale orangish slurry which was purified by flash column chromatography on silica gel (hexane/EtOAc 10:1) to yield 183 mg (78%) of the product. Ratio Z:E = 38:62.

Z isomer **185**: almost colourless oil: R_f 0.35 [hexane/EtOAc 7:3]; ν_{\max} (DCM film)/cm⁻¹ 3408, 2975, 1702, 1620, 1263, 1167, 742; δ_{H} (CDCl₃) 8.06 (1H, s, H4), 7.93 (1H, br, H1), 7.88-7.82 (3H, m), 7.75 (1H, s), 7.62-7.60 (1H, dd, *J* 8.5, *J* 1.5, H6), 7.56-7.48 (2H, m), 7.48-7.38 (1H, dd, *J* 8.5, *J* 1.5), 7.29 (1H, s, H1''), 7.25-7.23 (1H, d, *J* 8.5, H7), 6.45-6.44 (1H, d, *J* 1.0, H3), 4.42-4.34 (4H, m, 2xH3'', 2xH6''), 4.32 (2H, s, 2xH1'), 1.43-1.40 (3H, t, *J* 7.0, 3xH7''); δ_{C} (CDCl₃) 164.08 (C, C5''), 140.38, 138.80, 136.95, 135.56, 133.56, 132.42, 128.93 (7xC, C7a, C2', C2'', C5, C2, C3a', C7a'), 128.58 (CH), 127.71 (CH), 127.59-119.28 (C, q, *J* 277.0, C4''), 127.55, 127.48, 127.18, 127.15 126.34, 125.82 (6xCH), 124.38 (CH, C6), 124.30 (C, C3a), 123.39 (CH, C4), 110.64 (CH, C7), 102.00 (CH, C3), 68.34-67.30 (CH₂, q, *J* 35.0, C3''), 61.30 (CH₂, C6''), 34.88 (CH₂, C1'), 14.28 (CH₃, C7''); m/z (EI⁺) 453 ([M]⁺, 100), 342 (17), 141 (93); found [M+H]⁺, 453.1553, C₂₆H₂₂F₃NO₃ requires [M+H]⁺, 453.1552; Found: C, 68.8; H, 4.8; N, 2.9. Required: C, 68.9; H, 4.9; N, 3.1; Δ = 0.2 ppm.

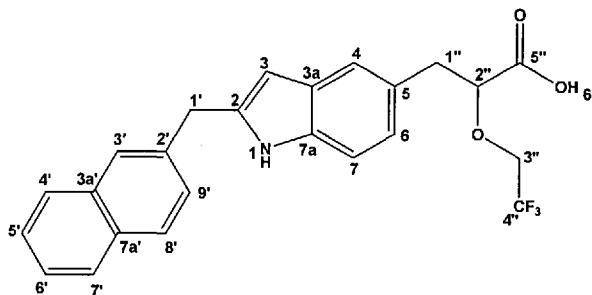
E isomer **186**: off-white powder: mp 123.0-124.5 °C (hexane/DCM 20:1); R_f 0.30 [hexane/EtOAc 7:3]; ν_{\max} (DCM film)/cm⁻¹ 3441, 2970-2850, 1709, 1645, 1267, 1132, 740; δ_{H} (CDCl₃) 7.86-7.79 (4H, m), 7.71 (1H, s, H1), 7.55 (1H, s, H4), 7.53-7.49 (2H, m), 7.38-7.34 (1H, dd, *J* 8.5, *J* 1.5), 7.17-7.15 (1H, d, *J* 8.5, H7), 7.10-7.08 (1H, dd, *J* 8.5, *J* 1.5), 6.72 (1H, s, H1''), 6.36 (1H, d, *J* 1.0, H3), 4.30-4.23 (4H, m, 2xH3'', 2xH1'), 4.23-4.18 (2H, q, *J* 14.0, *J* 7.0, 2xH6''), 1.18-1.15 (3H, t, *J* 7.0, 3xH7''); δ_{C} (CDCl₃) 163.51 (C, C5''), 143.33, 138.42, 136.08, 135.73, 133.54, 132.38, 128.58 (7xC, C7a, C2', C2'', C5, C2, C3a', C7a'), 128.49, 127.70, 127.53 (3xCH), 127.40-119.09 (CH₂, q, *J* 277.0, C4''), 127.16, 127.13, 126.31, 125.78 (4xCH), 124.37 (C, C3a), 122.82

($\underline{\text{C}}\text{H}$, C6), 121.82 ($\underline{\text{C}}\text{H}$, C1''), 121.00 ($\underline{\text{C}}\text{H}$, C4), 110.11 ($\underline{\text{C}}\text{H}$, C7), 101.49 ($\underline{\text{C}}\text{H}$, C3), 68.20-67.15 ($\underline{\text{C}}\text{H}_2$, q, J 35.0, C3''), 61.26 ($\underline{\text{C}}\text{H}_2$, C6''), 34.87 ($\underline{\text{C}}\text{H}_2$, C1'), 13.79 ($\underline{\text{C}}\text{H}_3$, C7''); m/z (EI⁺) 453 ([M]⁺, 61), 342 (10), 210 (100), 141 (46), 105 (69); found [M+H]⁺, 453.1548, C₂₆H₂₂F₃NO₃ requires [M+H]⁺, 453.1552 Found: C, 69.0; H, 5.0; N, 3.0. Required: C, 68.9; H, 4.9; N, 3.1; Δ = -0.9 ppm.

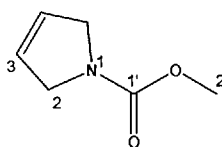
Methyl 3-(2-(naphthalen-2-ylmethyl)-1H-indol-5-yl)-2-(2,2,2-trifluoroethoxy)propanoate 190



To a mixture of the starting material **185** and **186** (14.7 mg, 0.032 mmol, 1.00 eq) and the magnesium turnings (19.2 mg, 0.790 mmol, 24.3 eq) at RT, under a constant flow of N₂, was added the anhydrous methanol (1.50 ml). A white slurry was observed, it was stirred at RT for 14 hr before being poured onto water (25.0 ml) and the aqueous phase was acidified with 1M HCl (2.00 ml). The 2 phases were separated and the aqueous phase was extracted with DCM (4x25.0 ml). After drying over MgSO₄, concentration *in vacuo* gave a pale yellow oil which was purified by flash column chromatography on silica gel (hexane/EtOAc 9:1, 8:2) to yield 11.3 mg (79%) of the product as a colourless oil: R_f 0.25 [hexane/EtOAc 7.5:2.5]; ν_{max} (DCM film)/cm⁻¹ 3403, 3054-2850, 1743, 1645, 1279, 1165, 739; δ_{H} (CDCl₃) 7.85-7.79 (3H, m), 7.77 (1H, br, H1), 7.72 (1H, s), 7.52-7.46 (2H, m), 7.42 (1H, s, H4), 7.39-7.37 (1H, dd, J 8.5, J 2.0), 7.17-7.15 (1H, d, J 8.0, H7), 7.00-6.98 (1H, dd, J 8.5, J 1.5, H6), 6.34 (1H, m, H3), 4.29 (2H, s, 2xH1'), 4.27-4.24 (1H, dd, J 7.5, J 5.0, H2''), 4.01-3.92 (1H, m, 1xH3''), 3.74 (3H, s, 3xH6''), 3.74-3.66 (1H, m, 1xH3''), 3.23-3.18 (1H, m, 1xH1''), 3.17-3.12 (1H, m, 1xH1''); δ_{C} (CDCl₃) 171.49 ($\underline{\text{C}}$, C5''), 138.05, 135.90, 135.44, 133.56, 132.38, 128.92 (7x $\underline{\text{C}}$, C7a, C2', C2'', C5, C2, C3a', C7a'), 128.46 ($\underline{\text{C}}\text{H}$), 127.74-119.42 ($\underline{\text{C}}$, q, J 277.0, C4''), 127.69 ($\underline{\text{C}}\text{H}$), 127.55 ($\underline{\text{C}}\text{H}$), 127.36 ($\underline{\text{C}}$), 127.24, 127.13, 126.26, 125.73 (4x $\underline{\text{C}}\text{H}$), 122.93 ($\underline{\text{C}}\text{H}$, C6), 120.60 ($\underline{\text{C}}\text{H}$, C4), 110.33 ($\underline{\text{C}}\text{H}$, C7), 101.07 ($\underline{\text{C}}\text{H}$, C3), 82.04 ($\underline{\text{C}}\text{H}$, C2''), 68.40-67.37 ($\underline{\text{C}}\text{H}_2$, q, J 34.5, C3''), 52.09 ($\underline{\text{C}}\text{H}_3$, C6''), 39.18 ($\underline{\text{C}}\text{H}_2$, C1''), 34.94 ($\underline{\text{C}}\text{H}_2$, C1'); m/z (EI⁺) 441 ([M]⁺, 56), 270 ([M-propanoate side chain]⁺, 100); found [M+H]⁺, 441.1548, C₂₅H₂₂F₃NO₃ requires [M+H]⁺, 441.1552; Found: C, 72.7; H, 4.9; N, 3.8. Required: C, 68.2; H, 5.0; N, 3.2; Δ = 0.9 ppm.

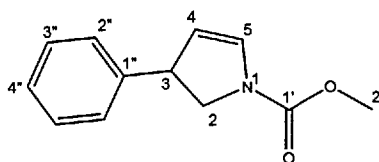
3-(2-(Naphthalen-2-ylmethyl)-1H-indol-5-yl)-2-(2,2,2-trifluoroethoxy)propanoic acid **43**

The starting material **190** (5.9 mg, 0.013 mmol, 1.00 eq) was refluxed with potassium hydroxide pellets (1.5 mg, 0.027 mmol, 2.00 eq) in a mixture of ethanol/water 1:1 (1.00 ml) at 78 °C for 15 hr. The light yellow solution was allowed to cool down to RT and concentrated *in vacuo*. With vigorous stirring in ice, was added 1M HCl (~2 drops) until a pH of 1 was reached. The desired acid crashed out as an off-white ppt. DCM was added and the 2 phases were separated. The aqueous phase was extracted with DCM (4x20.0 ml). The extracts were washed with water (25.0 ml). The aqueous phase was extracted with DCM (4x25.0 ml). After drying over MgSO₄, concentration *in vacuo* gave 5.6 mg (98%) of the product as a pale yellow oil: R_f 0.40 [Solvent B]; ν_{max} (DCM film)/cm⁻¹ 3441, 3000-2700, 1706, 1646, 1267, 1049, 740; δ_H (CDCl₃/MeOD 2:1) 9.53 (1H, br, H6''), 7.76-7.71 (3H, m), 7.65 (1H, s), 7.51 (1H, s, H4), 7.42-7.38 (2H, m), 7.35-7.32 (1H, dd, *J* 8.5, *J* 1.0), 7.17-7.15 (1H, d, *J* 8.5, H7), 7.09-7.07 (1H, m, H6), 6.59 (1H, s, H1''), 6.18 (1H, br, H3), 4.26-4.20 (4H, m, 2xH3'', 2xH1'); δ_C (CDCl₃) 174.21 (C, C5''), 138.19, 135.85, 135.50, 133.55, 132.38, 128.96 (7xC, C7a, C2', C2'', C5, C2, C3a', C7a'), 128.48, 127.69 (2xCH), 127.58-119.27 (C, q, *J* 277.0, C4''), 127.54, 127.23, 127.14 (3xCH), 126.98 (C), 126.27, 125.74 (2xCH), 122.91 (CH, C6), 120.70 (CH, C4), 110.46 (CH, C7), 101.07 (CH, C3), 81.65 (CH, C2''), 68.64-67.61 (CH₂, q, *J* 34.5, C3''), 38.98 (CH₂, C1'), 34.93 (CH₂, C1''); m/z (EI⁺) 427 ([M]⁺, 47), 270 (100), 141 (53); found [M+H]⁺, 427.1389, C₂₄H₂₀F₃NO₃ requires [M+H]⁺, 427.1395; Found: C, 67.3; H, 4.6; N, 3.2. Required: C, 67.4; H, 4.7; N, 3.3; Δ = 0.9 ppm.

1-(Methoxycarbonyl)-2,5-dihydropyrrole **210**²⁵⁷

To a round-bottomed flask were added 3-pyrroline (5.50 ml, 65% pure, 47.07 mmol, 1.00 eq), powdered potassium carbonate (19.5 g, 141 mmol, 3.00 eq) and anhydrous DCM (120 ml). The mixture was cooled to 0 °C and methyl chloroformate (6.10 ml, 78.9 mmol, 1.64 eq) was added dropwise *via* syringe pump over 100 min. The reaction mixture was allowed to warm up to RT over 14 hr. It turned yellowish. The reaction mixture was filtered and the filtrate concentrated *in vacuo*. Next, it was treated with 10% Na₂CO₃ (2x60.0 ml). After extracting the aqueous phase with DCM (4x120 ml) and drying over MgSO₄, concentration *in vacuo* yielded a yellow liquid which was purified by flash column chromatography on silica gel (hexane/EtOAc 8:2, 6:4) to yield 5.92 g (99%) of the product as a colourless liquid: R_f 0.25 [hexane/EtOAc 7.5:2.5]; ν_{\max} (film)/cm⁻¹ 3081-2850, 1707, 1548, 1462, 1393, 1120; δ_{H} (CDCl₃) 5.80-5.78 (2H, d, *J* 10.0, 2xH₃), 4.19-4.11 (4H, m, 4xH₂), 3.73 (3H, s, 3xH₂); δ_{C} (CDCl₃) 155.28 (C, C1'), 125.77 and 125.65 (CH, C3 rotamers), 53.39 and 52.84 (CH₂, rotamers, C2), 52.36 (CH₃, C2'); m/z (EI⁺) 127 ([M]⁺, 100), 112 ([M-Me]⁺, 85), 67 ([M-carbamate group]⁺, 63); found [M+H]⁺, 127.0629, C₆H₉NO₂ requires [M+H]⁺, 127.0633; Found: C, 56.5; H, 7.2.; N, 10.9. Required: C, 56.7; H, 7.1; N, 11.0; Δ = -0.8 ppm.

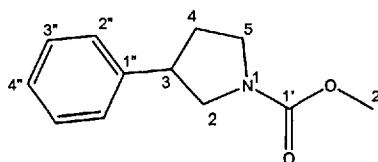
1-(Methoxycarbonyl)-3-phenyl-2,3-dihydropyrrole **211**²⁵⁷



To a stirred solution of pyrroline **210** (529 mg, 4.16 mmol, 9.91 eq) and molecular sieves 4Å in anhydrous DMF (1.00 ml), under N₂, were added iodobenzene (0.050 ml, 0.420 mmol, 1.00 eq), P(*o*-tol)₃ (15.3 mg, 0.050 mmol, 0.12 eq), Ag₂CO₃ (80.3 g, 0.291 mmol, 0.69 eq), Pd(OAc)₂ (5.0 mg, 0.022 mmol, 0.05 eq) and *i*Pr₂NEt (0.290 ml, 1.67 mmol, 3.96 eq). The brown reaction mixture was stirred at 100 °C for 19.5 hr. It was allowed to cool down, filtered over celite, and treated with 10% Na₂CO₃ (10.0 ml). After extracting the aqueous phase with ether (4x20.0 ml) and drying over MgSO₄, concentration *in vacuo* yielded a brown oil which was purified by flash column chromatography on silica gel (hexane/ether 10:1, 2:1) to yield 56.1 mg (66%) of the product as a yellow oil: R_f 0.25 [hexane/ether 2:1]; ν_{\max} (DCM film)/cm⁻¹ 3050-2850, 1707, 1549, 1452, 1384, 1126, 744; δ_{H} (CDCl₃) 7.36-7.32 (2H, m, 2xH³), 7.28-7.20 (3H, m, 2xH², H⁴), 6.84-6.69 (1H, m, rotamers, H⁵), 5.19-5.15 (1H, m, rotamers, H⁴), 4.21-4.11 (2H, m, H³, H²), 3.79-3.66 (4H, m, 3xH², H²); δ_{C} (CDCl₃)

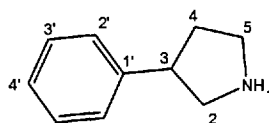
152.4, 152.3 (\underline{C} , C1' rotamers), 143.76 (\underline{C} , C1''), 130.36 and 129.45 (\underline{CH} , C5 rotamers), 128.69 (2x \underline{CH}), 127.11 (2x \underline{CH}), 126.89 (\underline{CH}), 112.41 and 112.07 (\underline{CH}_2 , C4 rotamers), 53.88 (\underline{CH}_3 , C2'), 52.60-52.53 (\underline{CH}_2 , C2), 48.27 and 47.10 (\underline{CH}_2 , C3 rotamers); m/z (EI⁺) 203 ([M]⁺, 81), 188 ([M-Me]⁺, 60), 144 ([M-carbamate group]⁺, 42), 115 (57), 84 (82); found [M+H]⁺, 203.0938, C₁₂H₁₃NO₂ requires [M+H]⁺, 203.0946; Found: C, 70.9; H, 6.4.; N, 7.0. Required: C, 70.9; H, 6.5; N, 6.9; Δ = -3.9 ppm.

1-(Methoxycarbonyl)-3-phenylpyrrolidine **218**²⁵⁷



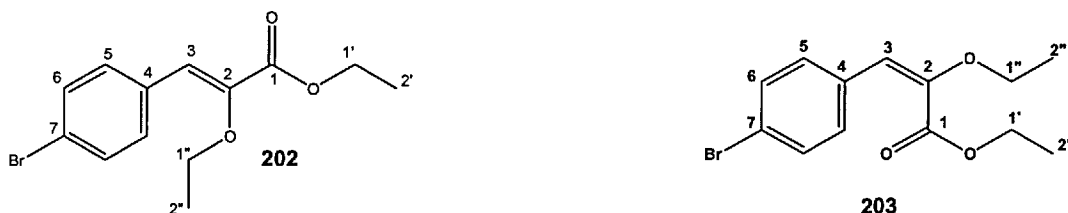
To a colourless solution of pyrrolidine **211** (647 mg, 3.18 mmol, 1.00 eq) in anhydrous MeOH (15.0 ml), under N₂, was added the platinum oxide (34.2 mg, 0.151 mmol, 0.05 eq). The reaction mixture was flushed with hydrogen gas and the RM was stirred at RT for 15.5 hr. The reaction mixture was flushed with N₂ and filtered over celite. Concentration *in vacuo* yielded an almost colourless oil which was purified by flash column chromatography on silica gel (hexane/ether 9:1, 8:2, 2:1) to yield 467 mg (72%) of the product as a colourless oil: R_f 0.15 [hexane/ether 2:1]; ν_{\max} (film)/cm⁻¹ 3050-2850, 1705, 1548, 1456, 1390, 1122, 760; δ_{H} (CDCl₃) 7.36-7.32 (2H, m, 2xH3''), 7.27-7.22 (3H, m, 2xH2'', H4''), 3.95-3.82 (1H, m, H5), 3.73 (3H, s, H2'), 3.70-3.30 (4H, m, H5, 2xH2, H3), 2.35-2.23 (1H, m, H4), 2.09-1.93 (1H, m, H4); δ_{C} (CDCl₃) 155.47 (\underline{C} , C1'), 141.21 (\underline{C} , C1''), 128.59, 126.96, 126.79 (3x \underline{CH} aromatic, C3'', C2'', C4''), 52.31 (\underline{CH}_3 , C2'), 52.28 and 52.08 (\underline{CH}_2 , C2 rotamers), 46.12 and 45.63 (\underline{CH}_2 , C5 rotamers), 44.15 and 43.24 (\underline{CH} , C3 rotamers), 33.25 and 32.39 (\underline{CH}_2 , C4 rotamers); m/z (EI⁺) 205 ([M]⁺, 64), 190 ([M-Me]⁺, 41), 117 (37), 101 (100), 42 (68); found [M+H]⁺, 205.1103, C₁₂H₁₅NO₂ requires [M+H]⁺, 205.1103; Found: C, 70.2; H, 7.5; N, 7.1. Required: C, 70.2; H, 7.4; N, 6.8; Δ = 0.0 ppm.

3-Phenylpyrrolidine **201**²⁵⁷



To a colourless solution of **218** (43.8 mg, 0.216 mmol, 1.00 eq) and molecular sieves 4Å in anhydrous DCM (4.00 ml), under N₂, was added iodotrimethylsilane (0.040 ml, 0.281 mmol, 1.30 eq). The reaction mixture turned yellow, it was stirred at RT for 16 hr. The reaction mixture was quenched with methanol (4.00 ml), filtered and concentrated *in vacuo*. Purification of the crude by flash column chromatography on silica gel (DCM, DCM/solvent B 9:1, 1:1, 0:1) to yield 27.0 mg (99%) of the product as a yellow powder: mp 83.5-85.0 °C (EtOAc); R_f 0.25 [Solvent B]; ν_{\max} (DCM film)/cm⁻¹ 3441, 3030-2850, 1548, 1068, 742; δ_{H} (CDCl₃/MeOD 2:1) 7.34-7.20 (5H, m, 2xH3', H4', 2xH2''), 3.73-3.66 (1H, dd, *J* 11.0, *J* 8.0, H2), 3.61-3.51 (2H, m, H3, H5), 3.44-3.35 (1H, m, 1xH5), 3.25-3.17 (1H, t, *J* 11.0, H2), 2.50-2.41 (1H, m, 1xH4), 2.20-2.08 (1H, m, 1xH4); δ_{C} (CDCl₃/MeOD 2:1) 138.49 (C, C1'), 129.34, 128.01, 127.54 (3xCH aromatic, C3'', C2'', C4''), 51.18 (CH₂, C2), 46.01 (CH₂, C5), 43.76 (CH, C3), 32.54 (CH₂, C4); m/z (EI⁺) 147 ([M]⁺, 20), 84 (66), 49 (74), 43 (100); found [M+H]⁺, 147.1043, C₁₀H₁₃N requires [M+H]⁺, 147.1048; Δ = -3.3 ppm.

(*Z*)-Ethyl 3-(4-bromophenyl)-2-ethoxyacrylate **202** and (*E*)-ethyl 3-(4-bromophenyl)-2-ethoxyacrylate **203**

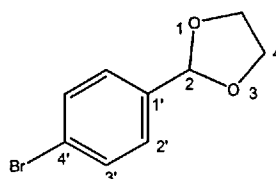


To a milky suspension of sodium hydride, 60% in oil (508.1 mg, 12.7 mmol, 2.20 eq) and molecular sieves 4Å in anhydrous THF (60.0 ml) at 0 °C, under a constant flow of N₂, was added dropwise, *via* syringe pump, phosphonoacetate **129** (2.79 g, 10.4 mmol, 1.80 eq) in THF (5.00 ml) over 54 min. The suspension turned pale yellow. It was stirred at 0 °C for 57 min before the dropwise addition of 4-bromobenzaldehyde (1.07 g, 5.78 mmol, 1.00 eq) in dry THF (5.00 ml) *via* syringe pump over 64 min. The solution which had turned yellow was left to stir in the ice bath over 39 hr. The dark yellowish orange solution was concentrated *in vacuo*, re-dissolved in EtOAc (60.0 ml) and washed with water (2x50.0 ml). An emulsion was observed, thus some NaCl was added. The aqueous phase was extracted with EtOAc (4x100 ml) and DCM (2x100 ml). After drying the organic extracts over MgSO₄, concentration *in vacuo* of the organic phase gave a yellow oil which was purified by flash column chromatography on silica gel (hexane/EtOAc 40:1, 30:1) to yield 1.34 g (78%) of the product. Ratio Z:E = 66:34.

Z isomer **202**: white amorphous solid: mp 31.0-32.0 °C (hexane/EtOAc); R_f 0.25 [hexane/ether 15:1]; ν_{\max} (nujol)/ cm^{-1} 3020-2850, 1726, 1645, 1548, 1045, 662; δ_H (CDCl_3) 7.67-7.64 (2H, m, 2xH2), 7.51-7.48 (2H, m, 2xH3), 6.90 (1H, s, H1'), 4.34-4.29 (2H, q, J 14.0, J 7.0, 2xH3'), 4.05-4.00 (2H, q, J 14.0, J 7.0, 2xH6'), 1.40-1.34 (6H, m, H4', H7'); δ_C (CDCl_3) 164.38 (\underline{C} , C1), 145.23 (\underline{C} , C2), 132.62 (\underline{C} , C4), 131.65 (2x \underline{CH}), 131.45 (2x \underline{CH}), 122.73 (\underline{C} , C7), 122.32 (\underline{CH} , C3), 67.75 (\underline{CH}_2 , C1'), 61.27 (\underline{CH}_2 , C1''), 15.54 (\underline{CH}_3), 14.27 (\underline{CH}_3); m/z (EI^+) 298 ($[\text{M}]^+$, 41), 196 ($[\text{M-ethoxy propanoic acid side chain}]^+$, 100), 89 (56); found $[\text{M+H}]^+$, 298.0207, $\text{C}_{13}\text{H}_{15}\text{O}_3\text{Br}$ requires $[\text{M+H}]^+$, 298.0205; Found: C, 52.1; H, 5.0. Required: C, 52.2; H, 5.1; Δ = 0.7 ppm.

E isomer **203**: colourless oil R_f 0.15 [hexane/ether 15:1]; ν_{\max} (film)/ cm^{-1} 2983, 1731, 1641, 1548, 1161, 662; δ_H (CDCl_3) 7.42-7.39 (2H, m, 2xH2), 7.08-7.06 (2H, m, 2xH3), 6.00 (1H, s, H1'), 4.18-4.13 (2H, q, J 14.5, J 7.0, 2xH3'), 3.96-3.91 (2H, q, J 14.0, J 7.0, 2xH6'), 1.45-1.41 (3H, t, J 7.0, H6'), 1.16-1.12 (3H, t, J 7.0, H3'); δ_C (CDCl_3) 164.25 (\underline{C} , C1'), 148.02 (\underline{C} , C2'), 134.06 (\underline{C} , C4), 131.13 (2x \underline{CH}), 130.05 (2x \underline{CH}), 120.61 (\underline{C} , C7), 107.83 (\underline{CH} , C3), 64.59 (\underline{CH}_2 , C1'), 61.41 (\underline{CH}_2 , C1''), 14.39 (\underline{CH}_3 , C2'), 13.69 (\underline{CH}_3 , C2''); m/z (EI^+) 298 ($[\text{M}]^+$, 38), 196 ($[\text{M-ethoxy propanoic acid side chain}]^+$, 100), 89 (60); found $[\text{M+H}]^+$, 298.0209, $\text{C}_{13}\text{H}_{15}\text{O}_3\text{Br}$ requires $[\text{M+H}]^+$, 298.0205; Found: C, 52.1; H, 5.0. Required: C, 52.2; H, 5.1; Δ = 0.9 ppm.

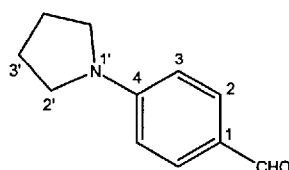
2-(4-Bromophenyl)-1,3-dioxolane **220**²⁶⁵



Ethylene glycol (0.450 ml, 8.07 mmol, 1.99 eq) and *para*-toluenesulfonic acid (36.3 mg, 0.191 mmol, 0.05 eq) were dissolved in dry toluene (7.50 ml) under N_2 in a Dean Stark apparatus. The mixture was vigorously stirred under reflux at 114 °C for 17 hr to remove the water from the ethylene glycol. It was allowed to cool down, 4-bromobenzaldehyde (749 mg, 4.05 mmol, 1.00 eq) dissolved in toluene (3.50 ml) was added and the mixture was refluxed at 116 °C for another 17.5 hr. The cooled reaction mixture was quenched with sat. NaHCO_3 and the product extracted with EtOAc (4x25.0 ml). The combined organic layers were washed with brine. After drying the organic extracts over MgSO_4 , concentration *in vacuo* of the organic phase gave a pale yellow oil which was purified by flash column chromatography on silica

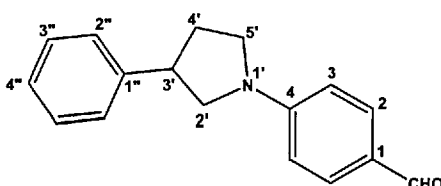
gel (hexane/ether 20:1, 15:1, 10:1) to yield 106 mg (14%) of the SM and 537 mg (57%) of the product as a pale yellow solid: mp 33.0-35.0 °C [lit.,²⁶⁵ 37-38 °C]; R_f 0.30 [Petroleum ether/ether 9:1]; ν_{\max} (nujol)/ cm^{-1} 2950-2850, 1646, 1078, 809, 662; δ_H (CDCl_3) 7.56-7.50 (2H, d, J 8.5, 2xH2'), 7.40-7.34 (2H, d, J 8.5, 2xH3'), 5.78 (1H, s, H2), 4.16-3.98 (4H, m, 2xH3, 2xH4); δ_C (CDCl_3) 136.99 (\underline{C} , C1'), 131.40 (2x \underline{CH}), 128.11 (2x \underline{CH}), 123.12 (\underline{C} , C4'), 102.93 (\underline{CH} , C2), 65.22 (\underline{CH}_2 , 2xC4); m/z (EI^+) 229 ($[\text{M} (^{81}\text{Br})]^+$, 100), 227 ($[\text{M} (^{79}\text{Br})]^+$, 97), 183 ($[\text{M-acetal}]^+$, 37), 149 ($[\text{M-bromo}]^+$, 41), 84 (56), 49 (65); found $[\text{M}+\text{H}]^+$, 227.9776, $\text{C}_9\text{H}_9\text{O}_2\text{Br}$ requires $[\text{M}+\text{H}]^+$, 227.9786; Found: C, 47.2; H, 4.0. Required: C, 47.2; H, 4.0; $\Delta = -4.4$ ppm.

4-(Pyrrolidin-1-yl)benzaldehyde **221**¹¹¹



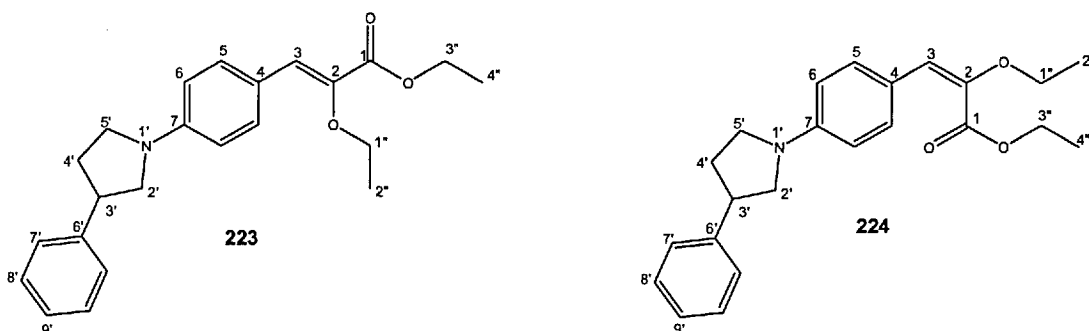
To a stirred solution of pyrrolidine (0.031 ml, 0.369 mmol, 1.20 eq) and acetal **220** (70.5 mg, 0.308 mmol, 1.00 eq) in anhydrous toluene (3.10 ml), under N_2 , were added $\text{Pd}_2(\text{dba})_3$ (6.0 mg, 0.007 mmol, 0.02 eq), (\pm)-BINAP (8.5 mg, 0.014 mmol, 0.04 eq) and sodium *tert*-butoxide (41.4 mg, 0.431 mmol, 1.40 eq) and the brown reaction mixture was stirred at 71 °C for 15.5 hr. It was allowed to cool down, diluted with ether, filtered over celite and the celite washed with ether. Concentration *in vacuo* yielded a bright yellowish orange oil which was purified by flash column chromatography on silica gel (hexane/ether 9:1, 8:2, 6:4) to yield 35.0 mg (65%) of the product as a white crystalline solid: R_f 0.20 [hexane/ether 6:4]; ν_{\max} (DCM film)/ cm^{-1} 3000-2900, 1658, 1610, 1533, 1157, 813; δ_H (CDCl_3) 9.72 (1H, s, $\underline{\text{CHO}}$), 7.45-7.71 (2H, dd, J 9.0, J 2.0, 2xH2), 6.59-6.56 (2H, d, J 9.0, 2xH3), 3.41-3.38 (4H, m, 4xH2'), 2.07-2.04 (4H, m, 4xH3'); δ_C (CDCl_3) 190.18 ($\underline{\text{CHO}}$), 151.95 (\underline{C} , C4), 132.12 (\underline{CH} , 2xC2), 124.84 (\underline{C} , C1), 111.17 (\underline{CH} , 2xC3), 47.62 (\underline{CH}_2 , 2xC2'), 25.39 (\underline{CH}_2 , 2xC3'); m/z (EI^+) 175 ($[\text{M}]^+$, 87), 174 (100), 119 (43), 84 (57), 49 (68); found $[\text{M}+\text{H}]^+$, 175.0989, $\text{C}_{11}\text{H}_{13}\text{NO}$ requires $[\text{M}+\text{H}]^+$, 175.0997; $\Delta = -4.6$ ppm.

4-(3-Phenylpyrrolidin-1-yl)benzaldehyde **222**



To a stirred solution of pyrrolidine **201** (63.7 mg, 0.433 mmol, 1.18 eq) and acetal **220** (83.7 mg, 0.365 mmol, 1.00 eq) in anhydrous toluene (3.60 ml), under N₂, were added Pd₂(dba)₃ (7.2 mg, 0.008 mmol, 0.02 eq), (±)-BINAP (9.5 mg, 0.015 mmol, 0.04 eq) and sodium *tert*-butoxide (50.0 mg, 0.520 mmol, 1.42 eq) and the brown reaction mixture was stirred at 71 °C for 15 hr. Some more acetal **220** (16.2 mg, 0.071 mmol, 0.19 eq), Pd₂(dba)₃ (6.5 mg, 0.007 mmol, 0.02 eq), (±)-BINAP (12.0 mg, 0.019 mmol, 0.05 eq) and sodium *tert*-butoxide (99.5 mg, 1.03 mmol, 2.83 eq) were added and the reaction was stirred at 71 °C for another 16 hr. It was allowed to cool down, diluted with ether, filtered over celite and the celite washed with ether. Concentration *in vacuo* yielded a dark orange oil which was purified by flash column chromatography on silica gel (hexane/ether 10:1, 8:2; 1:1) to yield 26.7 mg (25%) of the product as a bright yellow oil: R_f 0.25 [hexane/ether 8:2]; ν_{max} (DCM film)/cm⁻¹ 3020, 1691, 1646, 1265, 738; δ_H (CDCl₃) 9.76 (1H, s, CHO), 7.80-7.75 (2H, d, *J* 9.0, H2), 7.39-7.35 (2H, m, H3''), 7.30-7.28 (3H, m, H2'', H4''), 6.63-6.61 (2H, d, *J* 9.0, H3), 3.87-3.82 (1H, dd, *J* 7.5, *J* 2.0, H2'), 3.67-3.61 (1H, m, H5'), 3.59-3.52 (2H, m, H5', H3'), 3.48-3.44 (1H, m, H2'), 2.52-2.45 (1H, m, H4'), 2.25-2.16 (1H, m, H4'); δ_C (CDCl₃) 190.27 (CHO), 151.69 (C, C4), 141.42 (C, C1''), 132.19 (CH, 2xC2), 128.75 (CH, 2xC3''), 127.01 (CH, 2xC2'', C4''), 125.23 (C, C1), 111.20 (CH, 2xC3), 54.28 (CH₂, C2'), 47.66 (CH₂, C5'), 43.94 (CH, C3'), 32.94 (CH₂, C4'); m/z (EI⁺) 251 ([M]⁺, 100), 147 ([M-benzaldehyde]⁺, 71), 119 (85), 91 (47); found [M+H]⁺, 251.1303, C₁₇H₁₇NO requires [M+H]⁺, 251.1310; Δ = -2.8 ppm.

(*Z*)-ethyl 2-ethoxy-3-(4-(3-phenylpyrrolidin-1-yl)phenyl)acrylate **223** and (*E*)-ethyl 2-ethoxy-3-(4-(3-phenylpyrrolidin-1-yl)phenyl)acrylate **224**

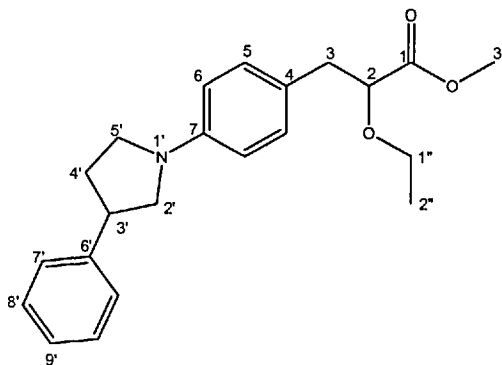


To a milky suspension of sodium hydride, 60% in oil (10.6 mg, 0.265 mmol, 2.47 eq) and molecular sieves 4Å in anhydrous THF (0.400 ml) at 0 °C, under a constant flow of N₂, was added dropwise, *via* syringe pump, phosphonoacetate **129** (56.5 mg, 0.211 mmol, 1.96 eq) in THF (0.500 ml) over 7 min. The suspension was stirred at

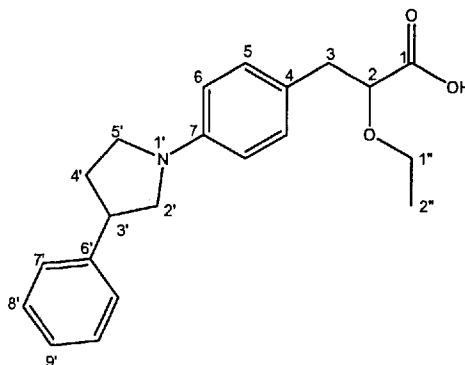
0 °C for 1 hr before the dropwise addition of aldehyde **222** (27.0 mg, 0.107 mmol, 1.00 eq) in dry THF (0.900 ml) *via* syringe pump over 31 min. The solution which had turned bright yellowish orange was left stirring in the ice bath over 45 hr. The RM was concentrated *in vacuo*, next re-dissolved in EtOAc (25.0 ml) and washed with water (25.0 ml). An emulsion was observed, thus some NaCl was added. The aqueous phase was extracted with EtOAc (4x25.0 ml). After drying the organic extracts over MgSO₄, concentration *in vacuo* of the organic phase gave a yellow oil which was purified by flash column chromatography on silica gel (hexane/ether 12:1, 10:1) to yield 36.0 mg (92%) of the product. Ratio Z:E = 63:37.

Z isomer: very pale yellow oil R_f 0.25 [hexane/ether 8:2]; ν_{\max} (DCM film)/cm⁻¹ 1747, 1706, 1604, 1178, 738; δ_{H} (CDCl₃) 7.76-7.72 (2H, d, *J* 8.8, 2xH₅), 7.38-7.33 (2H, m, 2xH₈'), 7.30-7.24 (3H, m, 2xH₇', H₉'), 7.00 (1H, s, H₃), 6.60-6.56 (2H, d, *J* 9.0, 2xH₆), 4.32-4.26 (2H, q, *J* 14.5, *J* 7.0, 2xH₃"'), 4.01-3.95 (2H, q, *J* 14.0, *J* 7.0, 2xH₁"'), 3.81-3.76 (1H, dd, *J* 7.5, *J* 1.5, 1xH₂''), 3.61-3.38 (4H, m, 2xH₅', H₃', 1xH₂''), 2.49-2.41 (1H, m, 1xH₄'), 2.21-2.12 (1H, m, 1xH₄'), 1.41-1.35 (6H, m, 3xH₄"', 3xH₂"'); δ_{C} (CDCl₃) 165.37 (C, C₁), 147.82 (C, C₇), 142.14, 141.09 (2xC), 131.90 (2xC₆), 128.64 (2xCH), 127.06 (2xCH), 126.77 (CH), 125.62 (CH, C₃), 121.25 (C, C₄), 111.35 (2xCH, 2xC₇), 67.26 (CH₂, C₁"'), 60.68 (CH₂, C₃"'), 54.21 (CH₂, C₂''), 47.46 (CH₂, C₅'), 44.02 (CH, C₃'), 33.12 (CH₂, C₄), 15.55 (CH₃), 14.38 (CH₃); *m/z* (ESI⁺) 366 ([M+H]⁺, 100); found [M+H]⁺, 366.2069, C₂₃H₂₈NO₃ requires [M+H]⁺, 366.2069; Found: C, 75.6; H, 7.4; N, 3.8. Required: C, 75.6; H, 7.5; N, 3.7; Δ = 0.0 ppm.

E isomer: pale yellow oil R_f 0.20 [hexane/ether 8:2]; ν_{\max} (DCM film)/cm⁻¹ 1743, 1706, 1531, 1265, 1053, 740; δ_{H} (CDCl₃) 7.38-7.32 (2H, m, 2xH₈'), 7.30-7.24 (3H, m, 2xH₇', H₉'), 7.20-7.16 (2H, d, *J* 8.5, 2xH₅), 6.54-6.50 (2H, d, *J* 8.5, 2xH₆), 6.17 (1H, s, H₃), 4.26-4.21 (2H, q, *J* 14.5, *J* 7.0, 2xH₃"'), 3.95-3.90 (2H, q, *J* 14.0, *J* 7.0, 2xH₁"'), 3.76-3.72 (1H, dd, *J* 7.5, *J* 1.0, 1xH₂''), 3.61-3.36 (4H, m, 2xH₅', H₃', 1xH₂''), 2.49-2.40 (1H, m, 1xH₄'), 2.21-2.10 (1H, m, 1xH₄'), 1.42-1.38 (3H, t, *J* 7.0, 3xH₂"'), 1.25-1.21 (3H, t, *J* 7.0, 3xH₄"'); δ_{C} (CDCl₃) 165.11 (C, C₁), 146.68 (C, C₇), 144.52, 142.49 (2xC), 129.85 (2xCH, 2xC₅), 128.58 (2xCH), 127.05 (2xCH), 126.66 (CH), 125.61 (CH), 121.57 (C, C₄), 113.07 (CH, C₃), 111.11 (2xCH, 2xC₆), 64.94 (CH₂, C₁"'), 60.99 (CH₂, C₃"'), 54.40 (CH₂, C₂''), 47.54 (CH₂, C₅'), 44.06 (CH, C₃'), 33.18 (CH₂, C₄), 14.63 (CH₃), 13.96 (CH₃); *m/z* (ESI⁺) 366 ([M+H]⁺, 100); found [M+H]⁺, 366.2063, C₂₃H₂₈NO₃ requires [M+H]⁺, 366.2069; Found: C, 75.6; H, 7.4; N, 3.8. Required: C, 75.6; H, 7.5; N, 3.7; Δ = -1.6 ppm.

Methyl 2-ethoxy-3-(4-(3-phenylpyrrolidin-1-yl)phenyl)propanoate 225

To a mixture of the starting materials **223** and **224** (30.0 mg, 0.082 mmol, 1.00 eq) and the magnesium turnings (52.0 mg, 2.14 mmol, 26.1 eq) at RT, under a constant flow of N₂, was added the anhydrous methanol (1.50 ml). The colourless solution turned into a milky white suspension, it was stirred for 20 hr before being poured onto water (20.0 ml) and 1M HCl (0.500 ml). The 2 phases were separated and the aqueous phase was extracted with DCM (4x25.0 ml). After drying over MgSO₄, concentration *in vacuo* gave a colourless oil which was purified by flash column chromatography on silica gel (hexane/ether 10:1, 9:1) to yield 20.0 mg (68%) of the product as a colourless oil: R_f 0.45 [hexane/ether 1:1]; ν_{max} (DCM film)/cm⁻¹ 1743, 1620, 1523, 1369, 1117, 737; δ_H (CDCl₃) 7.37-7.24 (5H, m, 2xH8', H9', 2xH7'), 7.14-7.12 (2H, d, *J* 8.5, 2xH6), 6.55-6.53 (2H, d, *J* 8.5, 2xH5), 4.03-3.99 (1H, t, *J* 6.5, H2), 3.75-3.70 (1H, m, 1xH2'), 3.73 (3H, s, 3xH3''), 3.65-3.58 (1H, m, 1xH1''), 3.57-3.43 (3H, m, 2xH5', 1xH3'), 3.41-3.34 (2H, m, 1xH1'', 1xH2''), 2.95-2.94 (2H, d, *J* 6.5, 2xH3), 2.46-2.39 (1H, m, 1xH4'), 2.19-2.09 (1H, m, 1xH4''), 1.22-1.18 (3H, t, *J* 7.0, 3xH2''); δ_C (CDCl₃) 173.22 (C, C1), 146.40 (C, C7), 142.68 (C), 130.11 (2xCH, 2xC6), 128.56 (2xCH), 127.12 (2xCH), 126.61 (CH), 123.95 (C), 111.47 (2xCH, 2xC5), 80.79 (CH, C2), 66.18 (CH₂, C1''), 54.58 (CH₂, C2'), 51.75 (CH₃, C3''), 47.69 (CH₂, C5'), 44.11 (CH, C3'), 38.52 (CH₂, C3), 33.24 (CH₂, C4'), 15.09 (CH₃, C2''); m/z (ESI⁺) 354 ([M+H]⁺, 100); found [M+H]⁺, 354.2071, C₂₂H₂₈NO₃ requires [M+H]⁺, 354.2069; Δ = -0.6 ppm.

2-Ethoxy-3-(4-(3-phenylpyrrolidin-1-yl)phenyl)propanoic acid 44

The starting material **225** (14.6 mg, 0.041 mmol, 1.00 eq) was refluxed with potassium hydroxide pellets (13.0 mg, 0.232 mmol, 5.66 eq) in a mixture of ethanol/water 1:1 (1.00 ml) at 81 °C for 8 hr. The clear colourless solution was allowed to cool down to RT, then concentrated *in vacuo*. With vigorous stirring in ice, was added dropwise, 1M HCl (~8 drops) until a pH of 1 was reached. The desired acid crashed out as a white ppt. DCM was added and the 2 phases were separated. The aqueous phase was extracted with DCM (4x25 ml). After drying over MgSO₄, concentration *in vacuo* gave 12.3 mg (88%) of the product as a colourless oil: R_f 0.50 [solvent B]; ν_{max} (DCM film)/cm⁻¹ 2921, 1730, 1647, 1517, 1115, 743; δ_H (CDCl₃) 7.36-7.24 (5H, m, 2xH8', H9', 2xH7'), 7.15-7.13 (2H, d, J 8.5, 2xH6), 6.56-6.54 (2H, d, J 8.0, 2xH5), 4.08-4.05 (1H, dd, J 7.5, J 4.0, H2), 3.74-3.70 (1H, t, J 8.0, 1xH2'), 3.65-3.41 (5H, m, 2xH1'', 2xH5', 1xH3'), 3.38-3.34 (1H, t, 1xH2''), 3.09-3.05 (1H, dd, J 14.0, J 4.0, 1xH3), 2.97-2.92 (1H, dd, J 14.0, J 7.5, 1xH3), 2.46-2.39 (1H, m, 1xH4'), 2.20-2.09 (1H, m, 1xH4'), 1.23-1.20 (3H, t, J 7.0, 3xH2''); δ_C (CDCl₃) 174.62 (C, C1), 146.50 (C, C7), 142.58 (C), 130.31 (2xCH, 2xC6), 128.59 (2xCH), 127.13 (2xCH), 126.66 (CH), 123.95 (C), 111.60 (2xCH, 2xC5), 80.11 (CH, C2), 66.83 (CH₂, C1''), 54.69 (CH₂, C2'), 47.77 (CH₂, C5'), 44.12 (CH, C3'), 37.72 (CH₂, C3), 33.23 (CH₂, C4'), 15.11 (CH₃, C2''); m/z (ESI⁺) 340 ([M+H]⁺, 100); found [M+H]⁺, 340.1917, C₂₁H₂₆NO₃ requires [M+H]⁺, 340.1913; Found: C, 74.2; H, 7.6; N, 4.1. Required: C, 74.3; H, 7.4; N, 4.1; Δ = 1.2 ppm.

6.3 Biological methods**6.3.1 Preparation of the samples for the PPAR activation assay**

Lipids: 25 mM solutions of lyso TTA-PC **34** and TTA-PG **36** were prepared in 0.1 M NaOH by heating to ca. 80 °C until complete dissolution, next they were slowly added

to pre-heated Foetal Bovine serum (Gibco Invitrogen, catalog no 10106169) at 37 °C. The final concentration of the lipids in serum was 0.74 mM. The solution of the lipids in serum was added to serum-free medium to the desired concentrations (1 to 75 μ M), and pure serum was added to get a total of 10% serum (v/v) in the medium. *Indoles*: The indole leads **38** to **43** were dissolved in DMSO, 0.1% (v/v). DMSO concentration was kept constant in all samples.

6.3.2 Transfection procedure

Human MCF-7 breast cancer cells were seeded at a density of 85,000 cells per well of a 12-well plate. The following day, they were transiently transfected by the SuperFect transfection procedure according to the manufacturer's protocol (Qiagen), using 0.9 μ g PPREx3-LUC reporter plasmid and 0.15 μ g of the plasmid vector, pcDNA3.1 humanPPAR $\alpha/\gamma/\delta$. The total amount of plasmid was kept constant at 2.65 μ g by compensating with promoterCMV-5. 24 hours after transfection, the cells were treated with the compounds to be tested or the PPAR specific agonists. 48 hours after transfection, the cells were washed once with PBS, lysed in 80 μ L lysis buffer containing 25 mM TAE, 2 mM DTT, 10% (v/v) Glycerol, 1% (v/v) Triton X-100 and de-ionised water. 35 μ L of the cell extracts were used for luciferase determination on a LUCY-1 luminometer (Anthos, Austria). The luciferase assay was performed in accordance with the protocol of the Luciferase Assay Kit (BIO Thema AB, Sweden).

CHAPTER 7

References

- (1) Berger, J.; Moller, D. E. *Annual Review of Medicine* **2002**, *53*, 409-435.
- (2) Hihi, A. K.; Michalik, L.; Wahli, W. *Cellular and Molecular Life Sciences* **2002**, *59*, 790-798.
- (3) Ahmed, W.; Ziouzenkova, O.; Brown, J.; Devchand, P.; Francis, S.; Kadakia, M.; Kanda, T.; Orasanu, G.; Sharlach, M.; Zandbergen, F.; Plutzky, J. *Journal of Internal Medicine* **2007**, *262*, 184-198.
- (4) Laudet, V.; Hanni, C.; Coll, J.; Catzeflis, F.; Stehelin, D. *Embo Journal* **1992**, *11*, 1003-1013.
- (5) Mangelsdorf, D. J.; Evans, R. M. *Cell* **1995**, *83*, 841-850.
- (6) Issemann, I.; Green, S. *Nature* **1990**, *347*, 645-650.
- (7) Everett, L.; Galli, A.; Crabb, D. *Liver* **2000**, *20*, 191-199.
- (8) Desvergne, B.; Wahli, W. *Endocrine Reviews* **1999**, *20*, 649-688.
- (9) Willson, T. M.; Brown, P. J.; Sternbach, D. D.; Henke, B. R. *Journal of Medicinal Chemistry* **2000**, *43*, 527-550.
- (10) Plutzky, J. *American Journal of Cardiology* **2003**, *92*, 34J-41J.
- (11) Delerive, P.; Fruchart, J. C.; Staels, B. *Journal of Endocrinology* **2001**, *169*, 453-459.
- (12) Samid, D.; Wells, M.; Greene, M. E.; Shen, W. Y.; Palmer, C. N. A.; Thibault, A. *Clinical Cancer Research* **2000**, *6*, 933-941.
- (13) Wahli, W. *Swiss Medical Weekly* **2002**, *132*, 83-91.
- (14) Feinstein, D. L. *Diabetes Technology & Therapeutics* **2003**, *5*, 67-73.
- (15) Berger, J.; Wagner, J. A. *Diabetes Technology & Therapeutics* **2002**, *4*, 163-174.
- (16) Henke, B. R. *Journal of Medicinal Chemistry* **2004**, *47*, 4118-4127.
- (17) Nolte, R. T.; Wisely, G. B.; Westin, S.; Cobb, J. E.; Lambert, M. H.; Kurokawa, R.; Rosenfeld, M. G.; Willson, T. M.; Glass, C. K.; Milburn, M. V. *Nature* **1998**, *395*, 137-143.
- (18) Xu, H. E.; Lambert, M. H.; Montana, V. G.; Parks, D. J.; Blanchard, S. G.; Brown, P. J.; Sternbach, D. D.; Lehmann, J. M.; Wisely, G. B.; Willson, T. M.; Kliewer, S. A.; Milburn, M. V. *Molecular Cell* **1999**, *3*, 397-403.
- (19) Xu, H. E.; Lambert, M. H.; Montana, V. G.; Plunket, K. D.; Moore, L. B.; Collins, J. L.; Oplinger, J. A.; Kliewer, S. A.; Gampe, R. T., Jr.; McKee, D. D.; Moore, J. T.; Willson, T. M. *Proceedings of the National Academy of Sciences* **2001**, *98*, 13919-13924.
- (20) Kliewer, S. A.; Forman, B. M.; Blumberg, B.; Ong, E. S.; Borgmeyer, U.; Mangelsdorf, D. J.; Umesono, K.; Evans, R. M. *Proceedings of the National Academy of Sciences of the United States of America* **1994**, *91*, 7355-7359.

- (21) Oberfield, J. L.; Collins, J. L.; Holmes, C. P.; Goreham, D. M.; Cooper, J. P.; Cobb, J. E.; Lenhard, J. M.; Hull-Ryde, E. A.; Mohr, C. P.; Blanchard, S. G.; Parks, D. J.; Moore, L. B.; Lehmann, J. M.; Plunket, K.; Miller, A. B.; Milburn, M. V.; Kliewer, S. A.; Willson, T. M. *Proceedings of the National Academy of Sciences of the United States of America* **1999**, *96*, 6102-6106.
- (22) Lemberger, T.; Desvergne, B.; Wahli, W. *Annual Review of Cell and Developmental Biology* **1996**, *12*, 335-&.
- (23) Tontonoz, P.; Hu, E.; Graves, R. A.; Budavari, A. I.; Spiegelman, B. M. *Genes & Development* **1994**, *8*, 1224-1234.
- (24) Tontonoz, P.; Hu, E. D.; Devine, J.; Beale, E. G.; Spiegelman, B. M. *Molecular and Cellular Biology* **1995**, *15*, 351-357.
- (25) Schoonjans, K.; PeinadoOnsurbe, J.; Lefebvre, A. M.; Heyman, R. A.; Briggs, M.; Deeb, S.; Staels, B.; Auwerx, J. *Embo Journal* **1996**, *15*, 5336-5348.
- (26) Schoonjans, K.; Staels, B.; Deeb, S.; Auwerx, J. *Circulation* **1995**, *92*, 2362-2362.
- (27) Kliewer, S. A.; Umesono, K.; Noonan, D. J.; Heyman, R. A.; Evans, R. M. *Nature* **1992**, *358*, 771-774.
- (28) Berger, J.; Bailey, P.; Biswas, C.; Cullinan, C. A.; Doebber, T. W.; Hayes, N. S.; Saperstein, R.; Smith, R. G.; Leibowitz, M. D. *Endocrinology* **1996**, *137*, 4189-4195.
- (29) Dowell, P.; Peterson, V. J.; Zabriskie, T. M.; Leid, M. *Journal of Biological Chemistry* **1997**, *272*, 2013-2020.
- (30) Xu, L.; Glass, C. K.; Rosenfeld, M. G. *Current Opinion in Genetics & Development* **1999**, *9*, 140-147.
- (31) Yin, Y. Z.; Yuan, H. Y.; Wang, C. G.; Pattabiraman, N.; Rao, M.; Pestell, R. G.; Glazer, R. I. *Molecular Endocrinology* **2006**, *20*, 268-278.
- (32) Murphy, G. J.; Holder, J. C. *Trends in Pharmacological Sciences* **2000**, *21*, 469-474.
- (33) Schoonjans, K.; Staels, B.; Auwerx, J. *Biochimica Et Biophysica Acta-Lipids and Lipid Metabolism* **1996**, *1302*, 93-109.
- (34) Semple, R. K.; Chatterjee, V. K. K.; O'Rahilly, S. *Journal of Clinical Investigation* **2006**, *116*, 581-589.
- (35) Schoonjans, K.; Watanabe, M.; Suzuki, H.; Mahfoudi, A.; Krey, G.; Wahli, W.; Grimaldi, P.; Staels, B.; Yamamoto, T.; Auwerx, J. *Journal of Biological Chemistry* **1995**, *270*, 19269-19276.
- (36) Wahli, W.; Braissant, O.; Desvergne, B. *Chemistry & Biology* **1995**, *2*, 261-266.
- (37) Kersten, S.; Desvergne, B.; Wahli, W. *Nature* **2000**, *405*, 421-424.

- (38) Devchand, P. R.; Keller, H.; Peters, J. M.; Vazquez, M.; Gonzalez, F. J.; Wahli, W. *Nature* **1996**, *384*, 39-43.
- (39) Lee, H.; Shi, W. B.; Tontonoz, P.; Wang, S.; Subbanagounder, G.; Hedrick, C. C.; Hama, S.; Borromeo, C.; Evans, R. M.; Berliner, J. A.; Nagy, L. *Circulation Research* **2000**, *87*, 516-521.
- (40) Staels, B.; Koenig, W.; Habib, A.; Merval, R.; Lebret, M.; Torra, I. P.; Delerive, P.; Fadel, A.; Chinetti, G.; Fruchart, J. C.; Najib, J.; Maclouf, J.; Tedgui, A. *Nature* **1998**, *393*, 790-793.
- (41) Combs, C. K.; Karlo, J. C.; Kao, S. C.; Landreth, G. E. *Journal of Neuroscience* **2001**, *21*, 1179-1188.
- (42) Streit, W. J.; Mrak, R. M.; Griffin, W. S. T. *Journal of Neuroinflammation* **2004**, *1*, 1-4.
- (43) Dreyer, C.; Krey, G.; Keller, H.; Givel, F.; Helftenbein, G.; Wahli, W. *Cell* **1992**, *68*, 879-887.
- (44) Werman, A.; Hollenberg, A.; Solanes, G.; Bjorbaek, C.; VidalPuig, A. J.; Flier, J. S. *Journal of Biological Chemistry* **1997**, *272*, 20230-20235.
- (45) Rosen, E. D.; Spiegelman, B. M. *Journal of Biological Chemistry* **2001**, *276*, 37731-37734.
- (46) Rangwala, S. M.; Lazar, M. A. *Trends in Pharmacological Sciences* **2004**, *25*, 331-336.
- (47) Kirkpatrick, P. *Nature Reviews Drug Discovery* **2002**, *1*, 169-169.
- (48) Schwartz, M. W.; Kahn, S. E. *Nature* **1999**, *402*, 860-861.
- (49) Martin, G.; Schoonjans, K.; Lefebvre, A. M.; Staels, B.; Auwerx, J. *Journal of Biological Chemistry* **1997**, *272*, 28210-28217.
- (50) Jiang, C. Y.; Ting, A. T.; Seed, B. *Nature* **1998**, *391*, 82-86.
- (51) Ricote, M.; Li, A. C.; Willson, T. M.; Kelly, C. J.; Glass, C. K. *Nature* **1998**, *391*, 79-82.
- (52) Dehmer, T.; Heneka, M. T.; Sastre, M.; Dichgans, J.; Schulz, J. B. *Journal of Neurochemistry* **2004**, *88*, 494-501.
- (53) Harris, S. G.; Phipps, R. P. *Immunology* **2002**, *105*, 23-34.
- (54) Padilla, J.; Leung, E.; Phipps, R. P. *Clinical Immunology* **2002**, *103*, 22-33.
- (55) Landreth, G. E.; Heneka, M. T. *Neurobiology of Aging* **2001**, *22*, 937-944.
- (56) Mrak, R. E.; Landreth, G. E. *Journal of Neuroinflammation* **2004**, *1*, 1-3.
- (57) Gross, B. S.; Fruchart, J. C.; Staels, B. *Drug Discovery Today: Therapeutic Strategies* **2005**, *2*, 237-243.
- (58) Tall, A. R.; Wang, N. *Journal of Clinical Investigation* **2000**, *106*, 1205-1207.
- (59) Marais, A. D. *Current Opinion in Lipidology* **2000**, *11*, 597-602.

- (60) Oliver, W. R.; Shenk, J. L.; Snaith, M. R.; Russell, C. S.; Plunket, K. D.; Bodkin, N. L.; Lewis, M. C.; Winegar, D. A.; Sznajdman, M. L.; Lambert, M. H.; Xu, H. E.; Sternbach, D. D.; Kliewer, S. A.; Hansen, B. C.; Willson, T. M. *Proceedings of the National Academy of Sciences of the United States of America* **2001**, *98*, 5306-5311.
- (61) Chawla, A.; Lee, C. H.; Barak, Y.; He, W. M.; Rosenfeld, J.; Liao, D.; Han, J.; Kang, H.; Evans, R. M. *Proceedings of the National Academy of Sciences of the United States of America* **2003**, *100*, 1268-1273.
- (62) Lee, C. H.; Chawla, A.; Urbiztondo, N.; Liao, D.; Boisvert, W. A.; Evans, R. M. *Science* **2003**, *302*, 453-457.
- (63) Saluja, I.; Granneman, J. G.; Skoff, R. P. *Glia* **2001**, *33*, 191-204.
- (64) Peters, J. M.; Lee, S. S. T.; Li, W.; Ward, J. M.; Gavrilova, O.; Everett, C.; Reitman, M. L.; Hudson, L. D.; Gonzalez, F. J. *Molecular and Cellular Biology* **2000**, *20*, 5119-5128.
- (65) Granneman, J.; Skoff, R.; Yang, X. Y. *Journal of Neuroscience Research* **1998**, *51*, 563-573.
- (66) Basu-Modak, S.; Braissant, O.; Escher, P.; Desvergne, B.; Honegger, P.; Wahli, W. *Journal of Biological Chemistry* **1999**, *274*, 35881-35888.
- (67) Forman, B. M.; Chen, J.; Evans, R. M. *Proceedings of the National Academy of Sciences of the United States of America* **1997**, *94*, 4312-4317.
- (68) Staels, B.; Vudac, N.; Schoonjans, K.; Kosykh, V.; Dallongeville, J.; Fruchart, J. C.; Auwerx, J. *Circulation* **1995**, *92*, 1385-1385.
- (69) Krey, G.; Braissant, O.; L'Horset, F.; Kalkhoven, E.; Perroud, M.; Parker, M. G.; Wahli, W. *Mol Endocrinol* **1997**, *11*, 779-791.
- (70) Lehmann, J. M.; Moore, L. B.; Smitholiver, T. A.; Wilkison, W. O.; Willson, T. M.; Kliewer, S. A. *Journal of Biological Chemistry* **1995**, *270*, 12953-12956.
- (71) Lehmann, J. M.; Lenhard, J. M.; Oliver, B. B.; Ringold, G. M.; Kliewer, S. A. *J. Biol. Chem.* **1997**, *272*, 3406-3410.
- (72) Kliewer, S. A.; Lehmann, J. u. r. M.; Willson, T. M. *Science* **1999**, *284*, 757-760.
- (73) Berger, J.; Leibowitz, M. D.; Doebber, T. W.; Elbrecht, A.; Zhang, B.; Zhou, G. C.; Biswas, C.; Cullinan, C. A.; Hayes, N. S.; Li, Y.; Tanen, M.; Ventre, J.; Wu, M. S.; Berger, G. D.; Mosley, R.; Marquis, R.; Santini, C.; Sahoo, S. P.; Tolman, R. L.; Smith, R. G.; Moller, D. E. *Journal of Biological Chemistry* **1999**, *274*, 6718-6725.
- (74) Kitamura, Y.; Shimohama, S.; Koike, H.; Kakimura, J.; Matsuoka, Y.; Nomura, Y.; Gebicke-Haerter, P. J.; Taniguchi, T. *Biochemical and Biophysical Research Communications* **1999**, *254*, 582-586.
- (75) Kitamura, Y.; Kakimura, J.; Matsuoka, Y.; Nomura, Y.; Gebicke-Haerter, P. J.; Taniguchi, T. *Neuroscience Letters* **1999**, *262*, 129-132.

- (76) Rouhi, A. M. *Chemical & Engineering News* **2004**, *82*, 83-99.
- (77) Scott, C. L. *American Journal of Cardiology* **2003**, *92*, 351-421.
- (78) Wingard, D. L.; Barrettconnor, E.; Criqui, M. H.; Suarez, L. *American Journal of Epidemiology* **1983**, *117*, 19-26.
- (79) Reaven, G. M. *Diabetes* **1988**, *37*, 1595-1607.
- (80) Alberti, K. G.; Zimmet, P. Z. *Diabetic medicine* **1998**, *15*, 539-553.
- (81) Eckel, R. H. *Proceedings of the Nutrition Society* **2007**, *66*, 82-95.
- (82) Denke, M. A. *Current Opinion in Lipidology* **2001**, *12*, 625-628.
- (83) Stolar, M. W. *American Journal of Health-System Pharmacy* **2002**, *59*, S3-S8.
- (84) Isomaa, B.; Almgren, P.; Tuomi, T.; Forsen, B.; Lahti, K.; Nissen, M.; Taskinen, M. R.; Groop, L. *Diabetes Care* **2001**, *24*, 683-689.
- (85) Stern, M. P.; Williams, K.; Gonzalez-Villalpando, C.; Hunt, K. J.; Haffner, S. M. *Diabetes Care* **2004**, *27*, 2676-2681.
- (86) *Diabetes action now, International Diabetes Foundation 2004.*
- (87) Image <http://fixedreference.org/2006-Wikipedia-CD-Selection/wp/i/Insulin.htm>.
- (88) Image <http://static.howstuffworks.com/gif/diabetes-pancreas.gif>.
- (89) Image <http://www.endocrineweb.com/images/sugar.gif>.
- (90) Skyler, J. S. *Journal of Medicinal Chemistry* **2004**, *47*, 4113-4117.
- (91) DeFronzo, R. A. *Diabetologia* **1992**, *35*, 389-397.
- (92) Gerich, J. E. *Mayo Clinic Proceedings* **2003**, *78*, 447-456.
- (93) Kahn, S. E. *Diabetologia* **2003**, *46*, 3-19.
- (94) Zimmet, P.; Alberti, K.; Shaw, J. *Nature* **2001**, *414*, 782-787.
- (95) Rotella, D. P. *Journal of Medicinal Chemistry* **2004**, *47*, 4111-4112.
- (96) Moller, D. E. *Nature* **2001**, *414*, 821-827.
- (97) Bohannon, N. J. V. *American Journal of Health-System Pharmacy* **2002**, *59*, S9-S13.
- (98) Misbin, R. I. *Annals of Internal Medicine* **1977**, *87*, 591-595.
- (99) Nattress, M.; Alberti, K. *Diabetologia* **1978**, *14*, 71-74.
- (100) Rosand, J.; Friedberg, J. W.; Yang, J. M. *Ann Intern Med* **1997**, *127*, 170-.
- (101) Cantello, B. C. C.; Cawthorne, M. A.; Haigh, D.; Hindley, R. M.; Smith, S. A.; Thurlby, P. L. *Bioorganic & Medicinal Chemistry Letters* **1994**, *4*, 1181-1184.
- (102) Olefsky, J.; Antonucci, T.; Lockwood, D.; Norris, R. *US patent* **1995**, 5,478,852.
- (103) Antonucci, T.; Lockwood, D.; Norris, R. *US patent* **1997**, 5,602,133.
- (104) Raskin, P.; Rappaport, E. B.; Cole, S. T.; Yan, Y.; Patwardhan, R.; Freed, M. I. *Diabetologia* **2000**, *43*, 278-284.
- (105) Ahmed, I.; Furlong, K.; Flood, J.; P., T. V.; Goldstein, B. *American Journal of Therapeutics* **2007**, *14*, 49-62.

- (106) Miller, A. R. *Drug Development Research* **2006**, *67*, 574-578.
- (107) Home, P. D.; Pocock, S. J.; Beck-Nielsen, H.; Gomis, R.; Hanefeld, M.; Jones, N. P.; Komajda, M.; McMurray, J. J. V. *New England Journal of Medicine* **2007**, *357*, 28-38.
- (108) Psaty, B. M.; Furberg, C. D. *New England Journal of Medicine* **2007**, *357*, 940-940.
- (109) Granberry, M. C.; Hawkins, J. B.; Franks, A. M. *American Journal of Health-System Pharmacy* **2007**, *64*, 931-936.
- (110) Sarabu, R.; Tilley, J. *Recent Advances in Therapeutic Approaches to Type 2 Diabetes*; 2004 Elsevier Inc., 2004; Vol. 39.
- (111) Magdolen, P.; Meciarova, M.; Toma, S. *Tetrahedron* **2001**, *57*, 4781-4785.
- (112) Knudsen, L. B. *Journal of Medicinal Chemistry* **2004**, *47*, 4128-4134.
- (113) Dalton, L. W. *Chemical & Engineering News* **2004**, *82*, 59-67.
- (114) Weber, A. E. *Journal of Medicinal Chemistry* **2004**, *47*, 4135-4141.
- (115) Haines, S. T. *Diabetes Educator* **2007**, *33*, 105S-110S.
- (116) Alberts, P.; Nilsson, C.; Selen, G.; Engblom, L. O. M.; Edling, N. H. M.; Norling, S.; Klingstrom, G.; Larsson, C.; Forsgren, M.; Ashkzari, M.; Nilsson, C. E.; Fiedler, M.; Bergqvist, E.; Ohman, B.; Bjorkstrand, E.; Abrahmsen, L. B. *Endocrinology* **2003**, *144*, 4755-4762.
- (117) Stulnig, T. M.; Waldhausl, W. *Diabetologia* **2004**, *47*, 1-11.
- (118) Edelman, S. V.; Darsow, T.; Frias, J. P. *International Journal of Clinical Practice* **2006**, *60*, 1647-1653.
- (119) Van Huijsduijnen, R. H.; Sauer, W. H. B.; Bombrun, A.; Swinnen, D. *Journal of Medicinal Chemistry* **2004**, *47*, 4142-4146.
- (120) Gilde, A. J.; Fruchart, J. C.; Staels, B. *Journal of the American College of Cardiology* **2006**, *48*, A24-A32.
- (121) Gervois, P.; Fruchart, J. C.; Staels, B. *International Journal of Clinical Practice* **2004**, *58*, 22-29.
- (122) Selkoe, D. J. *Nature* **1999**, *399*, A23-A31.
- (123) Image <http://www.ahaf.org/alzdis/about/AmyloidPlaques.htm>.
- (124) Image <http://www.ahaf.org/alzdis/about/BrainAlzheimer.htm>.
- (125) Vanduijn, C. M.; Hofman, A. *Neuroepidemiology* **1992**, *11*, 106-113.
- (126) Hebert, L. E.; Scherr, P. A.; Beckett, L. A.; Albert, M. S.; Pilgrim, D. M.; Chown, M. J.; Funkenstein, H. H.; Evans, D. A. *Jama-Journal of the American Medical Association* **1995**, *273*, 1354-1359.
- (127) McQualter, J. L.; Bernard, C. C. A. *Journal of Neurochemistry* **2007**, *100*, 295-306.
- (128) Image http://apu.sfn.org/images/brainbriefings/ms_illus_large.gif.

- (129) Keegan, B. M.; Noseworthy, J. H. *Annual Review of Medicine* **2002**, *53*, 285-302.
- (130) Pershadsingh, H. A.; Heneka, M. T.; Saini, R.; Amin, N. M.; Broeske, D. J.; Feinstein, D. G. *Journal of Neuroinflammation* **2004**, *1*, 1-4.
- (131) Feinstein, D. L. *Drug Discovery Today: Therapeutic Strategies* **2004**, *1*, 29-42.
- (132) Clarke, D. W.; Boyd, F. T.; Kappy, M. S.; Raizada, M. K. *Journal of Biological Chemistry* **1984**, *259*, 1672-1675.
- (133) Friedland, R. P.; Jagust, W. J.; Huesman, R. H.; Koss, E.; Knittel, B.; Mathis, C. A.; Ober, B. A.; Mazoyer, B. M.; Budinger, T. F. *Neurology* **1989**, *39*, 1427-1434.
- (134) Kumagai, A. K. *Diabetes-Metabolism Research and Reviews* **1999**, *15*, 261-273.
- (135) Bodor, N.; Brewster, M. E. *Pharmacology & Therapeutics* **1982**, *19*, 337-386.
- (136) Image <http://www-ermm.cbcu.cam.ac.uk/fig001pgc.gif>.
- (137) Image
<http://homepage.psy.utexas.edu/homepage/class/Psy332/Salinas/Cells/BBB.gif>.
- (138) Tsuzuki, N.; Hama, T.; Hibi, T.; Konishi, R.; Futaki, S.; Kitagawa, K. *Biochemical Pharmacology* **1991**, *41*, R5-R8.
- (139) Bodor, N.; Farag, H. H.; Brewster, M. E. *Science* **1981**, *214*, 1370-1372.
- (140) Bodor, N.; Prokai, L.; Wu, W. M.; Farag, H.; Jonalagadda, S.; Kawamura, M.; Simpkins, J. *Science* **1992**, *257*, 1698-1700.
- (141) Prokai, L.; Ouyang, X. D.; Wu, W. M.; Bodor, N. *Journal of the American Chemical Society* **1994**, *116*, 2643-2644.
- (142) Bodor, N. S. *US patent* **1983**, 4,540,564.
- (143) Bodor, N. S. *US patent* **1991**, 5,389,623.
- (144) Bodor, N. S. *US patent* **1992**, 5,525,727.
- (145) Farris, W.; Mansourian, S.; Chang, Y.; Lindsley, L.; Eckman, E. A.; Frosch, M. P.; Eckman, C. B.; Tanzi, R. E.; Selkoe, D. J.; Guenette, S. *Proceedings of the National Academy of Sciences of the United States of America* **2003**, *100*, 4162-4167.
- (146) Park, C. R. *Neuroscience & Biobehavioral Reviews* **2001**, *25*, 311-323.
- (147) Luchsinger, J. A.; Tang, M. X.; Shea, S.; Mayeux, R. *Neurology* **2004**, *63*, 1187-1192.
- (148) de la Torre, J. C. In *Alzheimers Disease: A Compendium of Current Theories* 2000; Vol. 924, p 136-152.
- (149) Heneka, M. T.; Gavriluk, V.; Landreth, G. E.; O'Banion, M. K.; Weinberg, G.; Feinstein, D. L. *Journal of Neurochemistry* **2003**, *85*, 387-398.
- (150) Heneka, M. T.; Landreth, G. E.; Feinstein, D. L. *Annals of Neurology* **2001**, *49*, 276-276.

- (151) Sastre, M.; Dewachter, I.; Landreth, G. E.; Willson, T. M.; Klockgether, T.; van Leuven, F.; Heneka, M. T. *J. Neurosci.* **2003**, *23*, 9796-9804.
- (152) Dello Russou, C.; Gavriilyuk, V.; Weinberg, G.; Almeida, A.; Bolanos, J. P.; Palmer, J.; Pelligrino, D.; Galea, E.; Feinstein, D. L. *Journal of Biological Chemistry* **2003**, *278*, 5828-5836.
- (153) Chain, D.; Cawthorne, M. *International patent* **2000**, WO0035437.
- (154) Cannella, B.; Raine, C. S. *Annals of Neurology* **1995**, *37*, 424-435.
- (155) Samoilova, E. B.; Horton, J. L.; Hilliard, B.; Liu, T. S. T.; Chen, Y. H. *Journal of Immunology* **1998**, *161*, 6480-6486.
- (156) Xu, J. H.; Storer, P. D.; Chavis, J. A.; Racke, M. K.; Drew, P. D. *Journal of Neuroscience Research* **2005**, *81*, 403-411.
- (157) Janabi, N. *Journal of Immunology* **2002**, *168*, 4747-4755.
- (158) Satoh, T.; Furuta, K.; Suzuki, M.; Watanabe, Y. *Biochemical and Biophysical Research Communications* **1999**, *258*, 50-53.
- (159) Heneka, M. T.; Klockgether, T.; Feinstein, D. L. *Journal of Neuroscience* **2000**, *20*, 1A-1A.
- (160) Feinstein, D. L.; Galea, E.; Gavriilyuk, V.; Brosnan, C. F.; Whitacre, C. C.; Dumitrescu-Ozimek, L.; Landreth, G. E.; Pershadsingh, H. A.; Weinberg, G.; Heneka, M. T. *Annals of Neurology* **2002**, *51*, 694-702.
- (161) Niino, M.; Iwabuchi, K.; Kikuchi, S.; Ato, M.; Morohashi, T.; Ogata, A.; Tashiro, K.; Onoe, K. *Journal of Neuroimmunology* **2001**, *116*, 40-48.
- (162) Diab, A.; Deng, C. S.; Smith, J. D.; Hussain, R. Z.; Phanavanh, B.; Lovett-Racke, A. E.; Drew, P. D.; Racke, M. K. *Journal of Immunology* **2002**, *168*, 2508-2515.
- (163) Ye, J. M.; Doyle, P. J.; Iglesias, M. A.; Watson, D. G.; Cooney, G. J.; Kraegen, E. W. *Diabetes* **2001**, *50*, 411-417.
- (164) Guerre-Millo, M.; Gervois, P.; Raspe, E.; Madsen, L.; Poulain, P.; Derudas, B.; Herbert, J. M.; Winegar, D. A.; Willson, T. M.; Fruchart, J. C.; Berge, R. K.; Staels, B. *Journal of Biological Chemistry* **2000**, *275*, 16638-16642.
- (165) Staels, B.; Dallongeville, J.; Auwerx, J.; Schoonjans, K.; Leitersdorf, E.; Fruchart, J. G. *Circulation* **1998**, *98*, 2088-2093.
- (166) Bergeron, R.; Yao, J.; Woods, J. W.; Zycband, E. I.; Liu, C.; Li, Z. H.; Adams, A.; Berger, J. P.; Zhang, B. B.; Moller, D. E.; Doebber, T. W. *Endocrinology* **2006**, *147*, 4252-4262.
- (167) Lohray, B. B.; Lohray, V. B.; Bajji, A. C.; Kalchar, S.; Poondra, R. R.; Padakanti, S.; Chakrabarti, R.; Vikramadithyan, R. K.; Misra, P.; Juluri, S.; Mamidi, N.; Rajagopalan, R. *Journal of Medicinal Chemistry* **2001**, *44*, 2675-2678.

- (168) Ljung, B.; Bamberg, K.; Dahllof, B.; Kjellstedt, A.; Oakes, N. D.; Ostling, J.; Svensson, L.; Camejo, G. *Journal of Lipid Research* **2002**, *43*, 1855-1863.
- (169) Hegarty, B. D.; Furler, S. M.; Oakes, N. D.; Kraegen, E. W.; Cooney, G. J. *Endocrinology* **2004**, *145*, 3158-3164.
- (170) Ye, J. M.; Iglesias, M. A.; Watson, D. G.; Ellis, B.; Wood, L.; Jensen, P. B.; Sorensen, R. V.; Larsen, P. J.; Cooney, G. J.; Wassermann, K.; Kraegen, E. W. *American Journal of Physiology-Endocrinology and Metabolism* **2003**, *284*, E531-E540.
- (171) Ide, T.; Nakazawa, T.; Mochizuki, T.; Murakami, K. *Metabolism-Clinical and Experimental* **2000**, *49*, 521-525.
- (172) Etgen, G. J.; Oldham, B. A.; Johnson, W. T.; Broderick, C. L.; Montrose, C. R.; Brozinick, J. T.; Misener, E. A.; Bean, J. S.; Bensch, W. R.; Brooks, D. A.; Shuker, A. J.; Rito, C. J.; McCarthy, J. R.; Ardecky, R. J.; Tyhonas, J. S.; Dana, S. L.; Bilakovics, J. M.; Paterniti, J. R.; Ogilvie, K. M.; Liu, S.; Kauffman, R. F. *Diabetes* **2002**, *51*, 1083-1087.
- (173) Chakrabarti, R.; Vikramadithyan, R. K.; Misra, P.; Hiriyan, J.; Raichur, S.; Damarla, R. K.; Gershon, C.; Suresh, J.; Rajagopalan, R. *British Journal of Pharmacology* **2003**, *140*, 527-537.
- (174) Shibata, T.; Takeuchi, S.; Yokota, S.; Kakimoto, K.; Yonemori, F.; Wakitani, K. *British Journal of Pharmacology* **2000**, *130*, 495-504.
- (175) Tozzo, E.; Ponticiello, R.; Swartz, J.; Farrelly, D.; Zebo, R.; Welzel, G.; Egan, D.; Kunselman, L.; Peters, A.; Gu, L. Q.; French, M.; Chen, S.; Devasthale, P.; Janovitz, E.; Staal, A.; Harrity, T.; Belder, R.; Cheng, P. T.; Whaley, J.; Taylor, S.; Hariharan, N. *Journal of Pharmacology and Experimental Therapeutics* **2007**, *321*, 107-115.
- (176) Henke, B. R.; Adkison, K. K.; Blanchard, S. G.; Leesnitzer, L. M.; Mook, R. A.; Plunket, K. D.; Ray, J. A.; Roberson, C.; Unwalla, R.; Willson, T. M. *Bioorganic & Medicinal Chemistry Letters* **1999**, *9*, 3329-3334.
- (177) Kuhn, B.; Hilpert, H.; Benz, J.; Binggeli, A.; Grether, U.; Humm, R.; Marki, H. P.; Meyer, M.; Mohr, P. *Bioorganic & Medicinal Chemistry Letters* **2006**, *16*, 4016-4020.
- (178) Spydevold, O.; Bremer, J. *Biochimica Et Biophysica Acta* **1989**, *1003*, 72-79.
- (179) Berge, R. K.; Aarsland, A.; Kryvi, H.; Bremer, J.; Aarsaether, N. *Biochimica Et Biophysica Acta* **1989**, *1004*, 345-356.
- (180) Berge, R. K.; Aarsland, A.; Kryvi, H.; Bremer, J.; Aarsaether, N. *Biochemical Pharmacology* **1989**, *38*, 3969-3979.

- (181) Raspe, E.; Madsen, L.; Lefebvre, A. M.; Leitersdorf, I.; Gelman, L.; Peinado-Onsurbe, J.; Dallongeville, J.; Fruchart, J. C.; Berge, R.; Staels, B. *Journal of Lipid Research* **1999**, *40*, 2099-2110.
- (182) Aarsland, A.; Aarsaether, N.; Bremer, J.; Berge, R. K. *Journal of Lipid Research* **1989**, *30*, 1711-1718.
- (183) Berge, R. K.; Hvattum, E. *Pharmacology & Therapeutics* **1994**, *61*, 345-383.
- (184) Madsen, L.; Guerre-Millo, M.; Flindt, E. N.; Berge, K.; Tronstad, K. J.; Bergene, E.; Sebokova, E.; Rustan, A. C.; Jensen, J.; Mandrup, S.; Kristiansen, K.; Klimes, I.; Staels, B.; Berge, R. K. *Journal of Lipid Research* **2002**, *43*, 742-750.
- (185) Hovik, R.; Osmundsen, H.; Berge, R.; Aarsland, A.; Bergseth, S.; Bremer, J. *Biochemical Journal* **1990**, *270*, 167-173.
- (186) Pettersen, R. J.; Muna, Z. A.; Kuiper, K. K. J.; Svendsen, E.; Muller, F.; Aukrust, P.; Berge, R. K.; Nordrehaug, J. E. *Cardiovascular Research* **2001**, *52*, 306-313.
- (187) Berge, K.; Tronstad, K. J.; Flindt, E. N.; Rasmussen, T. H.; Madsen, L.; Kristiansen, K.; Berge, R. K. *Carcinogenesis* **2001**, *22*, 1747-1755.
- (188) Westergaard, M.; Henningsen, J.; Svendsen, M. L.; Johansen, C.; Jensen, U. B.; Schroder, H. D.; Kratchmarova, I.; Berge, R. K.; Iversen, L.; Bolund, L.; Kragballe, K.; Kristiansen, K. *Journal of Investigative Dermatology* **2001**, *116*, 702-712.
- (189) Gunstone, F. *Fatty Acid and Lipid Chemistry*; Blackie A & P, 1996.
- (190) Image www.basisgmbh.com/images/mal1-e.gif.
- (191) Sciences, B.
http://arbl.cvmb.colostate.edu/hbooks/pathphys/digestion/smallgut/absorb_lipids.htm
I.
- (192) Warner, T. G.; Benson, A. A. *Journal of Lipid Research* **1977**, *18*, 548-552.
- (193) Hermetter, A.; Paltauf, F. *Chemistry and Physics of Lipids* **1981**, *29*, 225-233.
- (194) Charp, P. A.; Zhou, Q. Z.; Wood, M. G.; Raynor, R. L.; Menger, F. M.; Kuo, J. F. *Biochemistry* **1988**, *27*, 4607-4612.
- (195) Miller, A. D.; Jorgensen, M. R.; Berge, R.; Skorve, J. *International patent* **2003**, WO 2004/000854 A1.
- (196) Wang, P.; Schuster, M.; Wang, Y. F.; Wong, C. H. *Journal of the American Chemical Society* **1993**, *115*, 10487-10491.
- (197) Delfino, J. M.; Schreiber, S. L.; Richards, F. M. *Journal of the American Chemical Society* **1993**, *115*, 3458-3474.
- (198) Dewet, J. R.; Wood, K. V.; Deluca, M.; Helinski, D. R.; Subramani, S. *Molecular and Cellular Biology* **1987**, *7*, 725-737.
- (199) Cobb, J. E.; Henke, B. R.; Blanchard, S. G. *Diabetologia* **2000**, *43*, A189-A189.

- (200) Lipinski, C. A.; Lombardo, F.; Dominy, B. W.; Feeney, P. J. *Advanced Drug Delivery Reviews* **1997**, *23*, 3-25.
- (201) Xu, J.; Stevenson, J. *Journal of Chemical Information and Computer Sciences* **2000**, *40*, 1177-1187.
- (202) Wasserman, H. H.; Ho, W. B. *Journal of Organic Chemistry* **1994**, *59*, 4364-4366.
- (203) Kim, M. J.; Whitesides, G. M. *Journal of the American Chemical Society* **1988**, *110*, 2959-2964.
- (204) Kim, M. J.; Kim, J. Y. *Journal of the Chemical Society-Chemical Communications* **1991**, 326-327.
- (205) Iwamura, H.; Imahashi, Y.; Kushida, K.; Aoki, K.; Satoh, S. *Bulletin of the Chemical Society of Japan* **1976**, *49*, 1690-1696.
- (206) Hundesberger, M.; Shaw, E. R.; Fugger, J.; Ketcham, R.; Ledniger, D. **1955**, 394-399.
- (207) Belletire, J. L.; Spletzer, E. G.; Pinhas, A. R. *Tetrahedron Letters* **1984**, *25*, 5969-5972.
- (208) Rathke, M. W.; Lindert, A. *Tetrahedron Letters* **1971**, 3995-3998.
- (209) Wasserman, H. H.; Petersen, A. K. *Journal of Organic Chemistry* **1997**, *62*, 8972-8973.
- (210) Dalla, V.; Catteau, J. P.; Pale, P. *Tetrahedron Letters* **1999**, *40*, 5193-5196.
- (211) Liao, M.; Yao, W.; Wang, J. *Synthesis* **2004**, *16*, 2633-2636.
- (212) Barnett, J. E. G.; Kent, P. W. *Journal of the Chemical Society* **1963**, 2743-2747.
- (213) Roberts, E. M.; Gates, M.; Boekelheide, V. *J. Org. Chem.* **1955**, *20*, 1443-1447.
- (214) Fuson, R. C.; Rachlin, A. I. *Journal of the American Chemical Society* **1942**, *64*, 1567-1571.
- (215) Winneroski, L. L.; Xu, Y. *Journal of Organic Chemistry* **2004**, *69*, 4948-53.
- (216) Bays, D. E.; Webb, C. F. *UK patent* **1985**, GB 2 168 347 A.
- (217) Street, L. J.; Baker, R.; Castro, J. L.; Chambers, M. S.; Guiblin, A. R.; Hobbs, S. C.; Matassa, V. G.; Reeve, A. J.; Beer, M. S.; Middlemiss, D. N. *J Med Chem* **1993**, *36*, 1529-38.
- (218) Bentley, D. J.; Fairhurst, J.; Gallagher, P. T.; Manteuffel, A. K.; Moody, C. J.; Pinder, J. L. *Organic and Biomolecular Chemistry* **2004**, *2*, 701-8.
- (219) Glen, R. C.; Martin, G. R.; Hill, A. P.; Hyde, R. M.; Woollard, P. M.; Salmon, J. A.; Buckingham, J.; Robertson, A. D. *Journal of Medicinal Chemistry* **1995**, *38*, 3566-80.

- (220) Jandu, K. S.; Barrett, V.; Brockwell, M.; Cambridge, D.; Farrant, D. R.; Foster, C.; Giles, H.; Glen, R. C.; Hill, A. P.; Hobbs, H.; Honey, A.; Martin, G. R.; Salmon, J.; Smith, D.; Woollard, P.; Selwood, D. L. *Journal of Medicinal Chemistry* **2001**, *44*, 681-93.
- (221) Bosch, J.; Roca, T.; Armengol, M.; Fernandez-Forner, D. *Tetrahedron* **2001**, *57*, 1041-1048.
- (222) Robinson, B. *The Fischer Indole Synthesis*; John Wiley & Sons Ltd., 1982.
- (223) Iwanowicz, E. J.; Lau, W. F.; Lin, J.; Roberts, D. G. M.; Seiler, S. M. *Bioorganic & Medicinal Chemistry Letters* **1996**, *6*, 1339-1344.
- (224) Grell, W.; Machleidt, H. *Annalen. Chemie.* **1966**, *699*, 53-67.
- (225) Moody, C. J.; Sie, E.; Kulagowski, J. J. *Tetrahedron* **1992**, *48*, 3991-4004.
- (226) Haigh, D.; Birrell, H. C.; Cantello, B. C. C.; Hindley, R. M.; Ramaswamy, A.; Rami, H. K.; Stevens, N. C. *Tetrahedron-Asymmetry* **1999**, *10*, 1335-1351.
- (227) McElweewhite, L.; Goddard, W. A.; Dougherty, D. A. *Journal of the American Chemical Society* **1984**, *106*, 3461-3466.
- (228) Regitz, M.; Anschutz, W.; Liedhegener, A. *Chemische Berichte* **1968**, *101*, 3734-3743.
- (229) Lohray, B. B.; Lohray, V. B.; Bajji, A. C.; Kalchar, S.; Ramanujam, R.; Chakrabarti, R. *US patent* **2000**, 6,054,453.
- (230) Haigh, D. *Tetrahedron* **1994**, *50*, 3177-3194.
- (231) Zhang, W.; Cao, X. Y.; Zi, H.; Pei, J. *Organic Letters* **2005**, *7*, 959-962.
- (232) Liu, S. F.; Wu, Q. G.; Schmider, H. L.; Aziz, H.; Hu, N. X.; Popovic, Z.; Wang, S. N. *Journal of the American Chemical Society* **2000**, *122*, 3671-3678.
- (233) Wenkert, E.; Angell, E. C.; Ferreira, V. F.; Michelotti, E. L.; Piettre, S. R.; Sheu, J. H.; Swindell, C. S. *Journal of Organic Chemistry* **1986**, *51*, 2343-2351.
- (234) Zhou, X. M.; Wang, Z. Q.; Chang, J. Y.; Chen, H. X.; Cheng, Y. C.; Lee, K. H. *Journal of Medicinal Chemistry* **1991**, *34*, 3346-3350.
- (235) Gilman, H.; Soddy, T. S. *Journal of Organic Chemistry* **1957**, *22*, 565-566.
- (236) Shirley, D. A.; Roussel, P. A. *Journal of the American Chemical Society* **1952**, *75*, 375-378.
- (237) Hassan, H.; Spies, H. S.; Bredenkamp, M. W. *Polish Journal of Chemistry* **2000**, *74*, 1589-1598.
- (238) Sundberg, R. J.; Russell, H. F. *Journal of Organic Chemistry* **1973**, *38*, 3324-3330.
- (239) Lu, X. L.; Petersen, J. L.; Wang, K. K. *Organic Letters* **2003**, *5*, 3277-3280.
- (240) Adam, G.; Andrieux, J.; Plat, M. *Tetrahedron* **1985**, *41*, 399-407.
- (241) Ketcha, D. M.; Lieurance, B. A.; Homan, D. F. J.; Gribble, G. W. *Journal of Organic Chemistry* **1989**, *54*, 4350-4356.

- (242) Gribble, G. W.; Keavy, D. J.; Davis, D. A.; Saulnier, M. G.; Pelcman, B.; Barden, T. C.; Sibi, M. P.; Olson, E. R.; Belbruno, J. J. *Journal of Organic Chemistry* **1992**, *57*, 5878-5891.
- (243) Sakamoto, T.; Kondo, Y.; Takazawa, N.; Yamanaka, H. *Journal of the Chemical Society-Perkin Transactions 1* **1996**, 1927-1934.
- (244) Yang, Y. H.; Martin, A. R.; Nelson, D. L.; Regan, J. *Heterocycles* **1992**, *34*, 1169-1175.
- (245) Zhang, Q. Z.; Botting, N. P. *Tetrahedron* **2004**, *60*, 12211-12216.
- (246) Dvorak, C. A.; Apodaca, R.; Barbier, A. J.; Berridge, C. W.; Wilson, S. J.; Boggs, J. D.; Xiao, W.; Lovenberg, T. W.; Carruthers, N. I. *Journal of Medicinal Chemistry* **2005**, *48*, 2229-2238.
- (247) Vazquez, E.; Davies, I. W.; Payack, J. F. *Journal of Organic Chemistry* **2002**, *67*, 7551-7552.
- (248) Solladiecavallo, A.; Diepvohuule, A. *Journal of Organic Chemistry* **1995**, *60*, 3494-3498.
- (249) Saulnier, M. G.; Gribble, G. W. *Journal of Organic Chemistry* **1982**, *47*, 757-761.
- (250) Roy, S.; Gribble, G. W. *Tetrahedron Letters* **2005**, *46*, 1325-1328.
- (251) Paul, F.; Patt, J.; Hartwig, J. F. *Journal of the American Chemical Society* **1994**, *116*, 5969-5970.
- (252) Guram, A. S.; Buchwald, S. L. *Journal of the American Chemical Society* **1994**, *116*, 7901-7902.
- (253) Mizoroki, T.; Mori, K.; Ozaki, A. *Bulletin of the Chemical Society of Japan* **1971**, *44*, 581-581.
- (254) Heck, R. F.; Nolley, J. P. *Journal of Organic Chemistry* **1972**, *37*, 2320-&.
- (255) Loiseleur, O.; Hayashi, M.; Keenan, M.; Schmees, N.; Pfaltz, A. *Journal of Organometallic Chemistry* **1999**, *576*, 16-22.
- (256) Jeffery, T. *Tetrahedron* **1996**, *52*, 10113-10130.
- (257) Sonesson, C.; Larhed, M.; Nyqvist, C.; Hallberg, A. *Journal of Organic Chemistry* **1996**, *61*, 4756-4763.
- (258) David, O.; Blot, J.; Bellec, C.; Fargeau-Bellassoued, M. C.; Haviari, G.; Celerier, J. P.; Lhommet, G.; Gramain, J. C.; Gardette, D. *Journal of Organic Chemistry* **1999**, *64*, 3122-3131.
- (259) Donohoe, T. J.; Guyo, P. M.; Harji, R. R.; Helliwell, M.; Cousins, R. P. C. *Tetrahedron Letters* **1998**, *39*, 3075-3078.
- (260) Ablordeppey, S. Y.; Lyles-Eggleston, M.; Bricker, B.; Zhang, W.; Zhu, X.; Goodman, C.; Roth, B. L. *Bioorganic & Medicinal Chemistry Letters* **2006**, *16*, 3219-3223.

- (261) Lott, R. S.; Chauhan, V. S.; Stammer, C. H. *Journal of the Chemical Society-Chemical Communications* **1979**, 495-496.
- (262) Rawal, V. H.; Michoud, C. *Journal of Organic Chemistry* **1993**, *58*, 5583-5584.
- (263) Wolfe, J. P.; Wagaw, S.; Buchwald, S. L. *Journal of the American Chemical Society* **1996**, *118*, 7215-7216.
- (264) Wagaw, S.; Rennels, R. A.; Buchwald, S. L. *Journal of the American Chemical Society* **1997**, *119*, 8451-8458.
- (265) Cousin, D.; Mann, J.; Nieuwenhuyzen, M.; van den Berg, H. *Organic & Biomolecular Chemistry* **2006**, *4*, 54-62.
- (266) Still, W. C.; Kahn, M.; Mitra, A. *Journal of Organic Chemistry* **1978**, *43*, 2923-2925.
- (267) Daub, G. H.; Castle, R. N. *Journal of Organic Chemistry* **1954**, *19*, 1571-1574.

Appendices

Appendix 1 Crystal structure data for 2-benzylcyano indole 194

Crystal data and structure refinement for indole 194

Identification code	ADM0701
Empirical formula	C ₂₂ H ₁₆ N ₂ O ₂ S
Formula weight	372.43
Temperature	173 (2) K
Diffractometer, wavelength	OD Xcalibur 3, 0.71073 Å
Crystal system, space group	Monoclinic, P2(1)/n
Unit cell dimensions	a = 10.8591(3) Å α = 90° b = 10.0425(3) Å β = 100.888(3)° c = 17.0542(4) Å γ = 90°
Volume, Z	1826.32(9) Å ³ , 4
Density (calculated)	1.354 Mg/m ³
Absorption coefficient	0.197 mm ⁻¹
F(000)	776
Crystal colour / morphology	Colourless blocks
Crystal size	0.11 x 0.08 x 0.08 mm ³
θ range for data collection	3.79 to 28.96°
Index ranges	-14 ≤ h ≤ 14, -10 ≤ k ≤ 13, -22 ≤ l ≤ 22
Reflns collected / unique	12993 / 4231 [R(int) = 0.0606]
Reflns observed [F > 4σ(F)]	2710
Absorption correction	Analytical
Max. and min. transmission	0.988 and 0.976
Refinement method	Full-matrix least-squares on F ²
Data / restraints / parameters	4231 / 7 / 245
Goodness-of-fit on F ²	1.040
Final R indices [F > 4σ(F)]	R1 = 0.0438, wR2 = 0.1012
R indices (all data)	R1 = 0.0808, wR2 = 0.1155
Largest diff. peak, hole	0.248, -0.307 eÅ ⁻³
Mean and maximum shift/error	0.000 and 0.000

Bond lengths [Å] and angles [°] for indole 194

N(1)-C(9)	1.411	(2)
N(1)-C(2)	1.426	(2)
N(1)-S(10)	1.6757	(14)
C(2)-C(3)	1.339	(3)
C(2)-C(19)	1.499	(2)
C(3)-C(4)	1.419	(2)
C(4)-C(5)	1.388	(3)
C(4)-C(9)	1.411	(2)
C(5)-C(6)	1.375	(3)
C(6)-C(7)	1.406	(3)
C(6)-C(26)	1.442	(3)
C(7)-C(8)	1.372	(2)
C(8)-C(9)	1.390	(2)
S(10)-O(11)	1.4175	(14)
S(10)-O(12)	1.4217	(13)
S(10)-C(13)	1.7187	(15)
S(10)-C(13')	1.774	(4)
C(13)-C(14)	1.3900	
C(13)-C(18)	1.3900	
C(14)-C(15)	1.3900	
C(15)-C(16)	1.3900	
C(16)-C(17)	1.3900	
C(17)-C(18)	1.3900	
C(13')-C(14')	1.3900	
C(13')-C(18')	1.3900	
C(14')-C(15')	1.3900	
C(15')-C(16')	1.3900	
C(16')-C(17')	1.3900	
C(17')-C(18')	1.3900	
C(19)-C(20)	1.518	(2)
C(20)-C(21)	1.383	(2)
C(20)-C(25)	1.385	(2)
C(21)-C(22)	1.380	(2)
C(22)-C(23)	1.376	(3)
C(23)-C(24)	1.362	(3)
C(24)-C(25)	1.389	(3)

C(26)-N(26)	1.137	(3)
C(9)-N(1)-C(2)	107.88	(14)
C(9)-N(1)-S(10)	124.08	(11)
C(2)-N(1)-S(10)	128.00	(12)
C(3)-C(2)-N(1)	108.35	(15)
C(3)-C(2)-C(19)	126.30	(16)
N(1)-C(2)-C(19)	125.32	(16)
C(2)-C(3)-C(4)	109.55	(16)
C(5)-C(4)-C(9)	119.48	(16)
C(5)-C(4)-C(3)	133.01	(17)
C(9)-C(4)-C(3)	107.50	(16)
C(6)-C(5)-C(4)	118.96	(17)
C(5)-C(6)-C(7)	121.00	(18)
C(5)-C(6)-C(26)	119.20	(19)
C(7)-C(6)-C(26)	119.79	(18)
C(8)-C(7)-C(6)	121.05	(17)
C(7)-C(8)-C(9)	117.94	(17)
C(8)-C(9)-C(4)	121.56	(17)
C(8)-C(9)-N(1)	131.74	(16)
C(4)-C(9)-N(1)	106.68	(15)
O(11)-S(10)-O(12)	120.25	(9)
O(11)-S(10)-N(1)	106.64	(8)
O(12)-S(10)-N(1)	105.70	(7)
O(11)-S(10)-C(13)	106.10	(13)
O(12)-S(10)-C(13)	110.72	(13)
N(1)-S(10)-C(13)	106.66	(12)
O(11)-S(10)-C(13')	115.1	(2)
O(12)-S(10)-C(13')	103.9	(2)
N(1)-S(10)-C(13')	103.7	(3)
C(13)-S(10)-C(13')	9.0	(2)
C(14)-C(13)-C(18)	120.0	
C(14)-C(13)-S(10)	119.80	(13)
C(18)-C(13)-S(10)	120.19	(13)
C(15)-C(14)-C(13)	120.0	
C(14)-C(15)-C(16)	120.0	
C(17)-C(16)-C(15)	120.0	
C(16)-C(17)-C(18)	120.0	

C(17)-C(18)-C(13)	120.0	
C(14')-C(13')-C(18')	120.0	
C(14')-C(13')-S(10)	118.8	(3)
C(18')-C(13')-S(10)	121.1	(3)
C(13')-C(14')-C(15')	120.0	
C(16')-C(15')-C(14')	120.0	
C(17')-C(16')-C(15')	120.0	
C(18')-C(17')-C(16')	120.0	
C(17')-C(18')-C(13')	120.0	
C(2)-C(19)-C(20)	115.51	(14)
C(21)-C(20)-C(25)	118.04	(16)
C(21)-C(20)-C(19)	122.17	(16)
C(25)-C(20)-C(19)	119.76	(16)
C(22)-C(21)-C(20)	120.82	(17)
C(23)-C(22)-C(21)	120.37	(18)
C(24)-C(23)-C(22)	119.70	(17)
C(23)-C(24)-C(25)	120.15	(17)
C(20)-C(25)-C(24)	120.89	(18)
N(26)-C(26)-C(6)	179.8	(3)

Appendix 2 Crystal structure data for 2-naphthylmethylcyano indole 195

Crystal data and structure refinement for indole 195

Identification code	ADM0702
Empirical formula	C ₂₆ H ₁₈ N ₂ O ₂ S
Formula weight	422.48
Temperature	173(2) K
Diffractometer, wavelength	OD Xcalibur PX Ultra, 1.54248 Å
Crystal system, space group	Monoclinic, P2(1)/n
Unit cell dimensions	a = 18.0309 (4) Å α = 90° b = 5.88641 (15) Å β = 98.636 (2)° c = 19.5220 (4) Å γ = 90°
Volume, Z	2048.52(19) Å ³ , 4
Density (calculated)	1.370 Mg/m ³
Absorption coefficient	1.615 mm ⁻¹
F(000)	880
Crystal colour / morphology	Colourless needles
Crystal size	0.23 x 0.03 x 0.01 mm ³
θ range for data collection	3.11 to 63.12 °
Index ranges	-20 ≤ h ≤ 20, -6 ≤ k ≤ 6, -22 ≤ l ≤ 22
Reflns collected / unique	8932 / 3230 [R(int) = 0.0501]
Reflns observed [F > 4σ(F)]	1894
Absorption correction	Semi-empirical from equivalents
Max. and min. transmission	1.00000 and 0.81707
Refinement method	Full-matrix least-squares on F ²
Data / restraints / parameters	3230 / 0 / 280
Goodness-of-fit on F ²	0.867
Final R indices [F > 4σ(F)]	R1 = 0.0404, wR2 = 0.0764
R indices (all data)	R1 = 0.0879, wR2 = 0.0869
Largest diff. peak, hole	0.152, -0.256 eÅ ⁻³
Mean and maximum shift/error	0.000 and 0.000

Bond lengths [Å] and angles [°] for indole 195

N(1)-C(9)	1.415	(3)
N(1)-C(2)	1.434	(3)
N(1)-S(10)	1.6708	(19)
C(2)-C(3)	1.343	(3)
C(2)-C(19)	1.505	(3)
C(3)-C(4)	1.434	(3)
C(4)-C(5)	1.391	(3)
C(4)-C(9)	1.403	(3)
C(5)-C(6)	1.388	(3)
C(6)-C(7)	1.397	(3)
C(6)-C(30)	1.434	(4)
C(7)-C(8)	1.377	(3)
C(8)-C(9)	1.390	(3)
S(10)-O(11)	1.4261	(18)
S(10)-O(12)	1.4314	(15)
S(10)-C(13)	1.763	(3)
C(13)-C(18)	1.378	(3)
C(13)-C(14)	1.393	(4)
C(14)-C(15)	1.381	(4)
C(15)-C(16)	1.371	(4)
C(16)-C(17)	1.366	(4)
C(17)-C(18)	1.403	(4)
C(19)-C(20)	1.527	(3)
C(20)-C(21)	1.361	(3)
C(20)-C(29)	1.414	(3)
C(21)-C(22)	1.425	(3)
C(22)-C(23)	1.412	(3)
C(22)-C(27)	1.412	(3)
C(23)-C(24)	1.372	(3)
C(24)-C(25)	1.397	(3)
C(25)-C(26)	1.362	(3)
C(26)-C(27)	1.423	(3)
C(27)-C(28)	1.409	(3)
C(28)-C(29)	1.370	(3)
C(30)-N(30)	1.153	(3)

C(9)-N(1)-C(2)	107.78	(19)
C(9)-N(1)-S(10)	122.41	(15)
C(2)-N(1)-S(10)	126.61	(16)
C(3)-C(2)-N(1)	107.9	(2)
C(3)-C(2)-C(19)	127.1	(2)
N(1)-C(2)-C(19)	124.8	(2)
C(2)-C(3)-C(4)	109.9	(2)
C(5)-C(4)-C(9)	119.7	(2)
C(5)-C(4)-C(3)	133.3	(2)
C(9)-C(4)-C(3)	107.0	(2)
C(6)-C(5)-C(4)	118.3	(2)
C(5)-C(6)-C(7)	120.9	(3)
C(5)-C(6)-C(30)	119.5	(2)
C(7)-C(6)-C(30)	119.6	(2)
C(8)-C(7)-C(6)	121.9	(2)
C(7)-C(8)-C(9)	116.7	(2)
C(8)-C(9)-C(4)	122.5	(2)
C(8)-C(9)-N(1)	130.0	(2)
C(4)-C(9)-N(1)	107.45	(19)
O(11)-S(10)-O(12)	120.96	(11)
O(11)-S(10)-N(1)	106.20	(10)
O(12)-S(10)-N(1)	105.73	(10)
O(11)-S(10)-C(13)	109.86	(13)
O(12)-S(10)-C(13)	107.80	(12)
N(1)-S(10)-C(13)	105.14	(11)
C(18)-C(13)-C(14)	120.8	(3)
C(18)-C(13)-S(10)	119.3	(3)
C(14)-C(13)-S(10)	119.8	(2)
C(15)-C(14)-C(13)	119.3	(3)
C(16)-C(15)-C(14)	120.2	(3)
C(17)-C(16)-C(15)	120.7	(3)
C(16)-C(17)-C(18)	120.3	(3)
C(13)-C(18)-C(17)	118.6	(3)
C(2)-C(19)-C(20)	114.8	(2)
C(21)-C(20)-C(29)	119.5	(2)
C(21)-C(20)-C(19)	121.5	(2)
C(29)-C(20)-C(19)	118.9	(2)
C(20)-C(21)-C(22)	121.5	(2)

C(23)-C(22)-C(27)	119.0	(2)
C(23)-C(22)-C(21)	122.3	(2)
C(27)-C(22)-C(21)	118.7	(2)
C(24)-C(23)-C(22)	120.6	(2)
C(23)-C(24)-C(25)	120.6	(3)
C(26)-C(25)-C(24)	120.2	(2)
C(25)-C(26)-C(27)	120.9	(2)
C(28)-C(27)-C(22)	118.7	(2)
C(28)-C(27)-C(26)	122.7	(2)
C(22)-C(27)-C(26)	118.6	(2)
C(29)-C(28)-C(27)	121.5	(2)
C(28)-C(29)-C(20)	120.1	(2)
N(30)-C(30)-C(6)	179.7	(3)